

Figure 1: Map of the Lobster Fishing Areas in Atlantic Canada using the boundaries identified in the Atlantic fishery regulations.

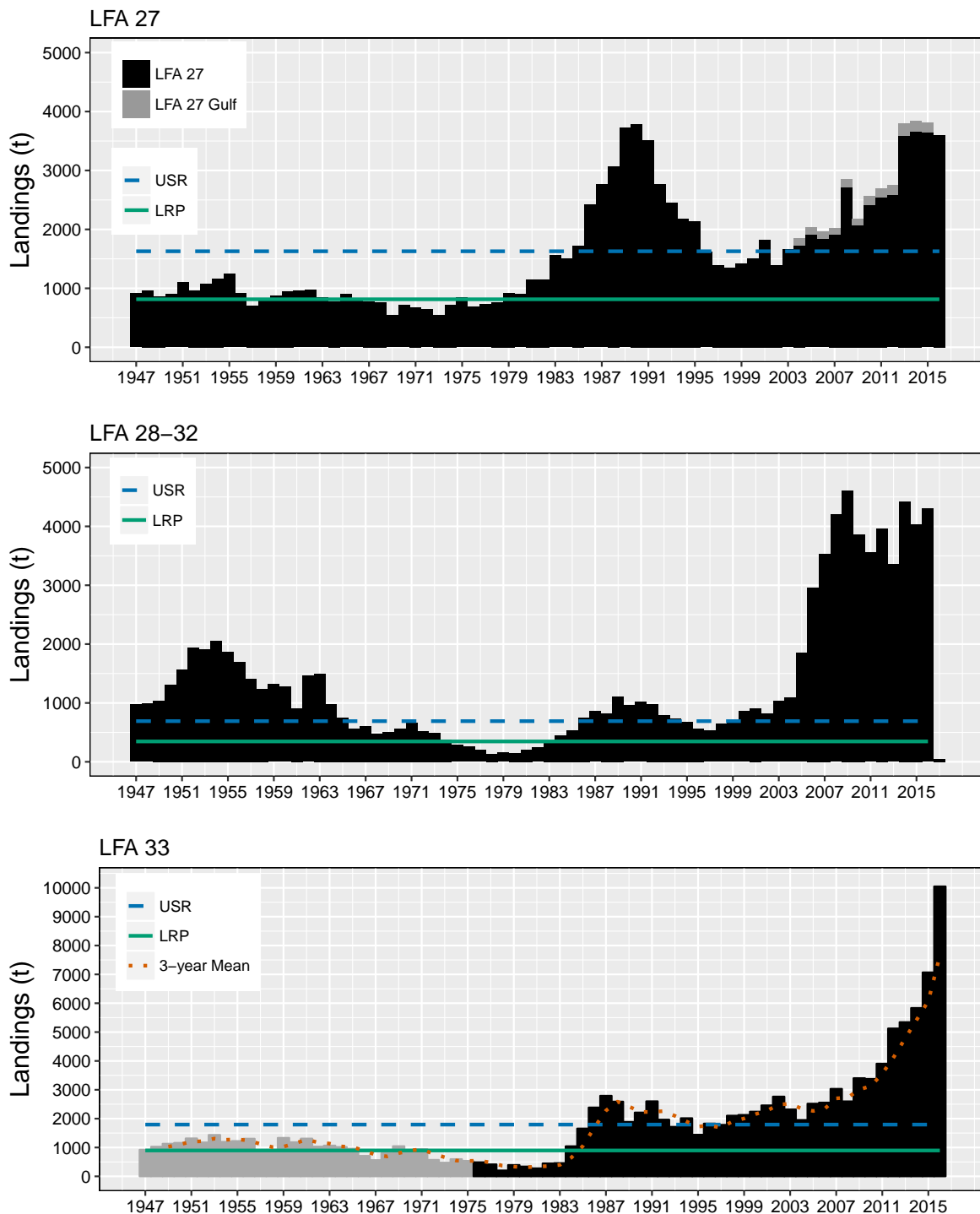


Figure 2: Time series of Lobster landings by LFA.

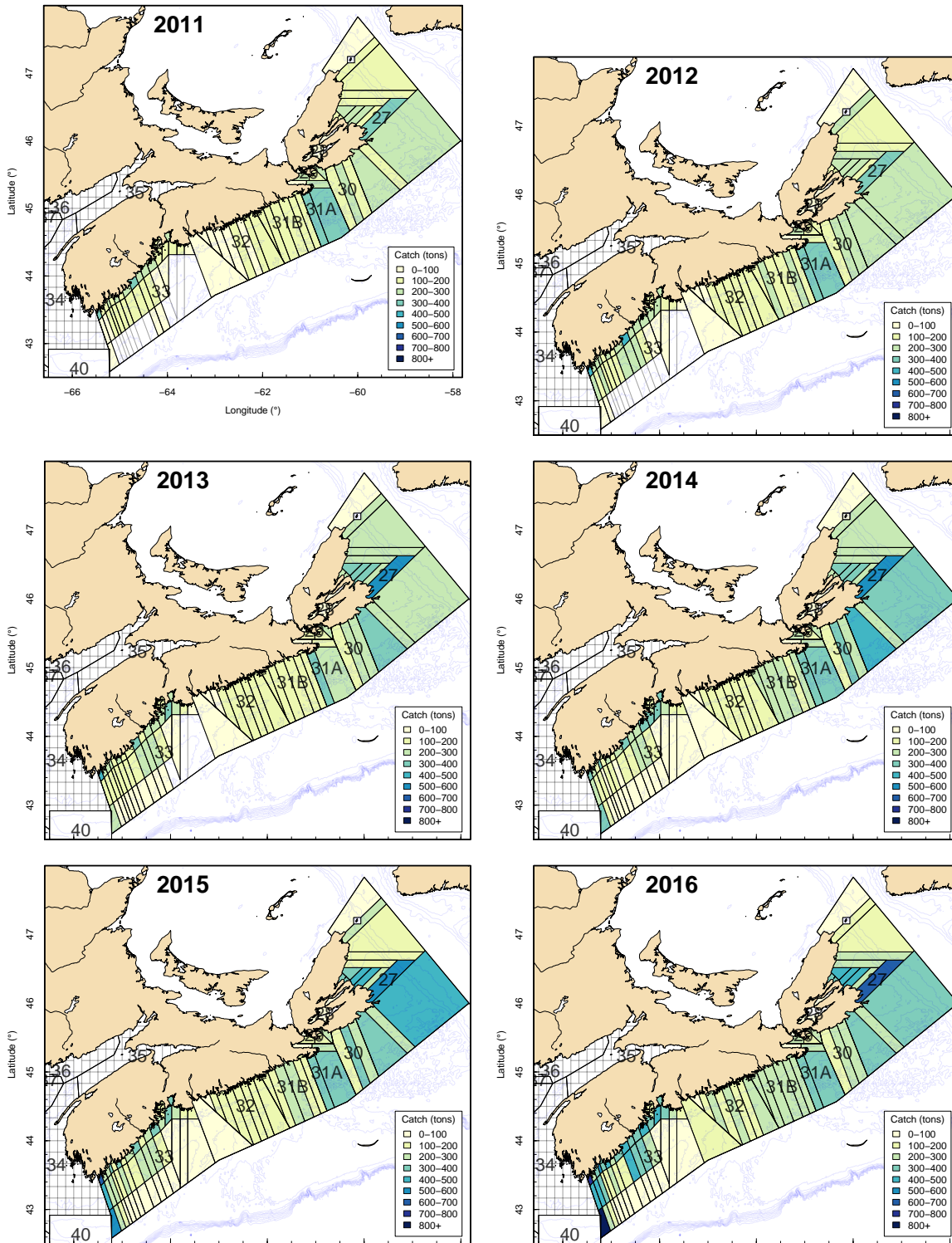


Figure 3: Map of the fishery footprint expressed as the amount of landings in each grid of LFAs 27 - 33 from 2011-2016.

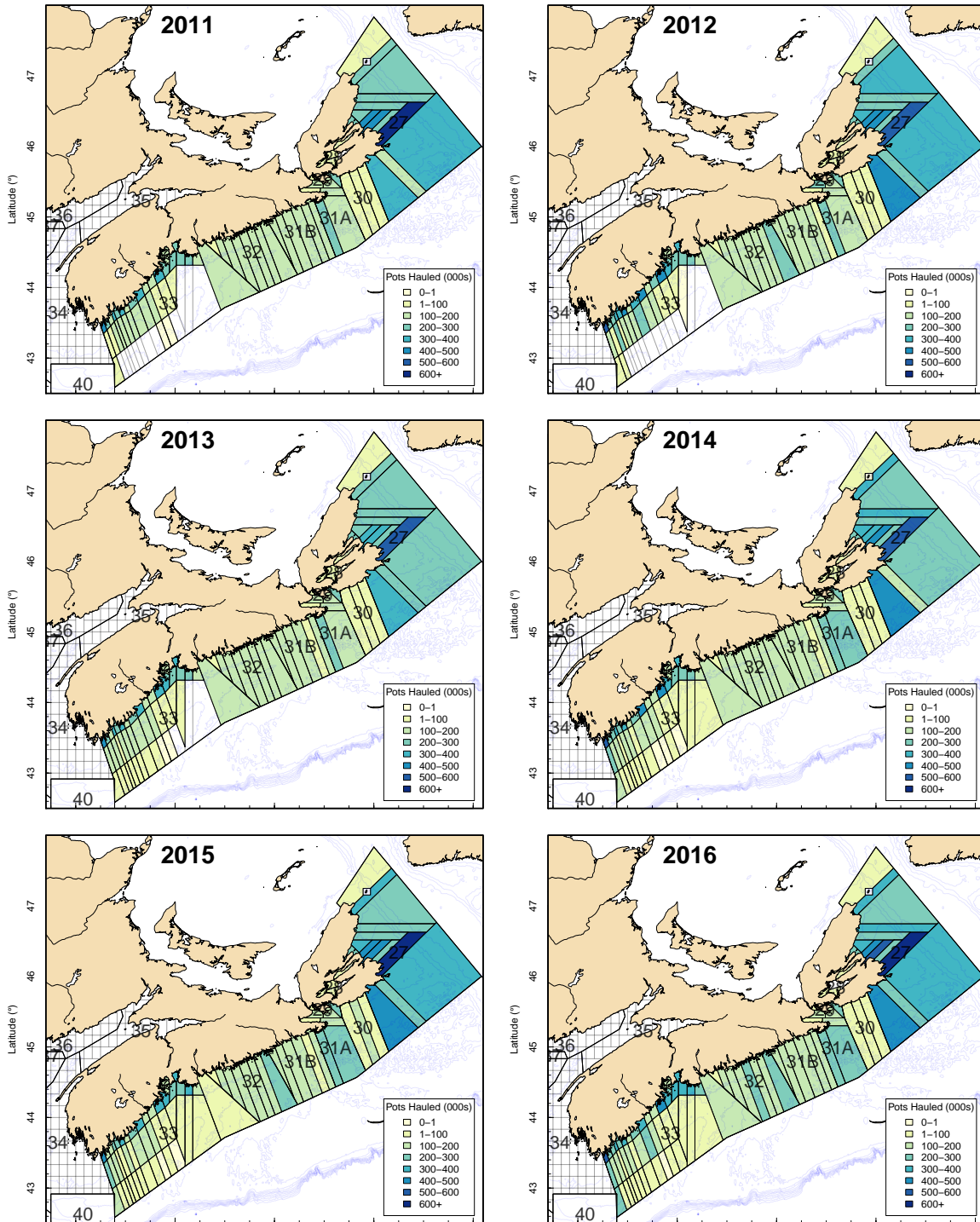


Figure 4: Map of the fishery footprint expressed as the amount of effort in each grid of LFAs 27 - 33 from 2011-2016.

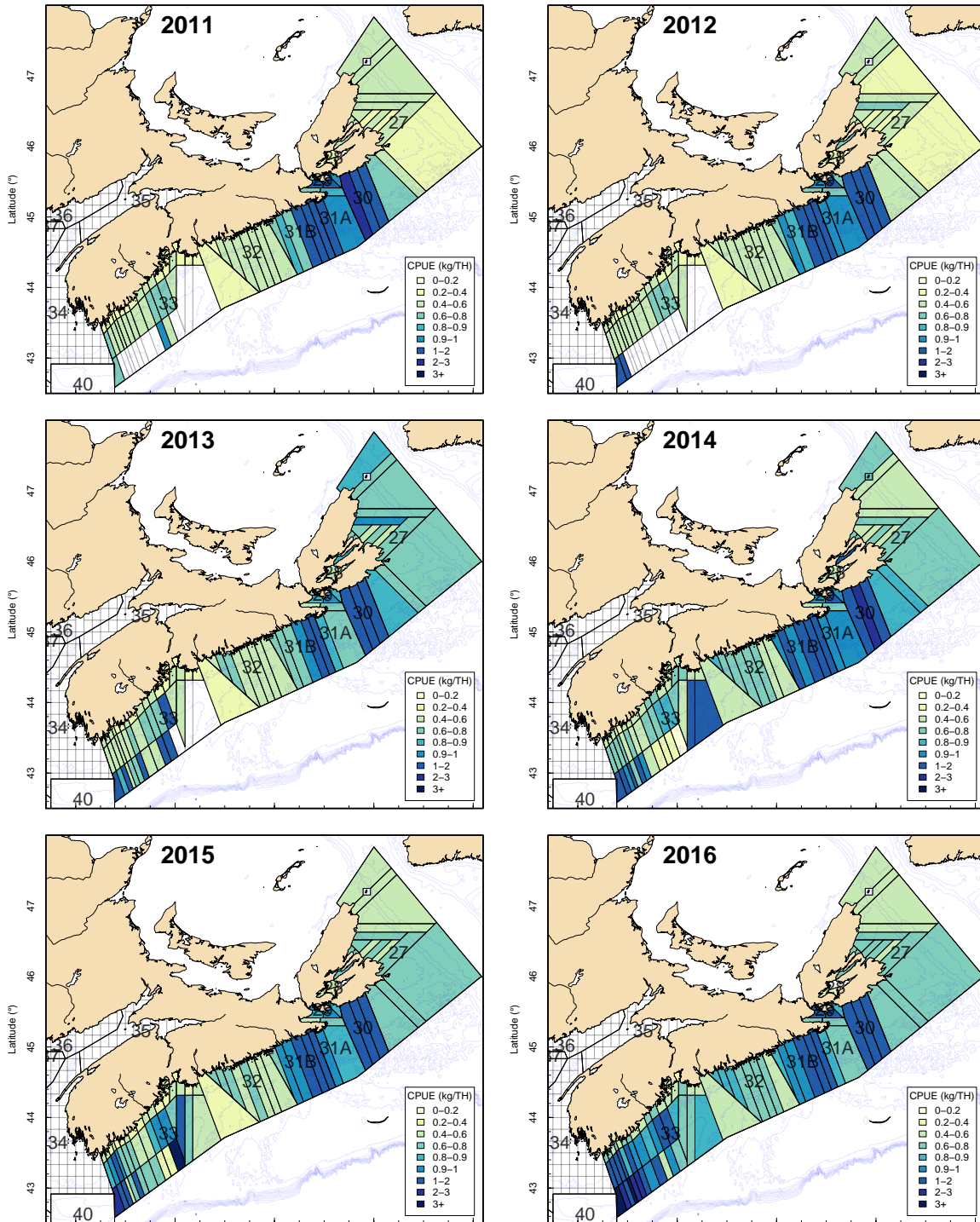


Figure 5: Map of the fishery footprint expressed as the amount of CPUE in each grid of LFAs 27 - 33 from 2011-2016.

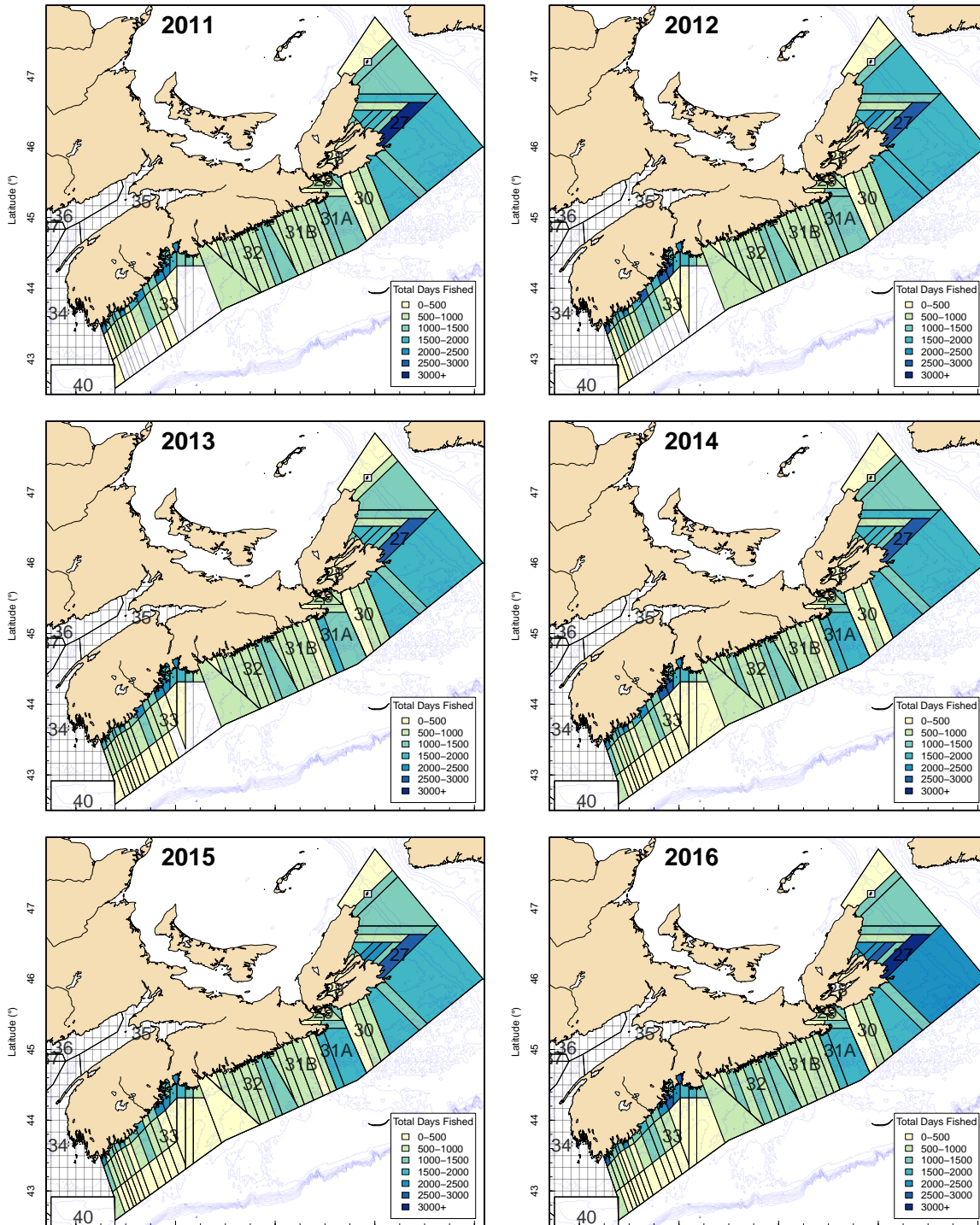


Figure 6: Map of the fishery footprint expressed as the amount of days fished in each grid of LFAs 27 - 33 from 2011-2016.

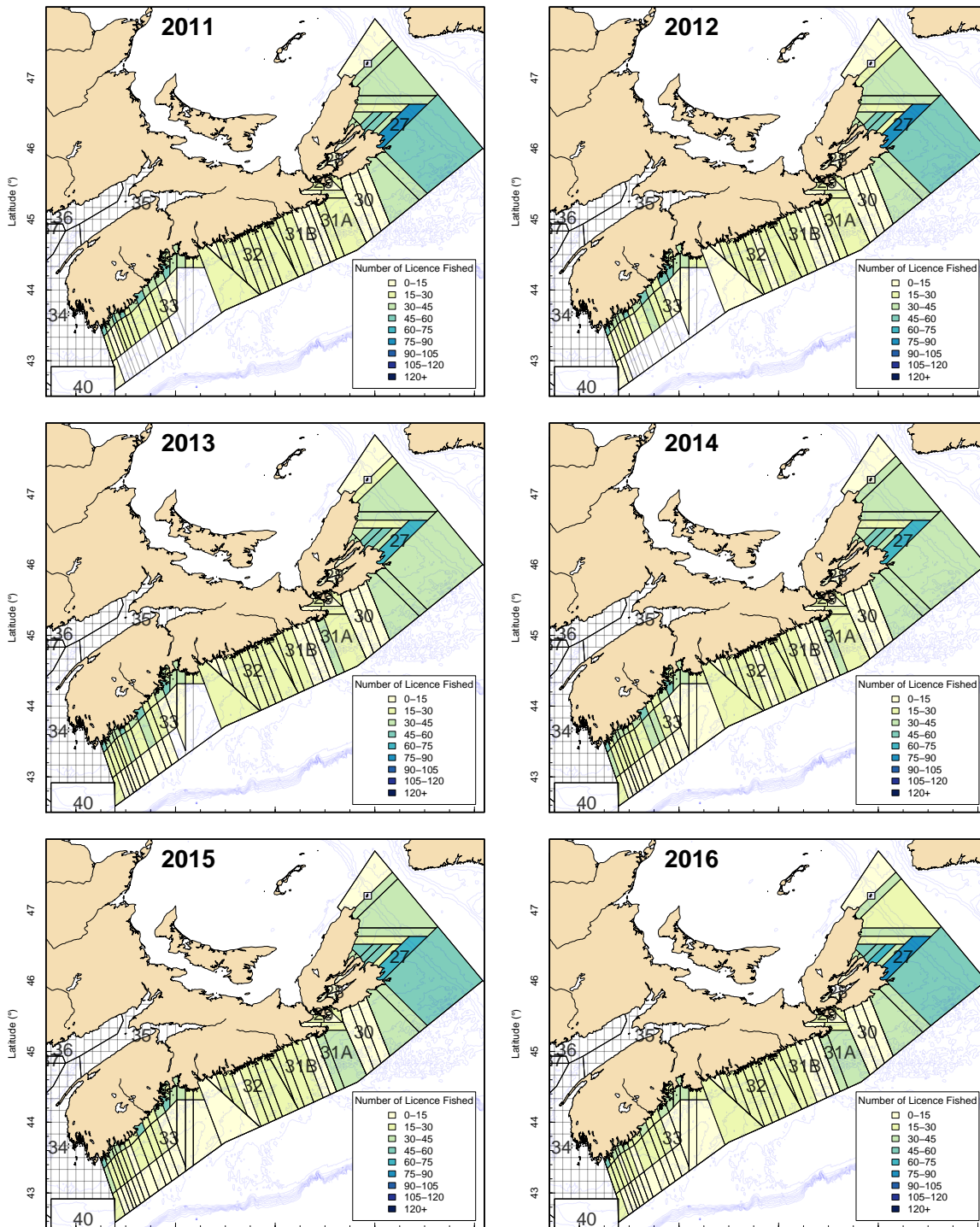


Figure 7: Map of the fishery footprint expressed as the amount of licences in each grid of LFAs 27 - 33 from 2011-2016.

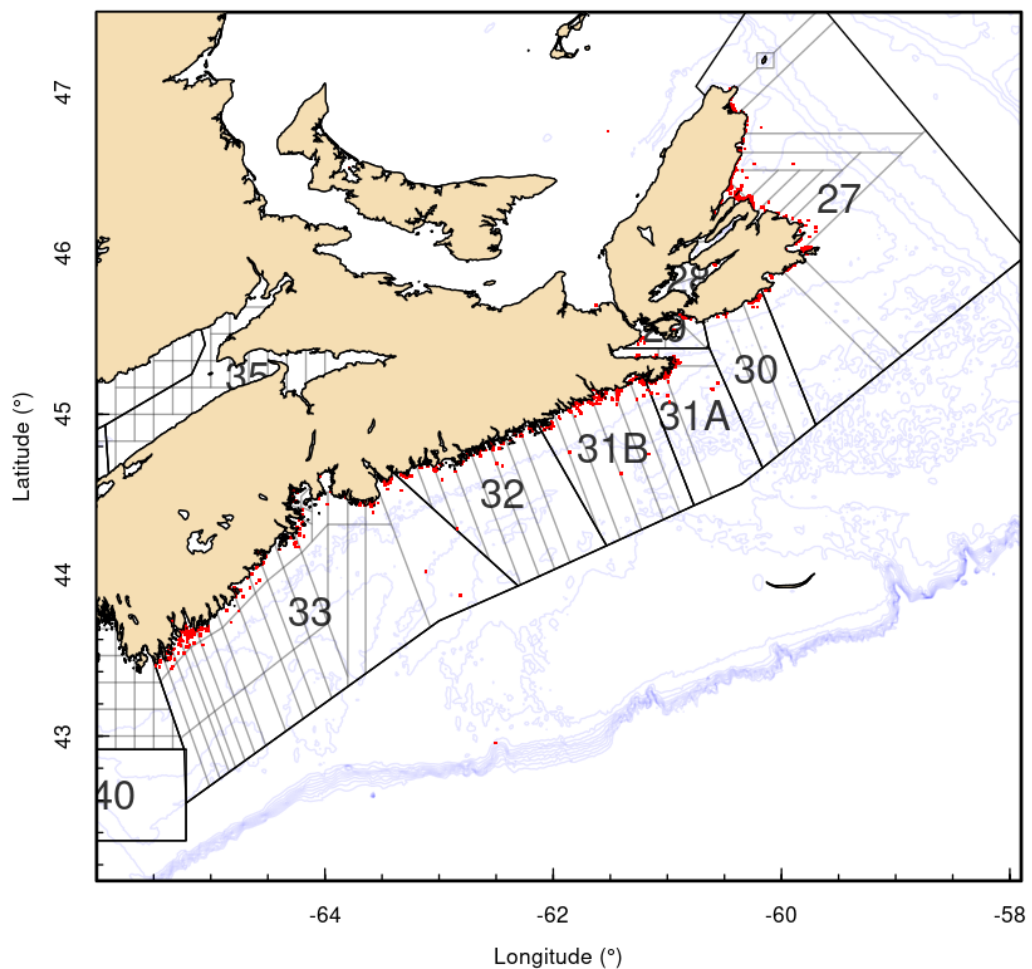


Figure 8: Centroid of the at sea sampling trips across LFA 27-33 bewteen 1977 and current.

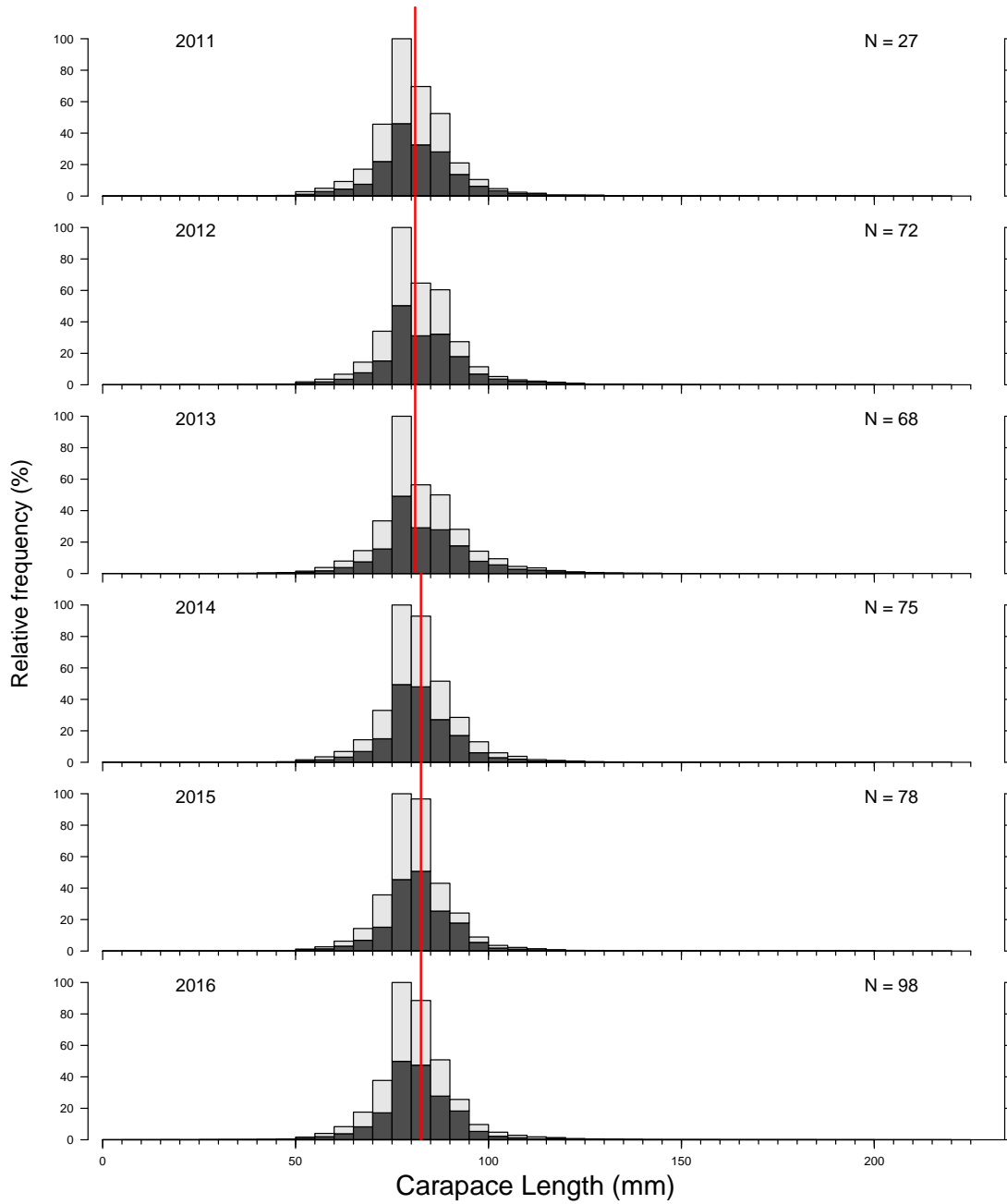


Figure 9: Carapace Length Frequencies from at sea sampling in LFA 27. Dark grey: males, light grey: females, red line: minimum legal size.

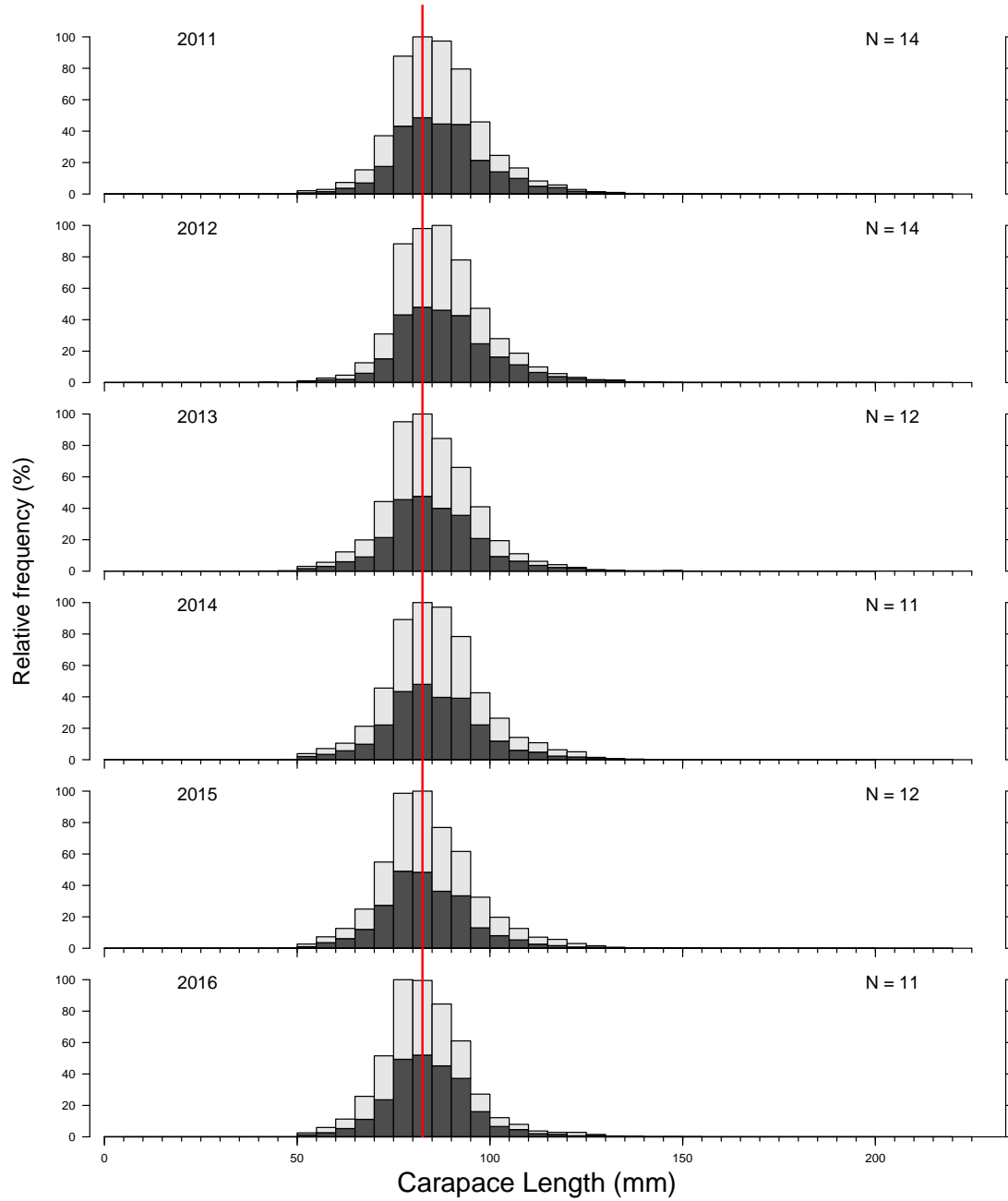


Figure 10: Carapace Length Frequencies from at sea sampling in LFA 31A. Dark grey: males, light grey: females, red line: minimum legal size.

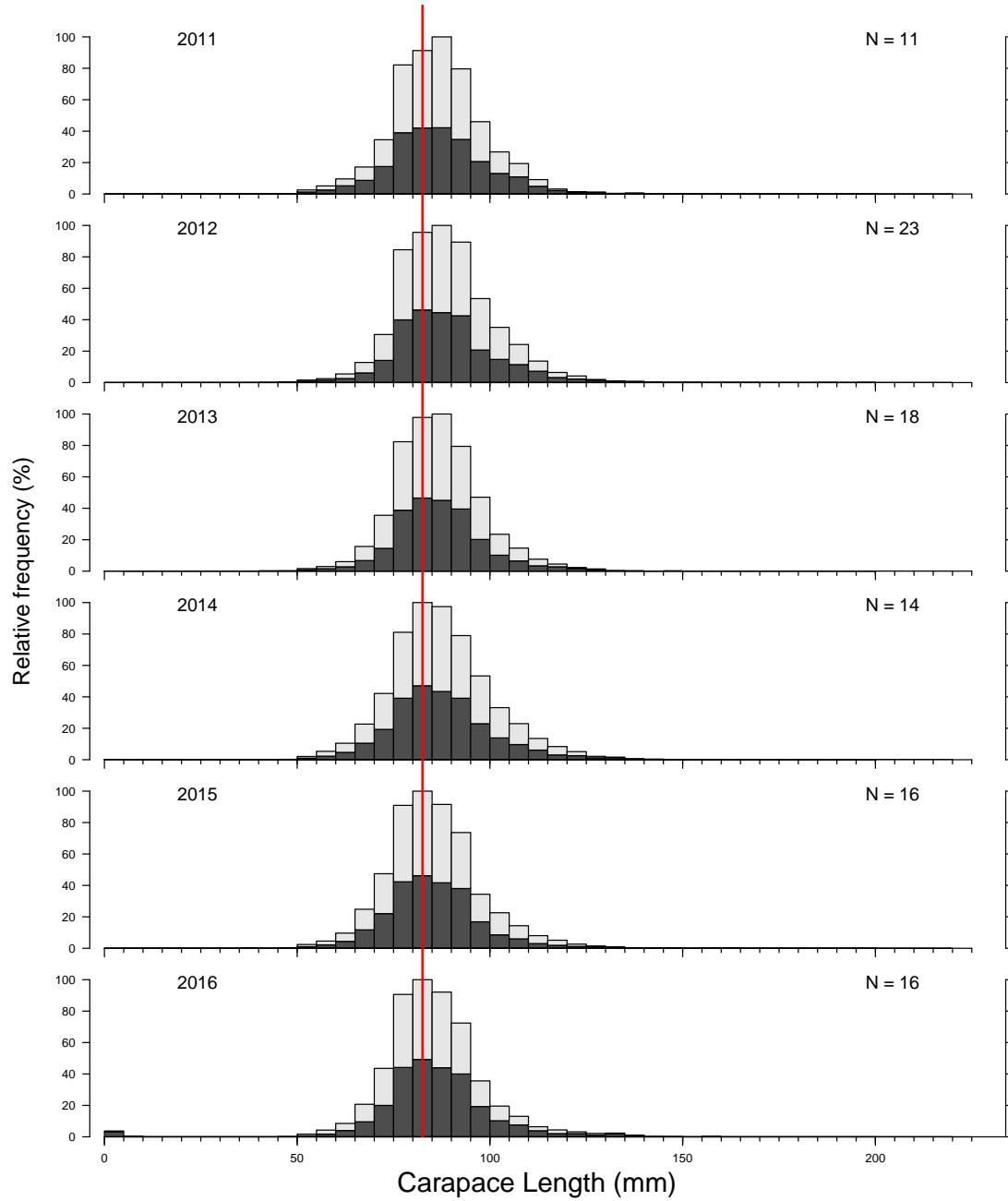


Figure 11: Carapace Length Frequencies from at sea sampling in LFA 31B. Dark grey: males, light grey: females, red line: minimum legal size.

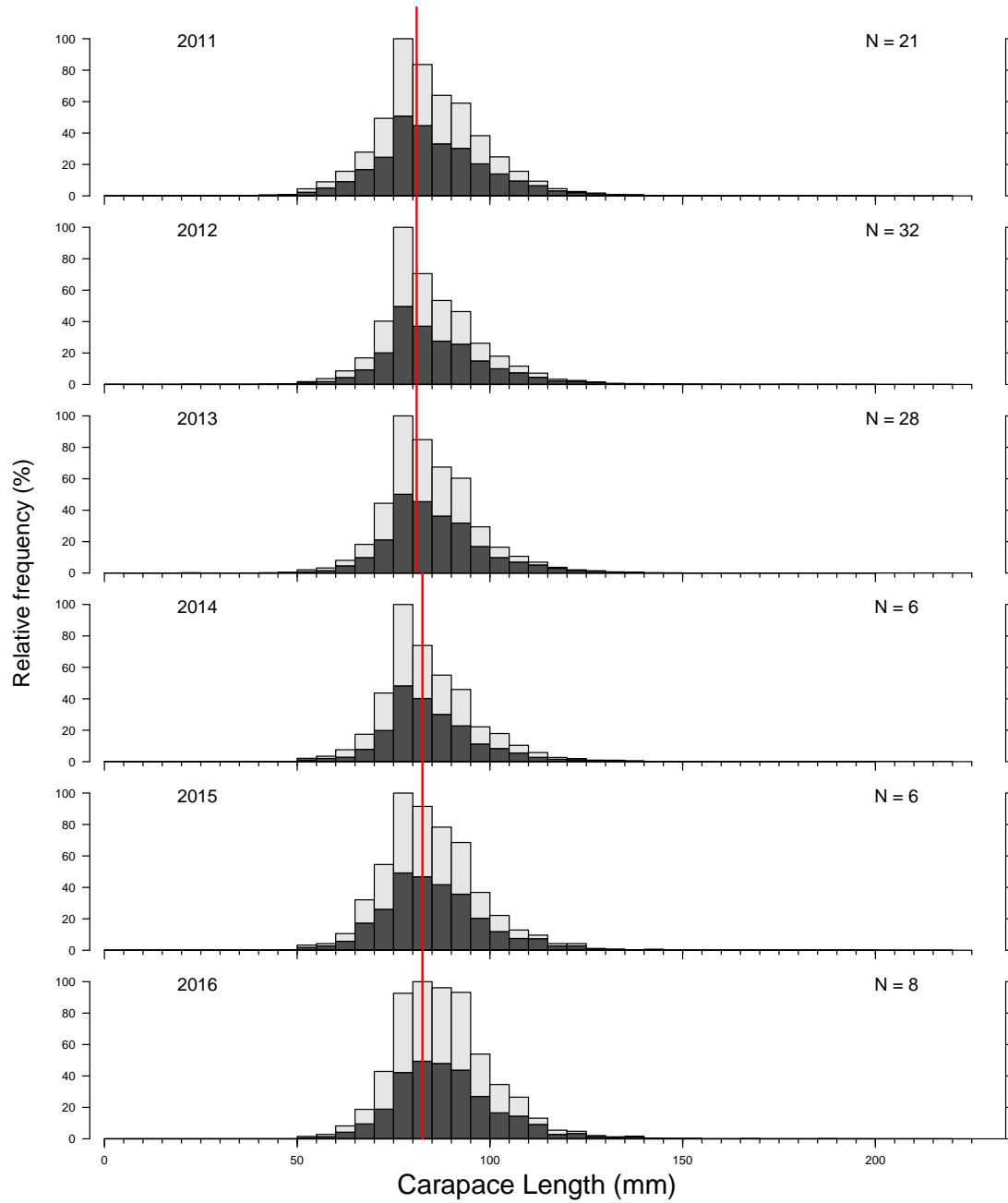


Figure 12: Carapace Length Frequencies from at sea sampling in LFA 32. Dark grey: males, light grey: females, red line: minimum legal size.

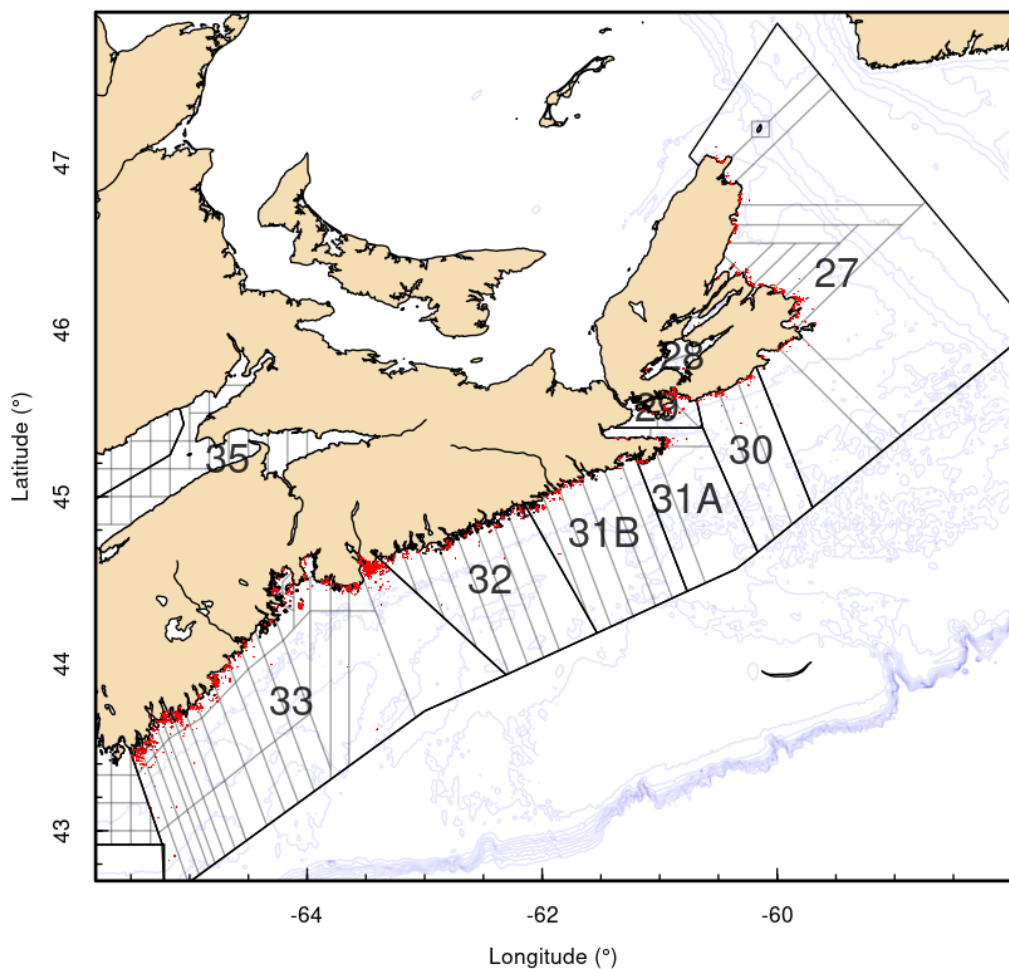


Figure 13: Location of the FSRS recruitment trap samples collected between 2004 and 2017.

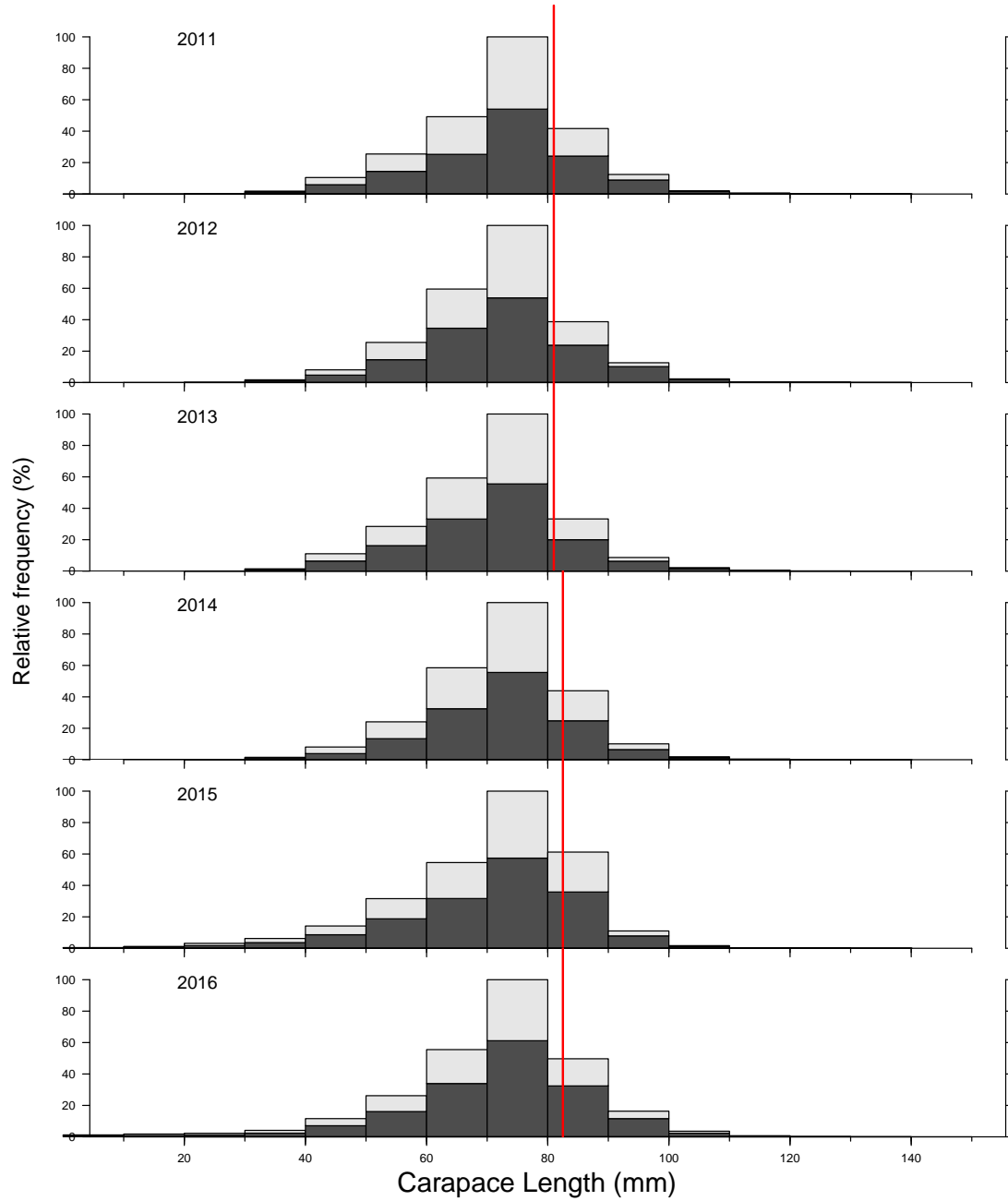


Figure 14: Carapace Length Frequencies from FSRS recruitment traps in LFA 27. Dark grey: males, light grey: females, red line: minimum legal size.

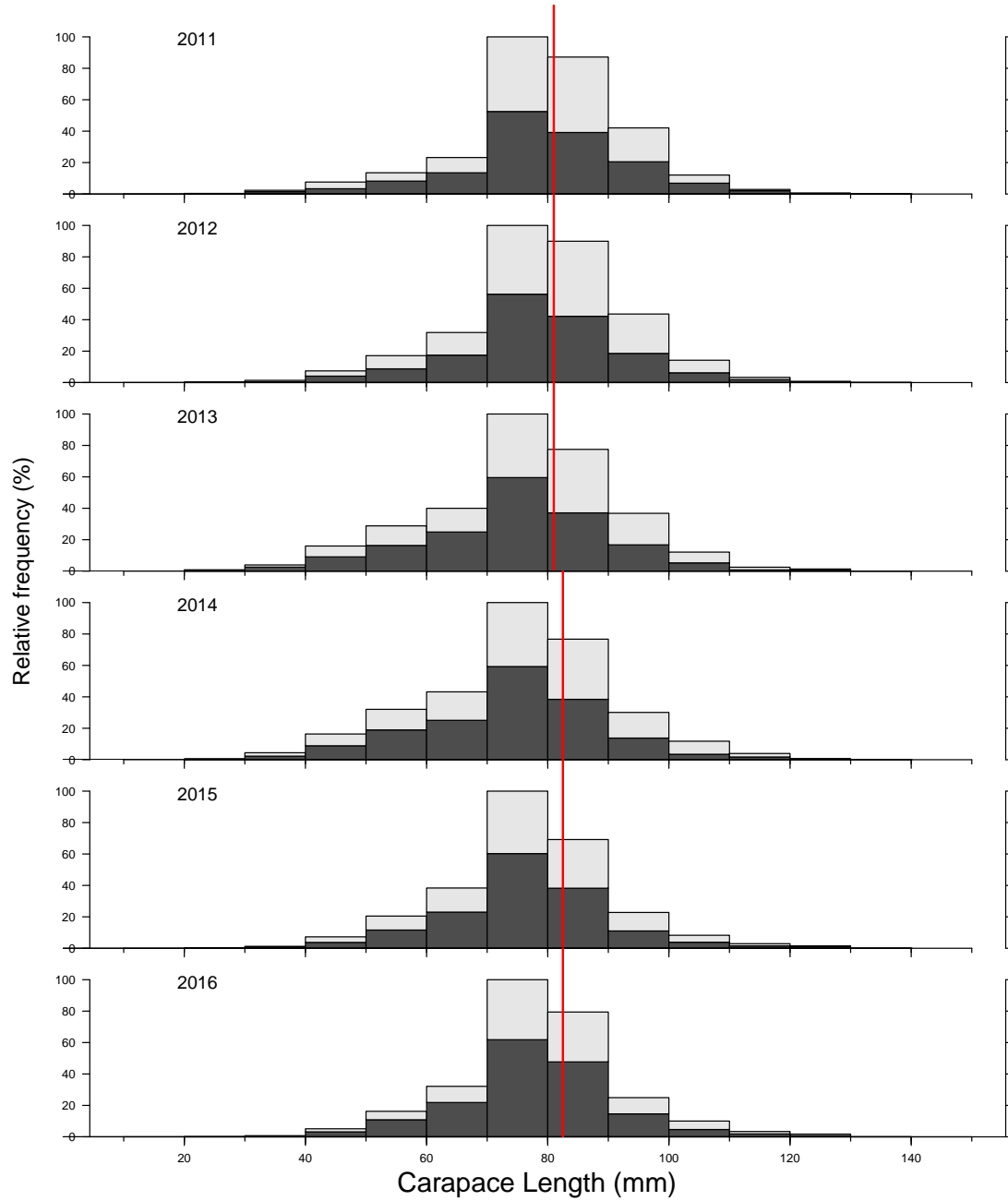


Figure 15: Carapace Length Frequencies from FSRS recruitment traps in LFA 29. Dark grey: males, light grey: females, red line: minimum legal size.

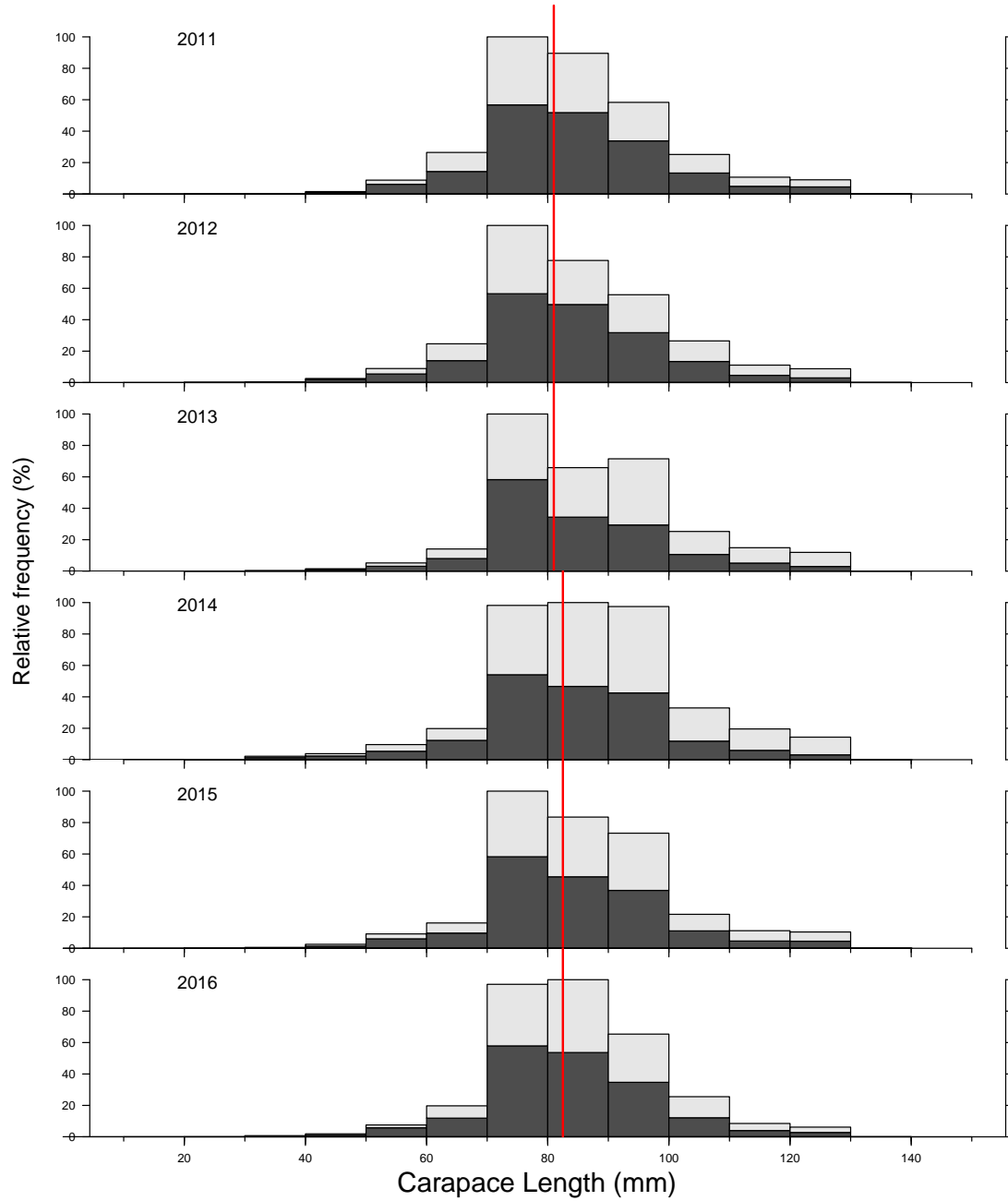


Figure 16: Carapace Length Frequencies from FSRS recruitment traps in LFA 30. Dark grey: males, light grey: females, red line: minimum legal size.

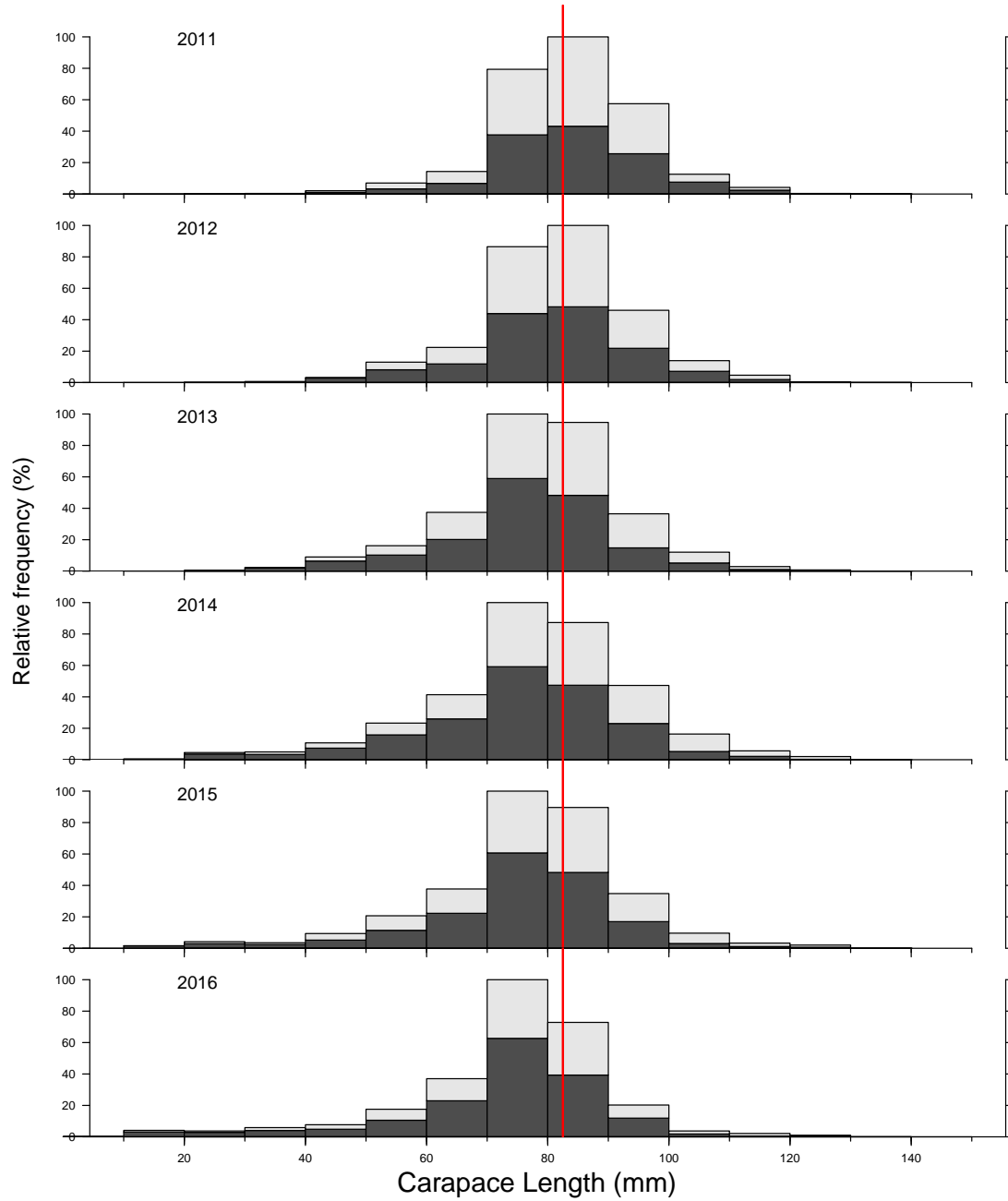


Figure 17: Carapace Length Frequencies from at FSRS recruitment traps in LFA 31A. Dark grey: males, light grey: females, red line: minimum legal size.

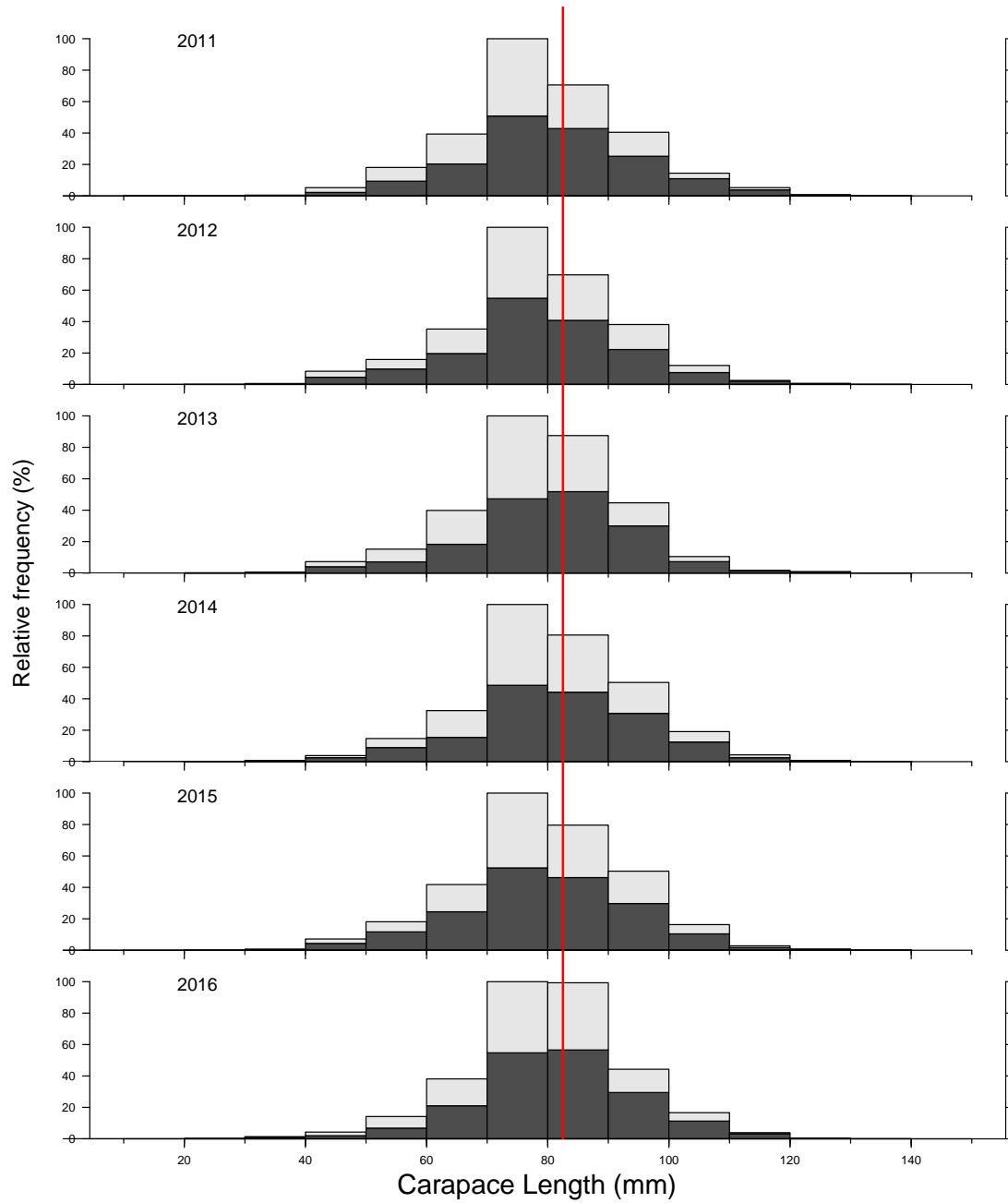


Figure 18: Carapace Length Frequencies from at FSRS recruitment traps in LFA 31B. Dark grey: males, light grey: females, red line: minimum legal size.

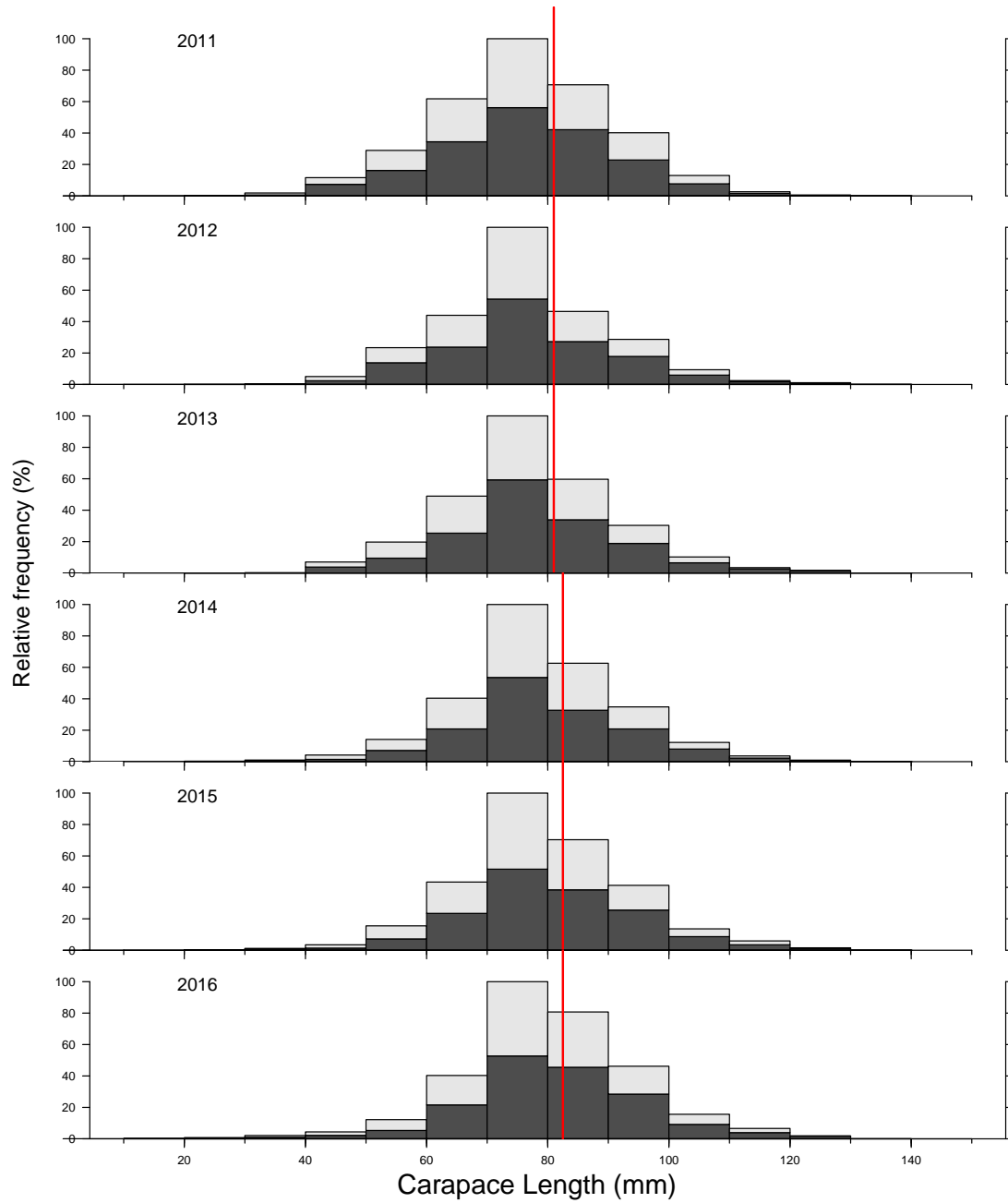


Figure 19: Carapace Length Frequencies from FSRS recruitment traps in LFA 32. Dark grey: males, light grey: females, red line: minimum legal size.

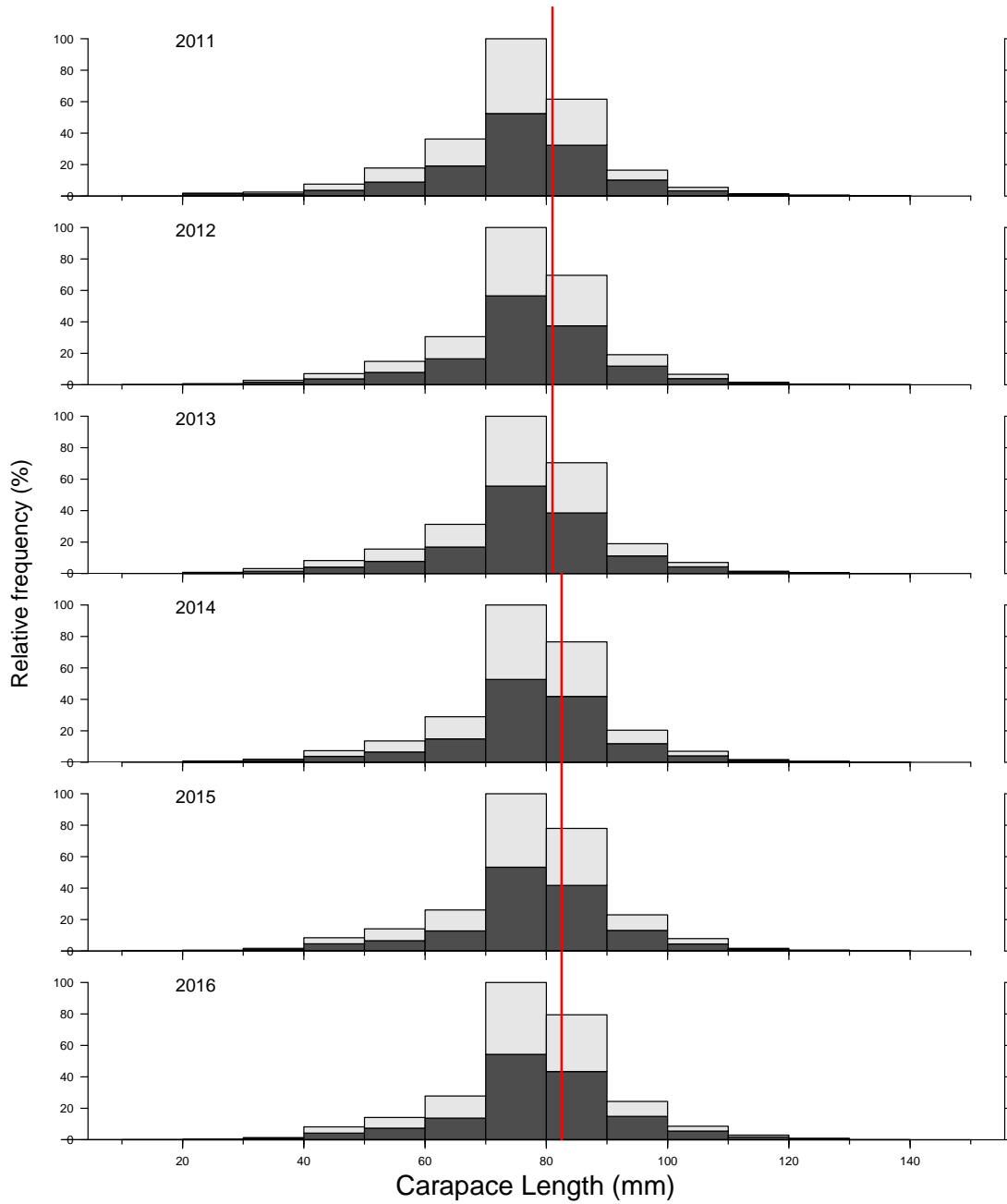


Figure 20: Carapace Length Frequencies from FSRS recruitment traps in LFA 33. Dark grey: males, light grey: females, red line: minimum legal size.

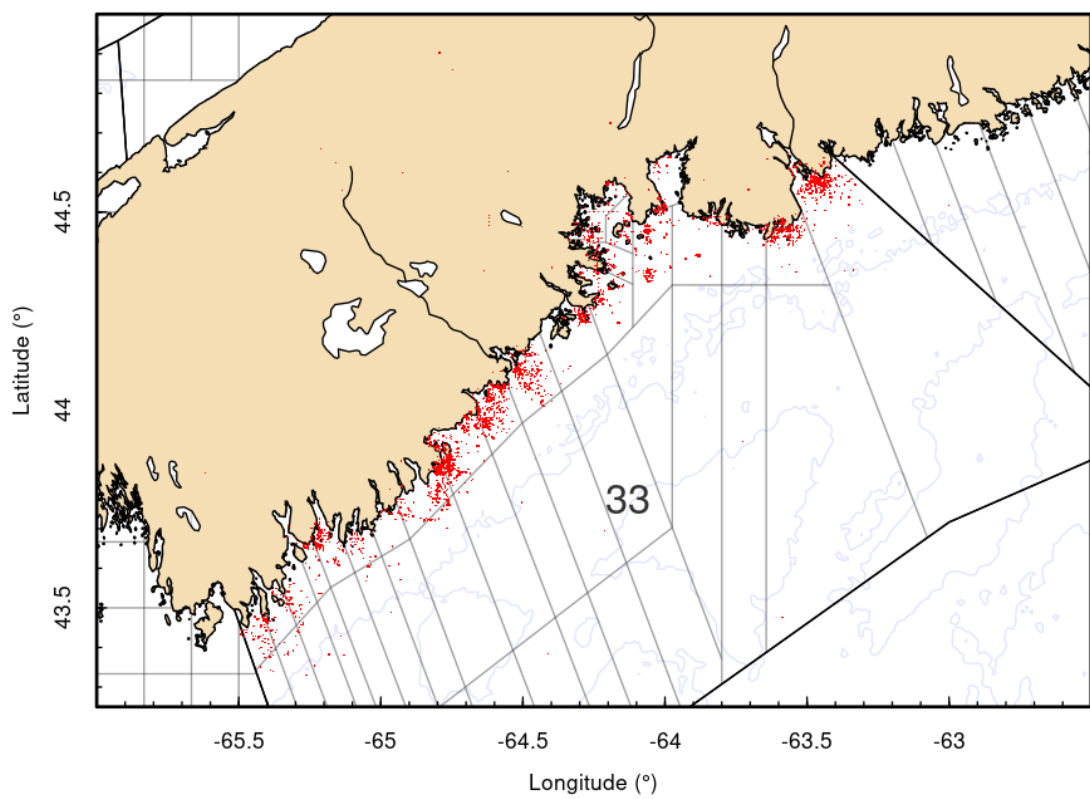


Figure 21: Location of the FSRS commercial trap samples collected between 2004 and 2017.

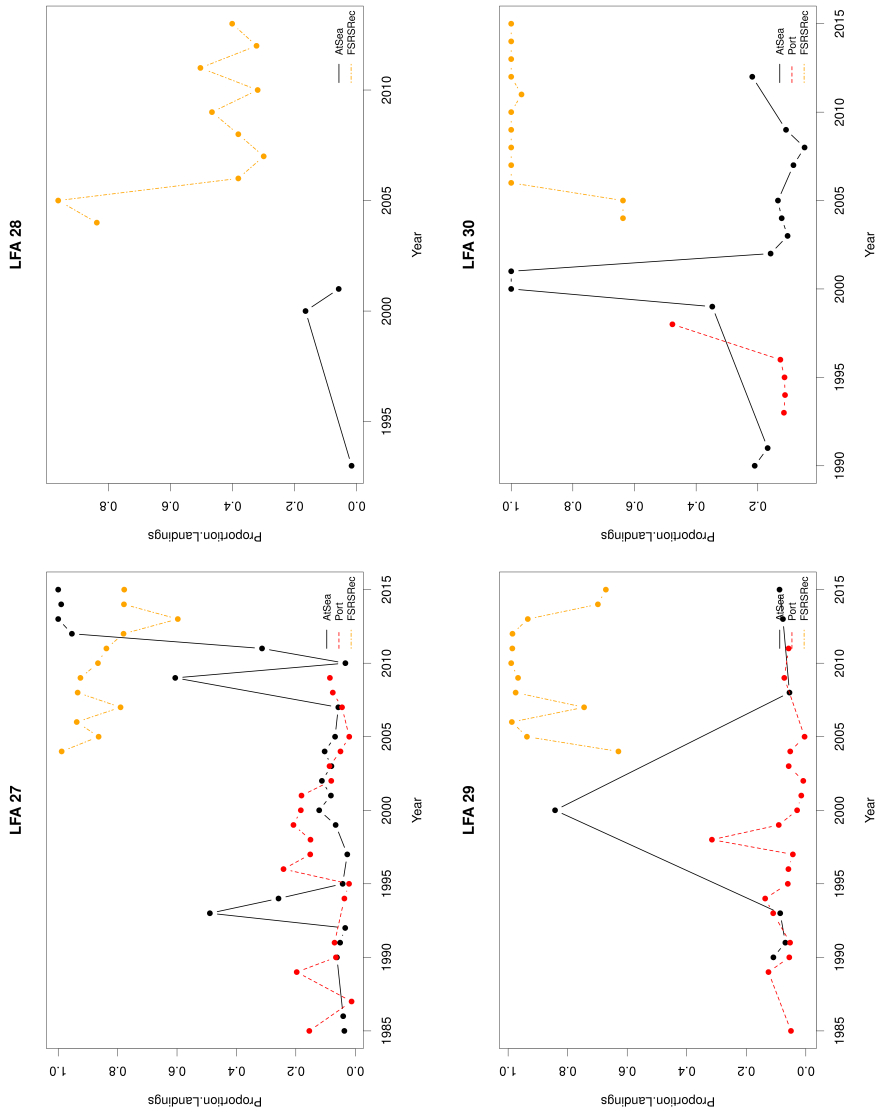


Figure 22: Estimated proportion of the week of season x area (grid or port) landings accounted for by the different biological sampling methods.

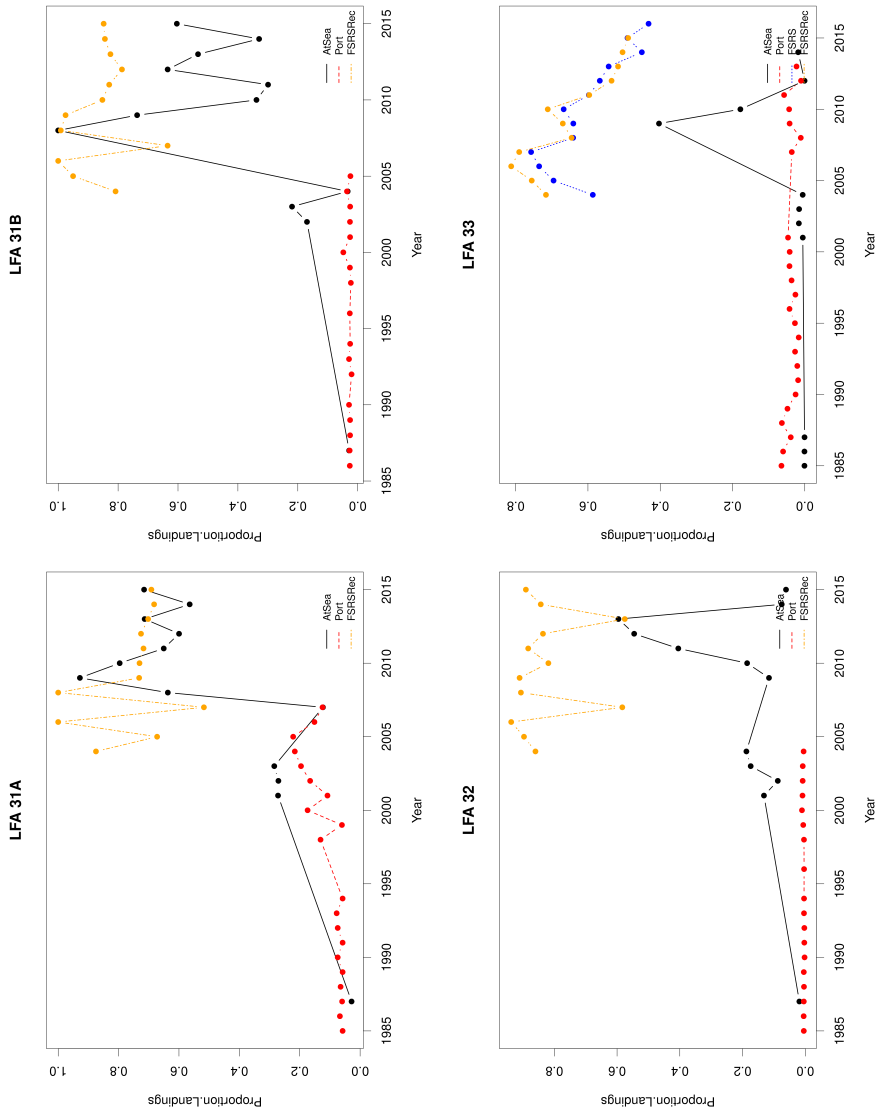


Figure 23: Estimated proportion of the week of season x area (grid or port) landings accounted for by the different biological sampling methods.

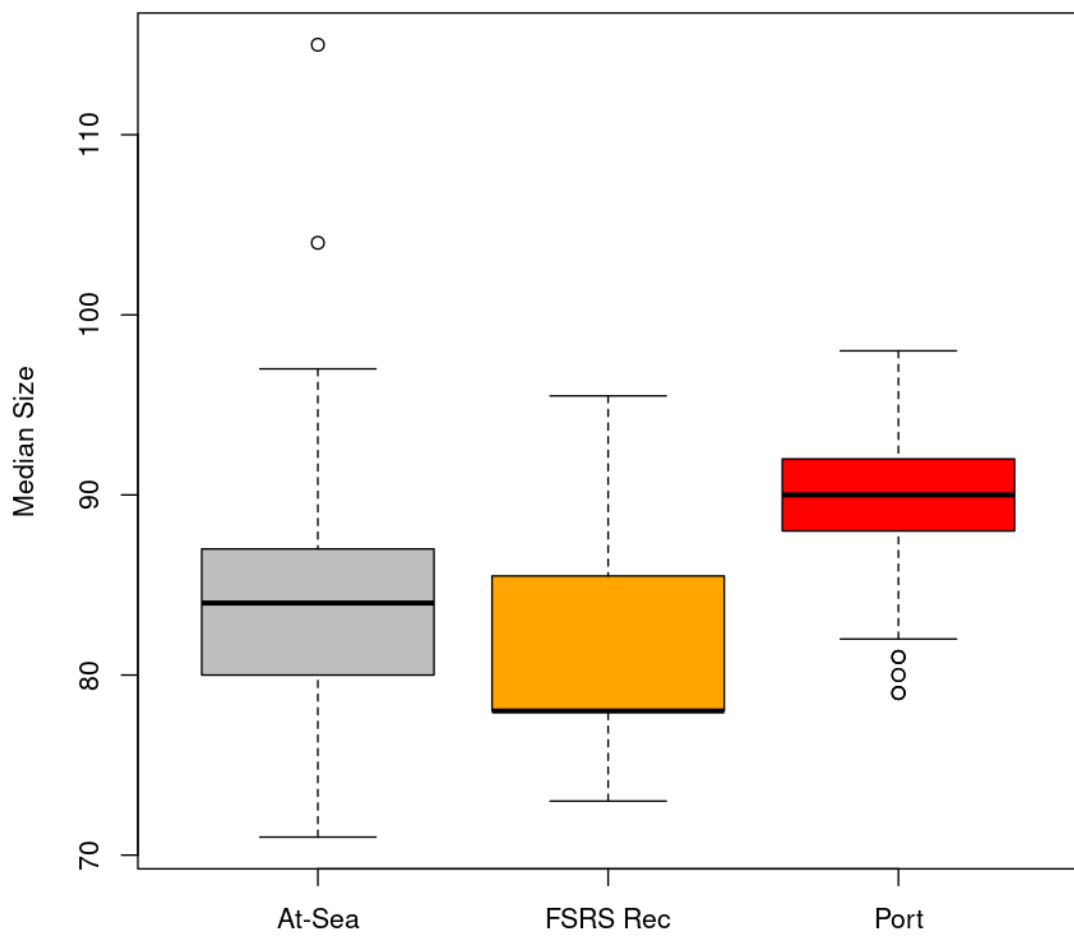


Figure 24: Boxplot of the combined estimates of median size by data source.

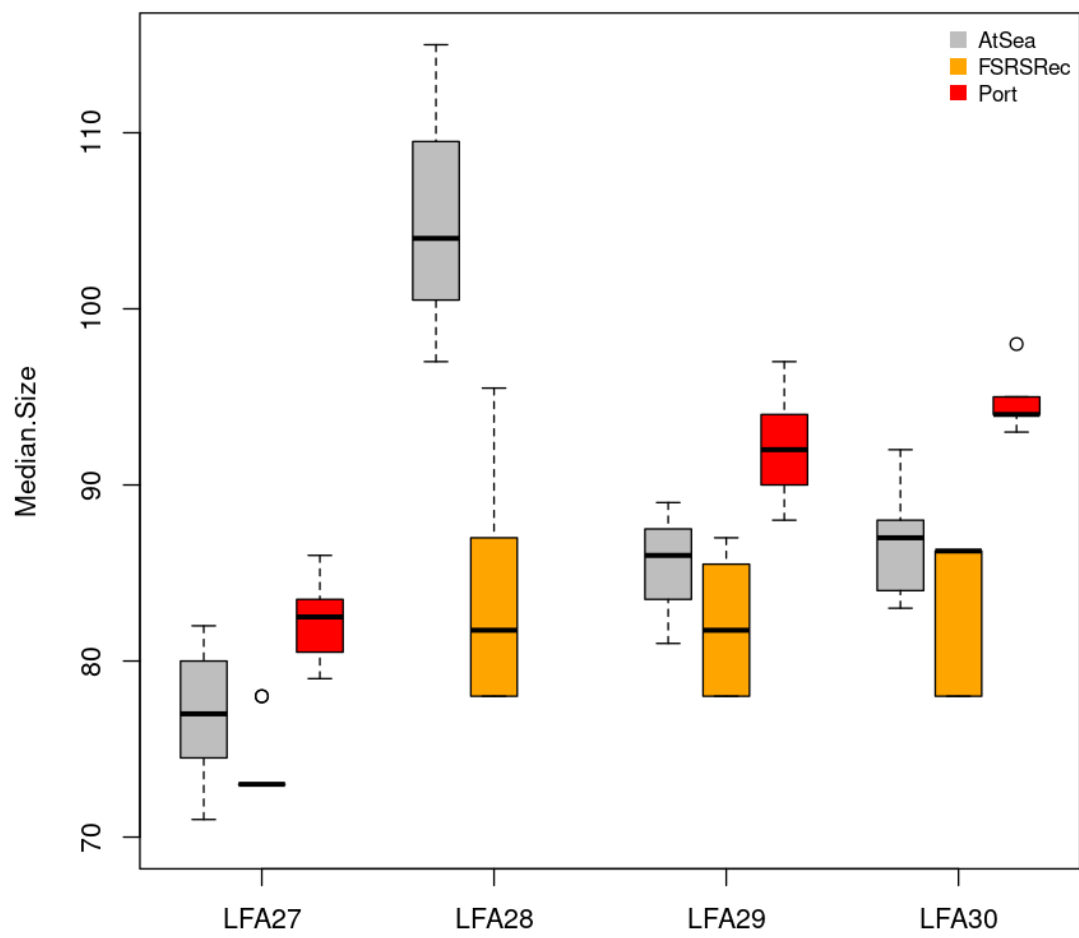


Figure 25: Boxplot of the annual estimates of median size by data source for LFA 27-30.

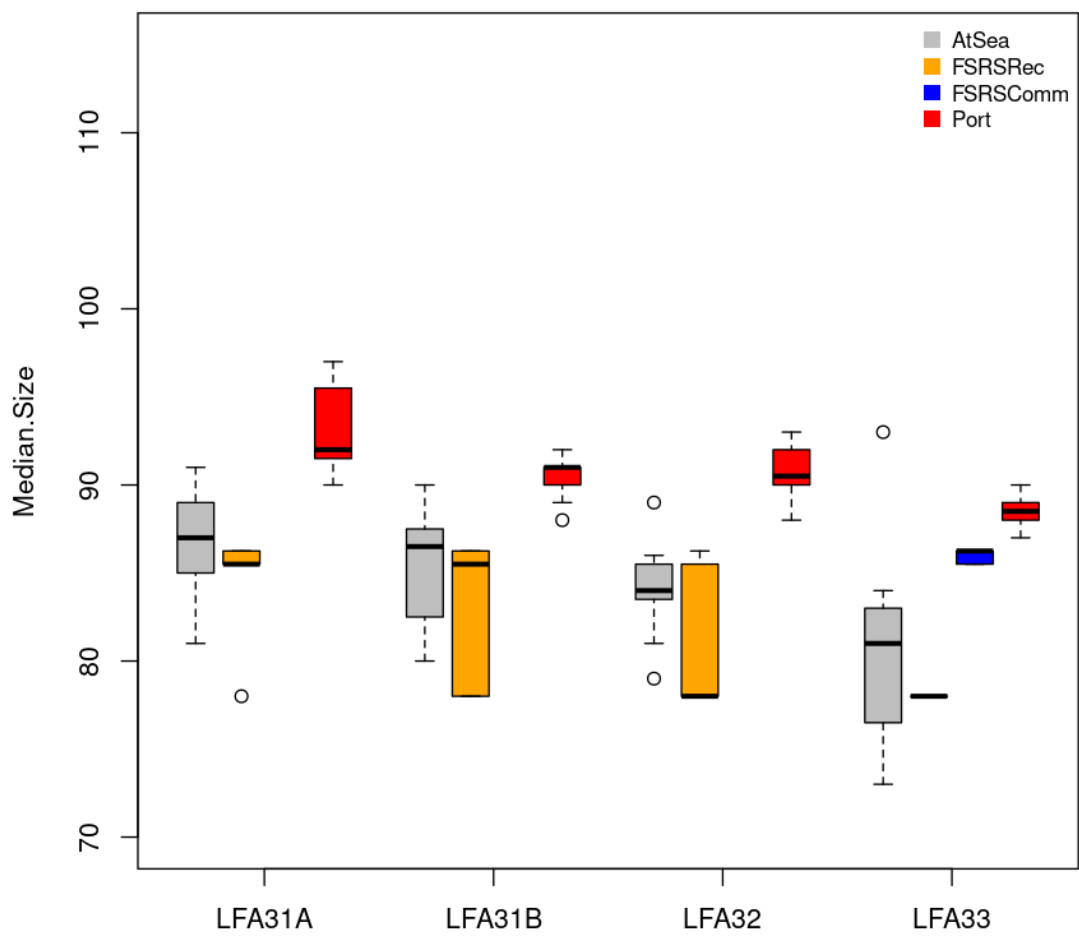


Figure 26: Boxplot of the annual estimates of median sizes by data source for LFA 31A-33.

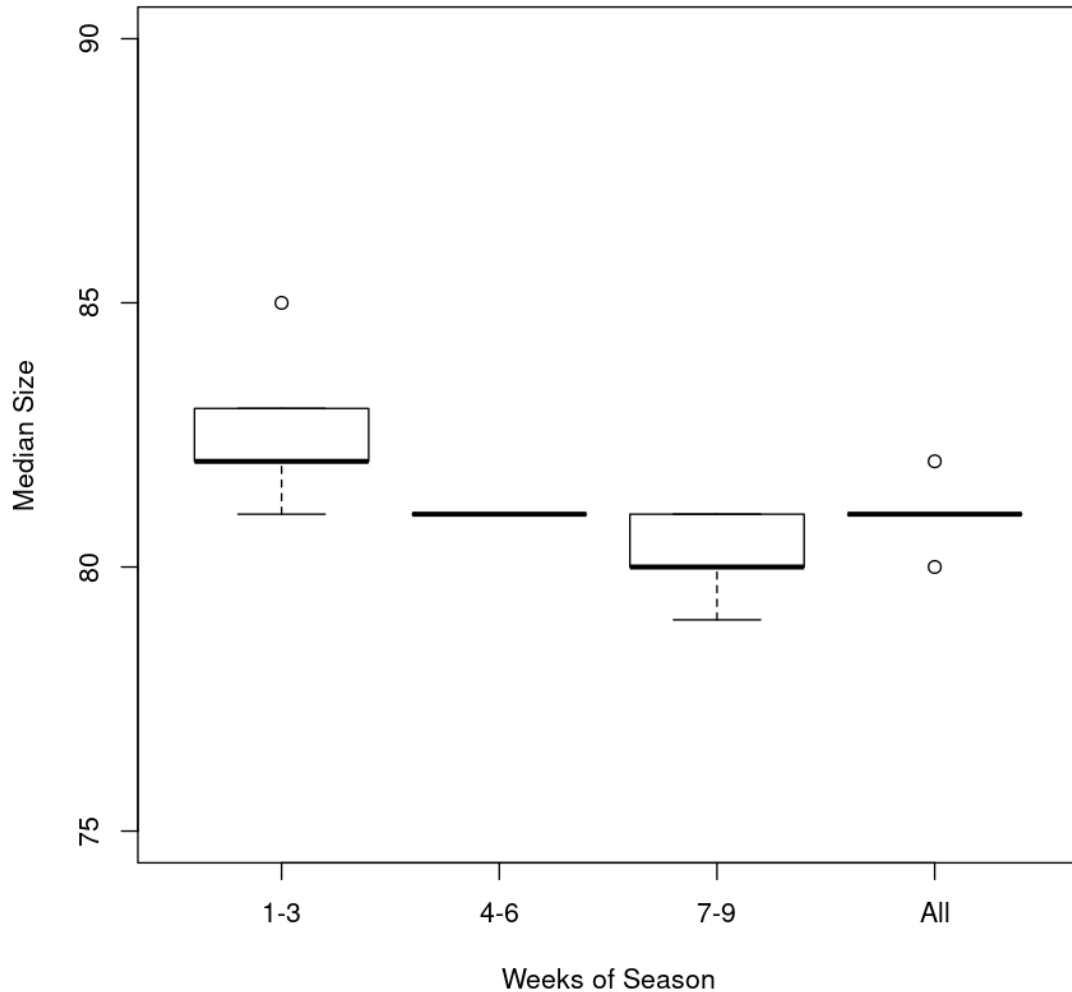


Figure 27: Boxplots of estimated median carapace length from sea sampling dates (weeks of season) observed from LFA 27 during the 2011-2015 seasons.

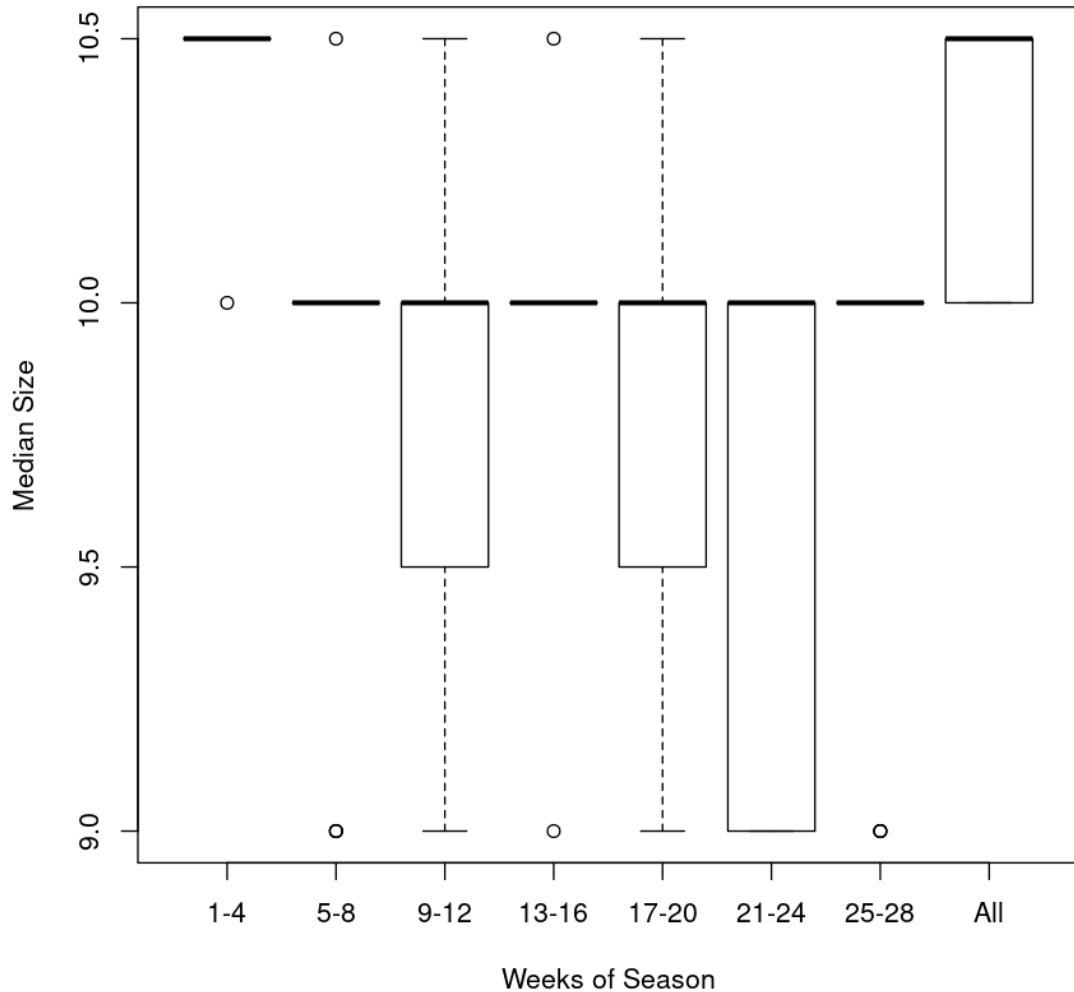


Figure 28: Boxplots of estimated median carapace length from FSRS commercial sampling dates (weeks of season) observed from LFA 33 during the 2004-2016 seasons.

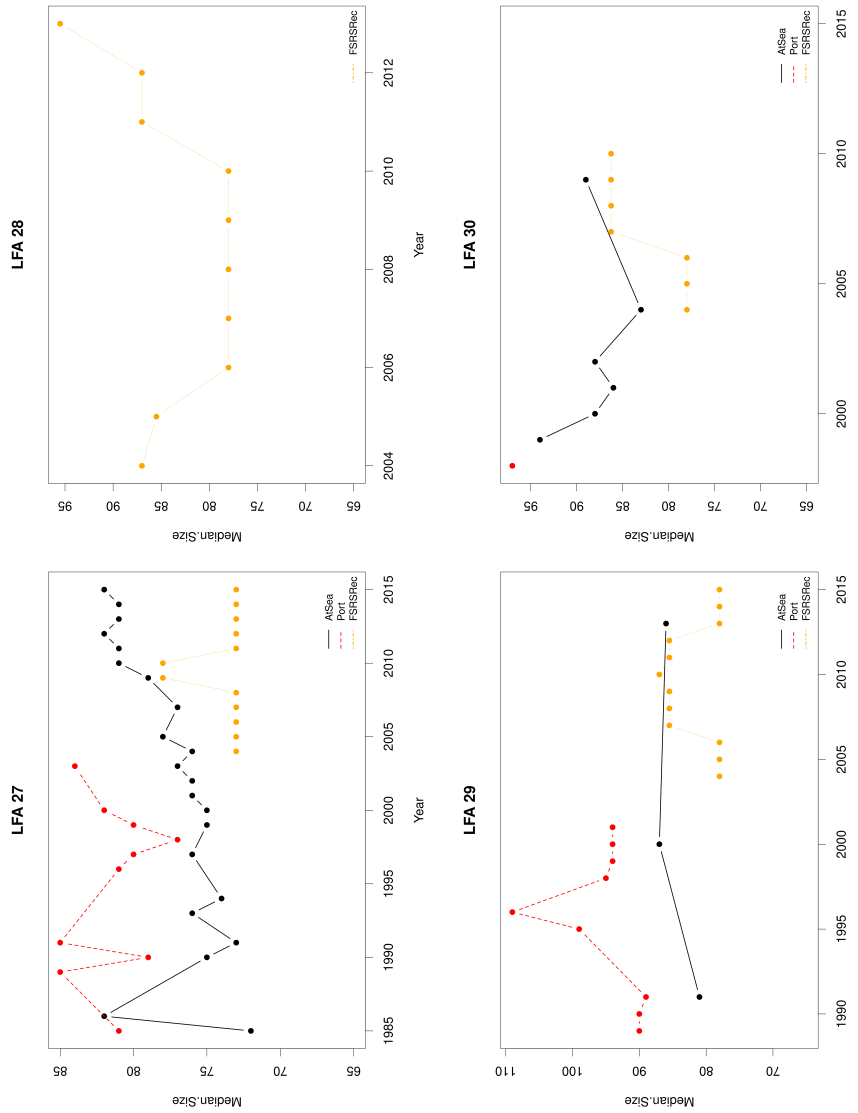


Figure 29: Estimated median carapace length of lobster samples taken from at sea samples, port samples, and / or the FSRS recruitment trap project. Median sizes from FSRS recruitment traps represent the center of the size bin converted to mm from the gauge used to measure carapace length of lobsters. Results represent mid-season samples only.

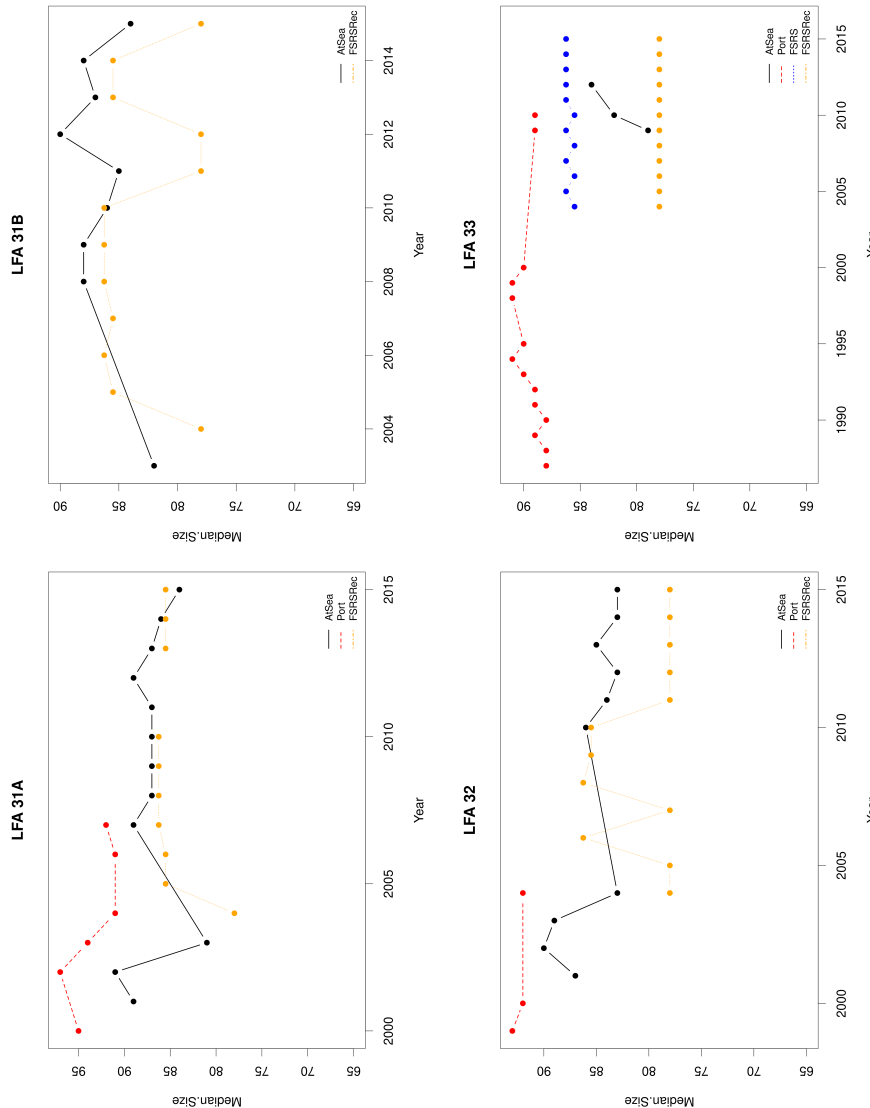


Figure 30: Estimated median carapace length of lobster samples taken from at sea samples, port samples, and / or the FSRS recruitment trap project. Median sizes from FSRS recruitment or commercial traps represent the center of the size bin converted to mm from the gauge used to measure carapace length of lobsters. Results represent mid-season samples only

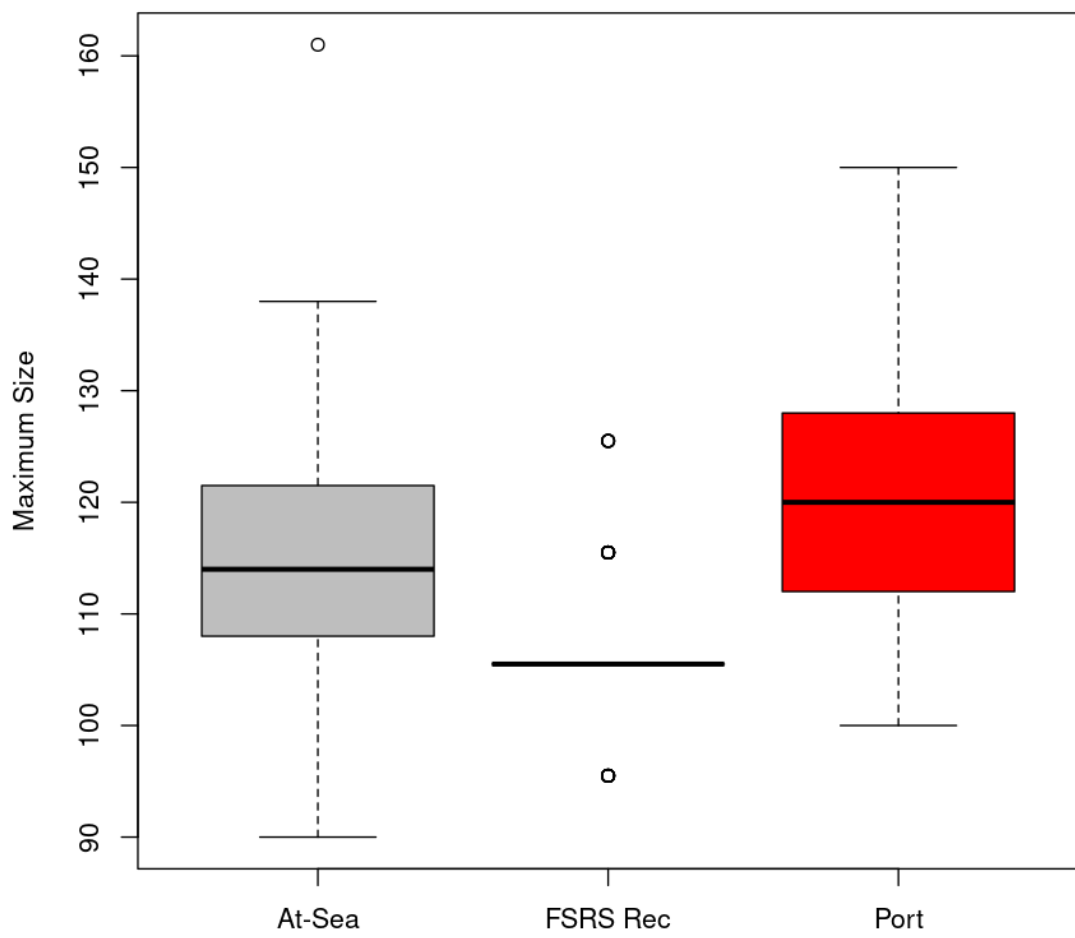


Figure 31: Boxplot of the combined estimates of maximum sizes by data source.

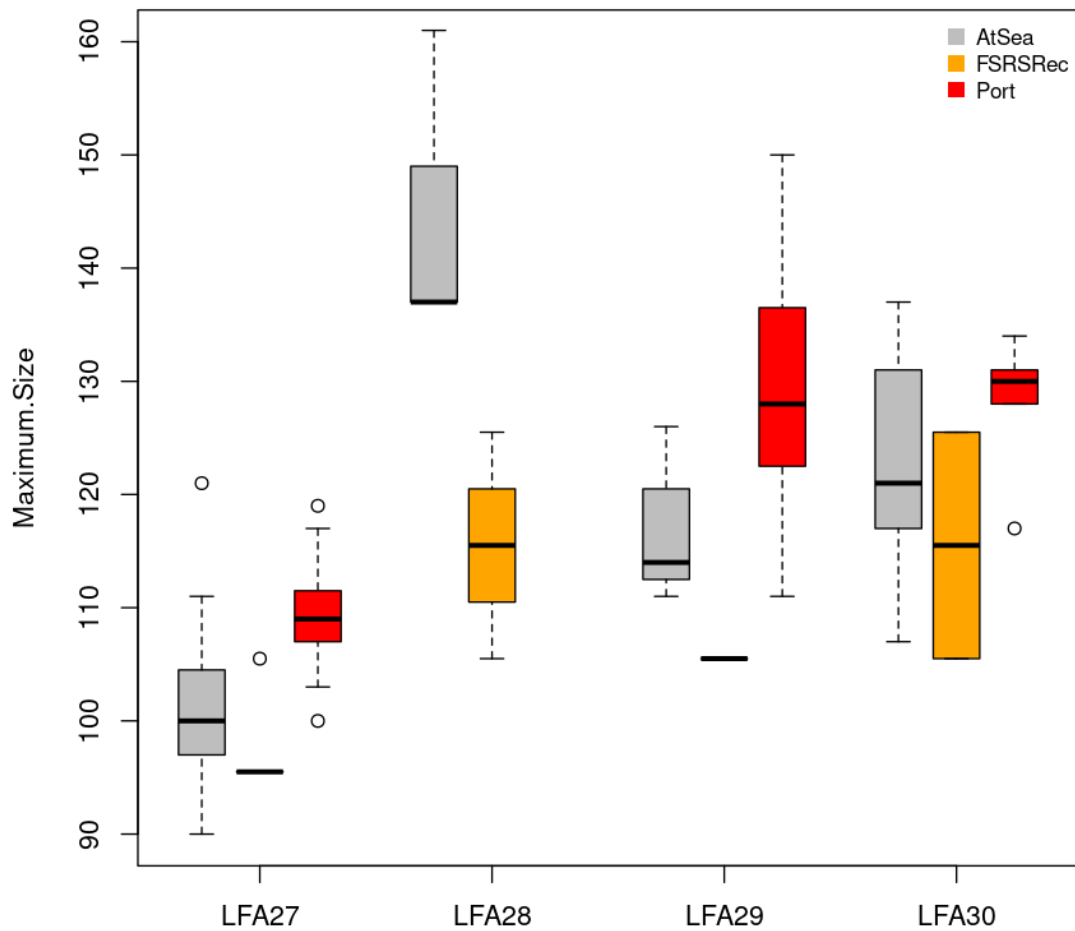


Figure 32: Boxplot of the annual estimates of maximum sizes by data source for LFA 27-30. Within LFAs FSRS samples where maximum size was in the largest size category were not included.

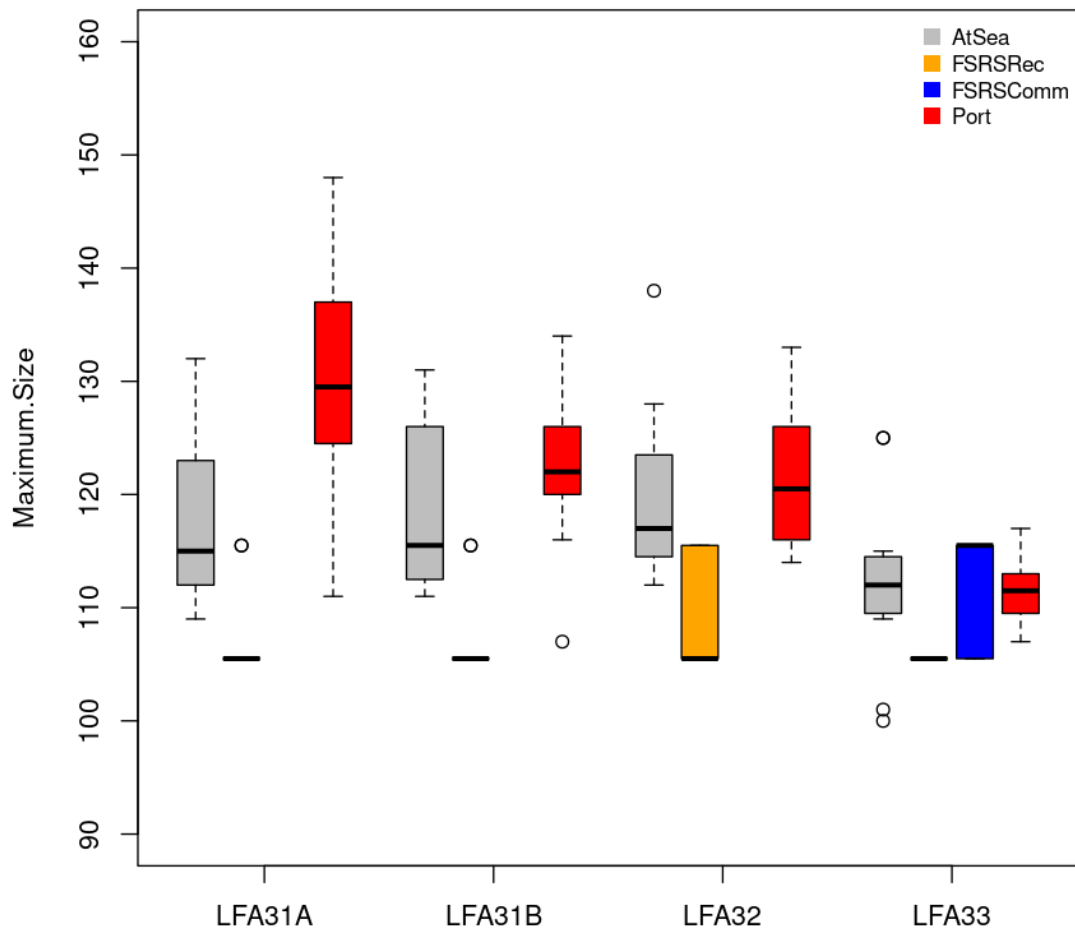


Figure 33: Boxplot of the annual estimates of maximum sizes by data source for LFA 31A-33. Within LFAs FSRS samples where maximum size was in the largest size category were not included

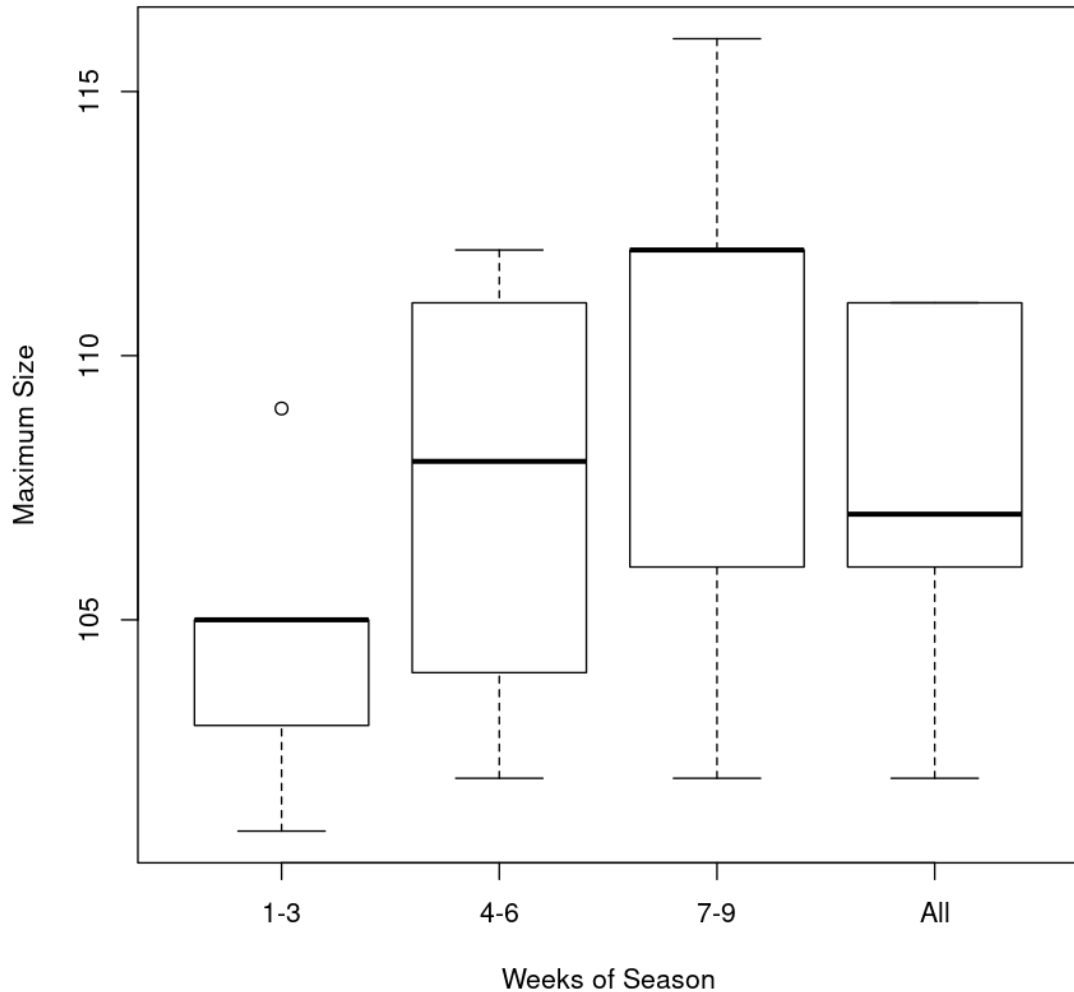


Figure 34: Boxplots of estimated maximum carapace length from sea sampling dates (weeks of season) observed from LFA 27 during the 2011-2015 seasons.

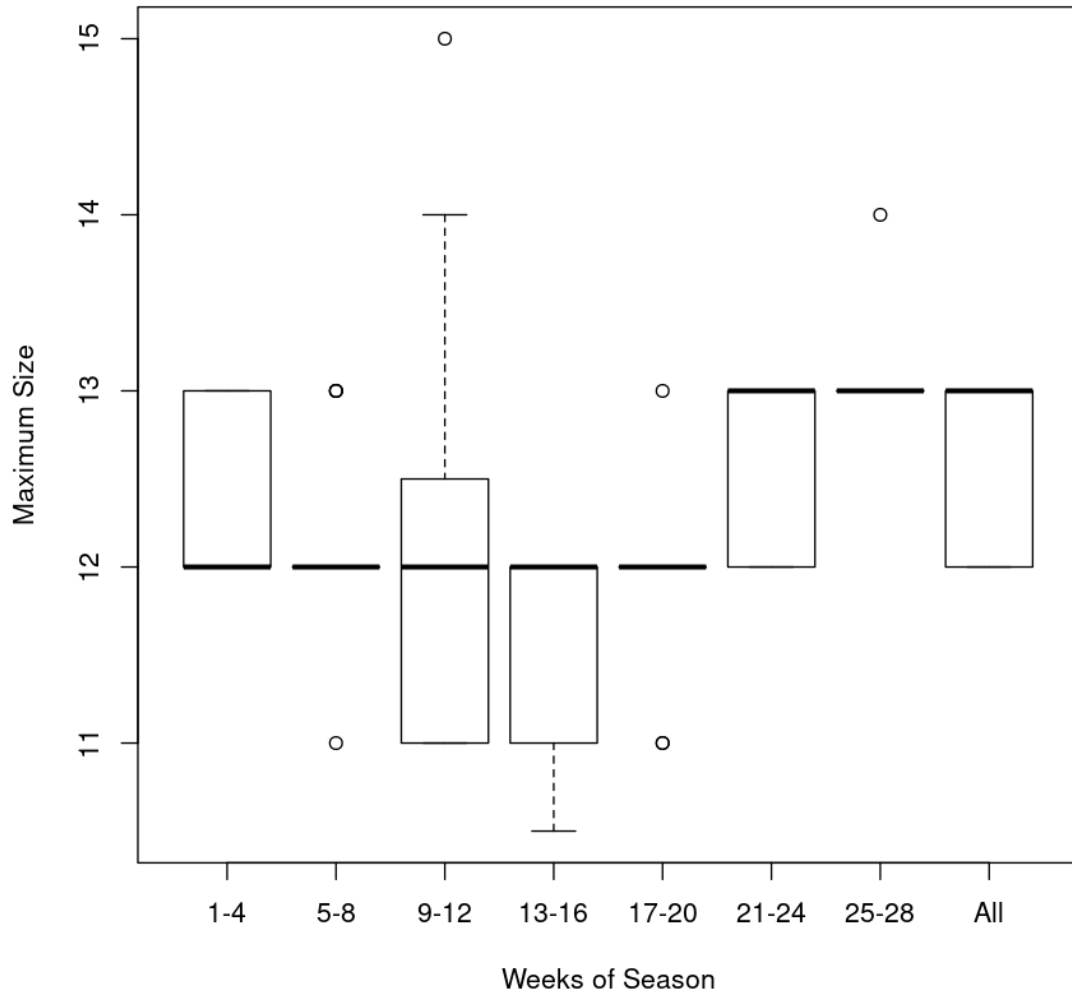


Figure 35: Boxplots of estimated maximum carapace length from FSRS commercial sampling dates (weeks of season) observed from LFA 33 during the 2004-2016 seasons.

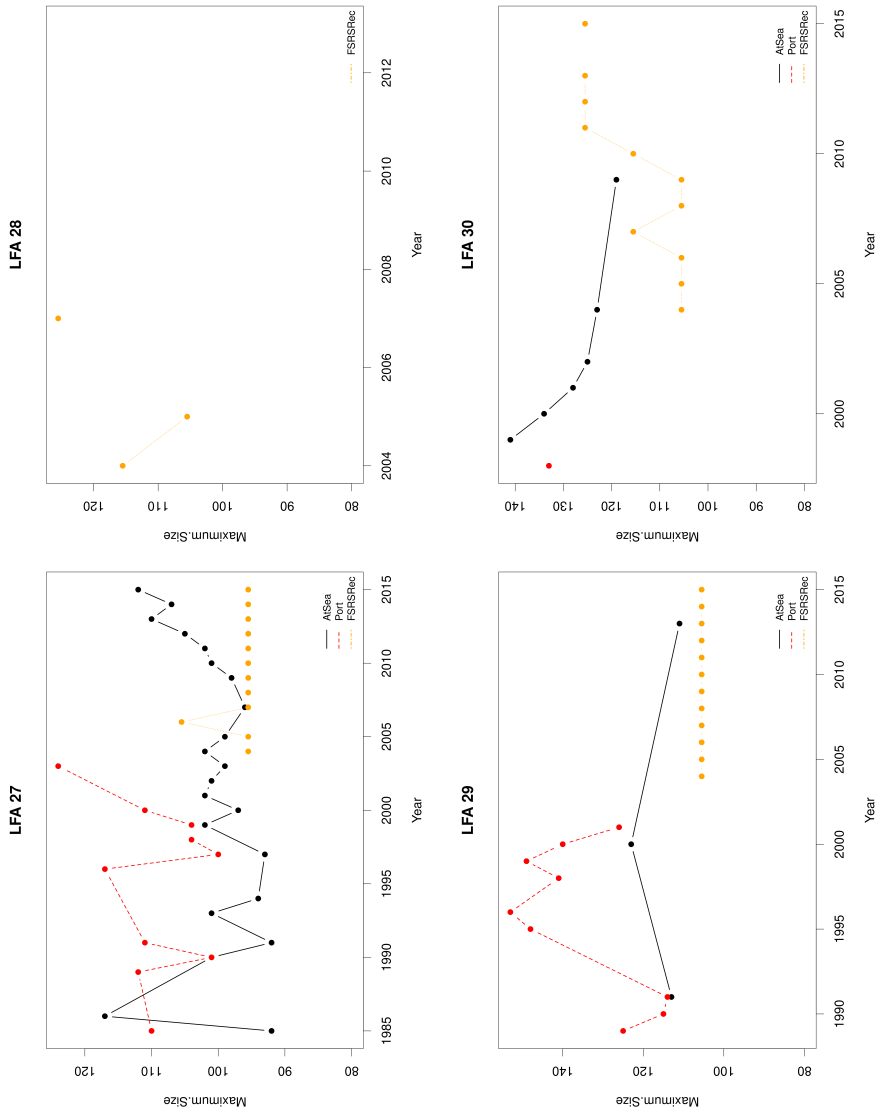


Figure 36: Estimated maximum carapace length (upper 95th percentile) of lobster samples taken from at sea samples, port samples, and / or the FSR recruitment trap project. Maximum sizes from FSRS recruitment traps represent the center of the size bin converted to mm from the gauge used to measure carapace length of lobsters. FSRS results with maximum sizes in the largest size bin were not included in these figures. Data were only from mid season samples.

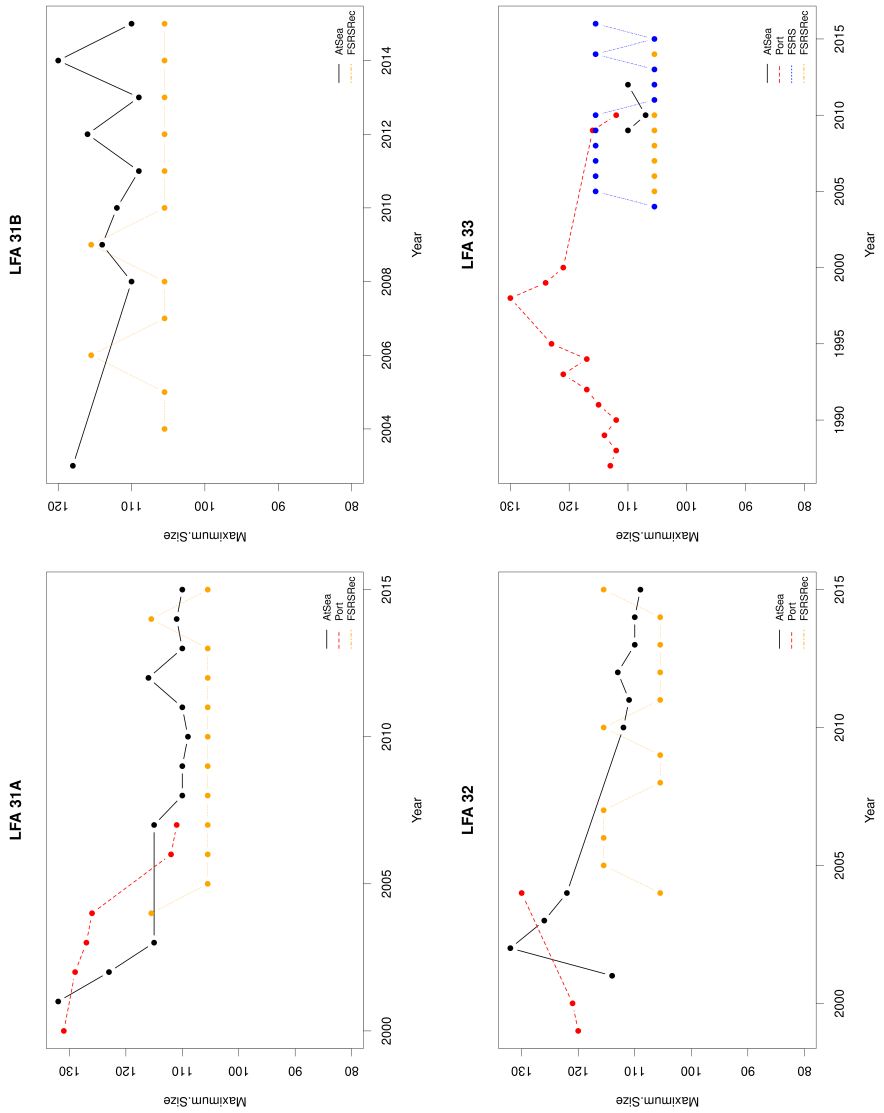


Figure 37: Estimated maximum carapace length (upper 95th percentile) of lobster samples taken from at sea samples, port samples, and / or the FSRS recruitment trap project. Maximum sizes from FSRS recruitment or commercial traps represent the center of the size bin converted to mm from the gauge used to measure carapace length of lobsters. FSRS results with maximum sizes in the largest size bin were not included in these figures. Data were only from mid season samples.

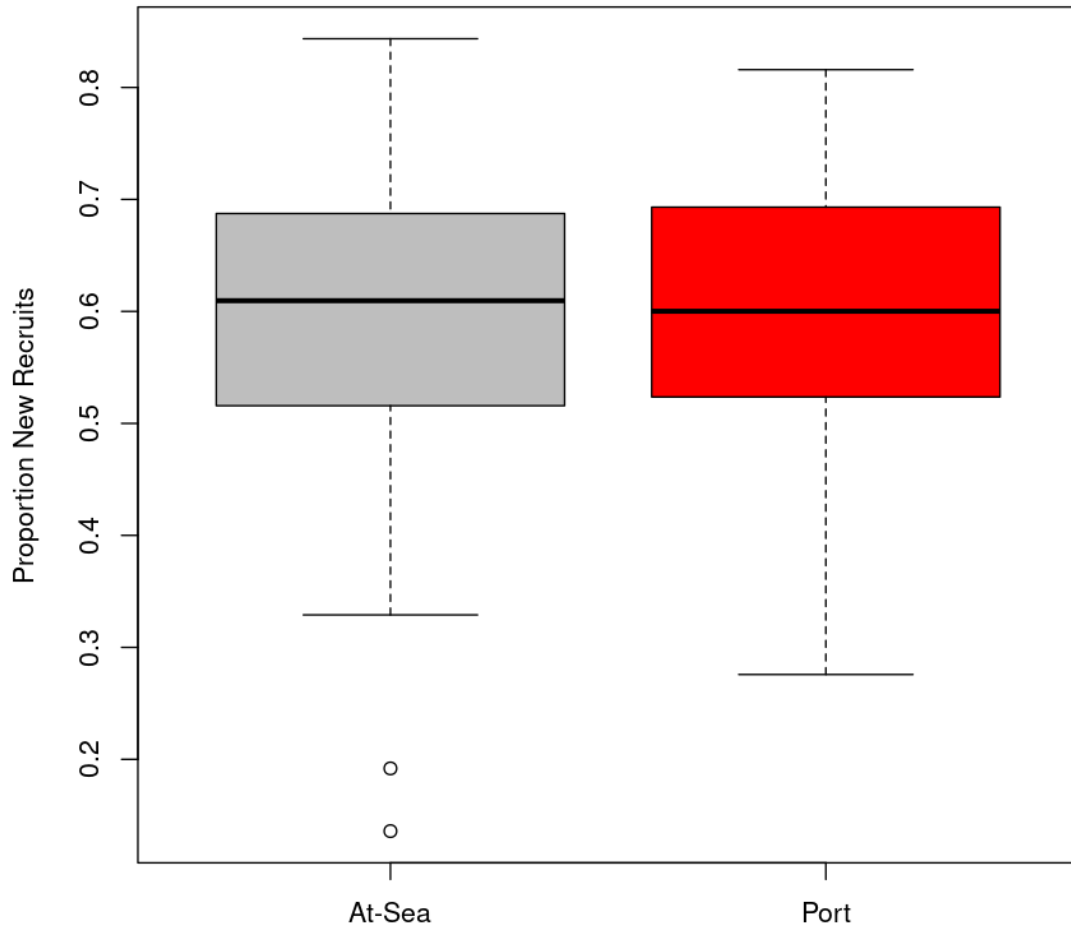


Figure 38: Boxplot of the combined estimates of the proportion of new recruits (size ranging from MLS - MLS + 11mm) sizes by data source.

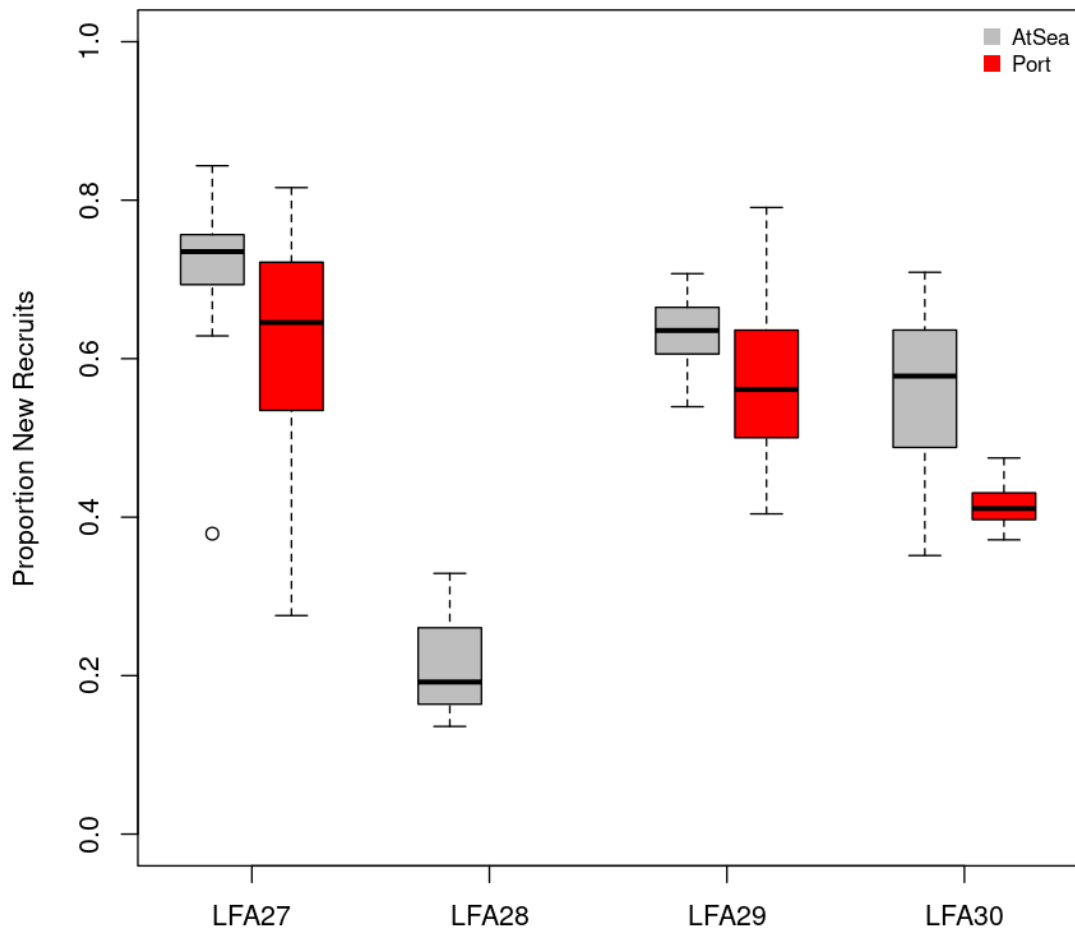


Figure 39: Boxplot of the annual estimates of proportion of total numbers landed represented by new recruits (minimum legal size : minimum legal size + 11 mm) by data source for LFA 27-30. FSRS recruitment traps not included in this analysis.

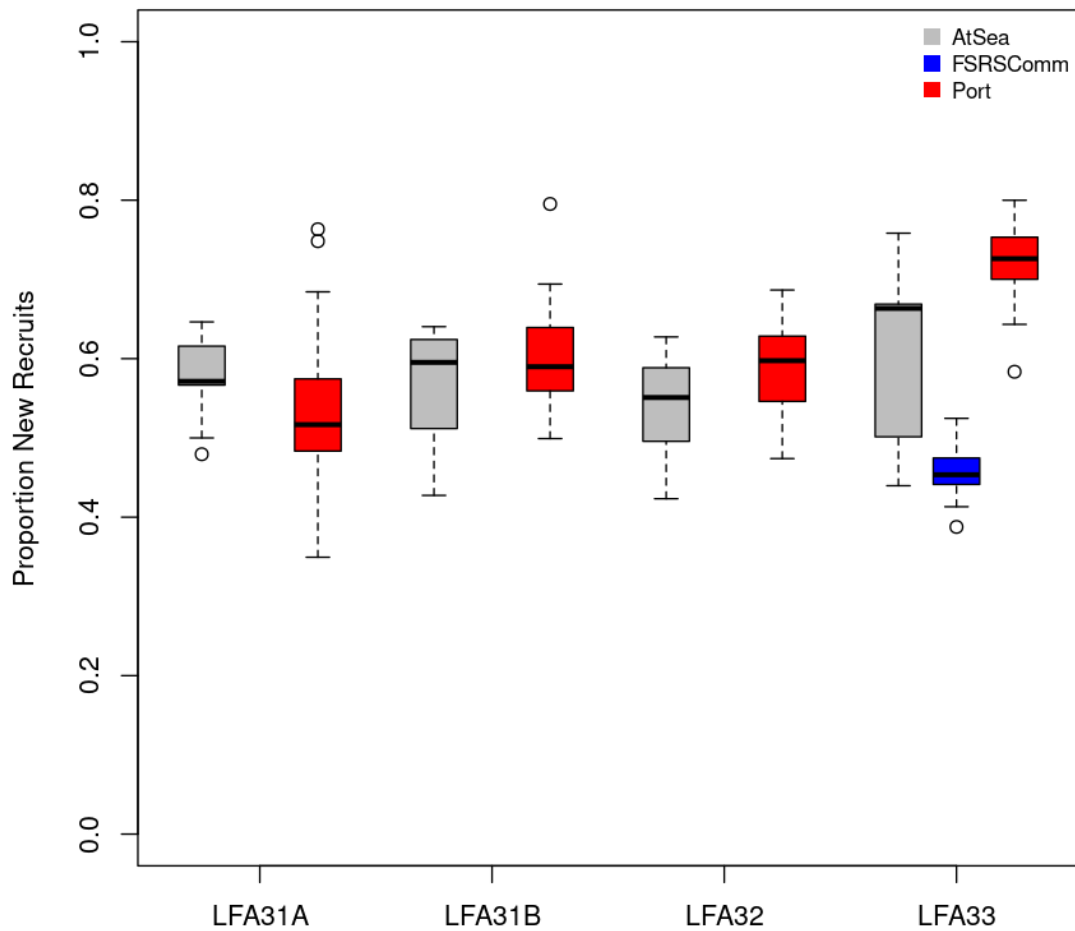


Figure 40: Boxplot of the annual estimates of proportion of total numbers landed represented by new recruits (minimum legal size : minimum legal size + 11 mm) by data source for LFA 31A-33. FSRS recruitment traps not included in this analysis.

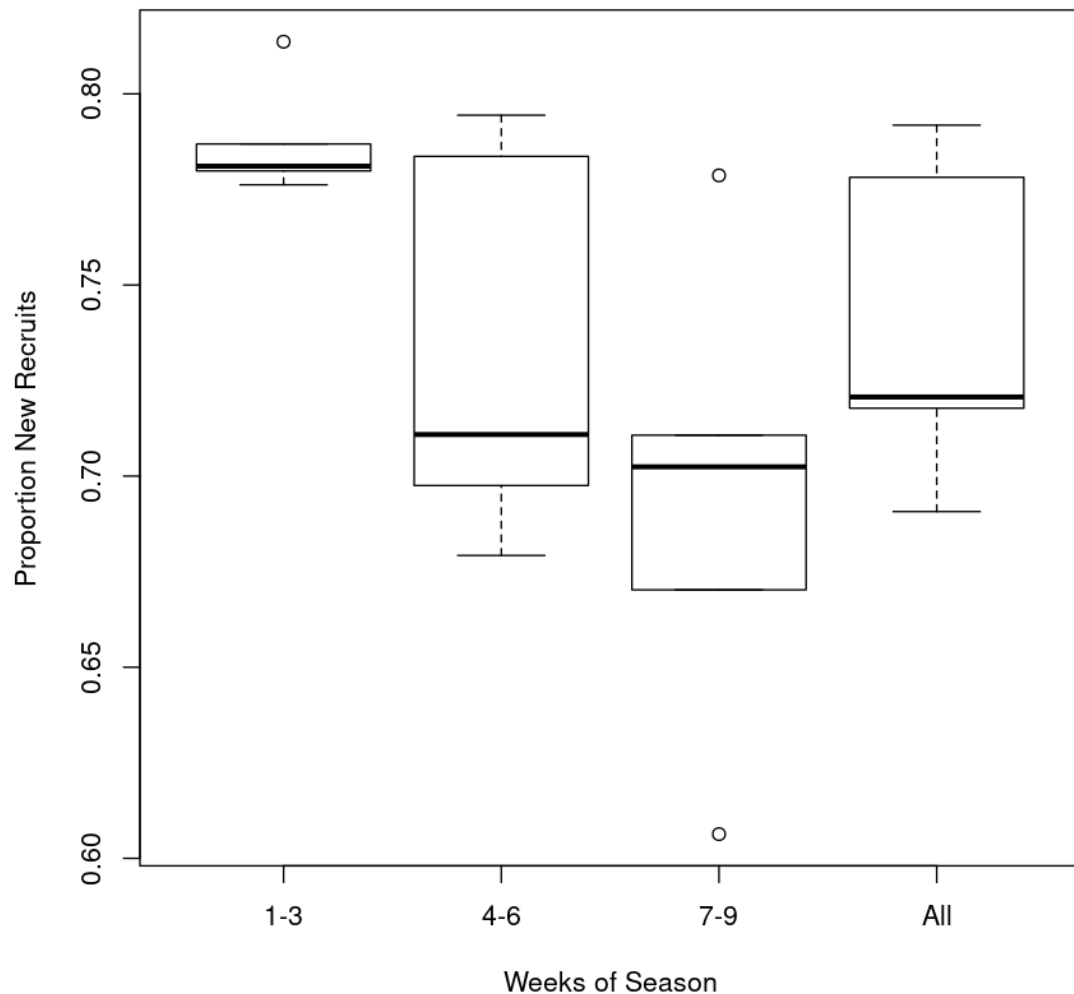


Figure 41: Boxplots of estimated proportion of total numbers landed represented by new recruits (minimum legal size : minimum legal size + 11 mm) from sea sampling dates (weeks of season) observed from LFA 27 during the 2011-2015 seasons.

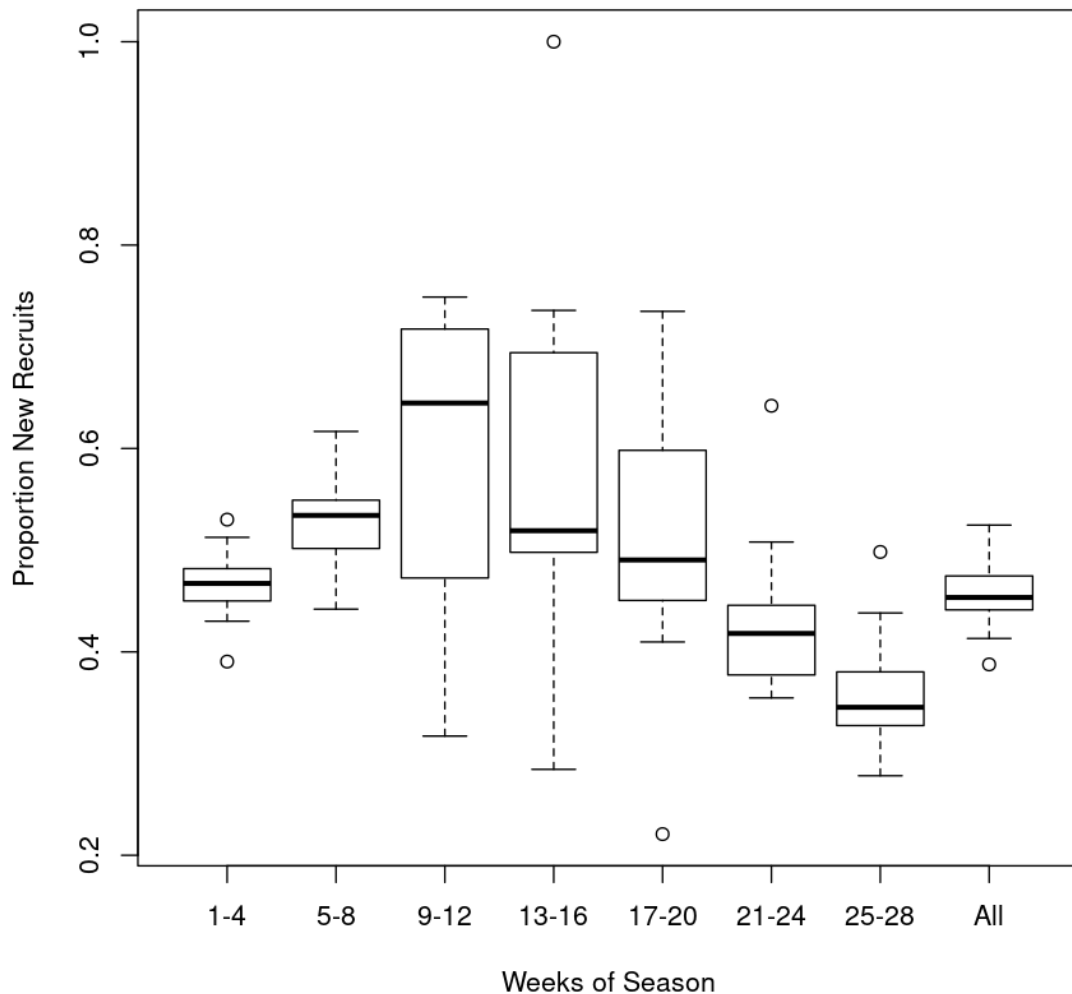


Figure 42: Boxplots of estimated proportion of total numbers landed represented by new recruits (minimum legal size : minimum legal size + 11 mm) from FSRS commercial sample dates (weeks of season) observed from LFA 33 during the 2004-2016 seasons.

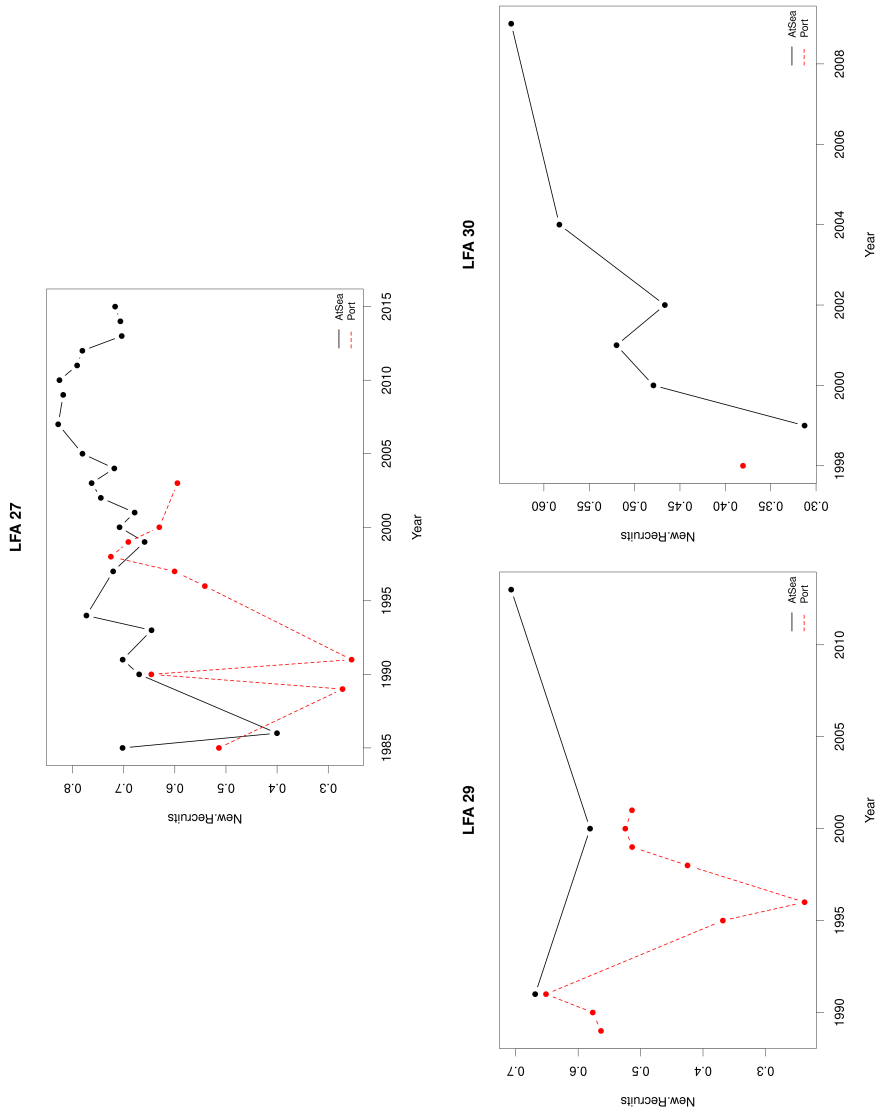


Figure 43: Time series of the proportion of total numbers landed represented by new recruits (minimum legal size : minimum legal size + 11 mm) taken from at sea samples, and /or port samples. Data was limited to mid-season samples.

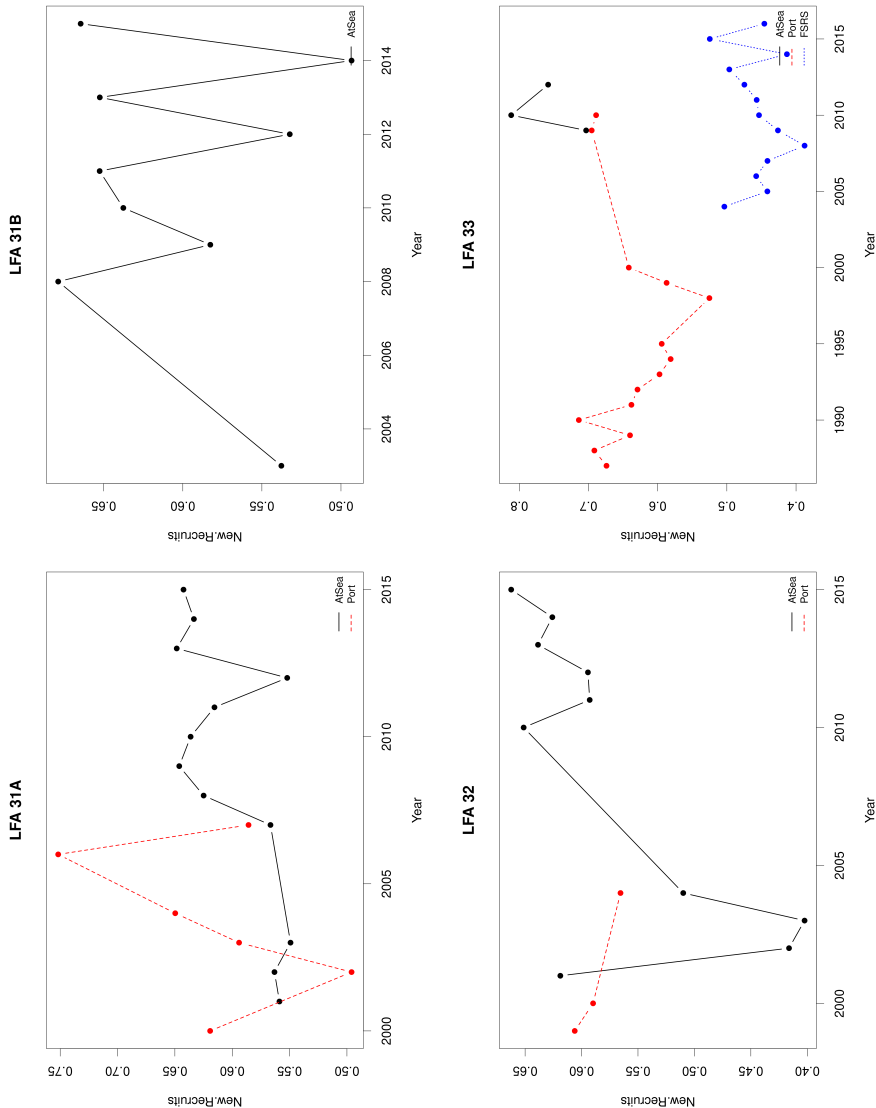


Figure 44: Time series of the proportion of total numbers landed represented by new recruits (minimum legal size : minimum legal size + 11 mm) taken from at sea samples, and /or port samples. Data was limited to mid-season samples.

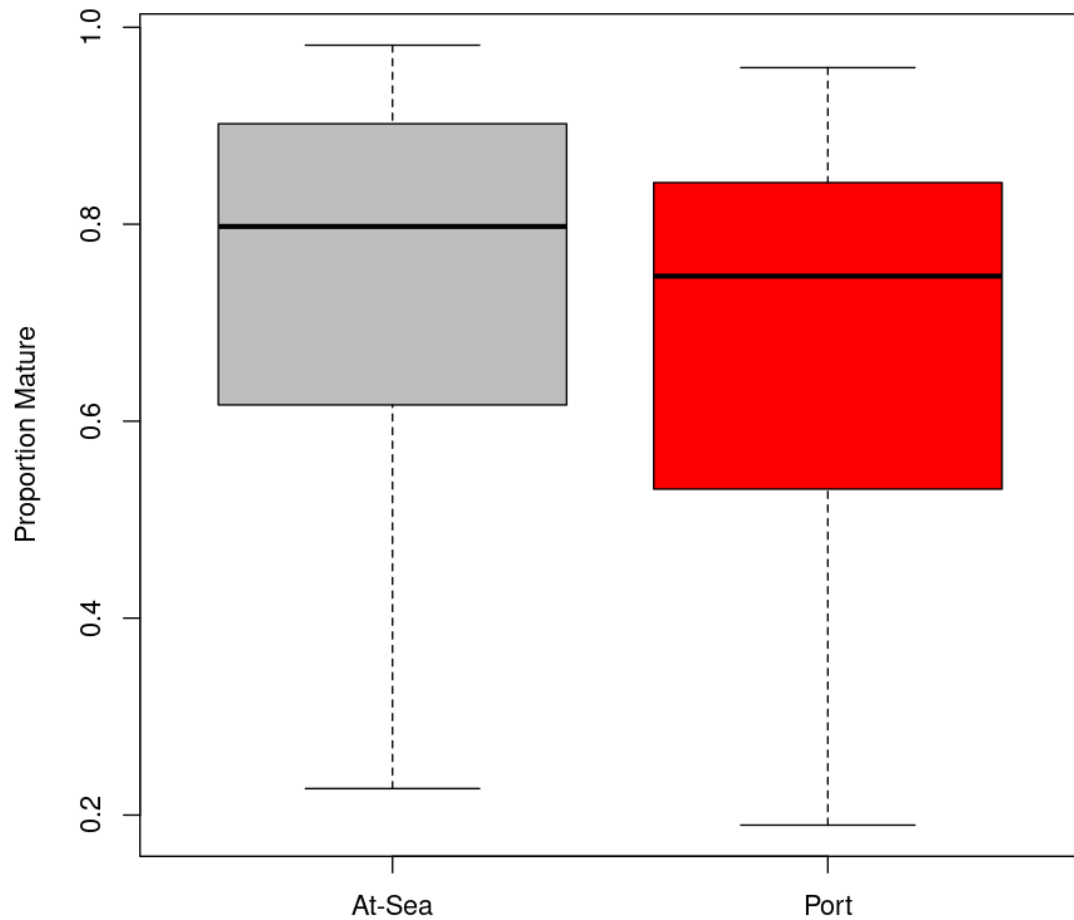


Figure 45: Boxplot of the estimates of proportion mature lobster in the landings, separated by data source.

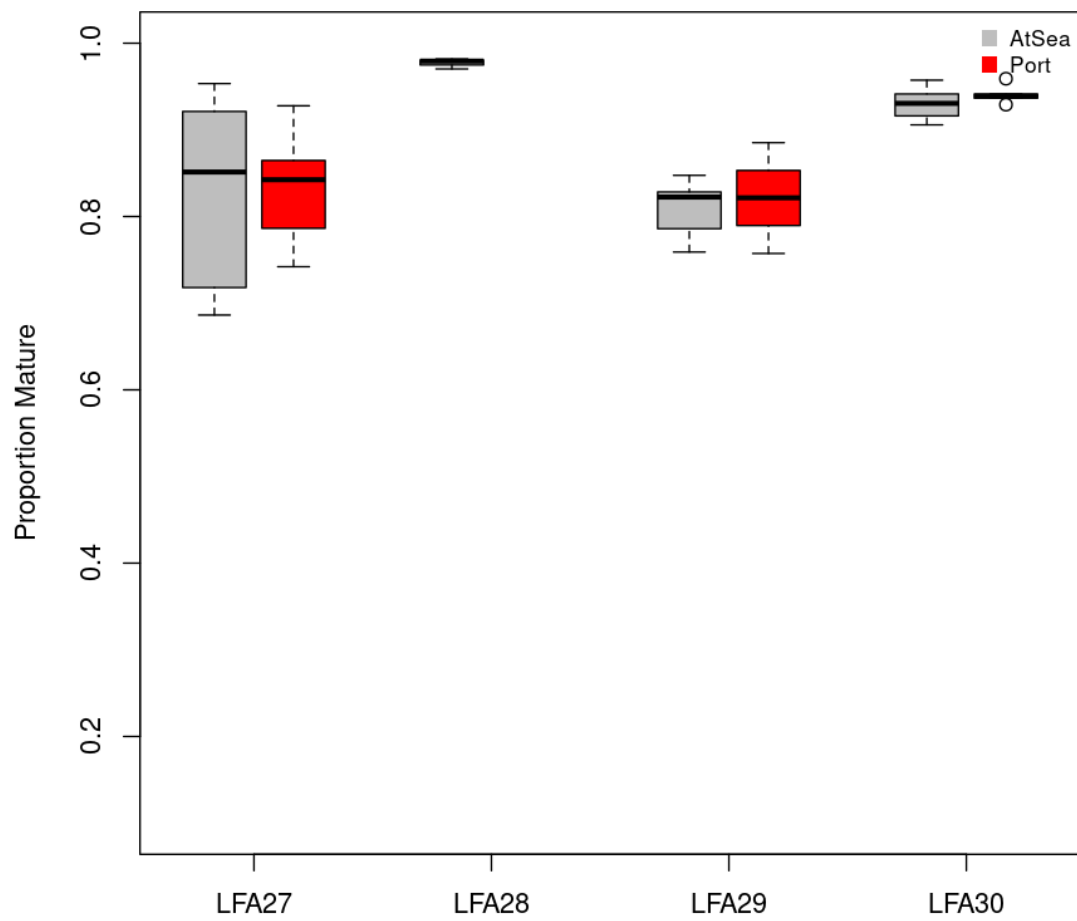


Figure 46: Boxplot of the annual estimates of proportion mature lobster in the landings separated by data source for LFA 27-30. FSRS data sets not included in this analysis.

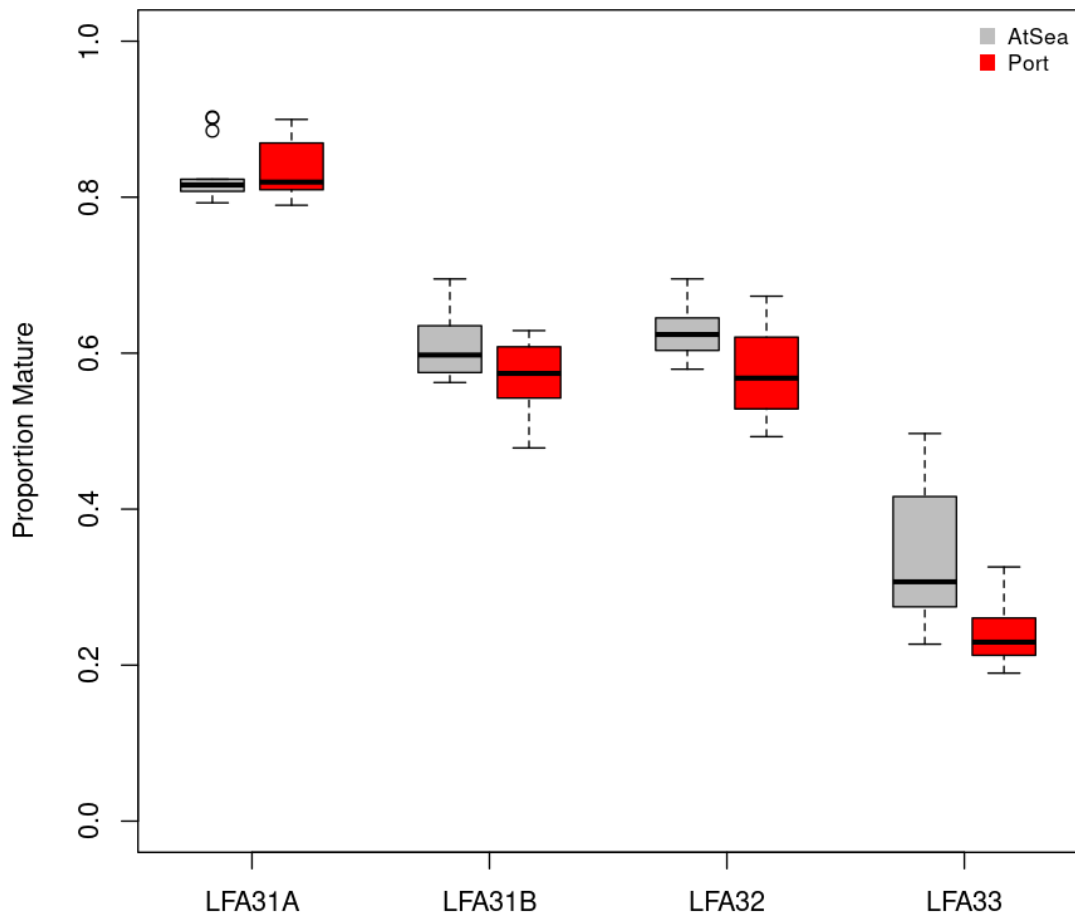


Figure 47: Boxplot of the annual estimates of proportion mature lobster in the landings, separated by data source for LFA 31A-33. FSRS data set not included in this analysis.

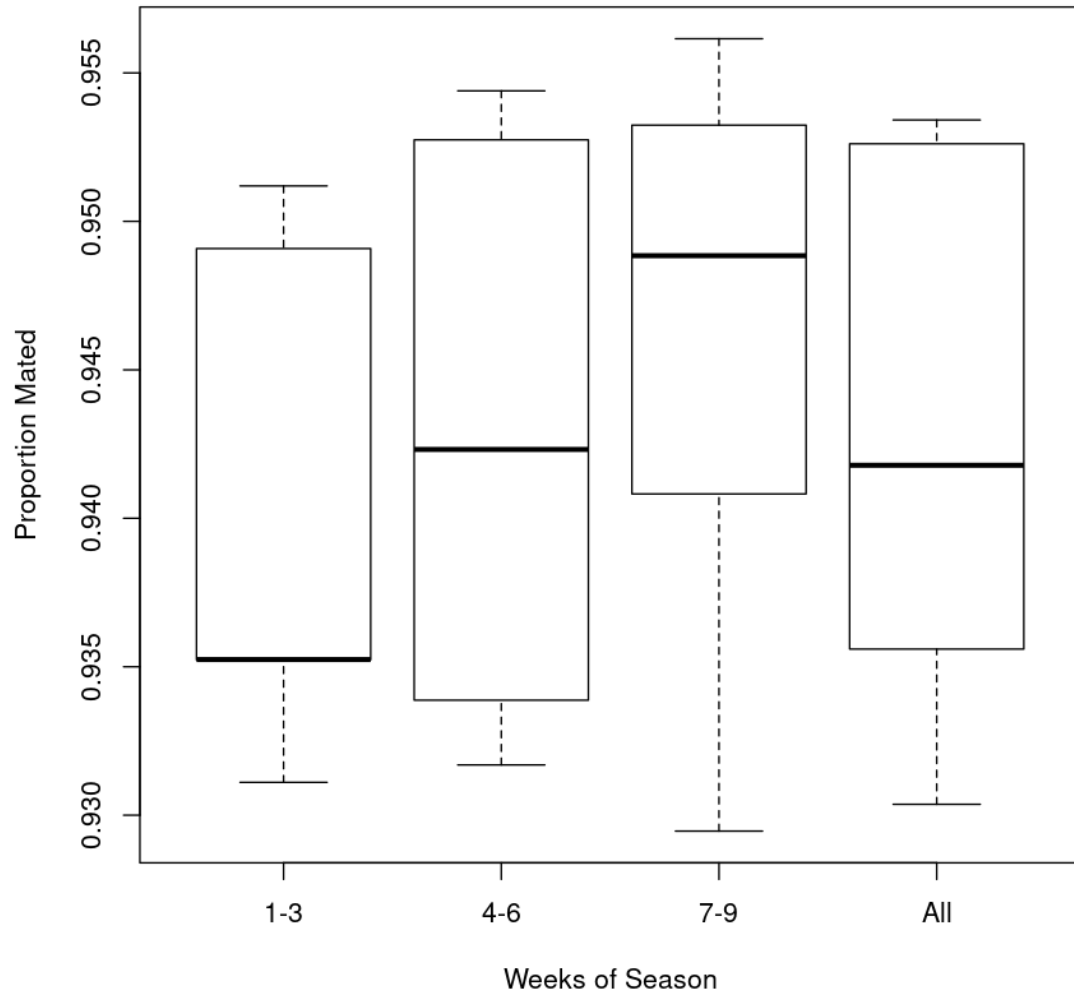


Figure 48: Boxplots of estimated proportion of the proportion mature lobster in the landings from sea sampling dates (weeks of season) observed from LFA 27 during the 2011-2015 seasons.

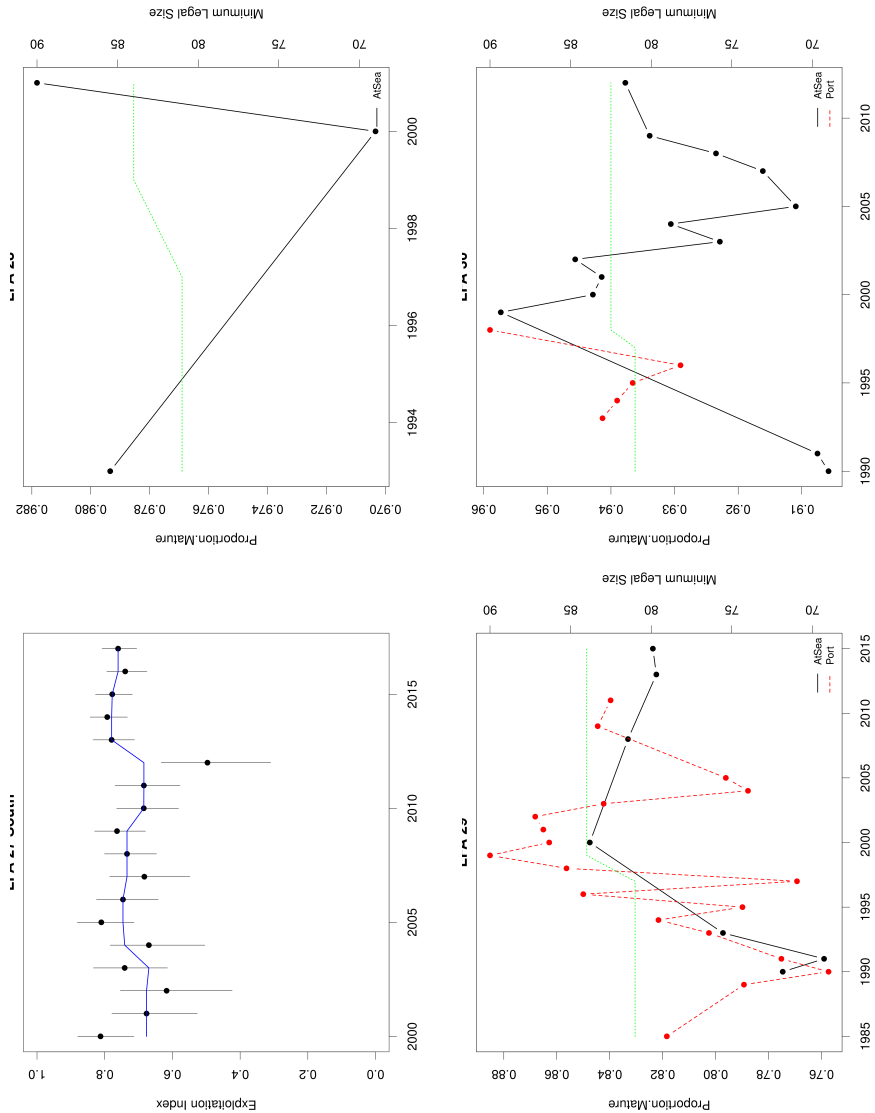


Figure 49: Time series of the proportion mature lobster in the landings from at sea samples, and / or port samples. Time series of changes in minimum legal sizes are shown in green.

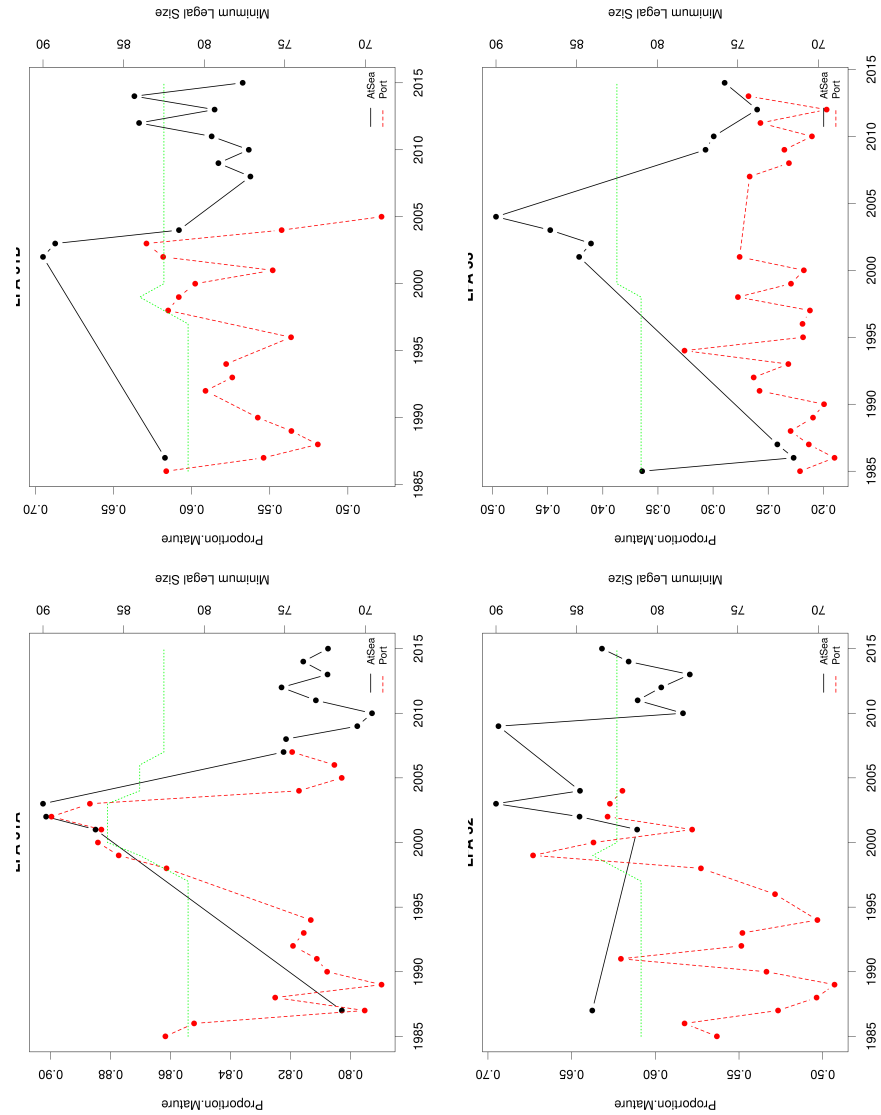


Figure 50: Time series of the proportion mature lobster in the landings at sea samples, and /or port samples. Time series of changes in minimum legal sizes are shown in green.

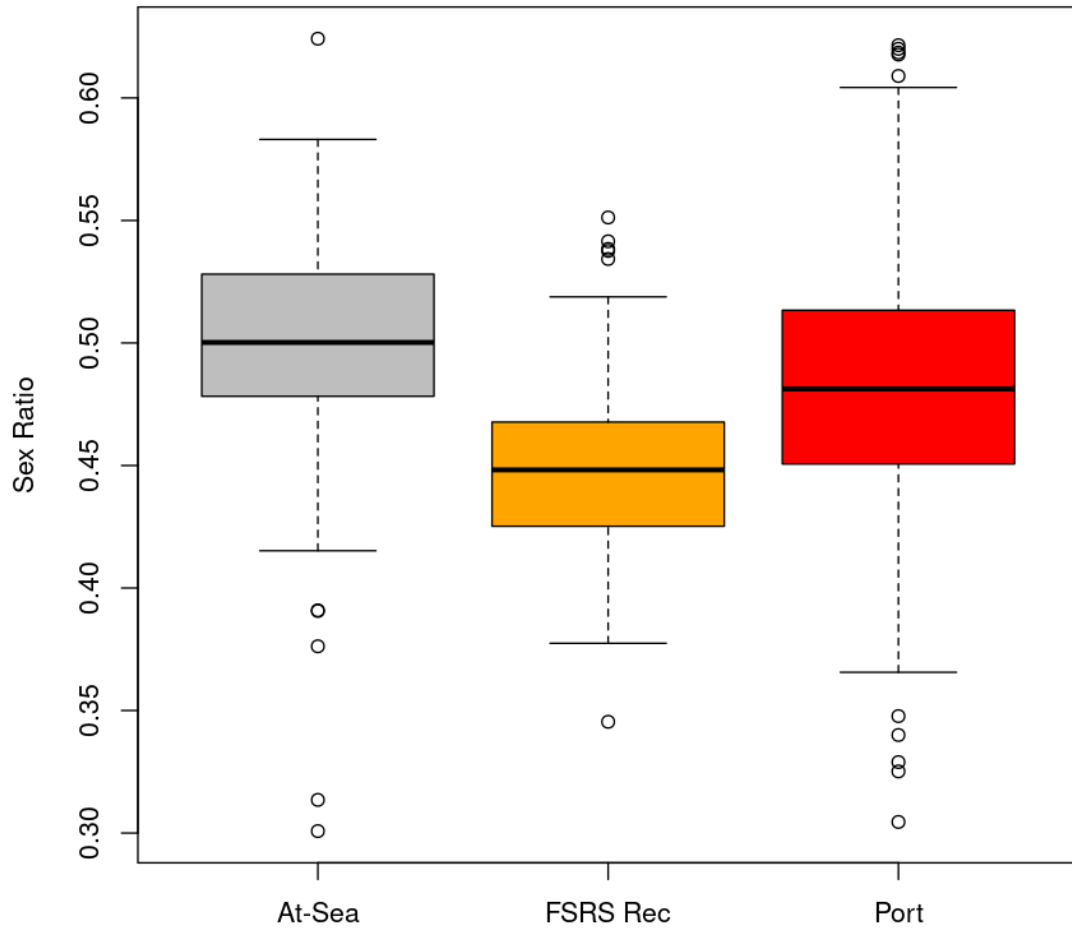


Figure 51: Boxplot of the estimates of sex ratio (proportion of female) lobsters separated by data source.

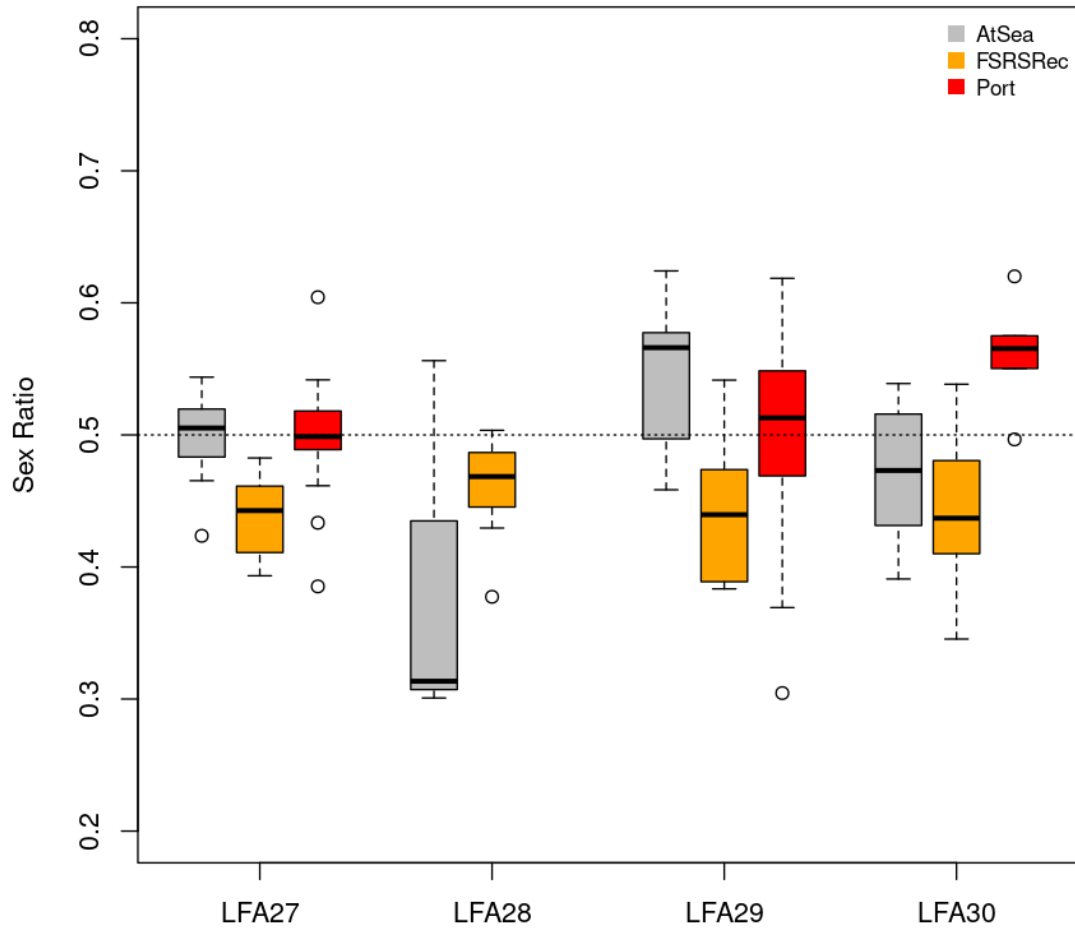


Figure 52: Boxplot of the annual estimates of sex ratio (proportion of female) lobsters sampled by data source for LFA 27-30.

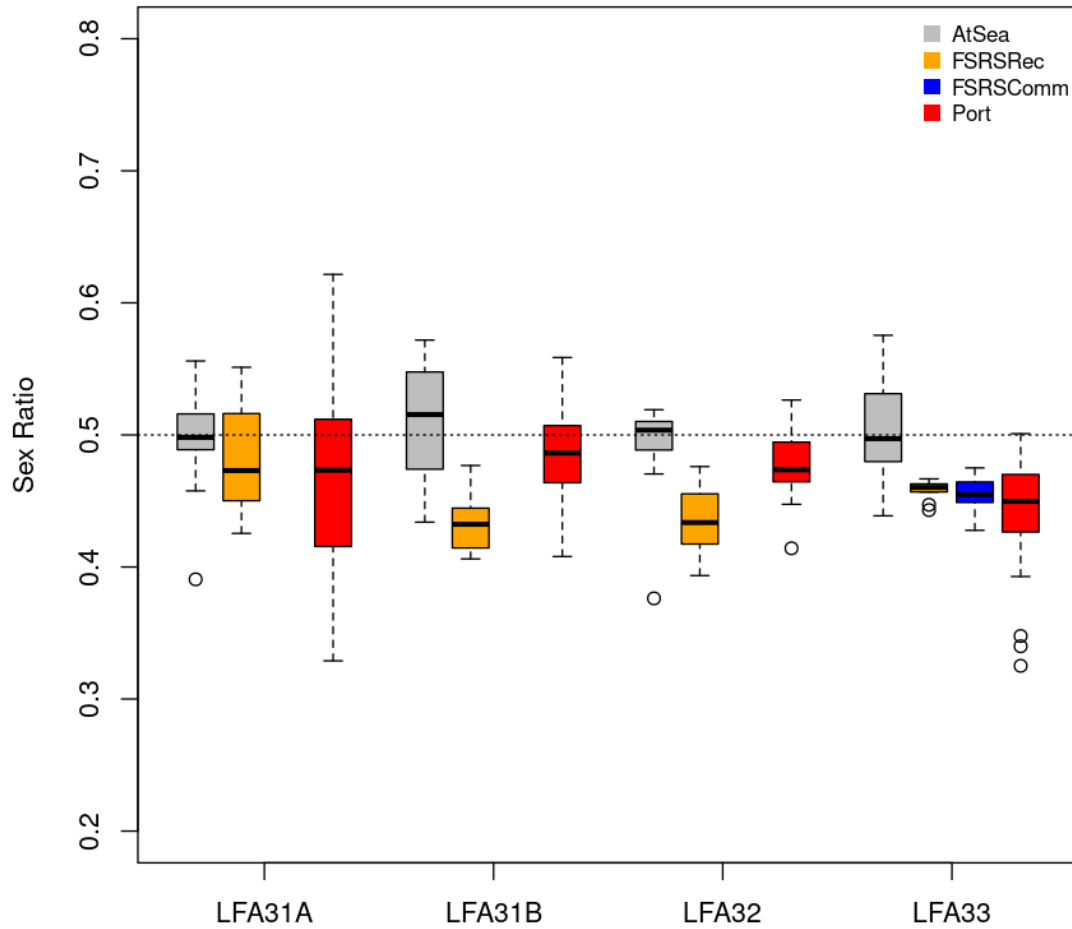


Figure 53: Boxplot of the annual estimates of sex ratio (proportion of female) lobsters sampled by data source for LFA 31A-33.

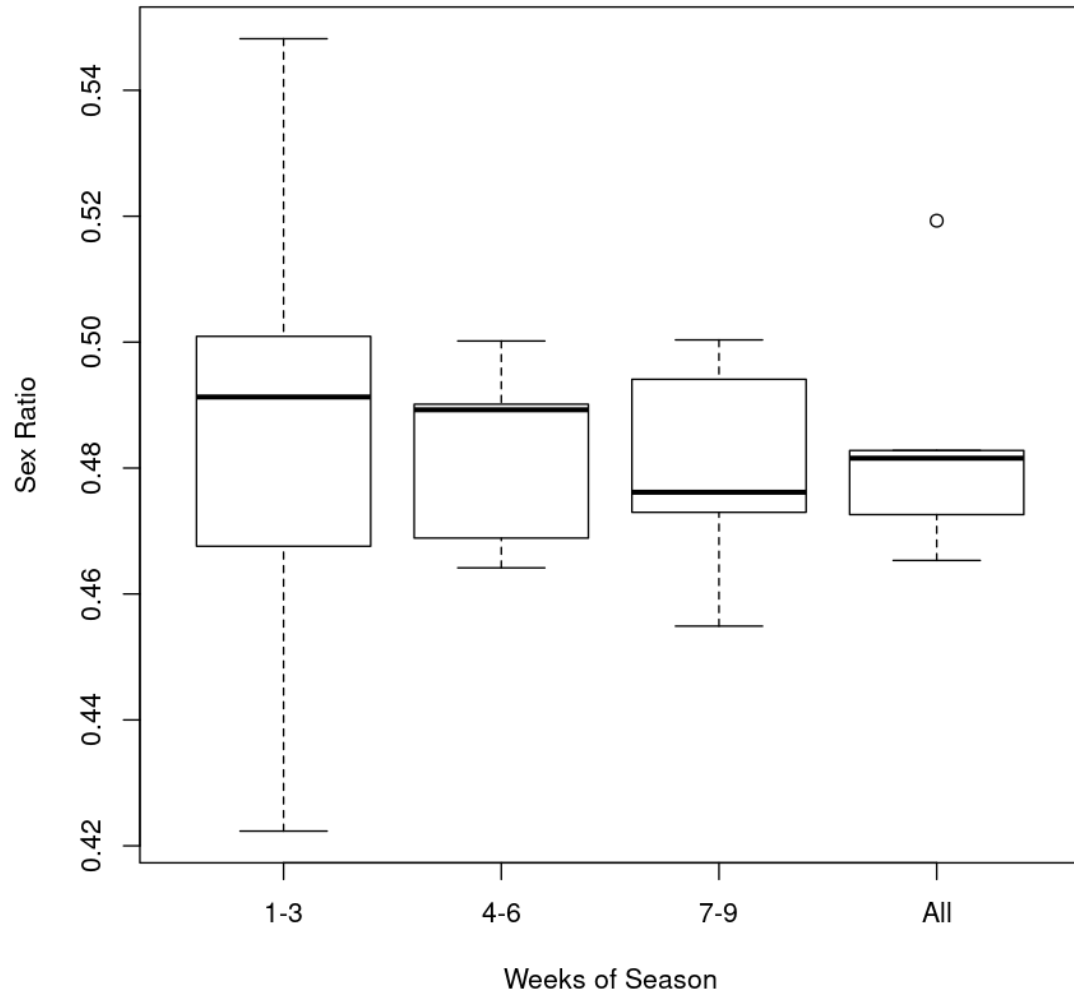


Figure 54: Boxplots of estimated sex ratio (proportion of females) from sea sampling dates (weeks of season) observed from LFA 27 during the 2011-2015 seasons.

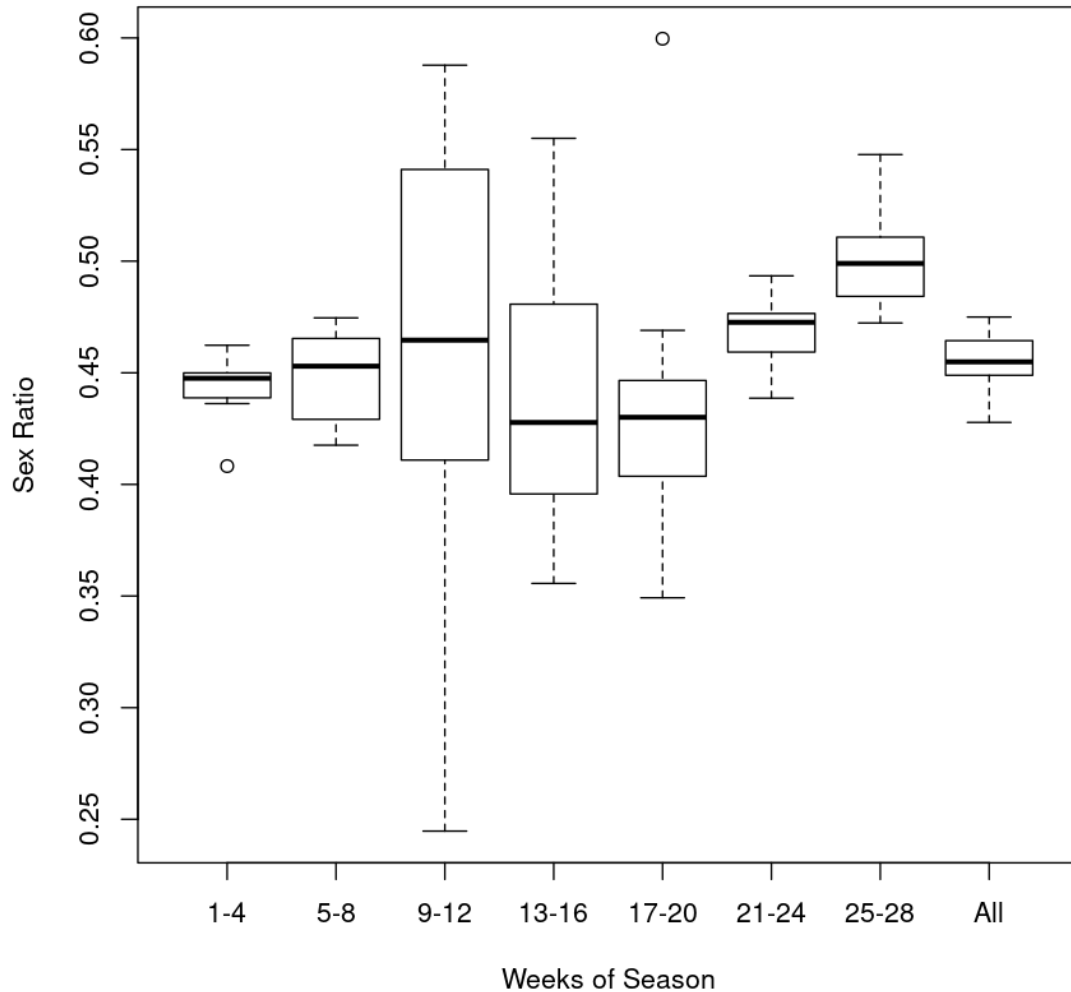


Figure 55: Boxplots of estimated sex ratio (proportion of females) from FSRS commercial sampling dates (weeks of season) observed from LFA 33 during the 2004-2016 seasons.

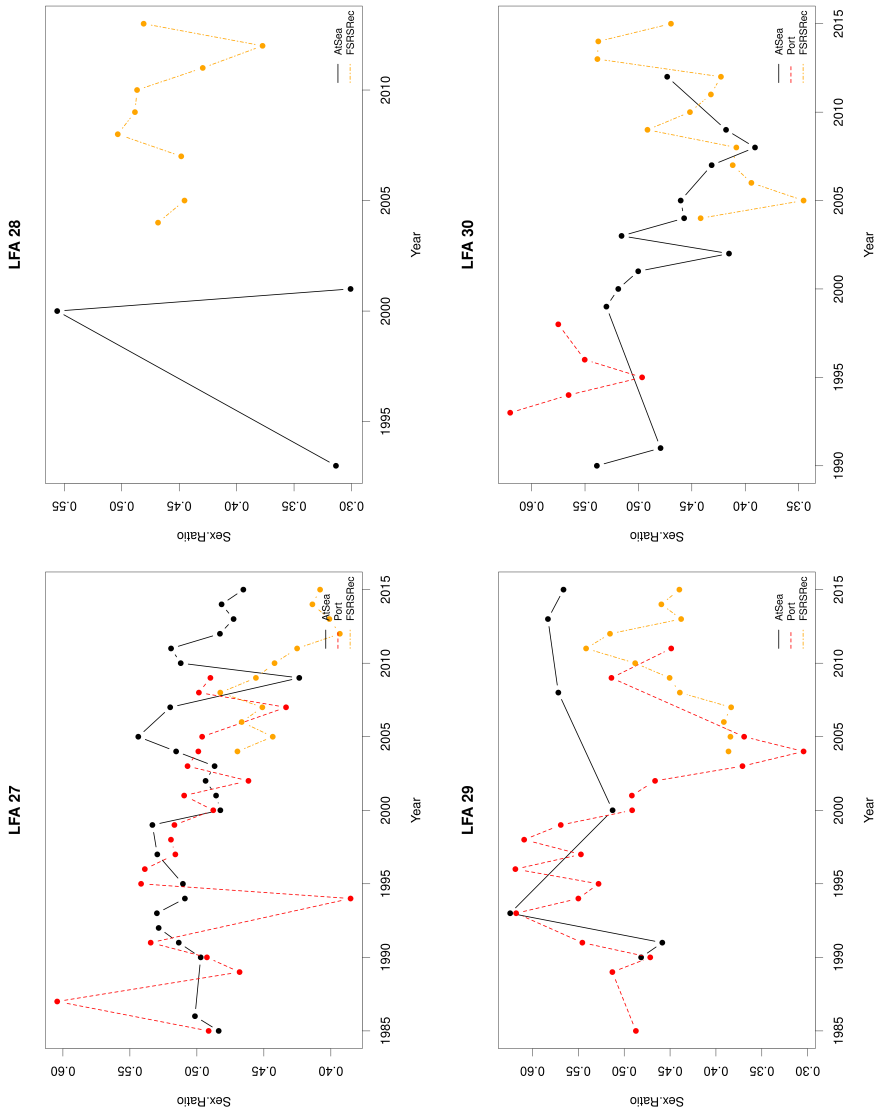


Figure 56: Time series of the sex ratio (proportion female) lobsters by data source across LFAs.

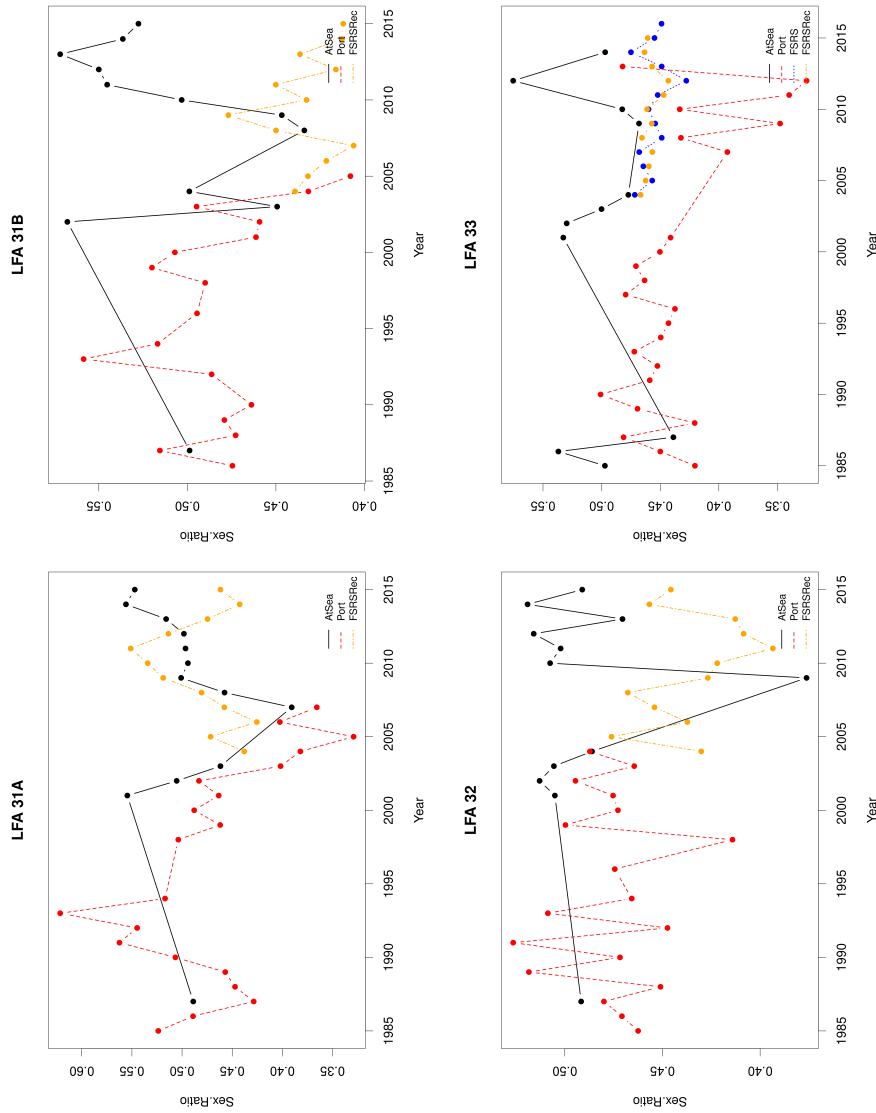


Figure 57: Time series of the sex ratio (proportion female) lobsters by data source across LFAs

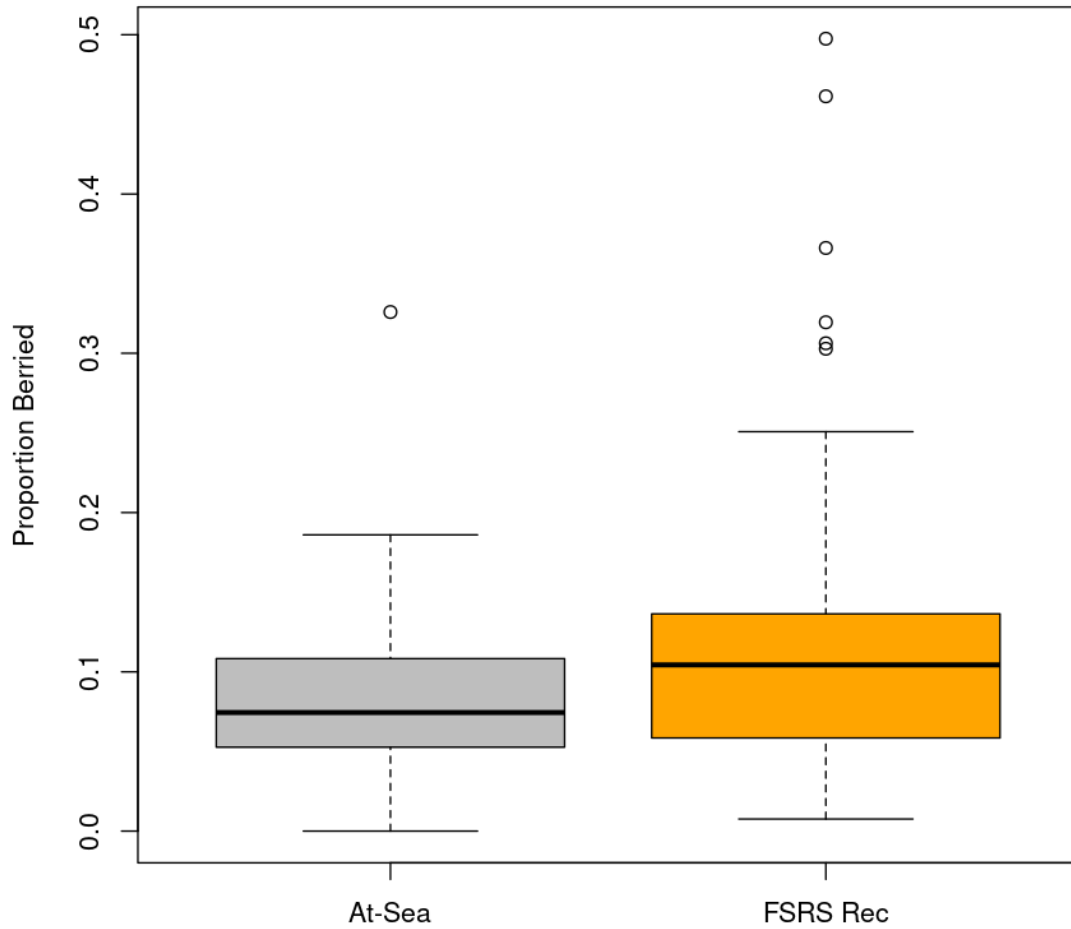


Figure 58: Boxplot of the estimates of proportion of berried female lobsters sampled by data source across all LFAs.

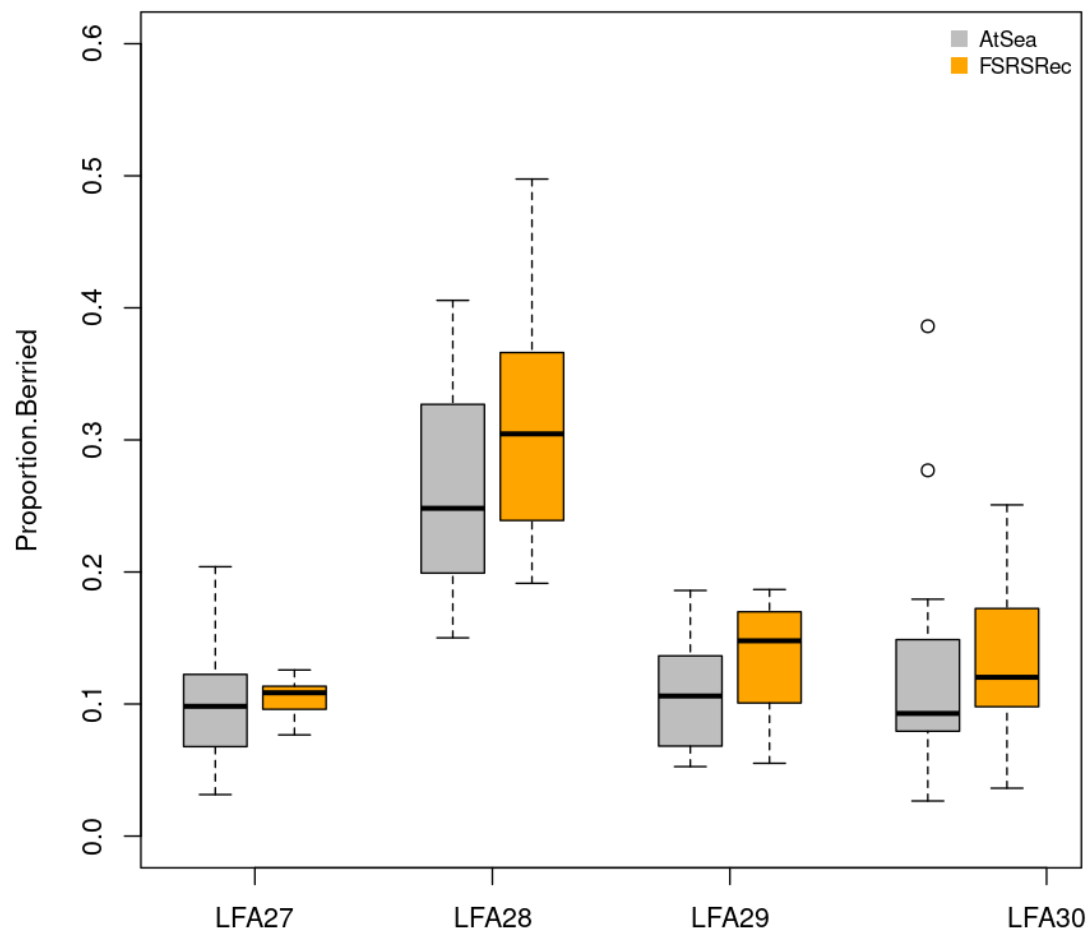


Figure 59: Boxplot of the time series of proportion of berried female lobsters sampled by data source for LFA 27-30.

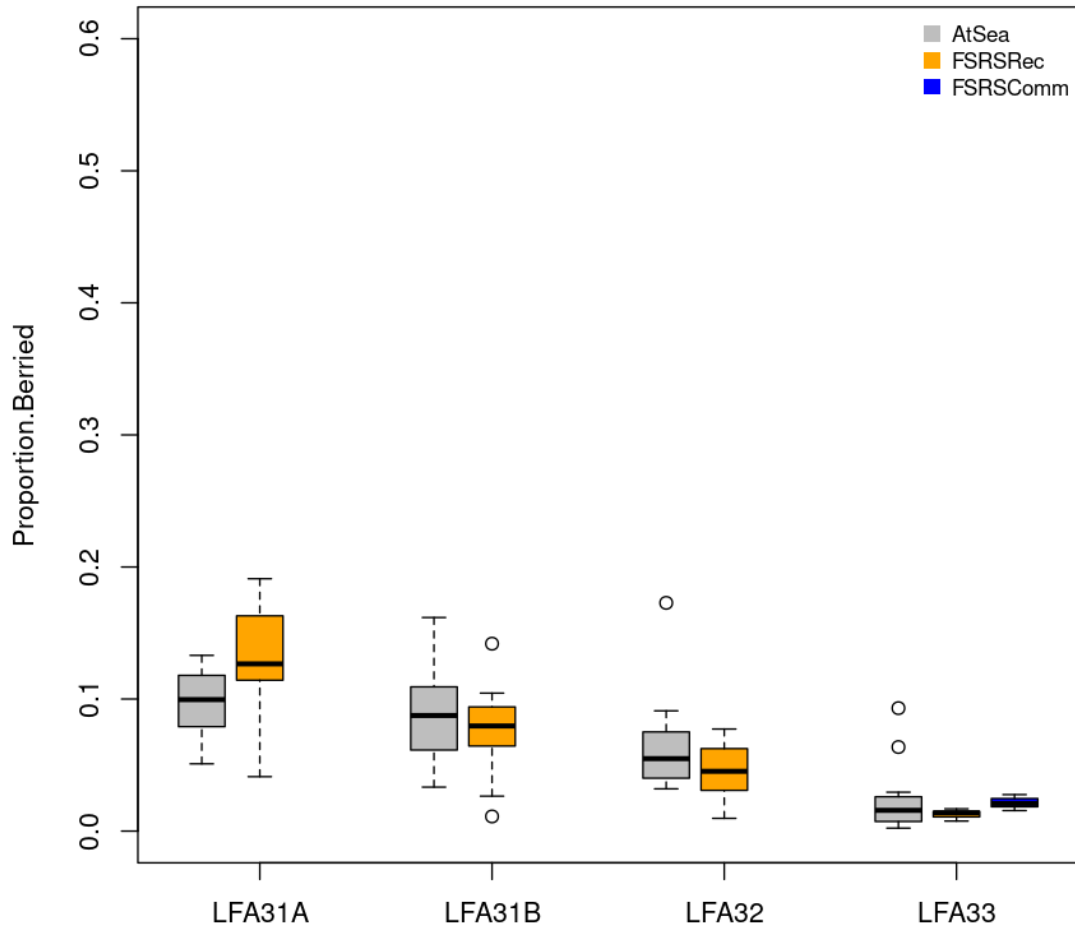


Figure 60: Boxplot of the time series of proportion of berried female lobsters sampled by data source for LFA 31A-33.

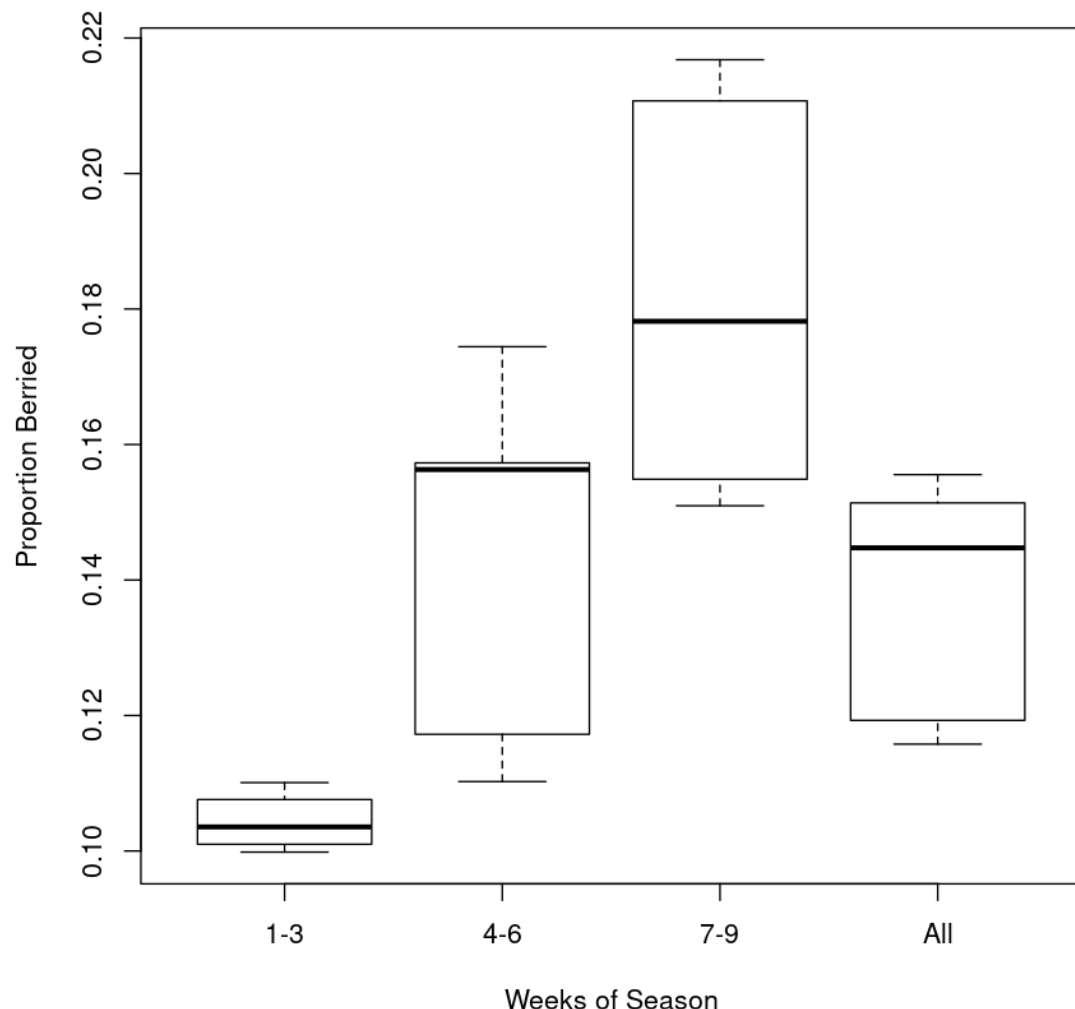


Figure 61: Boxplots of estimated proportion of berried females from sea sampling dates (weeks of season) observed from LFA 27 during the 2011-2015 seasons.

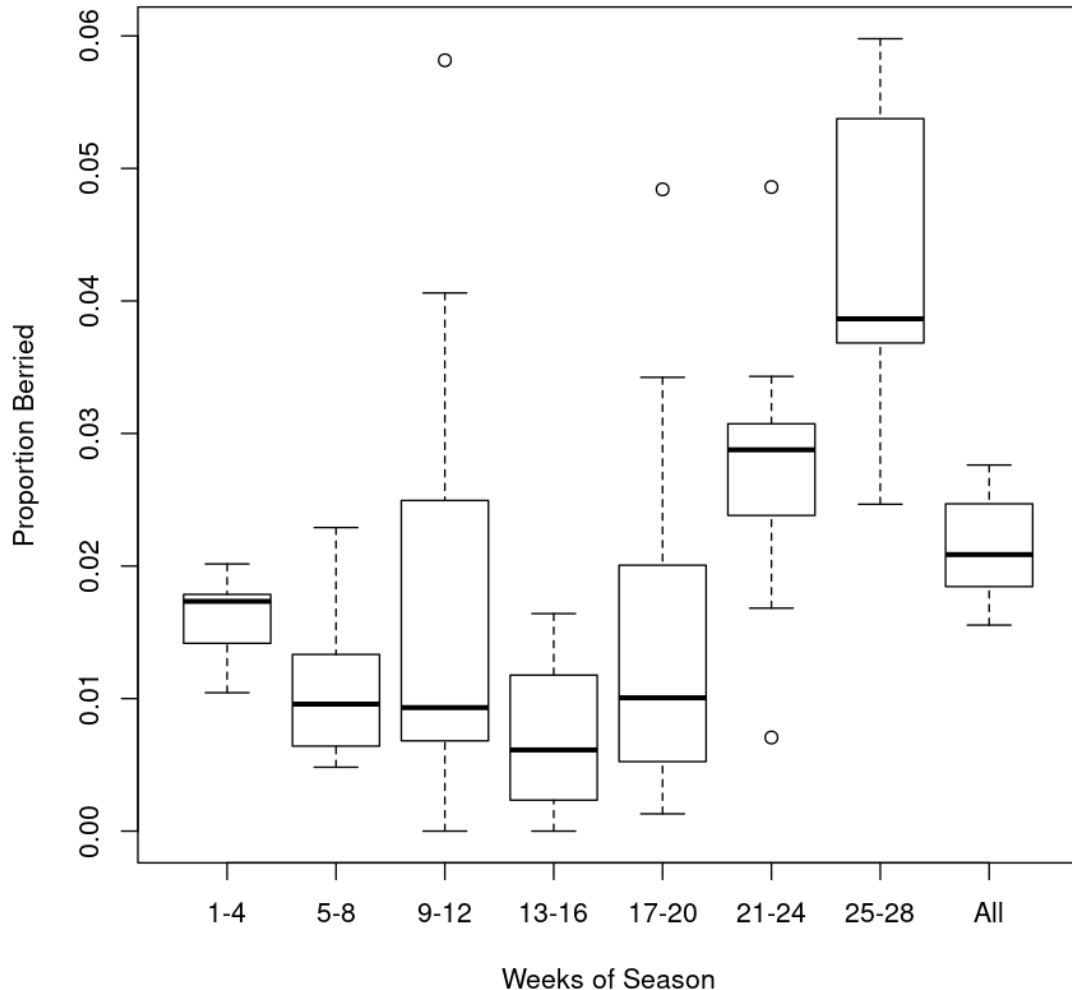


Figure 62: Boxplots of estimated proportion of berried females from FSRS commercial sampling dates (weeks of season) observed from LFA 33 during the 2004-2016 seasons.

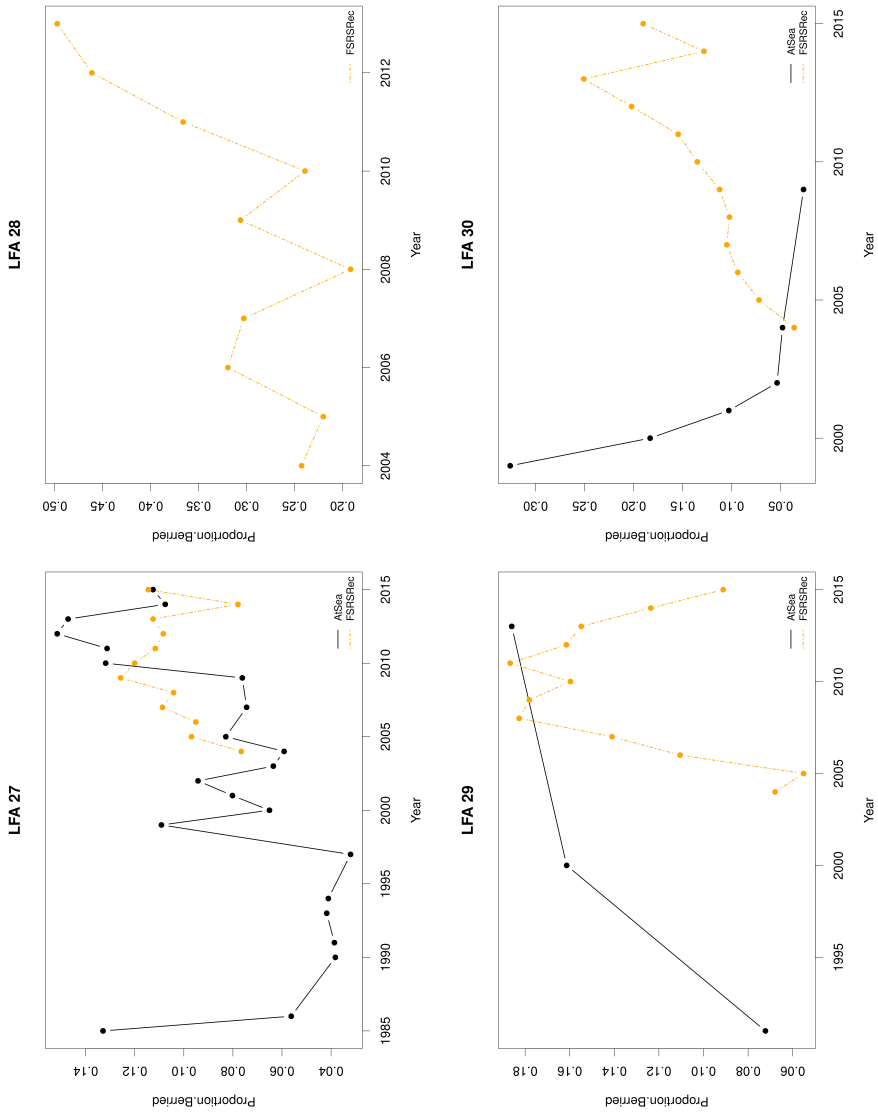


Figure 63: Time series of the proportion of berried female lobsters by data source across LFAs. Data was limited to mid-season samples.

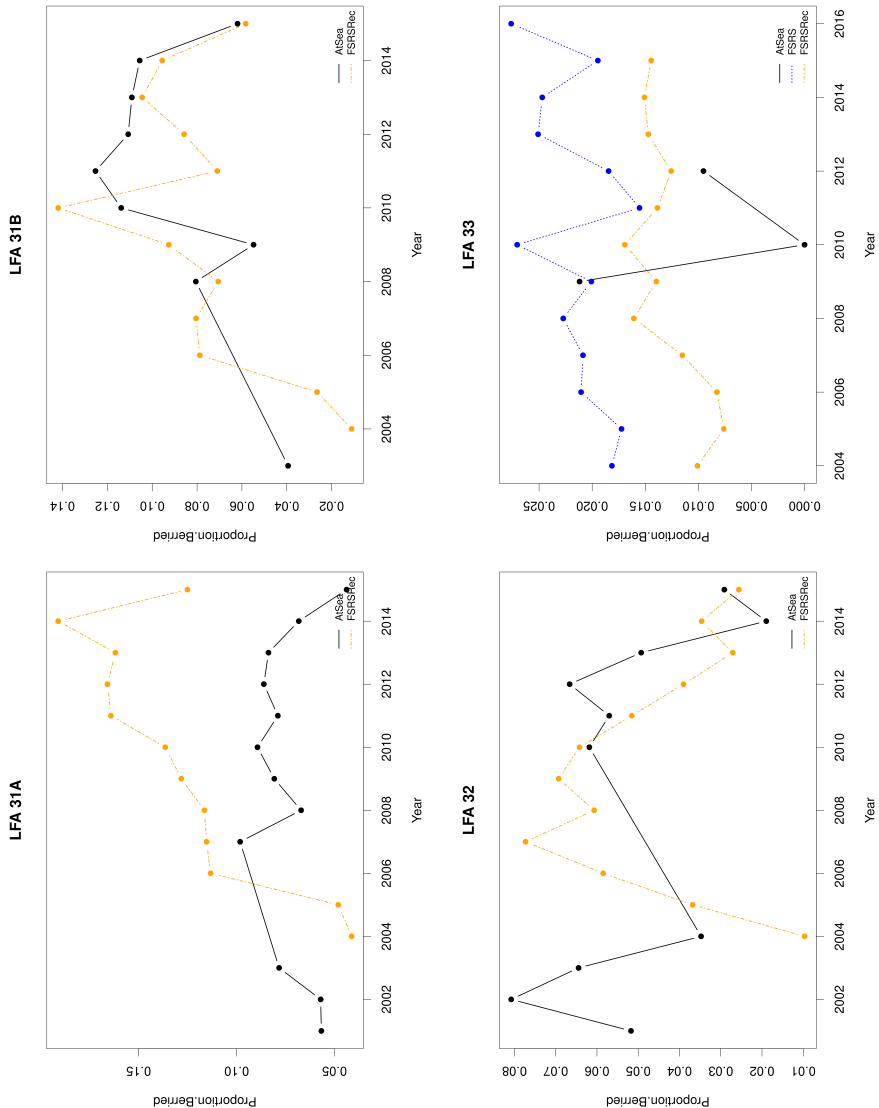


Figure 64: Time series of the proportion berried female lobsters by data source across LFAs. Data was limited to mid-season samples.

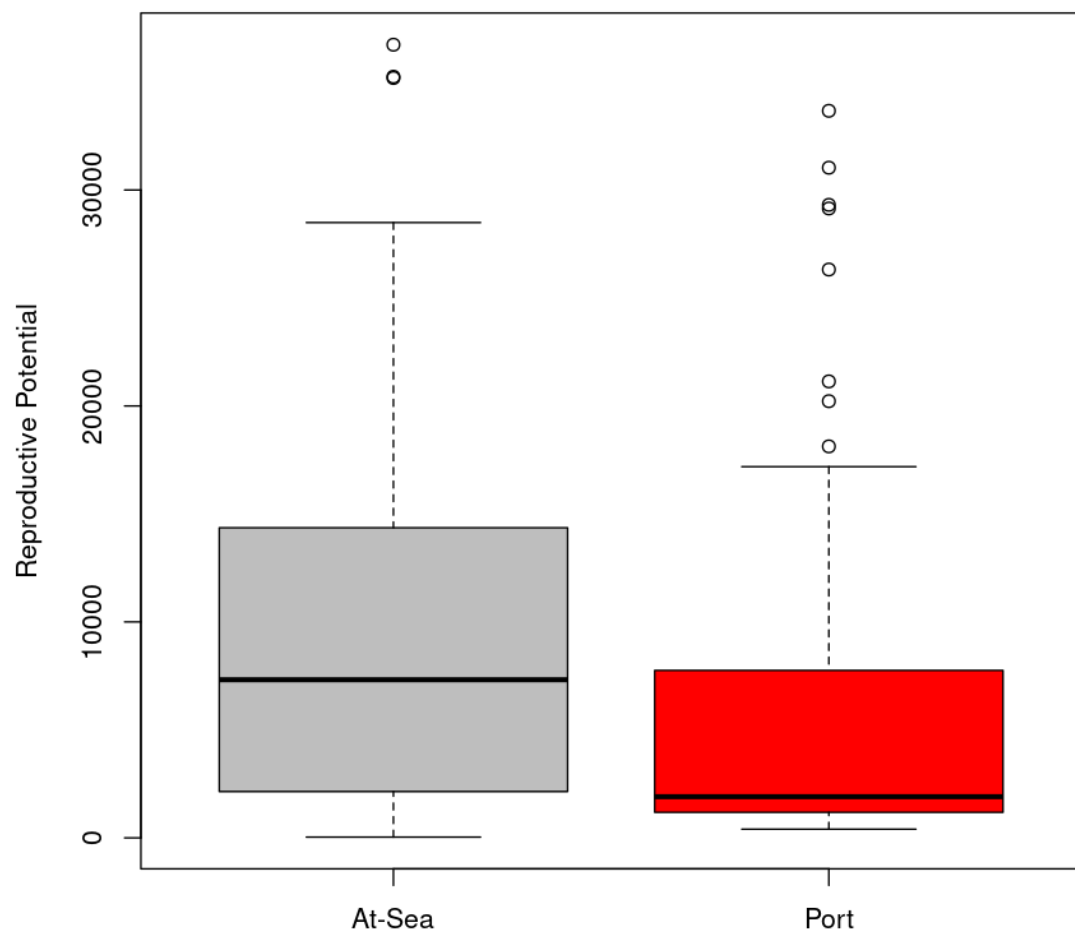


Figure 65: Boxplot of the estimates of reproductive potential by data source across all LFAs.

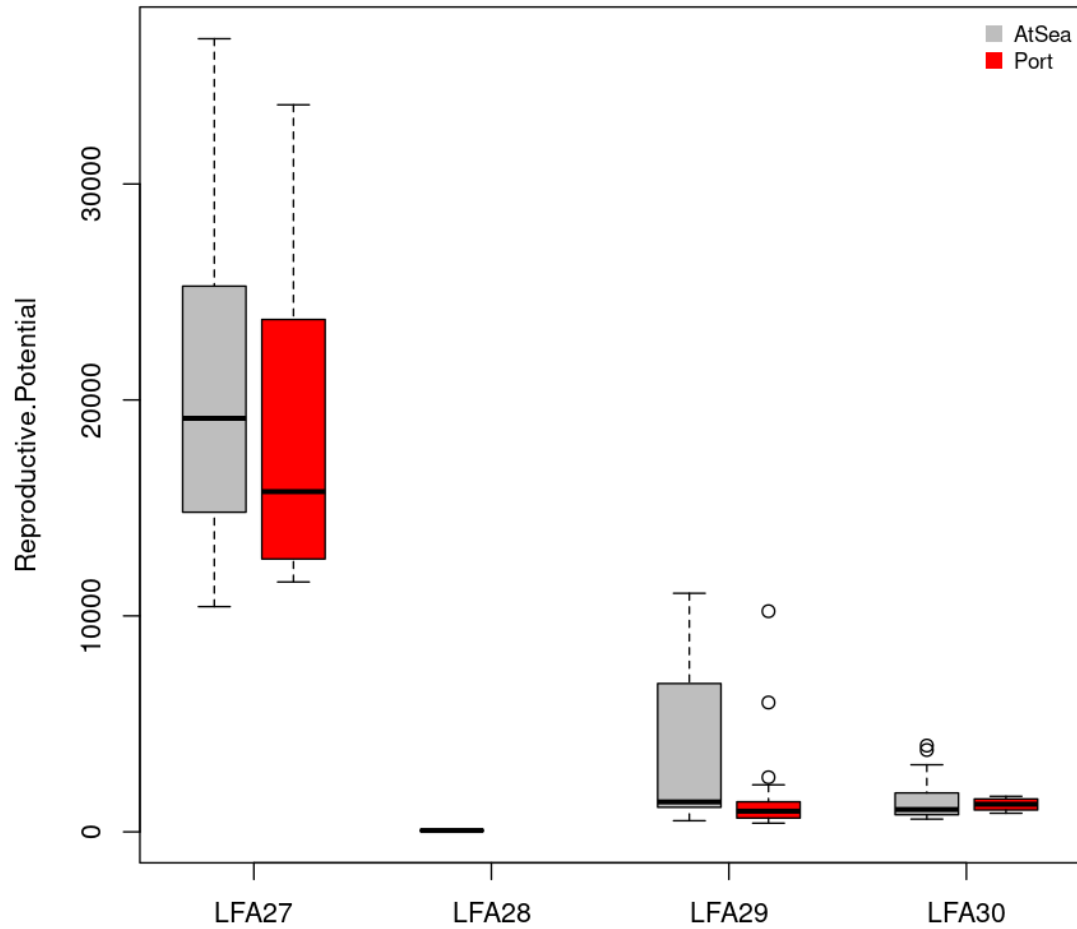


Figure 66: Boxplot of the time series of reproductive potential for lobsters sampled by data source for LFA 27-30.

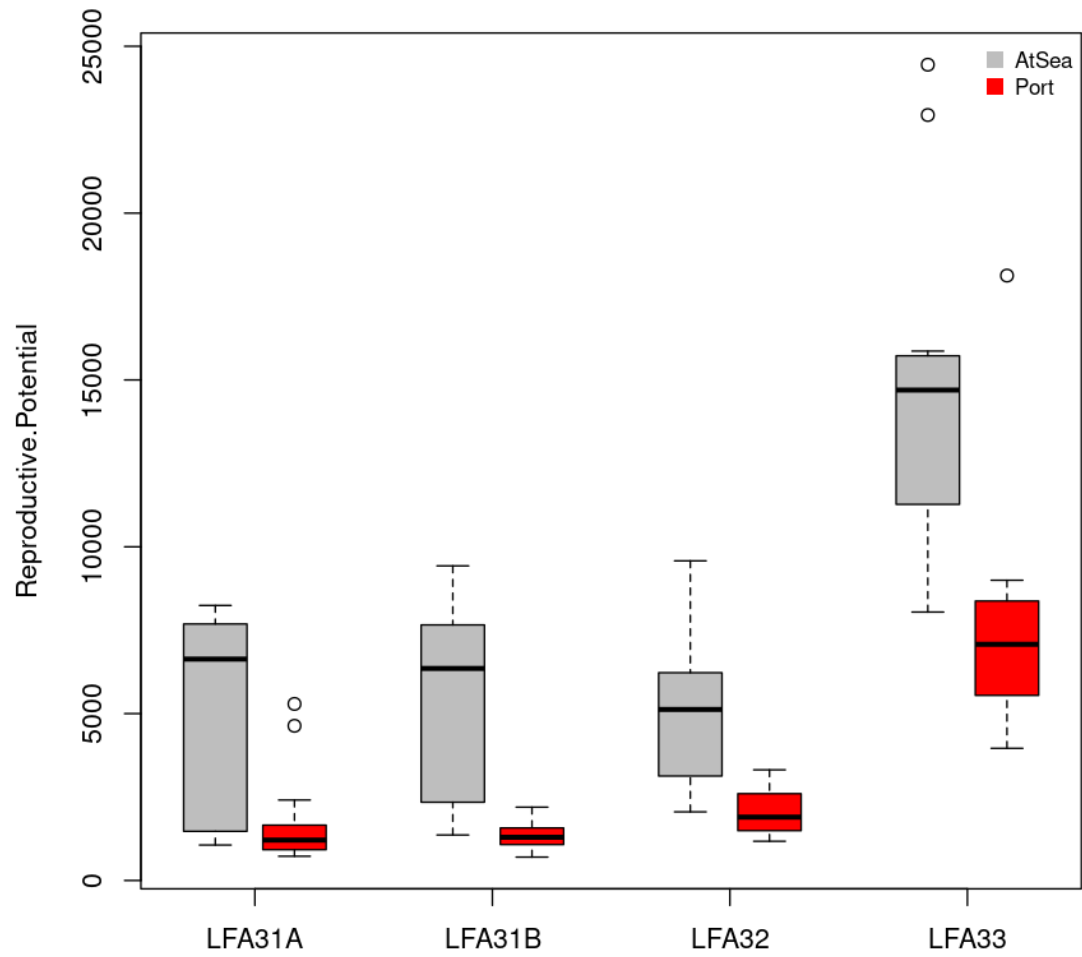


Figure 67: Boxplot of the time series of reproductive potential for lobsters sampled by data source for LFA 31A-33.

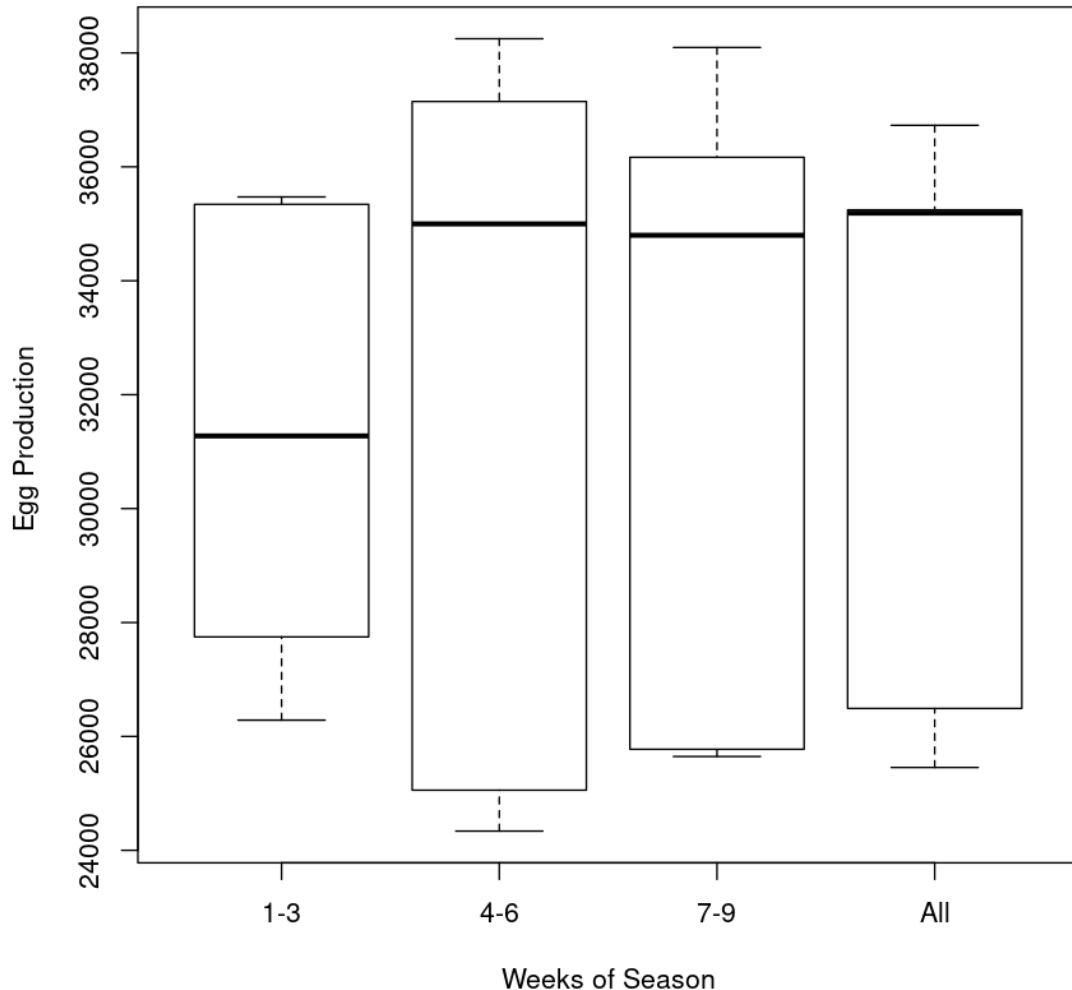


Figure 68: Boxplots of estimated reproductive potential from sea sampling dates (weeks of season) observed from LFA 27 during the 2011-2015 seasons.

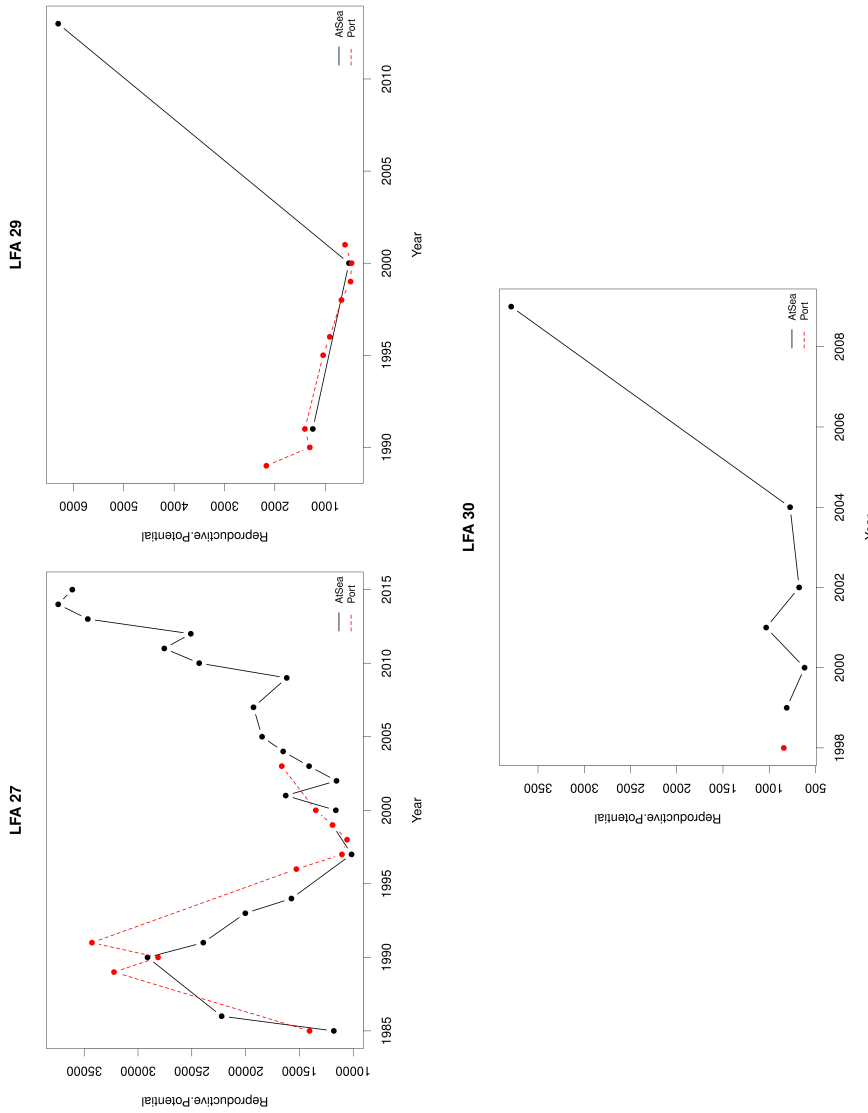


Figure 69: Time series of the reproductive potential by data source across LFAs. Data was limited to mid-season samples.

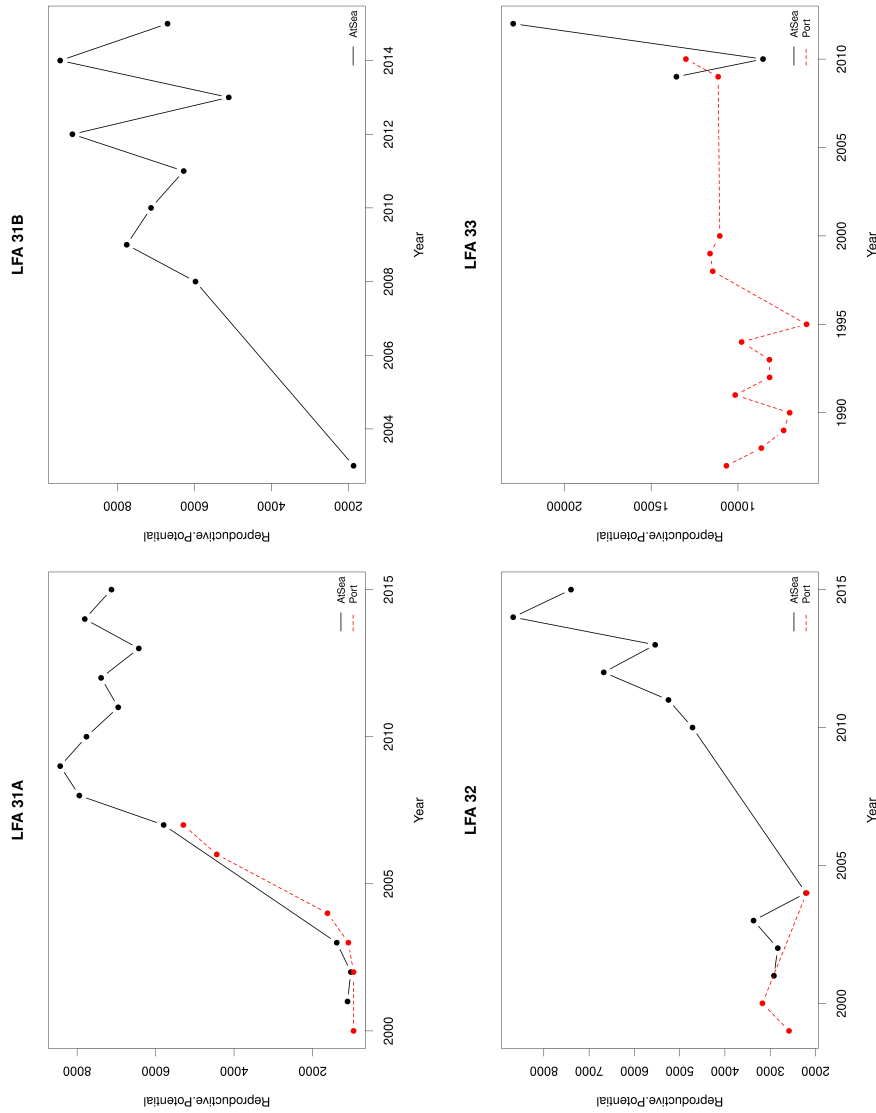


Figure 70: Time series of the reproductive potential by data source across LFAs. Data was limited to mid-season samples.

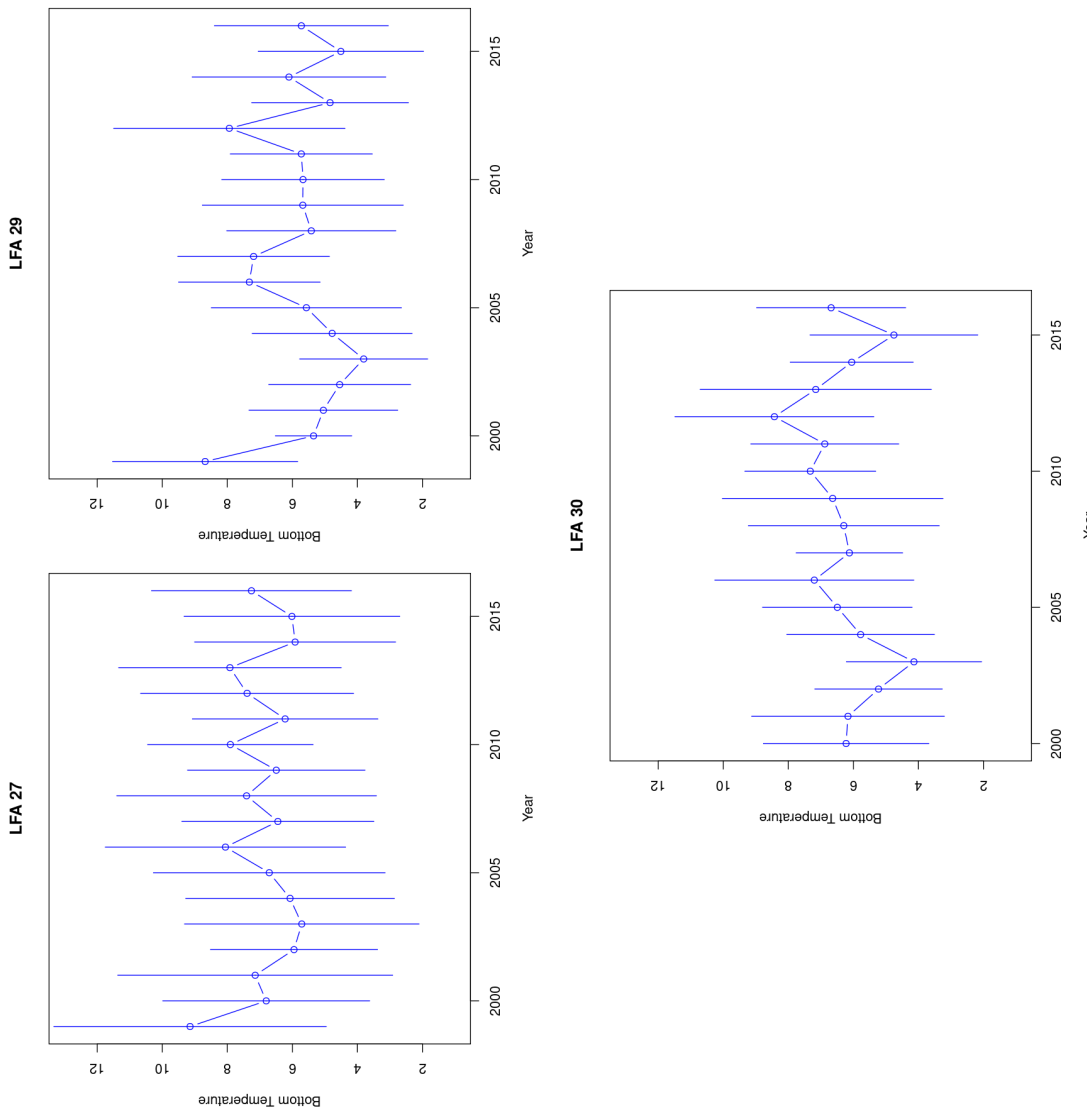


Figure 71: Time series of bottom temperatures across LFAs. Data represents the mean and standard deviation of the fishing season from the FSRS recruitment traps.

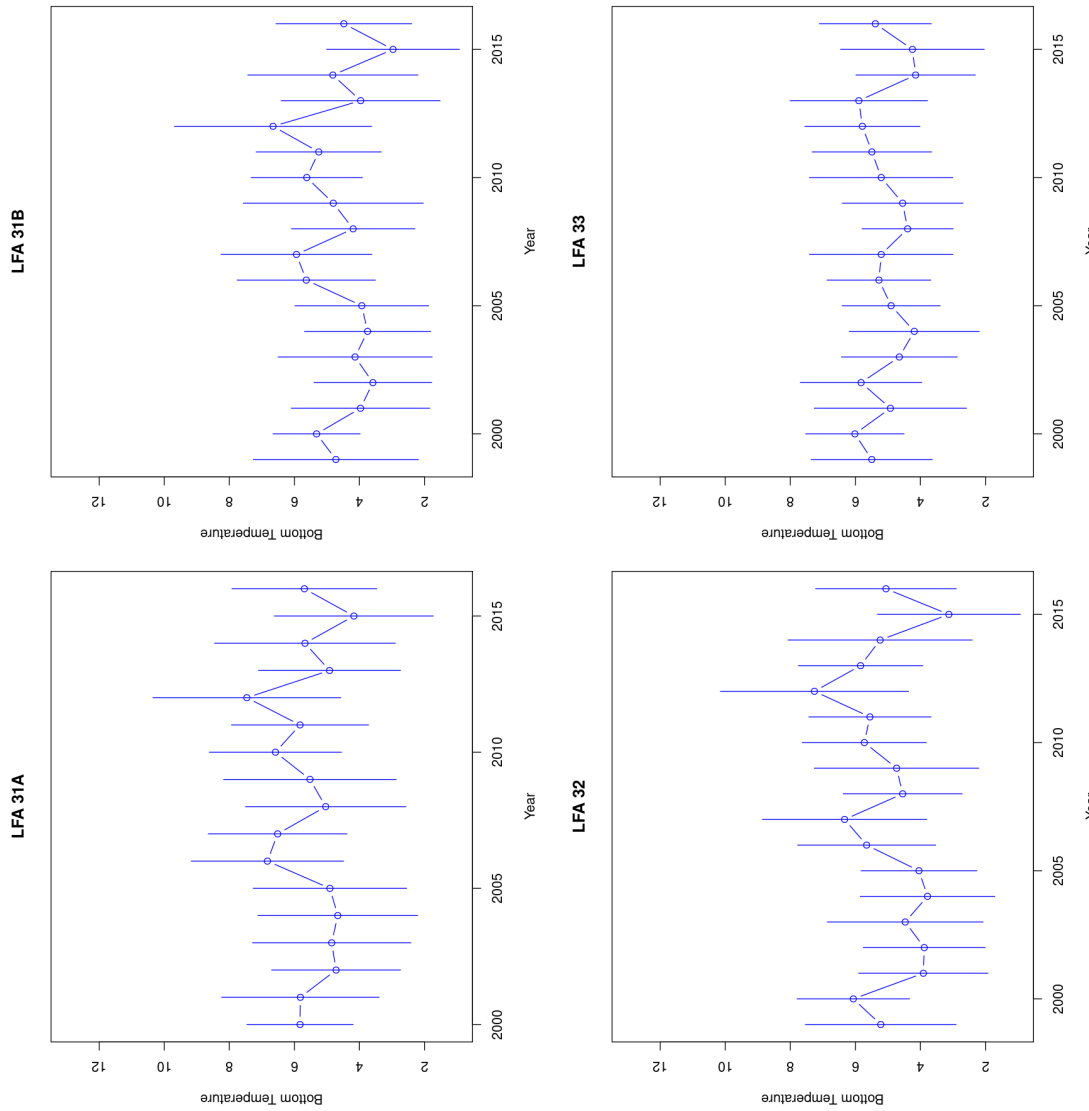


Figure 72: Time series of bottom temperatures across LFAs. Data represents the mean and standard deviation of the fishing season from the FSRS recruitment traps.

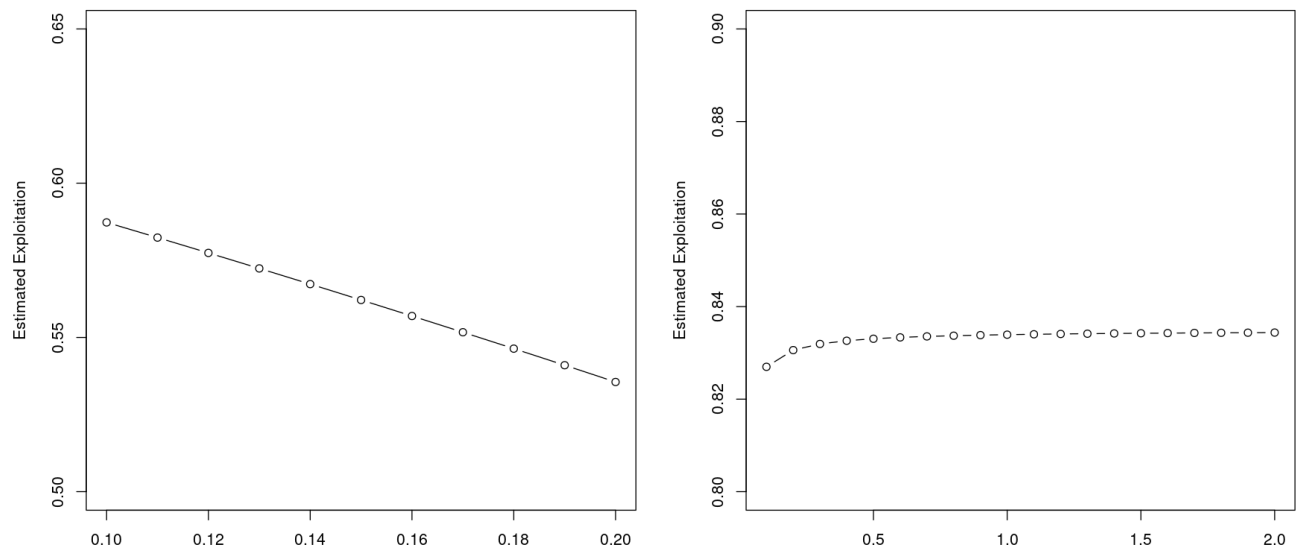


Figure 73: Sensitivity of cohort analysis to changing natural mortality (left) or changing fishing mortality on the oldest ages (right) on estimated exploitation rates. Size frequency data for sensitivity analyses were from LFA 33 sampled in 2015.

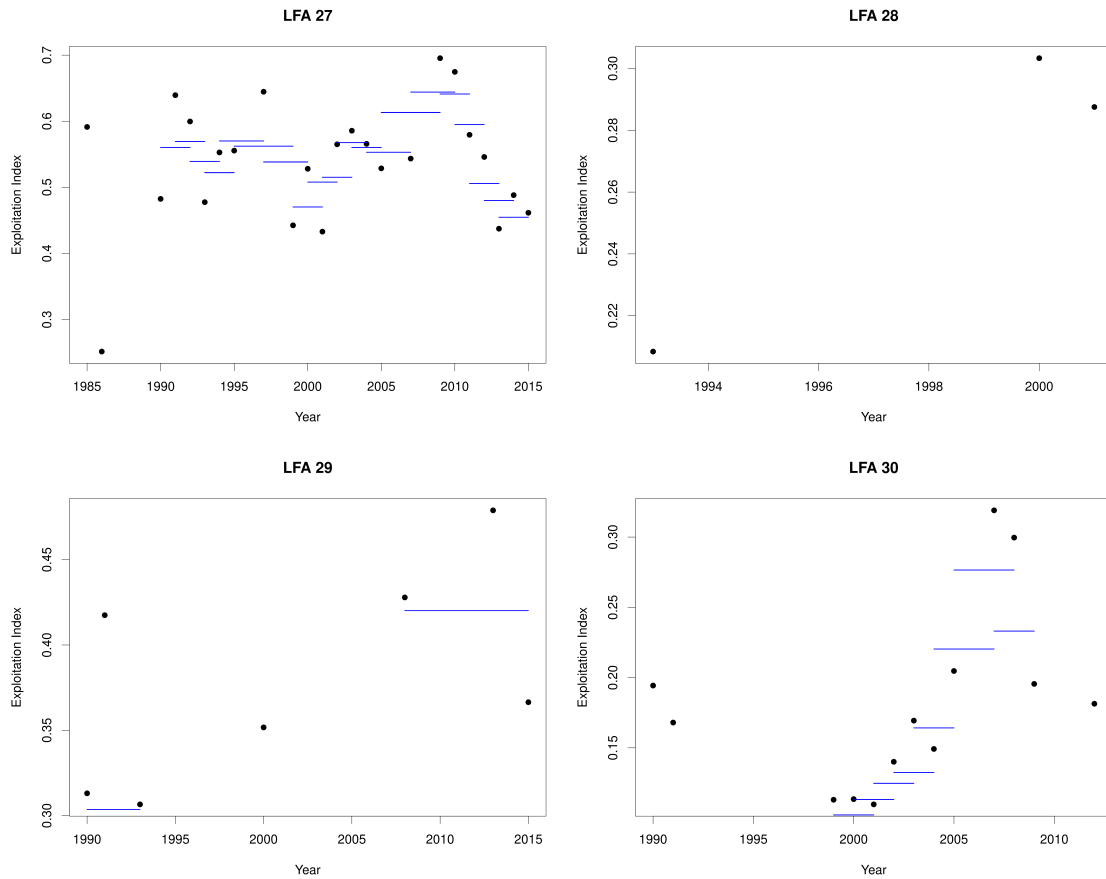


Figure 74: Estimates of exploitation from cohort analysis by year (black points) and by aggregate years (blue lines) within each LFA from at sea samples. The range of y-axes are not shared across plots.

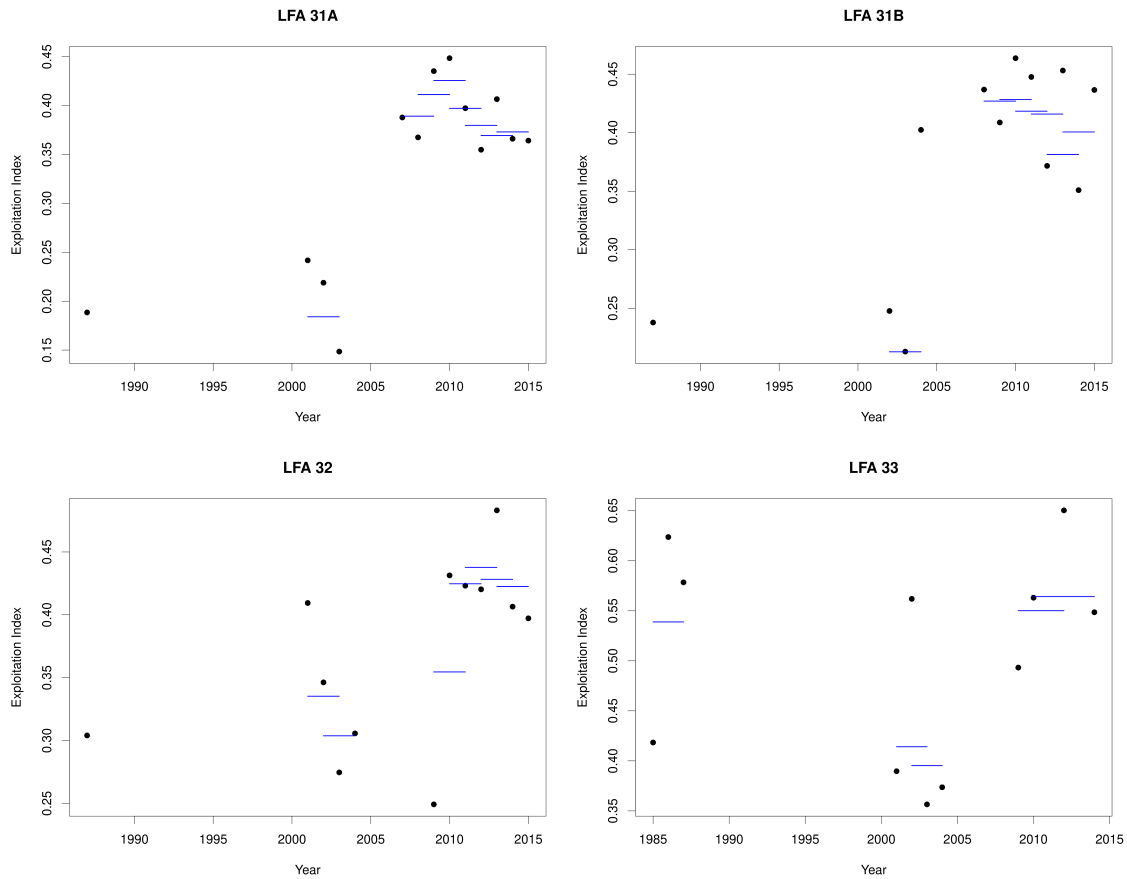


Figure 75: Estimates of exploitation from cohort analysis by year (black points) and by aggregate years (blue lines) within each LFA from at sea samples. The range of y-axes are not shared across plots

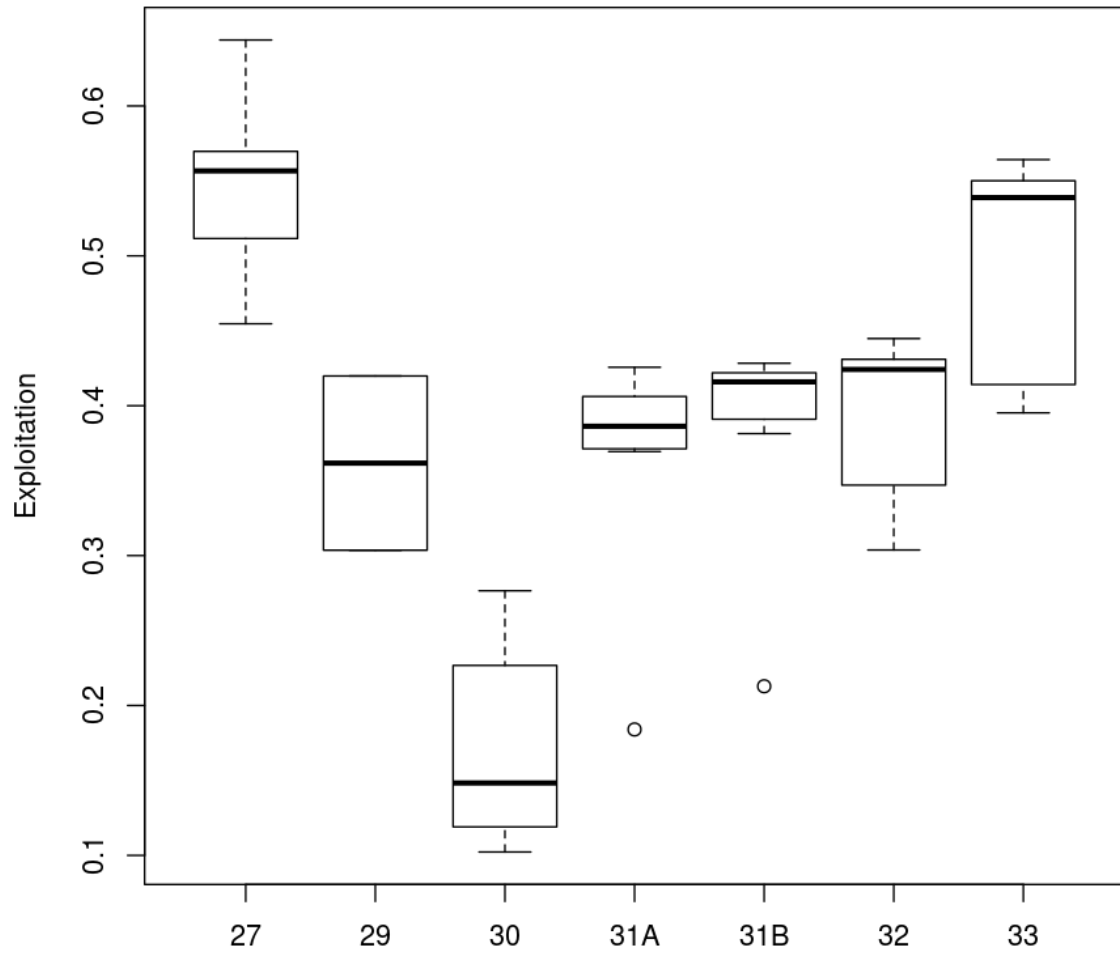


Figure 76: Boxplots of mean exploitation by LFA using the three year accumulated length frequencies from at sea sampled data.

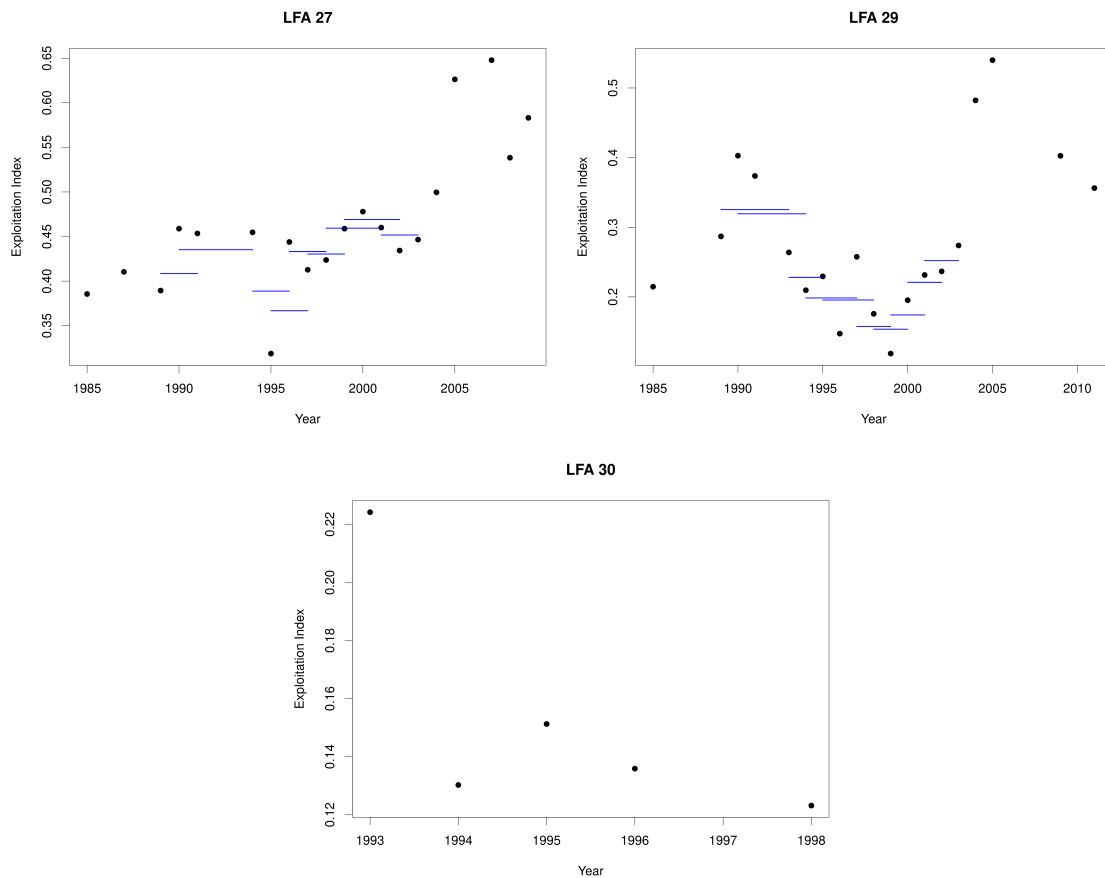


Figure 77: Estimates of exploitation from cohort analysis by year (black points) and by aggregate years (blue lines) within each LFA from port samples. The range of y-axes are not shared across plots.

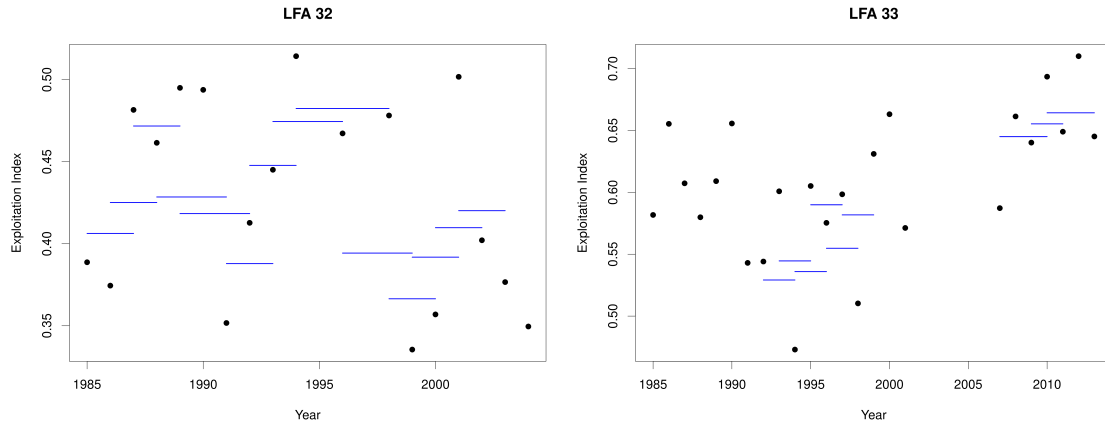


Figure 78: Estimates of exploitation from cohort analysis by year (black points) and by aggregate years (blue lines) within each LFA from port samples. The range of y-axes are not shared across plots

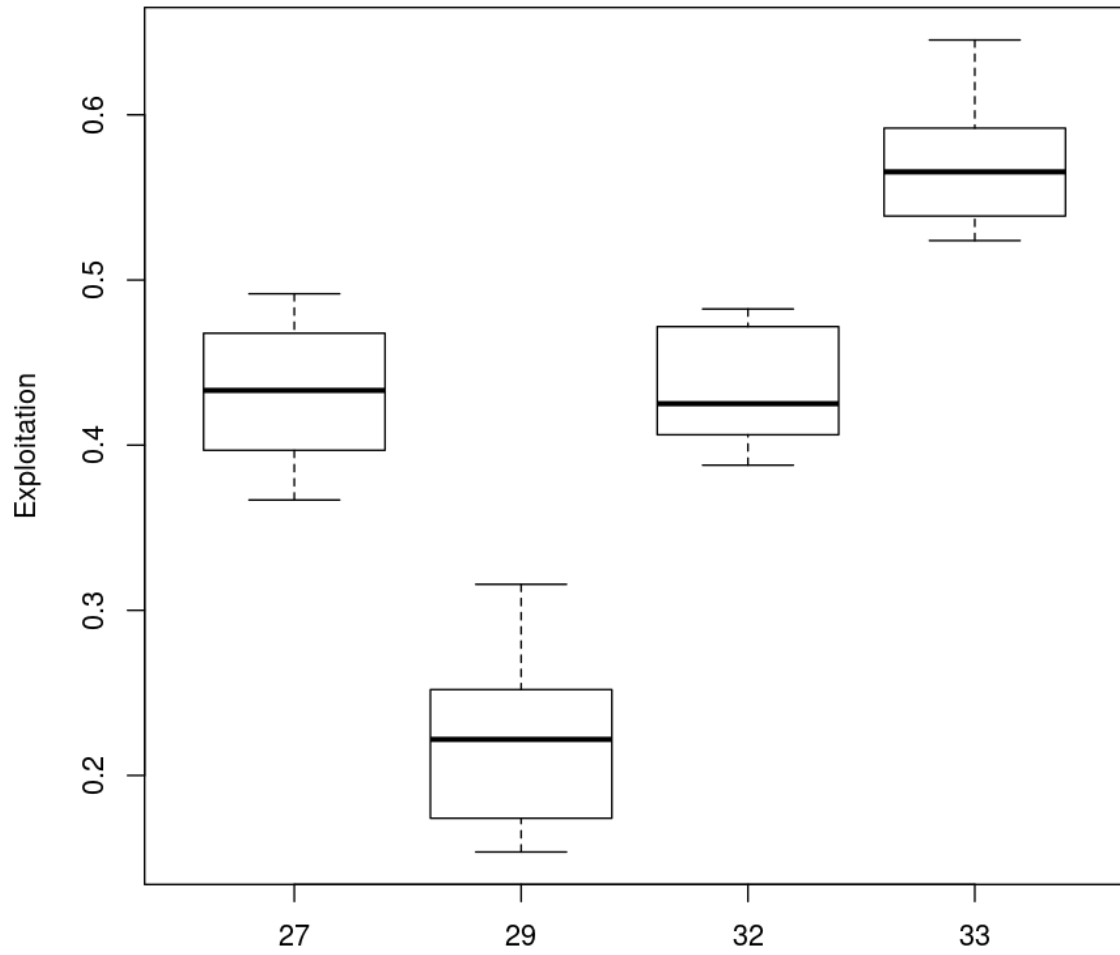


Figure 79: Boxplots of mean exploitation by LFA using the three year accumulated length frequencies from port sampled data.

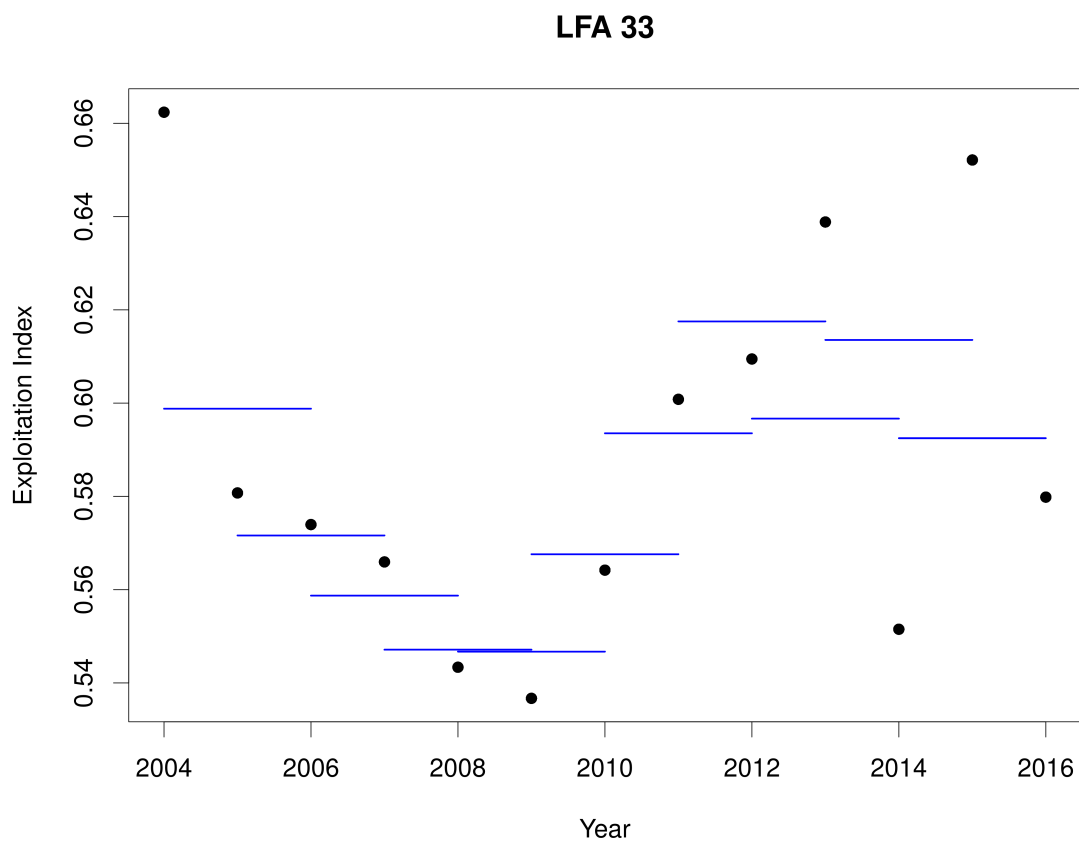


Figure 80: Estimates of exploitation from cohort analysis by year (black points) and by aggregate years (blue lines) from FSRS commercial trap data.

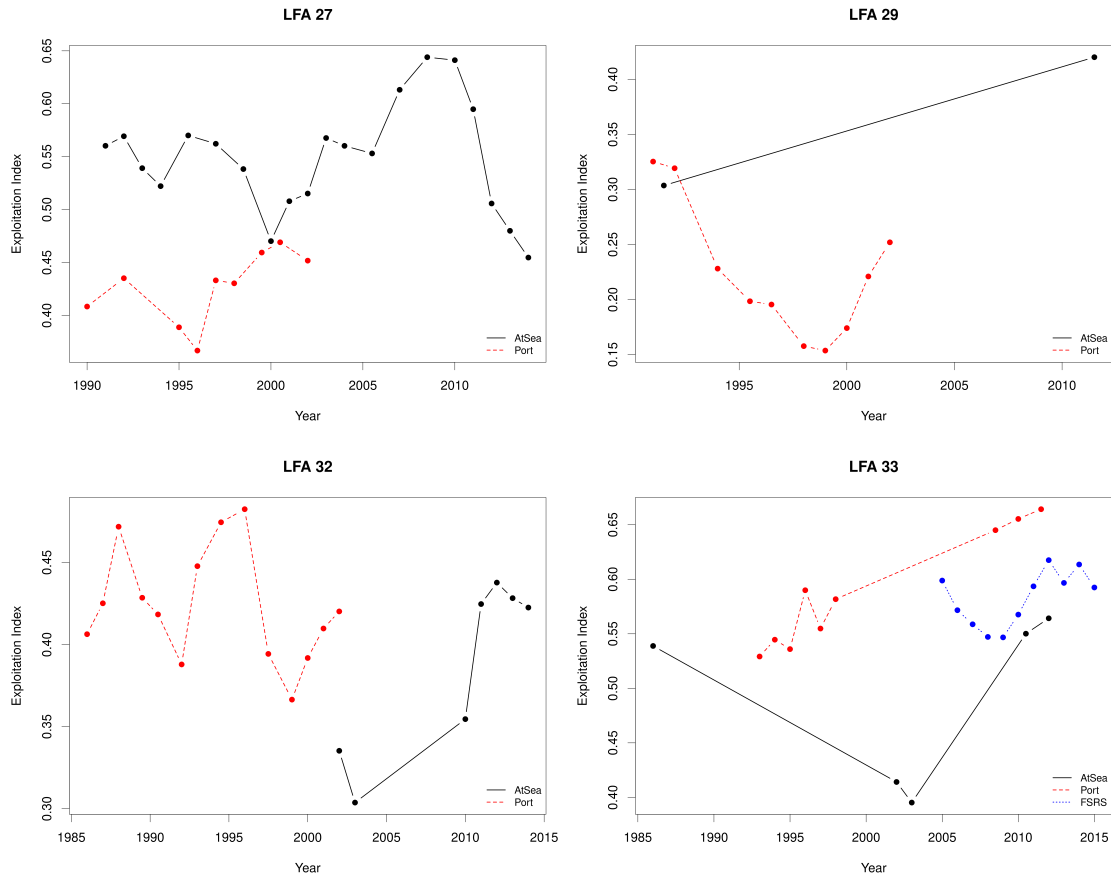


Figure 81: Estimates of three year aggregated exploitation (points represents the mean of the three years) from cohort analysis by year and data source. Black solid lines represent at sea collected data, red dashed lines represent port sampled data and blue dotted lines (LFA 33 only) represent FSRS commercial trap samples. The range of y-axes are not shared across plots

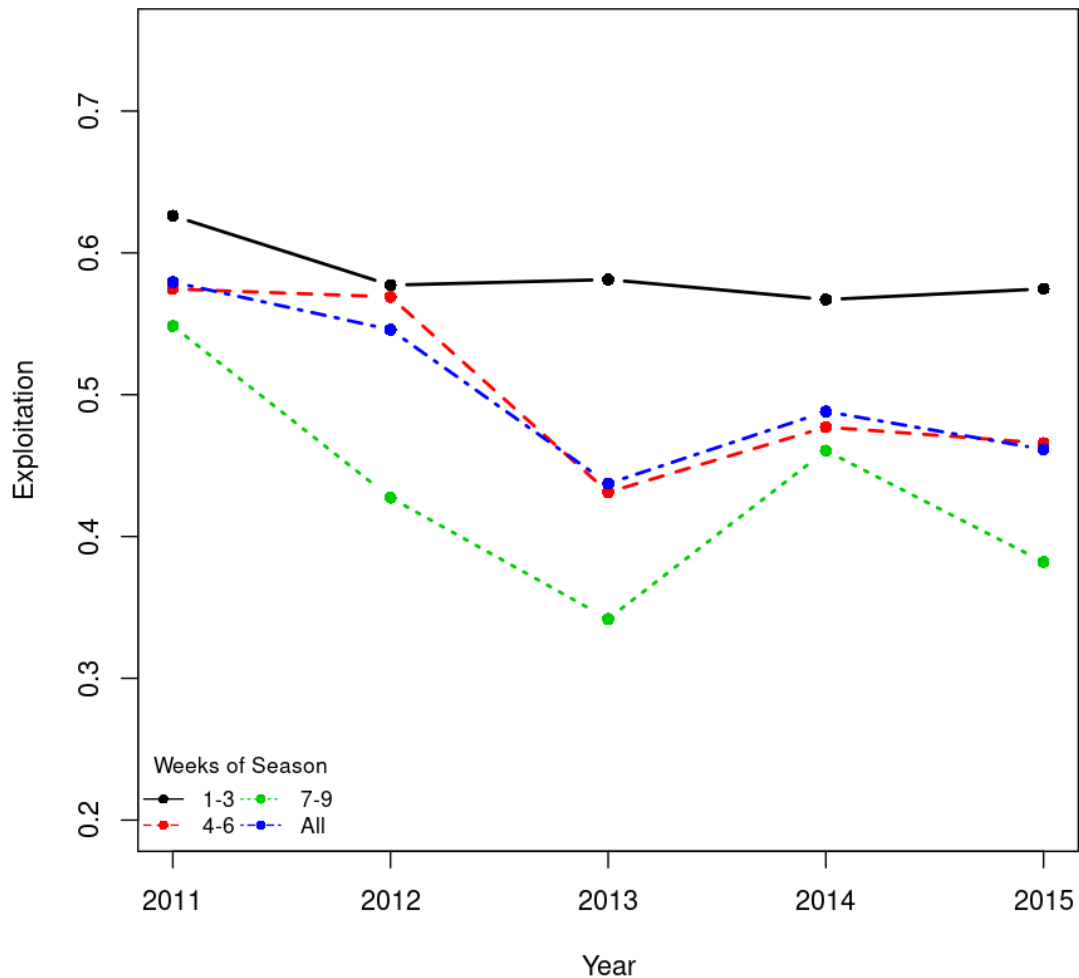


Figure 82: Impact of at sea sampling dates on estimated exploitation estimates from LFA 27 during the 2011-2015 seasons. Lines represent the landings weighted estimated exploitation from cohort analysis with size frequencies from each week of season block.

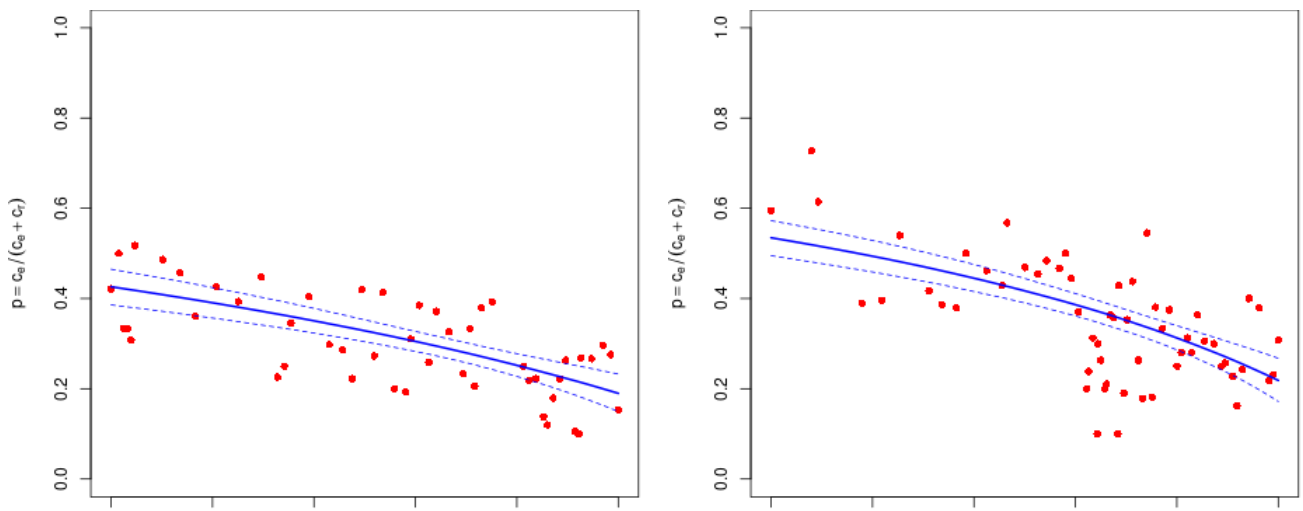


Figure 83: Example change in ratio of exploitable to total sample against cumulative scaled landings. Solid blue line represents CCIR median predictions whereas dashed blue lines represent 95% credible intervals. Left panel represents the results from LFA 27 south in 2007. Right panel represents results from LFA 33 east in 2009.

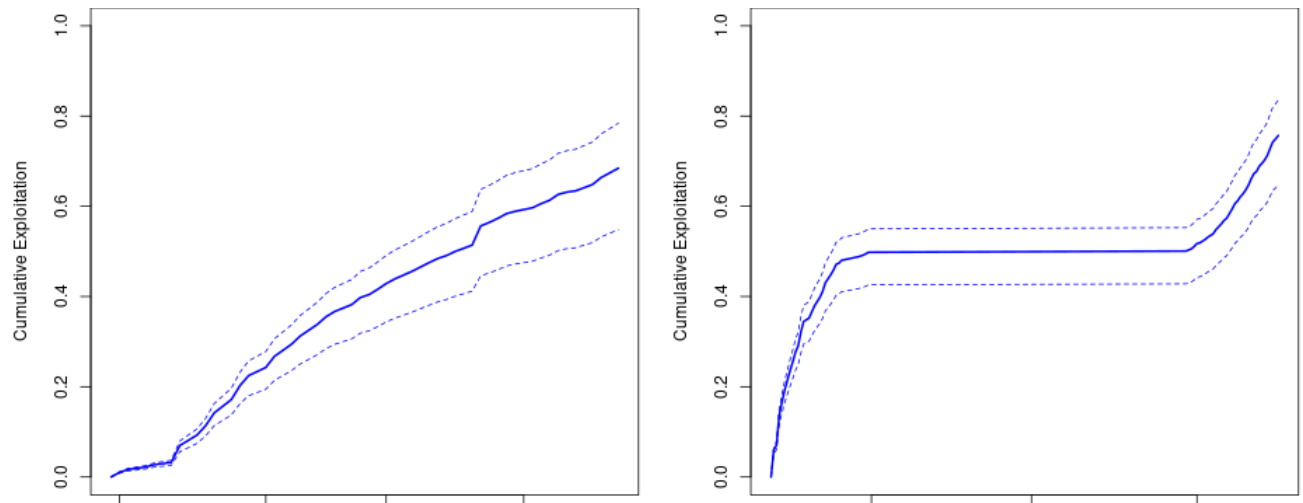


Figure 84: Within season CCIR estimated exploitation indices. Solid blue line represents CCIR median predicted exploitation whereas dashed blue lines represent 95% credible intervals. Left panel represents the results from LFA 27 south in 2007. Right panel represents results from LFA 33 east in 2009.

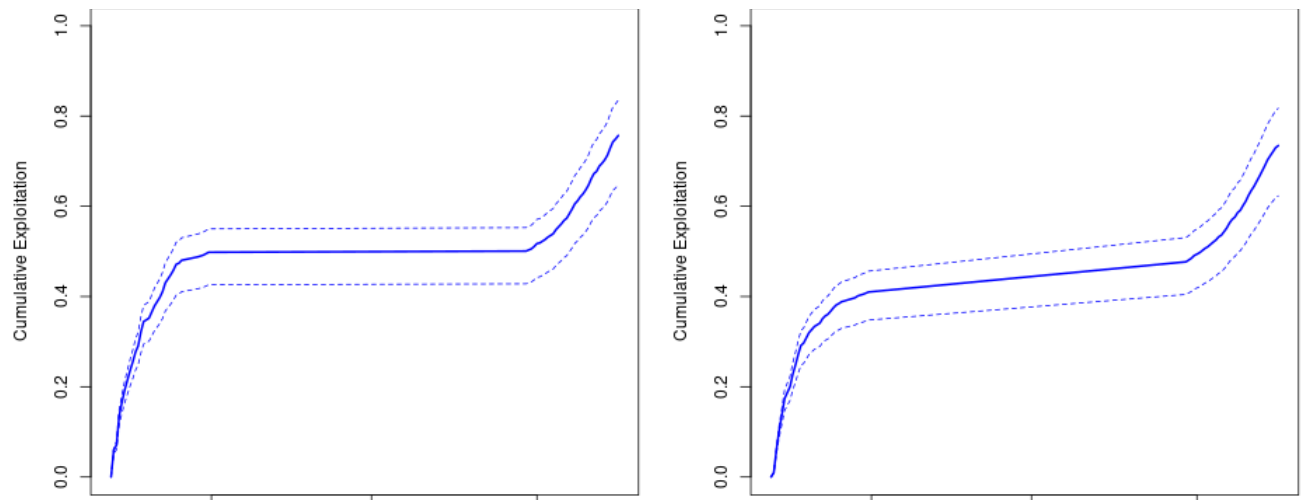


Figure 85: Comparison of within season CCIR estimated exploitation indices estimated using either the cumulative monitoring effort (left) or cumulative landings (right). Solid blue line represents CCIR median predicted exploitation whereas dashed blue lines represent 95% credible intervals. Both panels represent results from LFA 33 east in 2009.

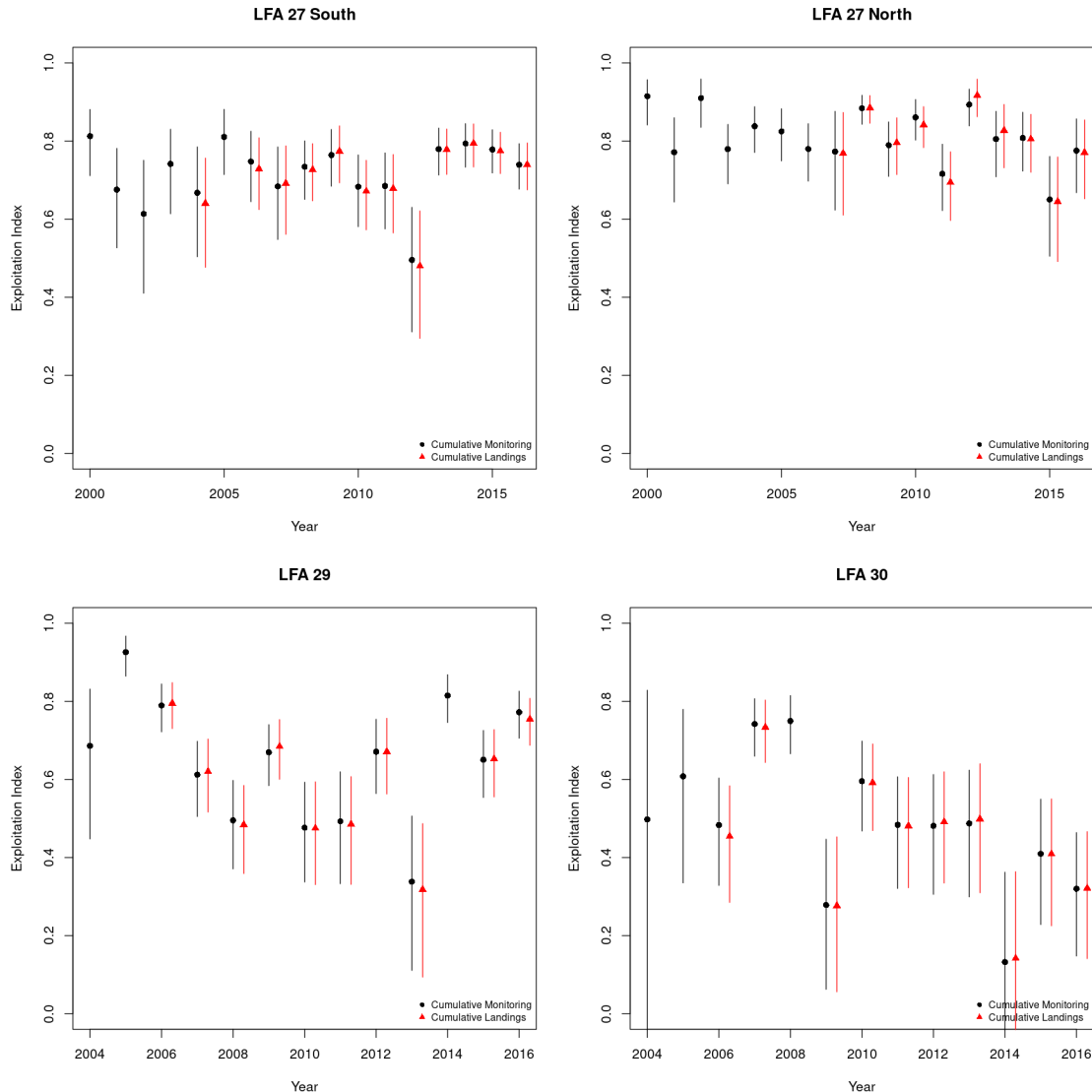


Figure 86: Comparison of predictor variables (cumulative monitoring - black or cumulative landings - red) on CCIR estimated end of season exploitation (points) with 95% credible intervals (vertical lines) by year within LFA 27 south and north, LFA 29 and LFA 30.

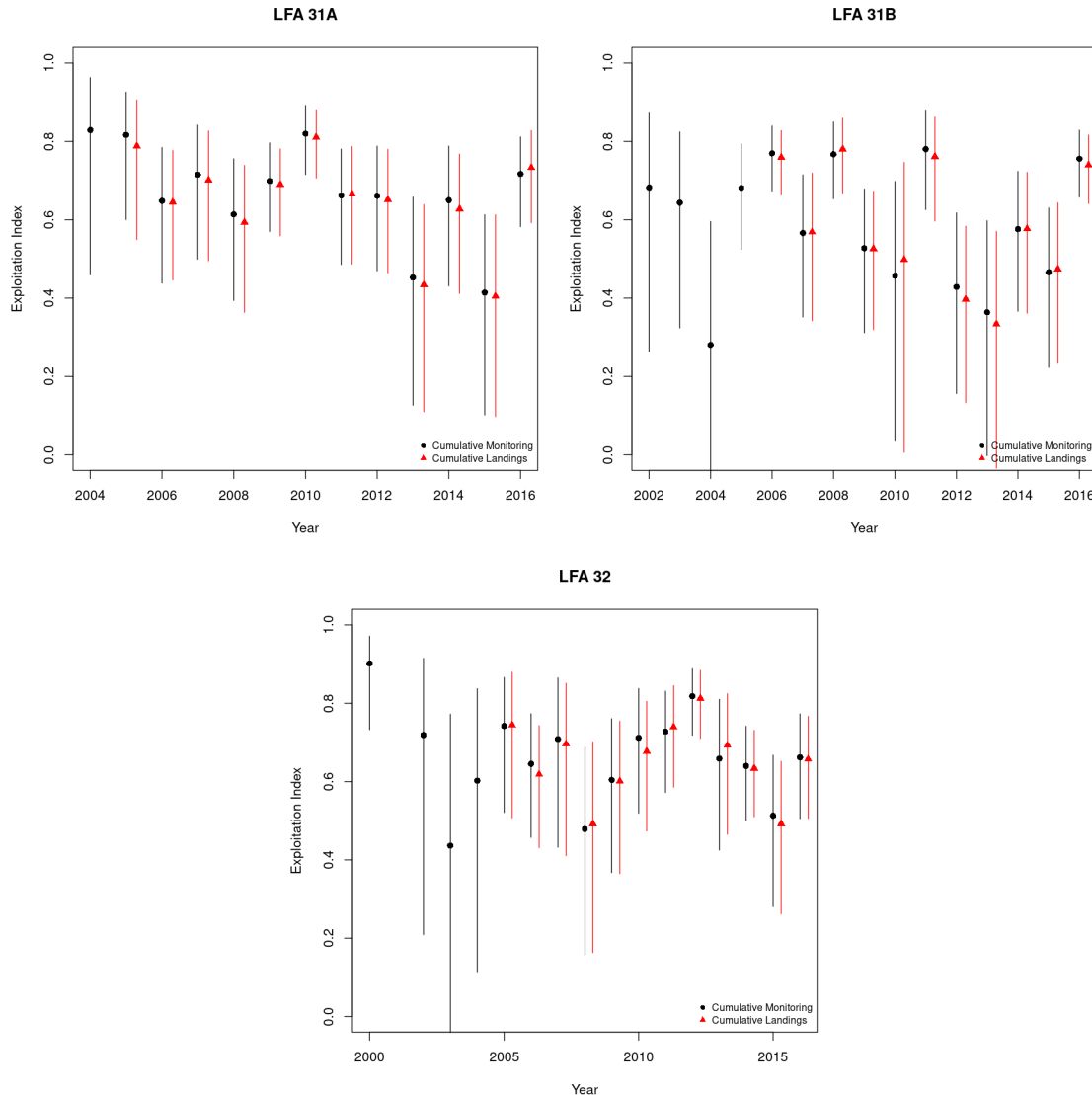


Figure 87: Comparison of predictor variables (cumulative monitoring - black or cumulative landings - red) on CCIR estimated end of season exploitation (points) with 95% credible intervals (vertical lines) by year within LFA 31A, LFA 31B and LFA 32.

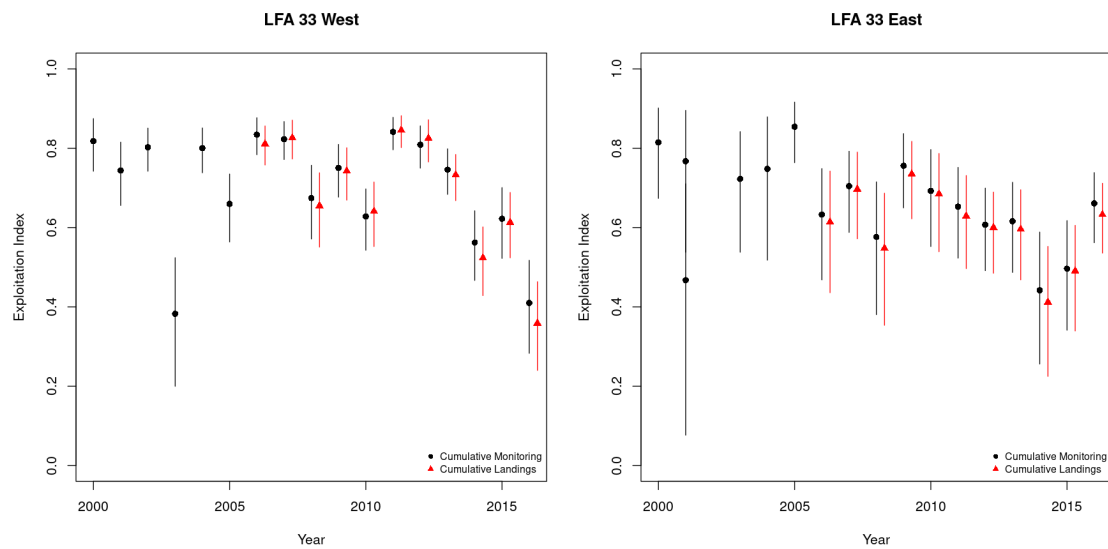


Figure 88: Comparison of predictor variables (cumulative monitoring - black or cumulative landings - red) on CCIR estimated end of season exploitation (points) with 95% credible intervals (vertical lines) by year within LFA 33 east and west.

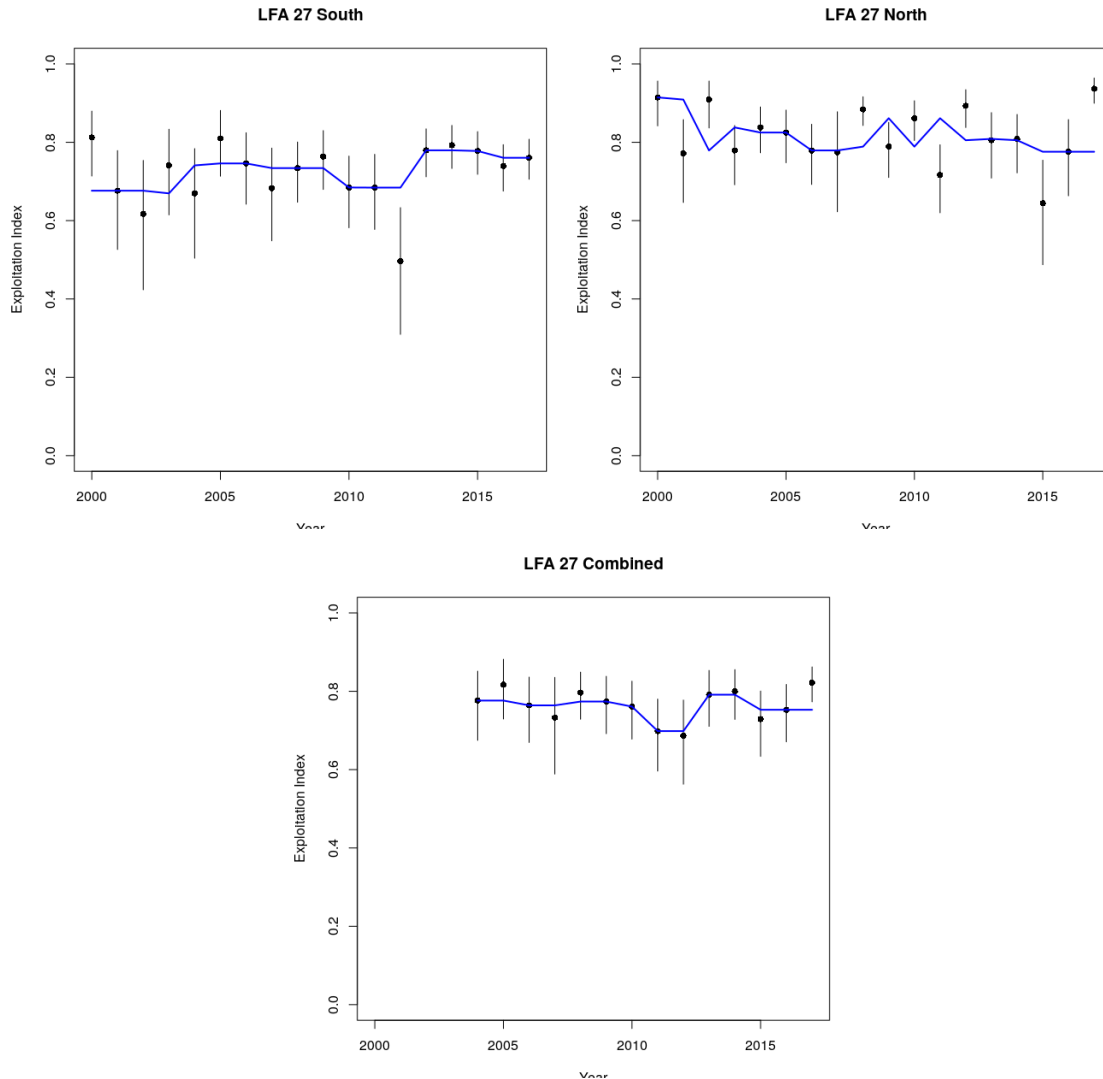


Figure 89: CCIR estimated end of season exploitation (points) with 95% credible intervals (vertical lines) by year within LFA 27 south, north or combined. The combined LFA 27 north and south represents the landings weighted annual exploitation. Within plots blue lines represent 3-year running median of exploitation estimates.

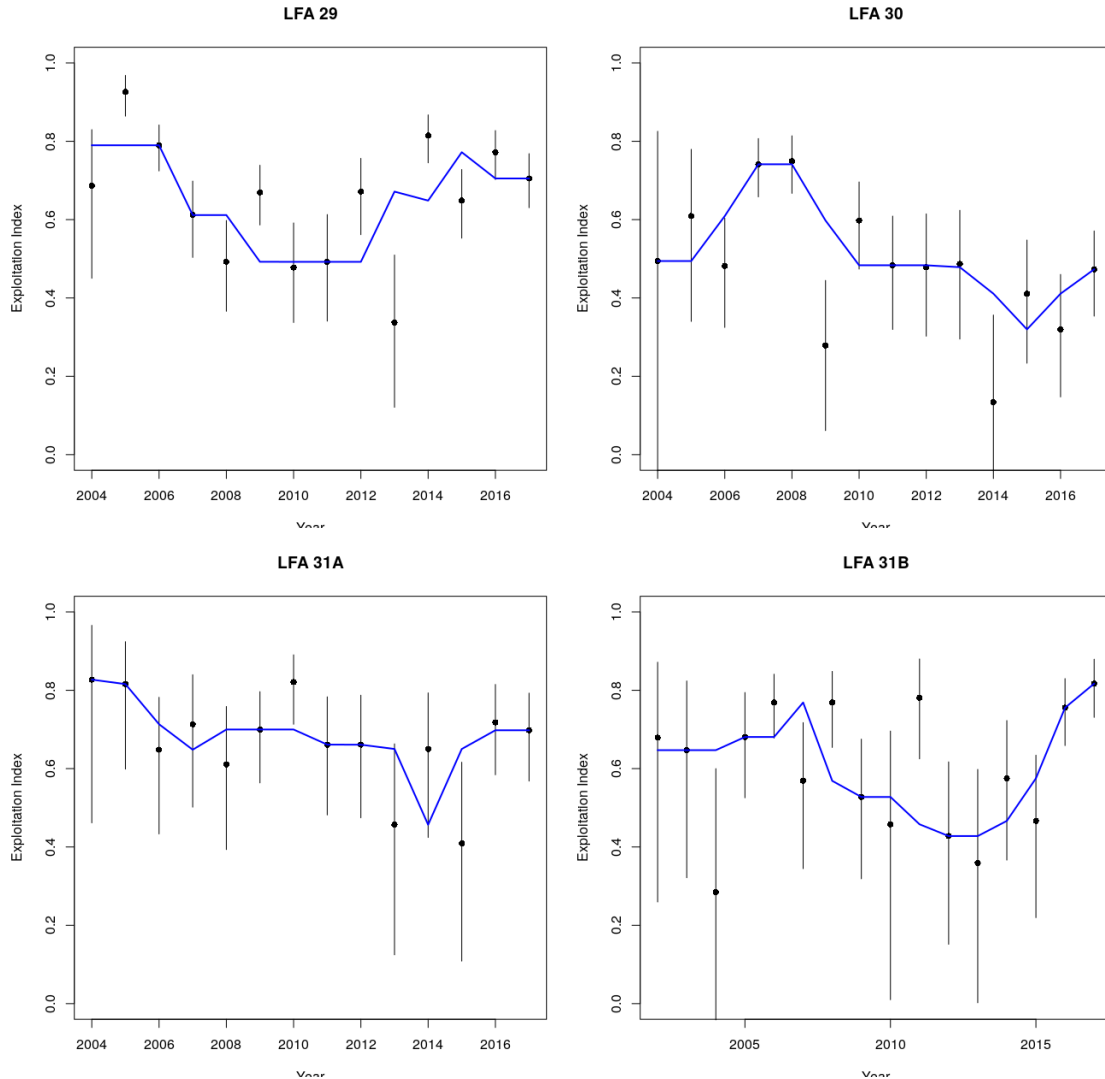


Figure 90: CCIR estimated end of season exploitation (points) with 95% credible intervals (vertical lines) by year within LFAs. Within plots blue lines represent 3-year running median of exploitation estimates.

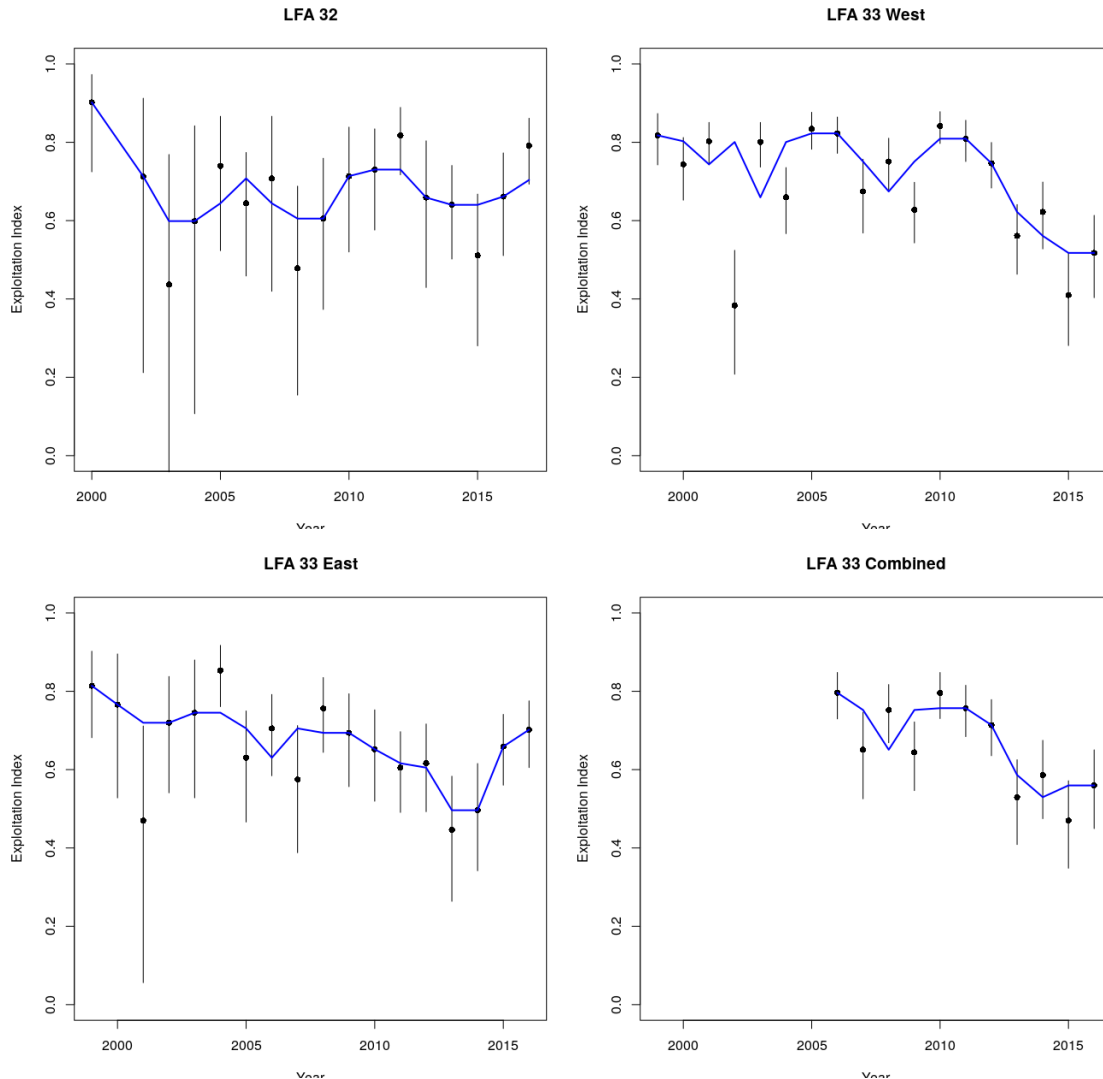


Figure 91: CCIR estimated end of season exploitation (points) with 95% credible intervals (vertical lines) by year within LFA 32, LFA 33 east, LFA 33 west and LFA 33 combined. The combined LFA 33 represents the landings weighted annual exploitation from the east and west combined. Within plots blue lines represent 3-year running median of exploitation estimates.

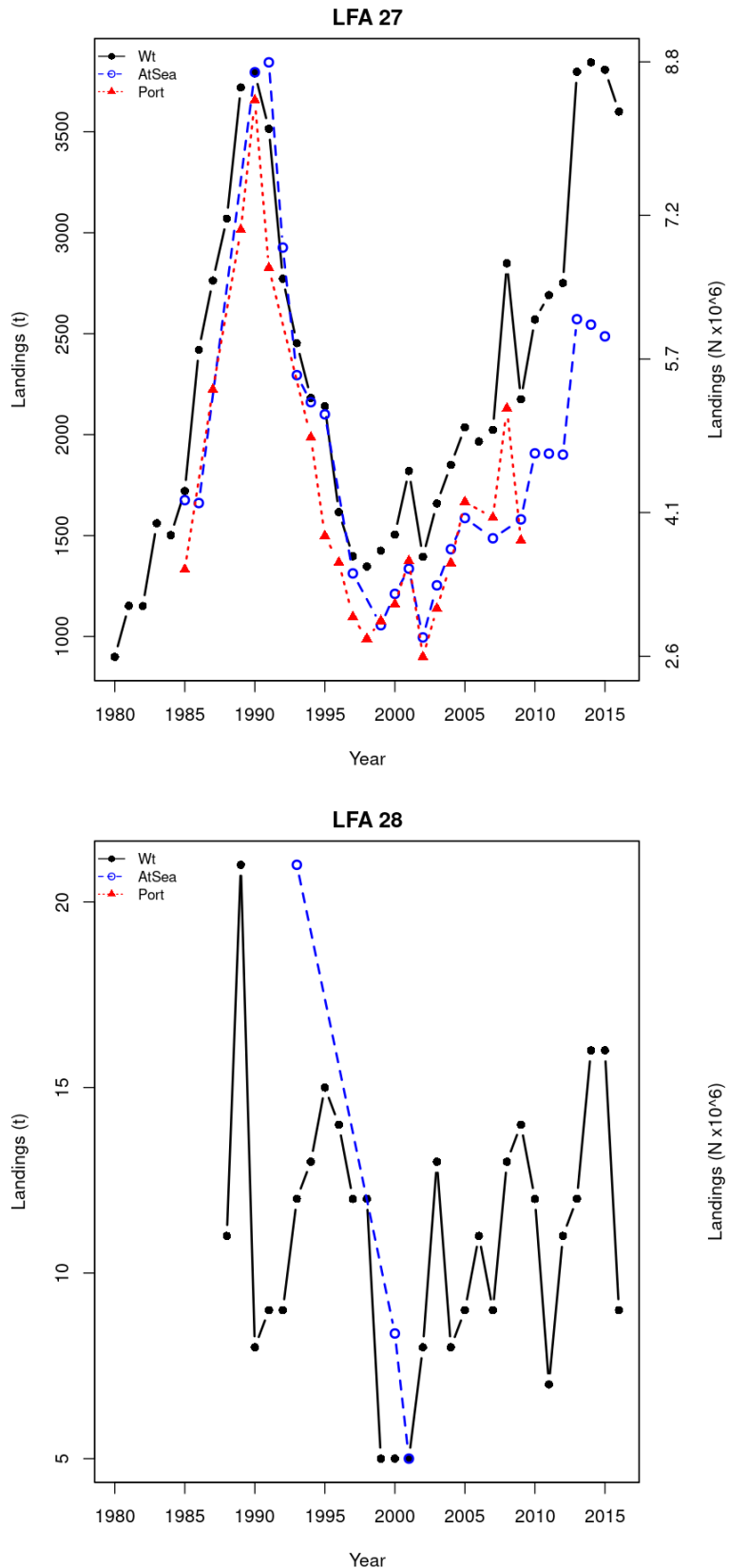


Figure 92: Time series of total landings in tons (black lines) and total landings in numbers estimated using length frequencies from At-Sea (blue) or Port samples (red).

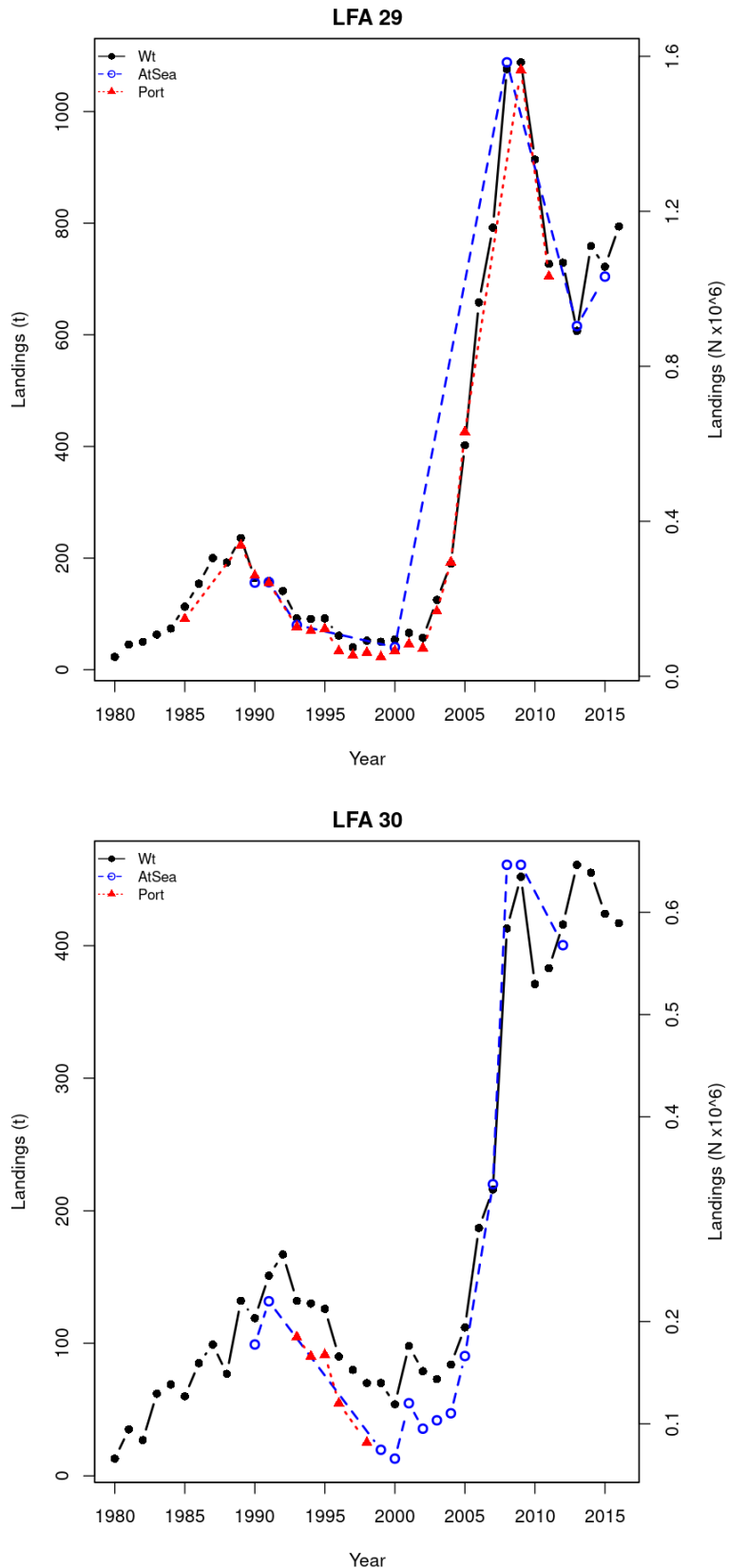


Figure 93: Time series of total landings in tons (black lines) and total landings in numbers estimated using length frequencies from At-Sea (blue) or Port samples (red).

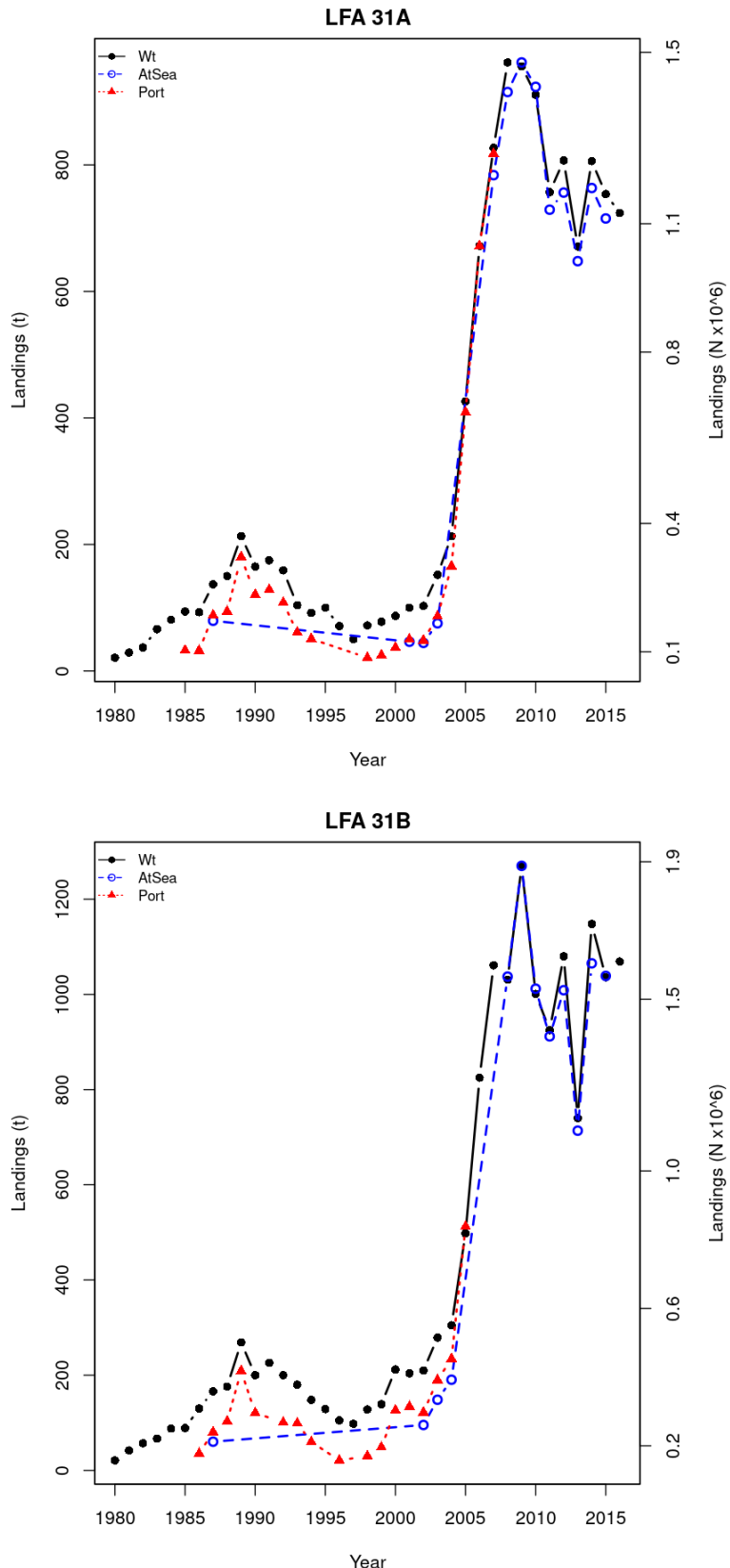


Figure 94: Time series of total landings in tons (black lines) and total landings in numbers estimated using length frequencies from At-Sea (blue) or Port samples (red).

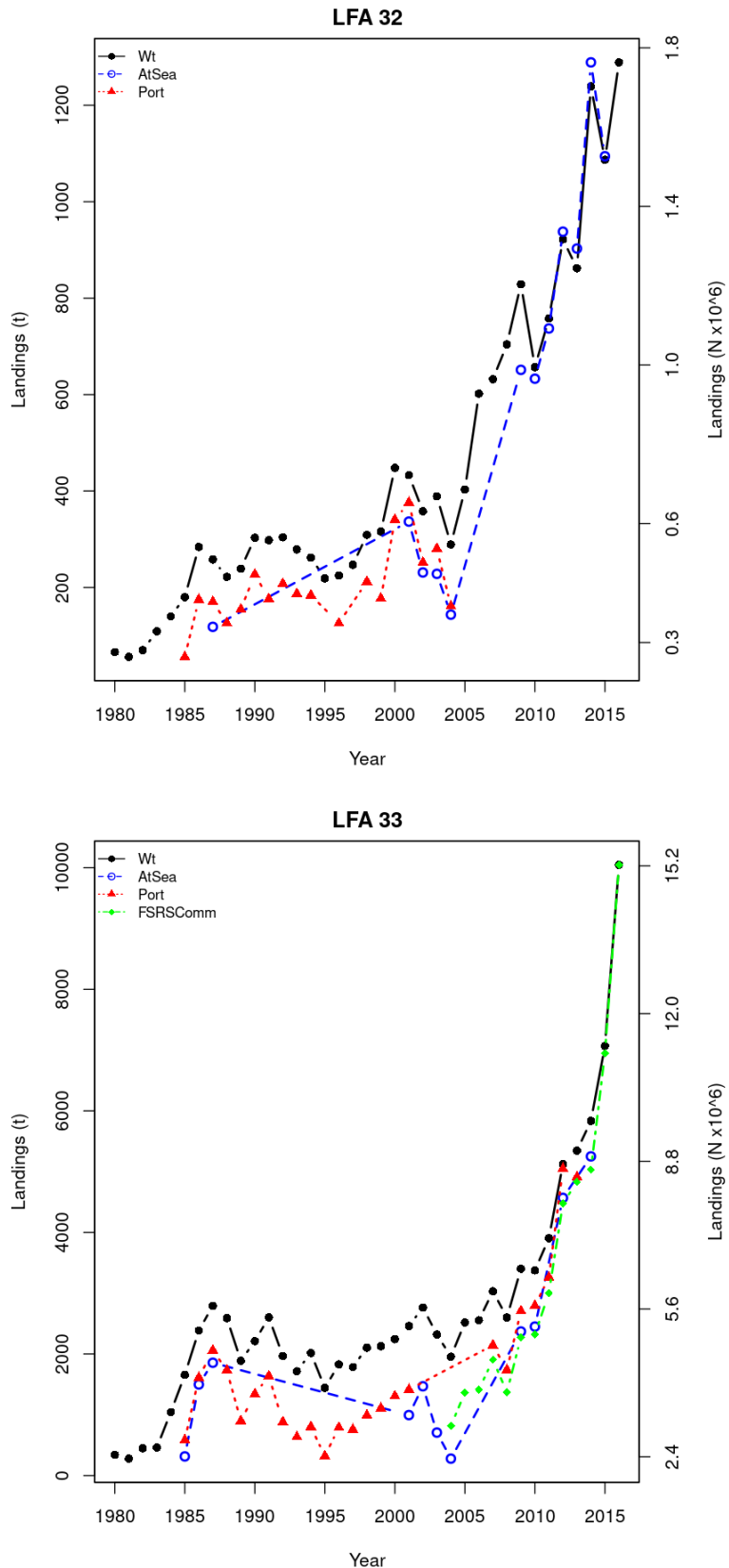


Figure 95: Time series of total landings in tons (black lines) and total landings in numbers estimated using length frequencies from At-Sea (blue) or Port samples (red), or FSRS commercial samples (green).

January 10, 2018

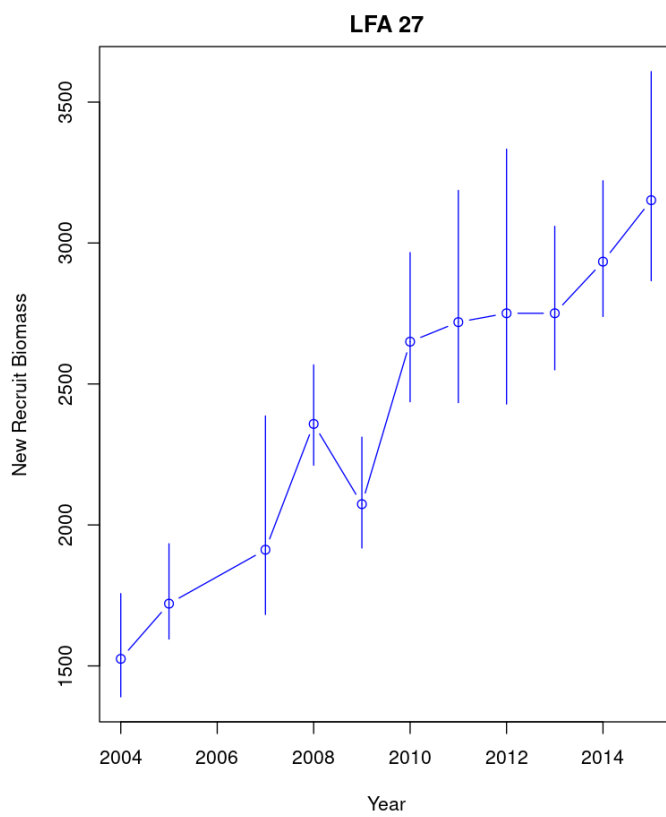


Figure 96: Time series of estimated recruitment biomass in tons with associated 95% error bounds.

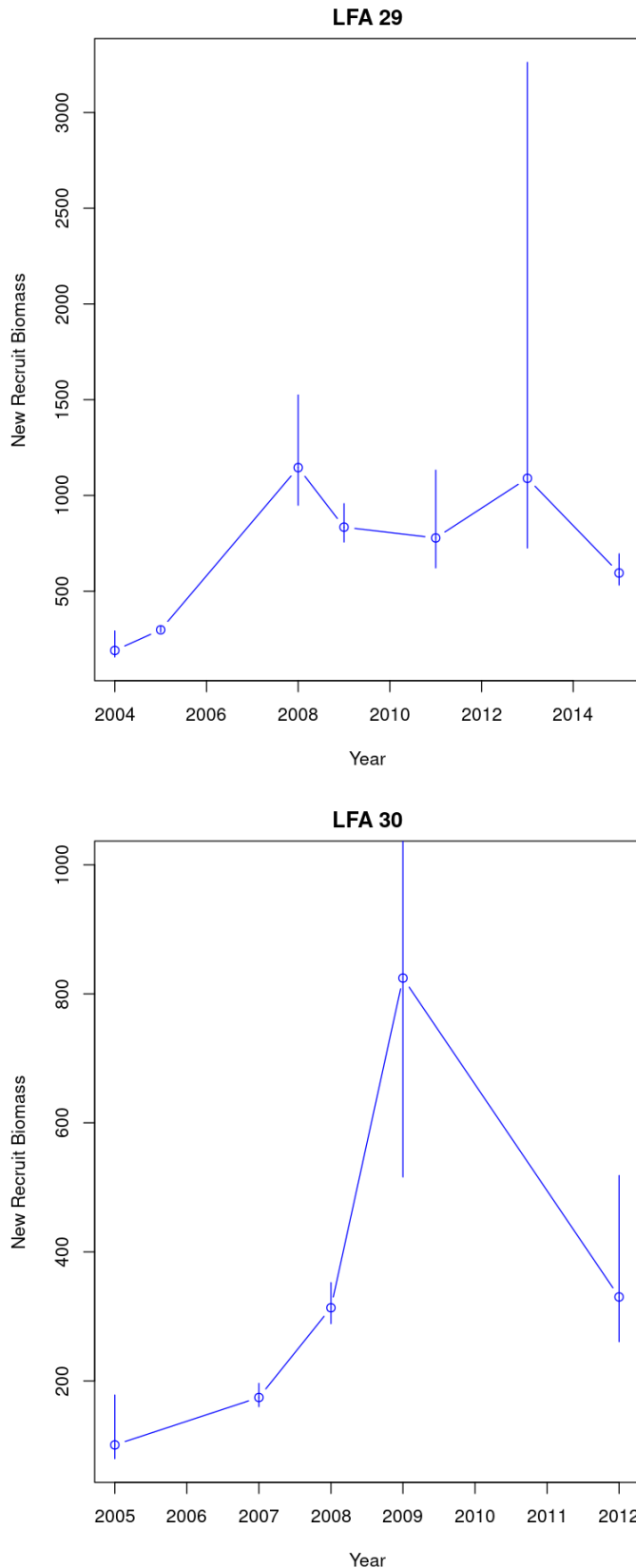


Figure 97: Time series of estimated recruitment biomass in tons with associated 95% error bounds. Upper bounds in LFA 30 in 2009 were not shown (4195 t). The full range of error was not shown as lower credible intervals on exploitation rates were not well defined.

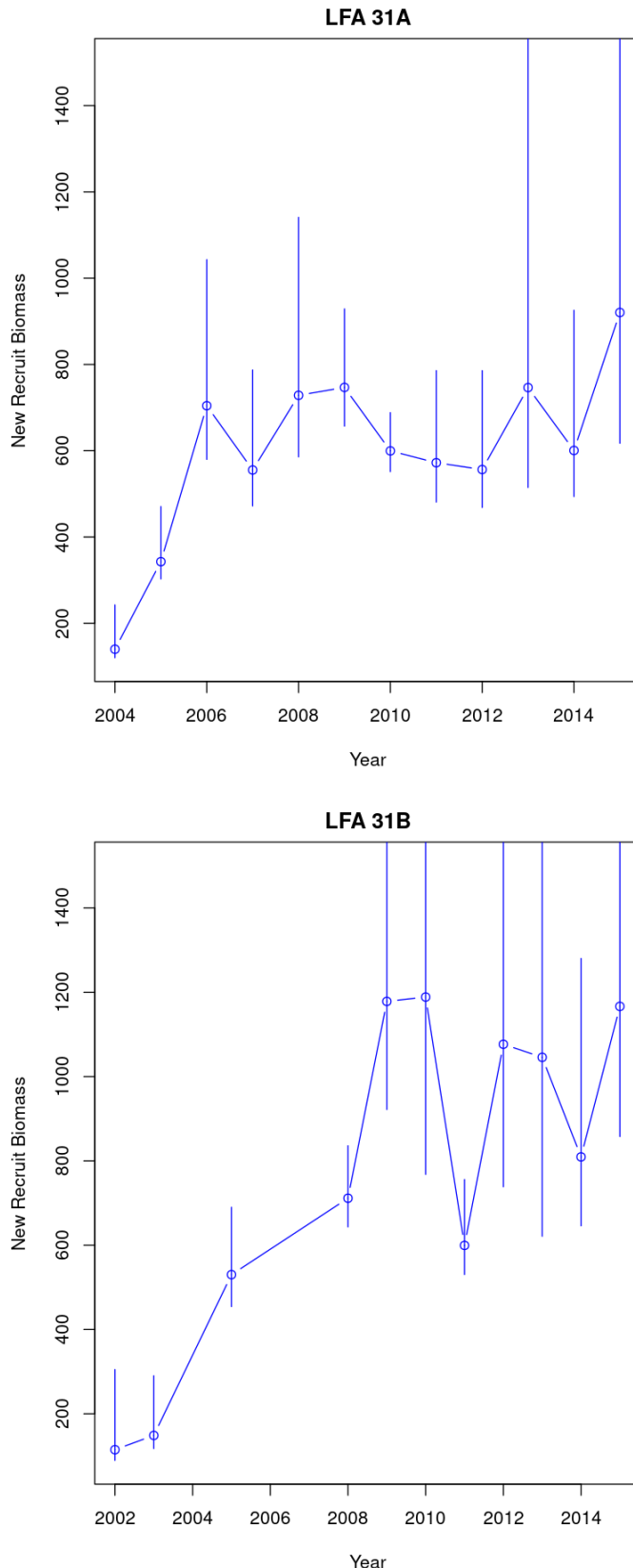


Figure 98: Time series of estimated recruitment biomass in tons with associated 95% error bounds. Upper bounds in LFA 31A for 2013 and 2015 were >2990t. Upper bounds for LFA 31B in 2010 and 2013 were >3000t. The full range of error was not shown as lower credible intervals on exploitation rates were not well defined.

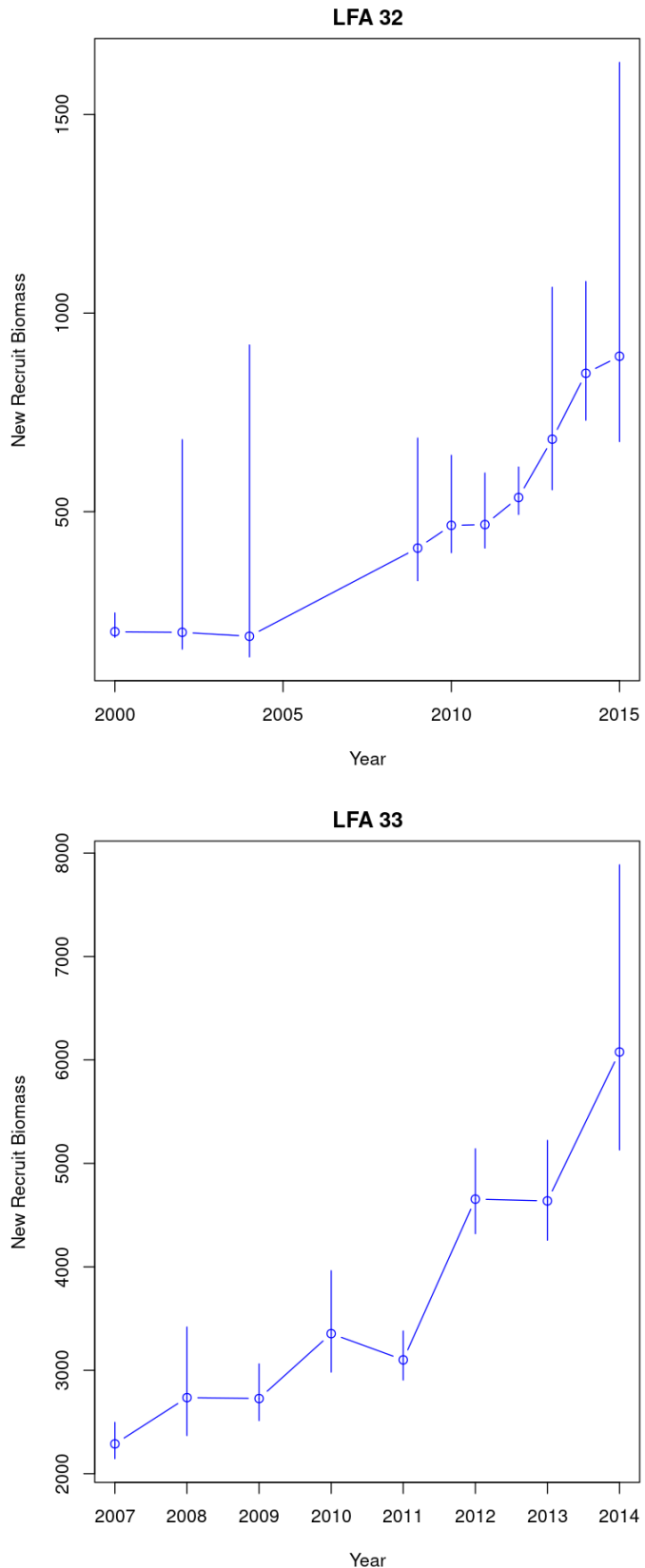


Figure 99: Time series of estimated recruitment biomass in tons with associated 95% error bounds

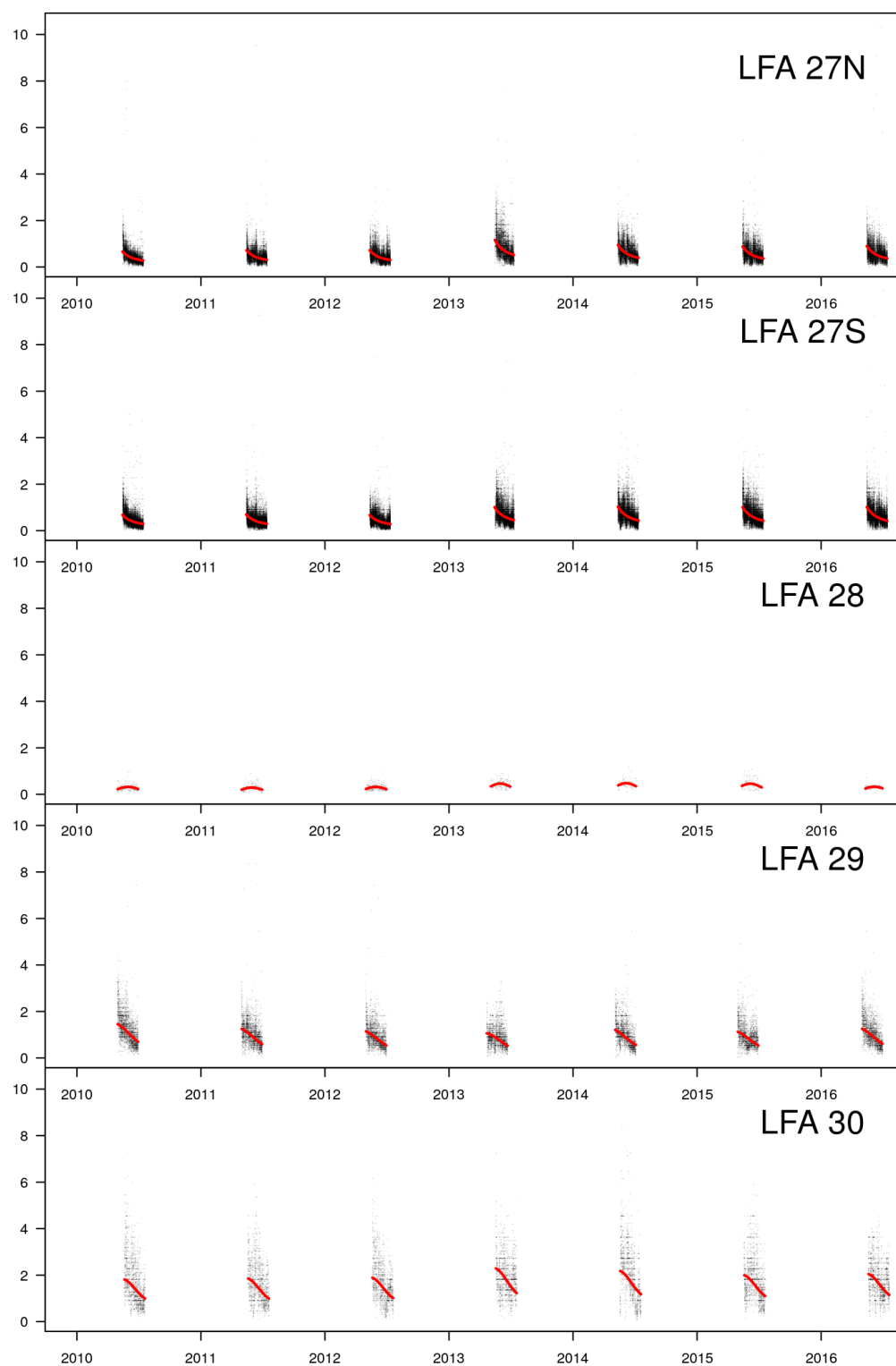


Figure 100: Predictions of Catch per unit effort (kg/trap haul) from the model for each day (red line), overlaid on the raw data for LFAs 27-30.

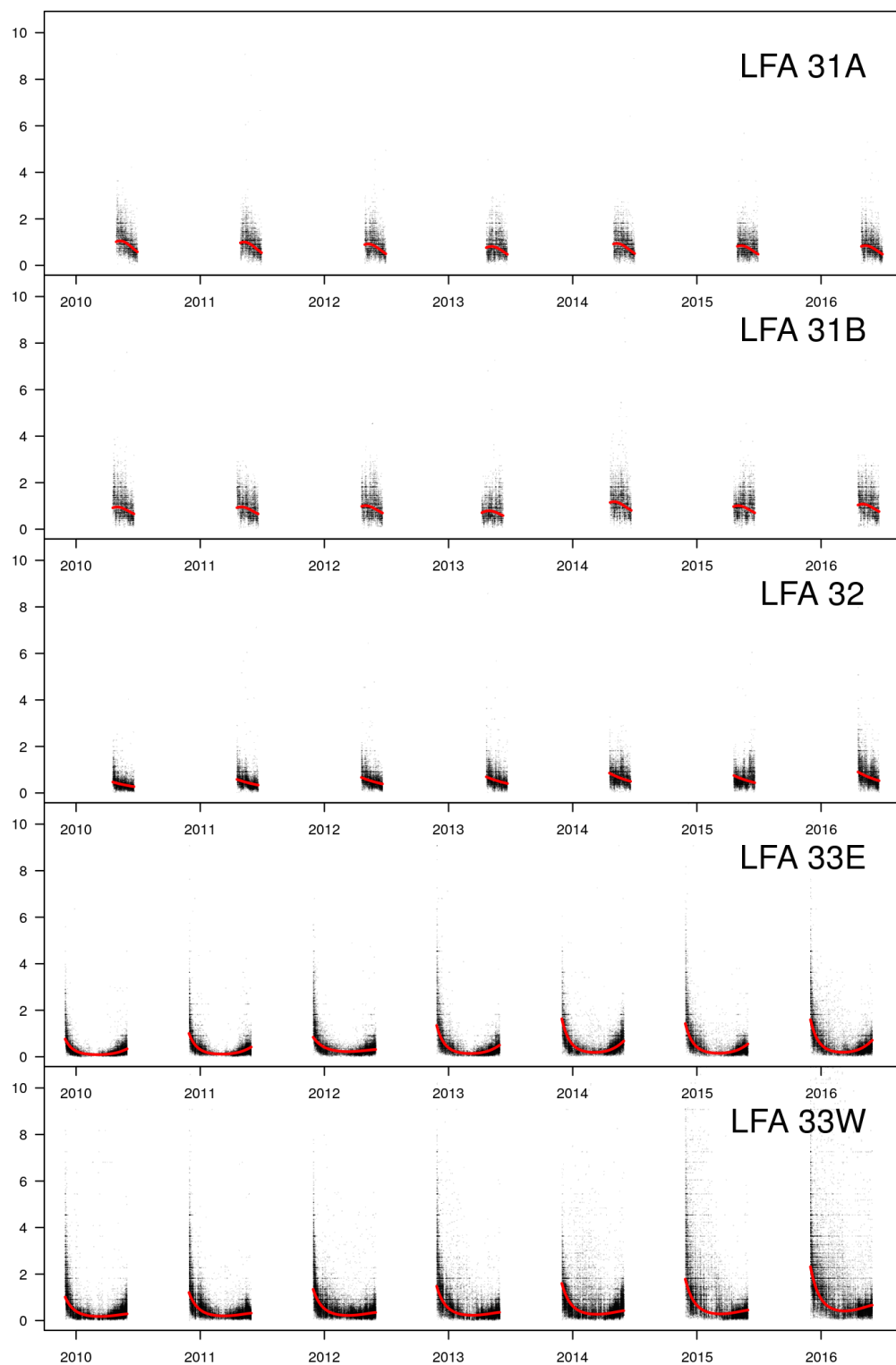


Figure 101: Predictions of Catch per unit effort (kg/trap haul) from the model for each day (red line), overlaid on the raw data for LFAs 31-33.

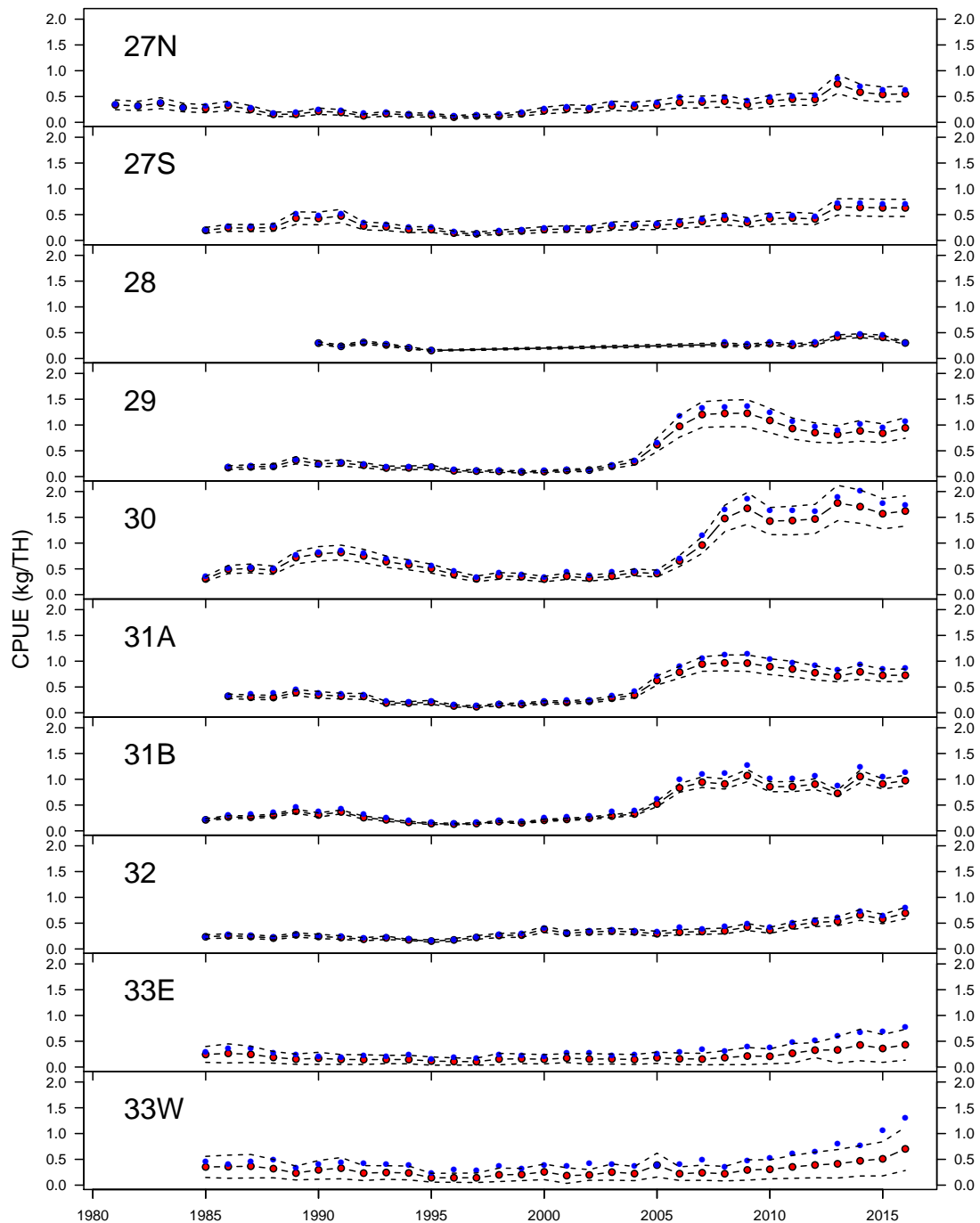


Figure 102: The predicted mean and standard deviation for seasonal and LFA Catch per unit effort (CPUE) indices from the CPUE model (red dots, dashed line). Unmodelled mean CPUE for each season and LFA (blue dots).

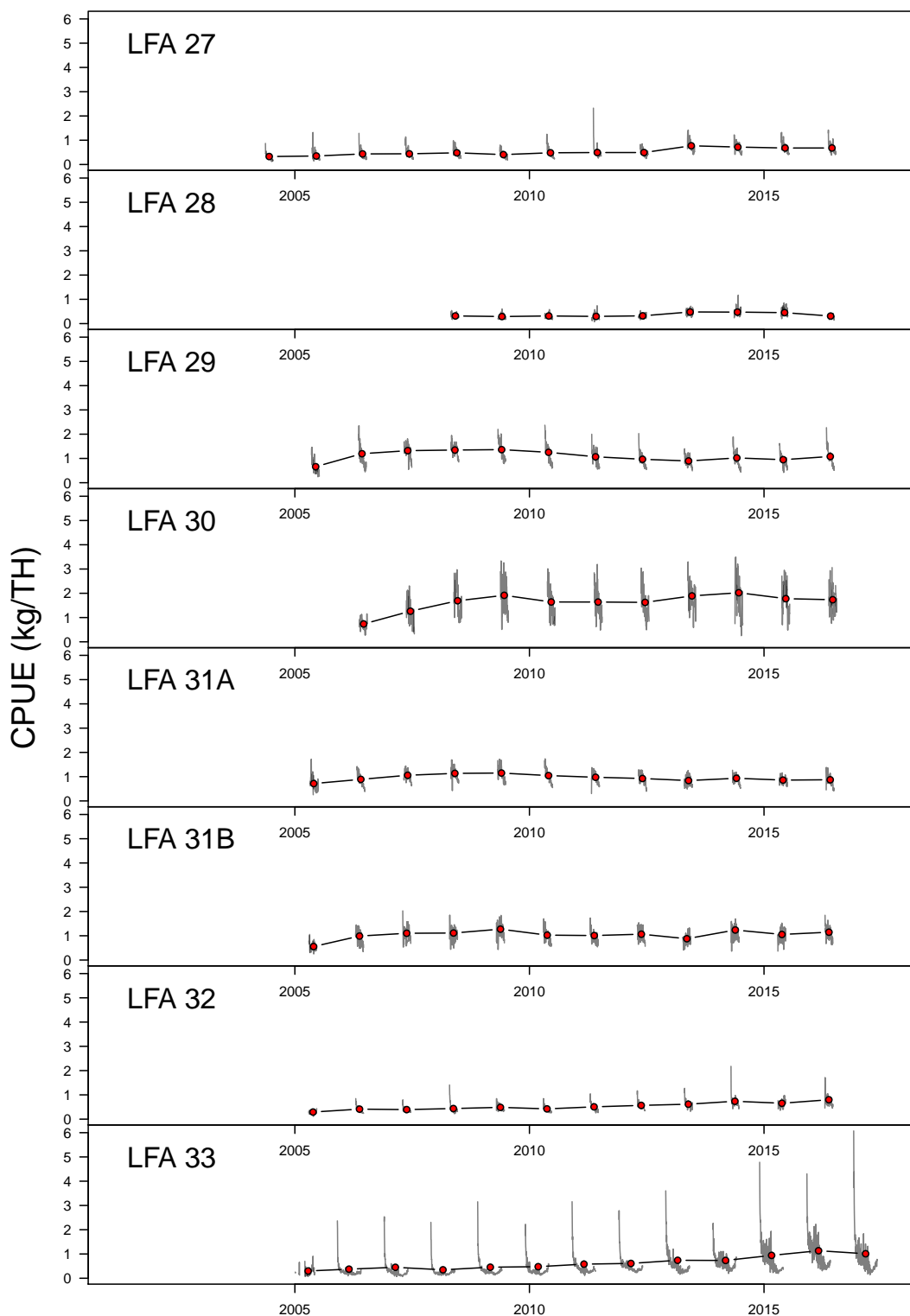


Figure 103: Daily (grey line) and Annual (red dot) mean Catch per unit effort (kg/Trap Haul) for each LFA.

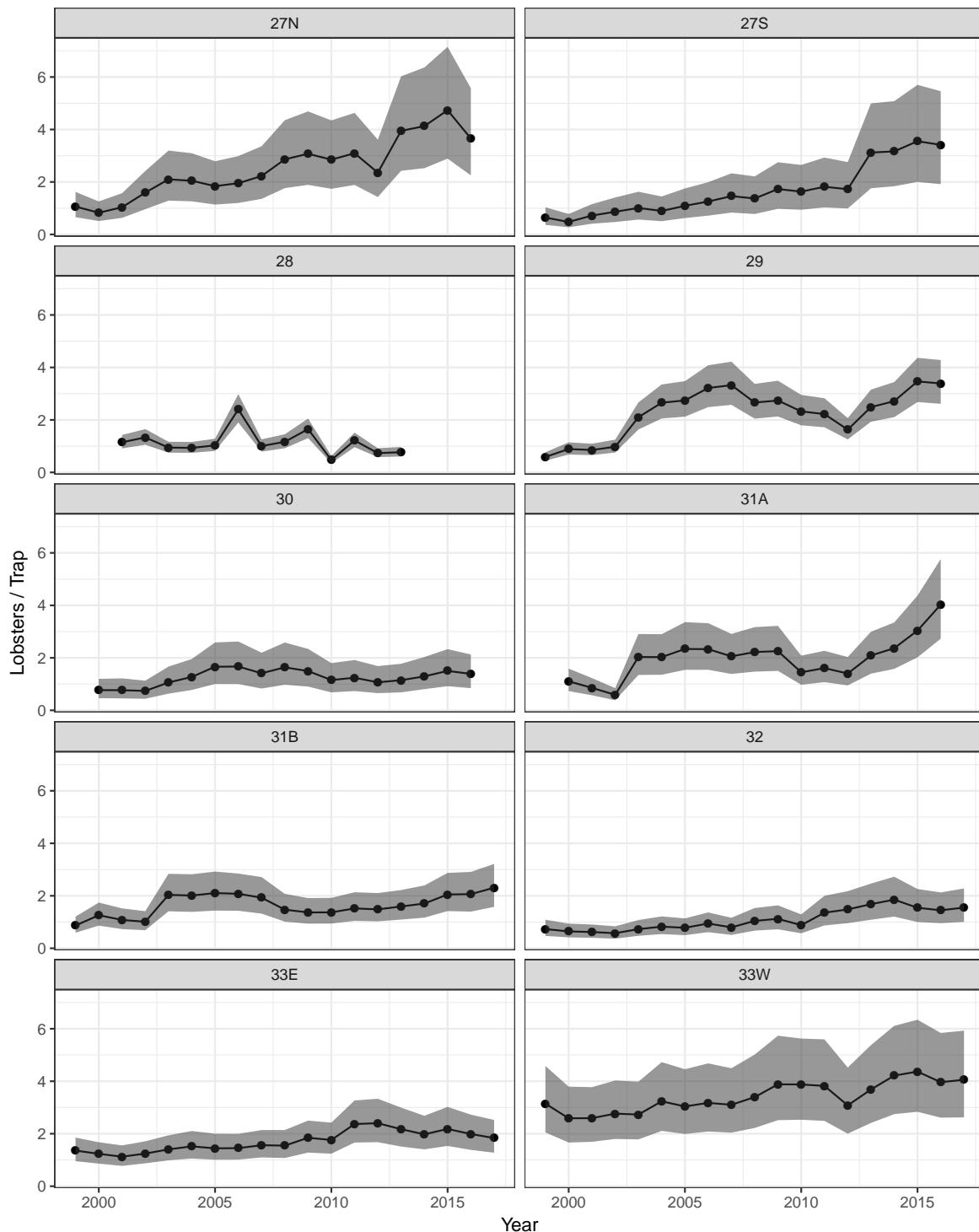


Figure 104: Annual index of sublegal sized (<82.5 mm) lobsters from the FSRS model with 95% credible intervals for each LFA.

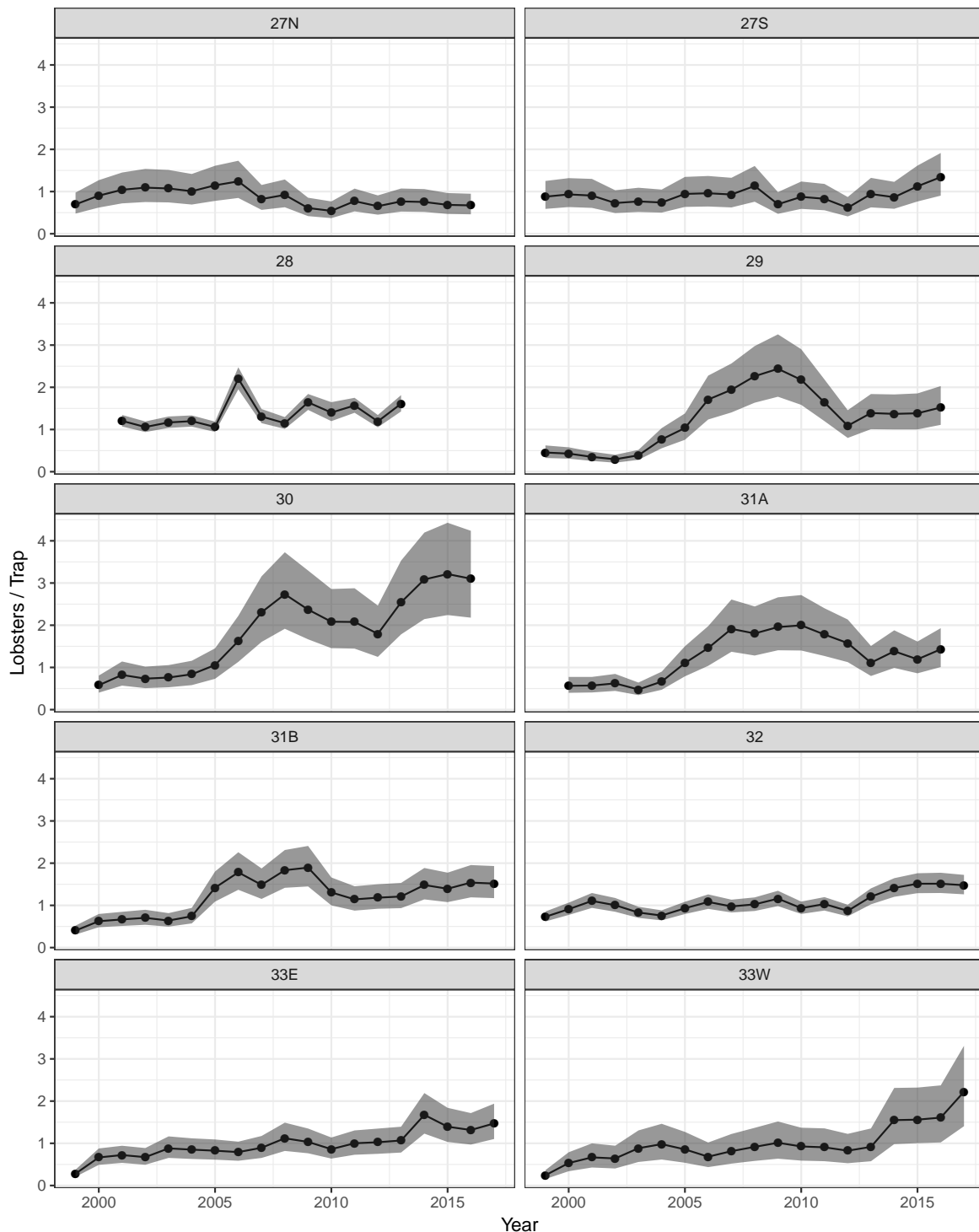


Figure 105: Annual index of legal sized (>82.5 mm) lobsters from the FSRS model with 95% credible intervals for each LFA.

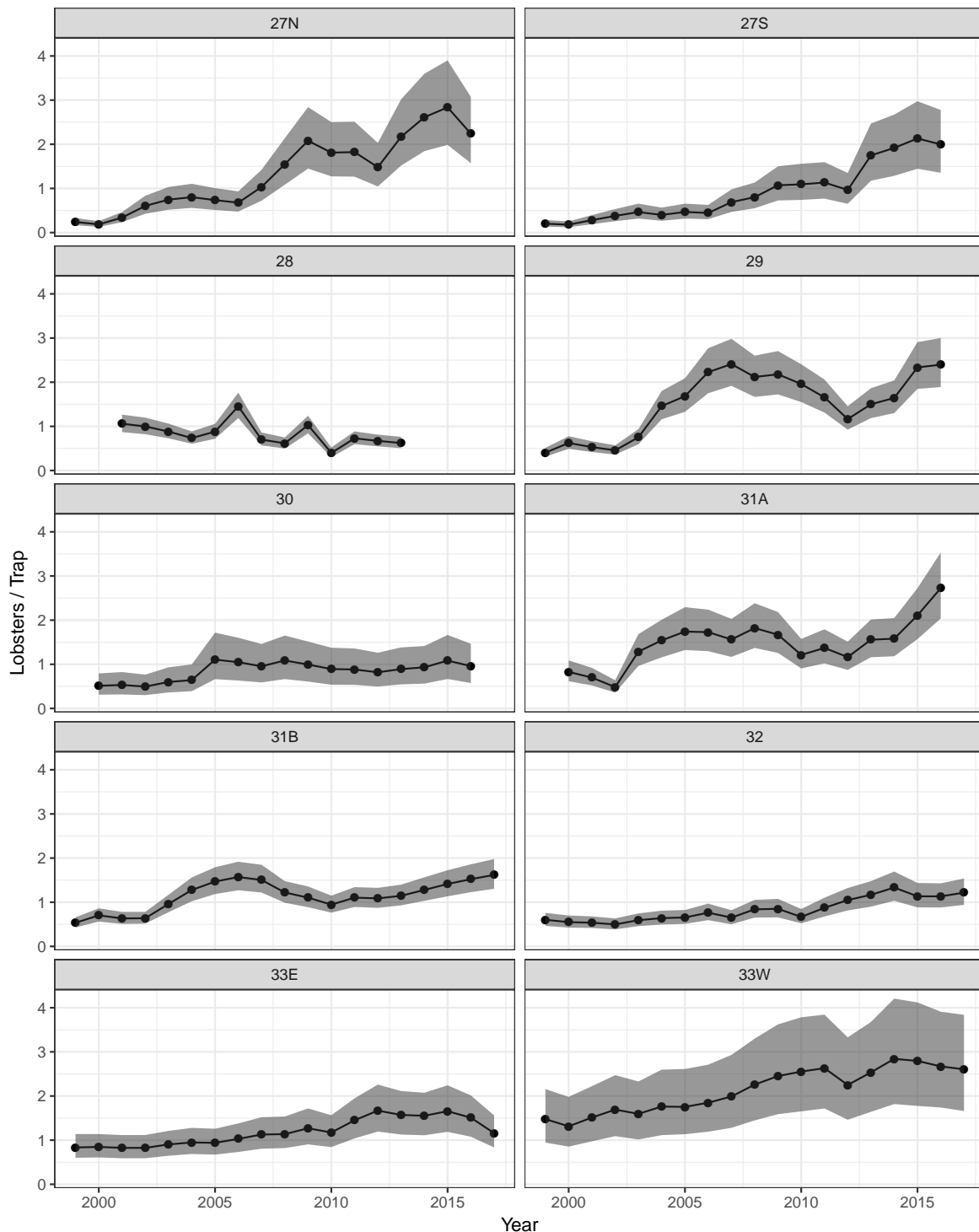


Figure 106: Annual index of recruit sized (75-82.5 mm) lobsters from the FSRS model with 95% credible intervals for each LFA.

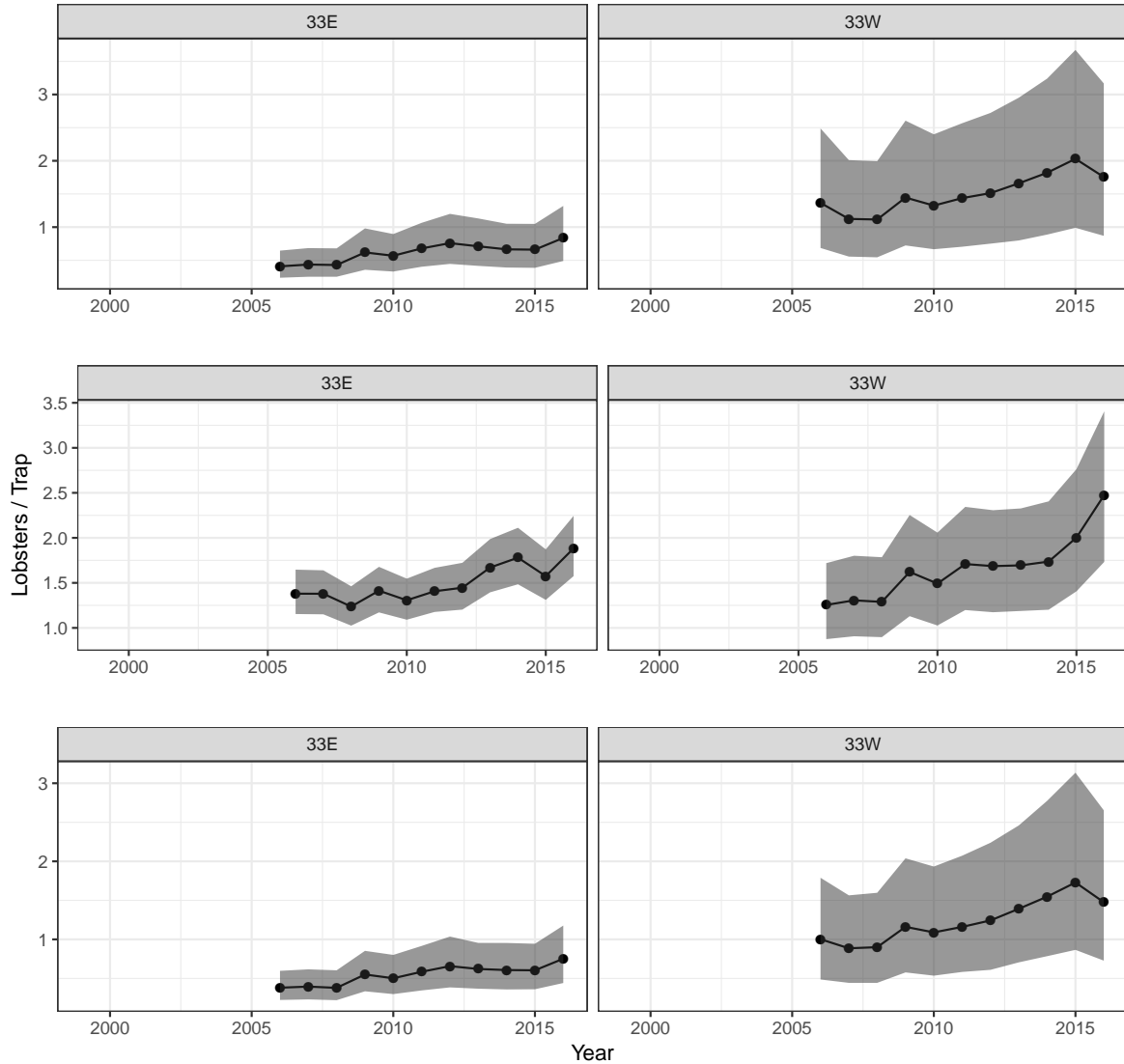


Figure 107: Model predictions from the FSRS commercial sampling program in LFA 33. top to bottom: sublegal sized (<82.5 mm) , legal sized (>82.5 mm) and recruit sized (75-82.5 mm).

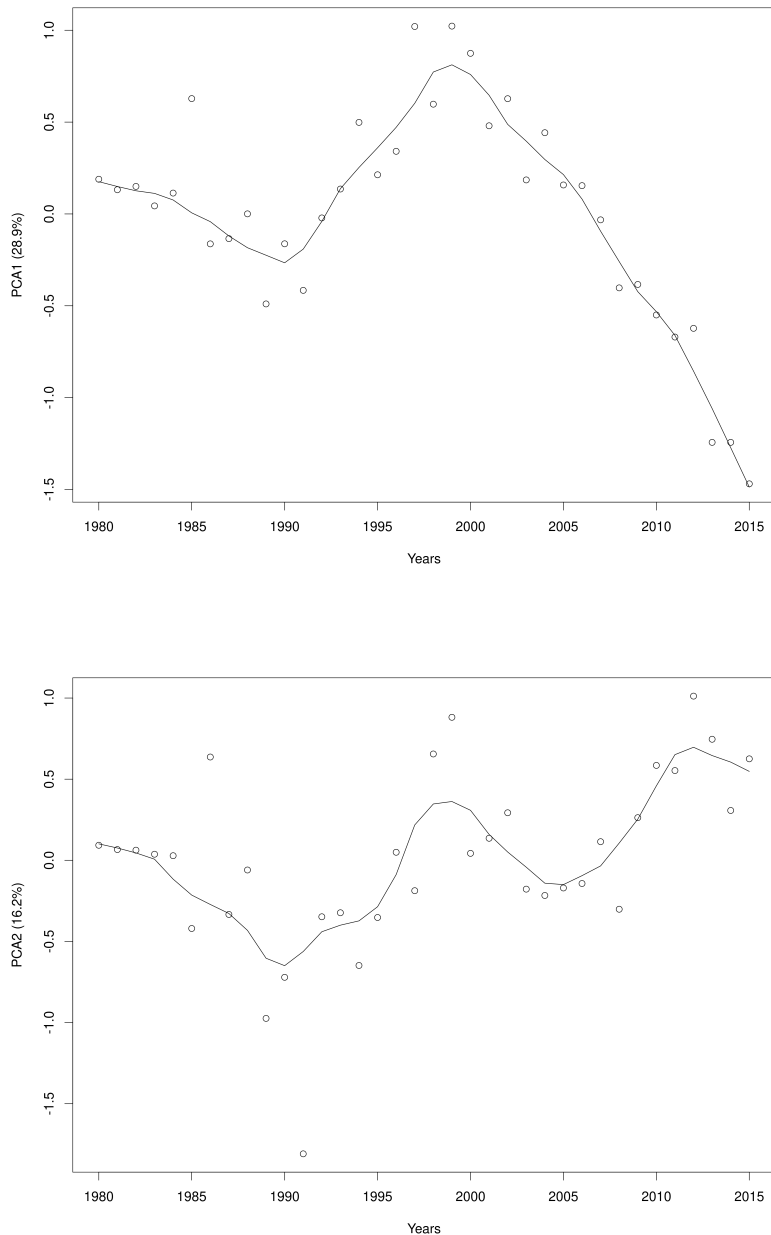


Figure 108: The first two principle components of a multivariate ordination of indicators representing the lobster stock and fishery in LFA 27. Solid line represents a loess smooth.

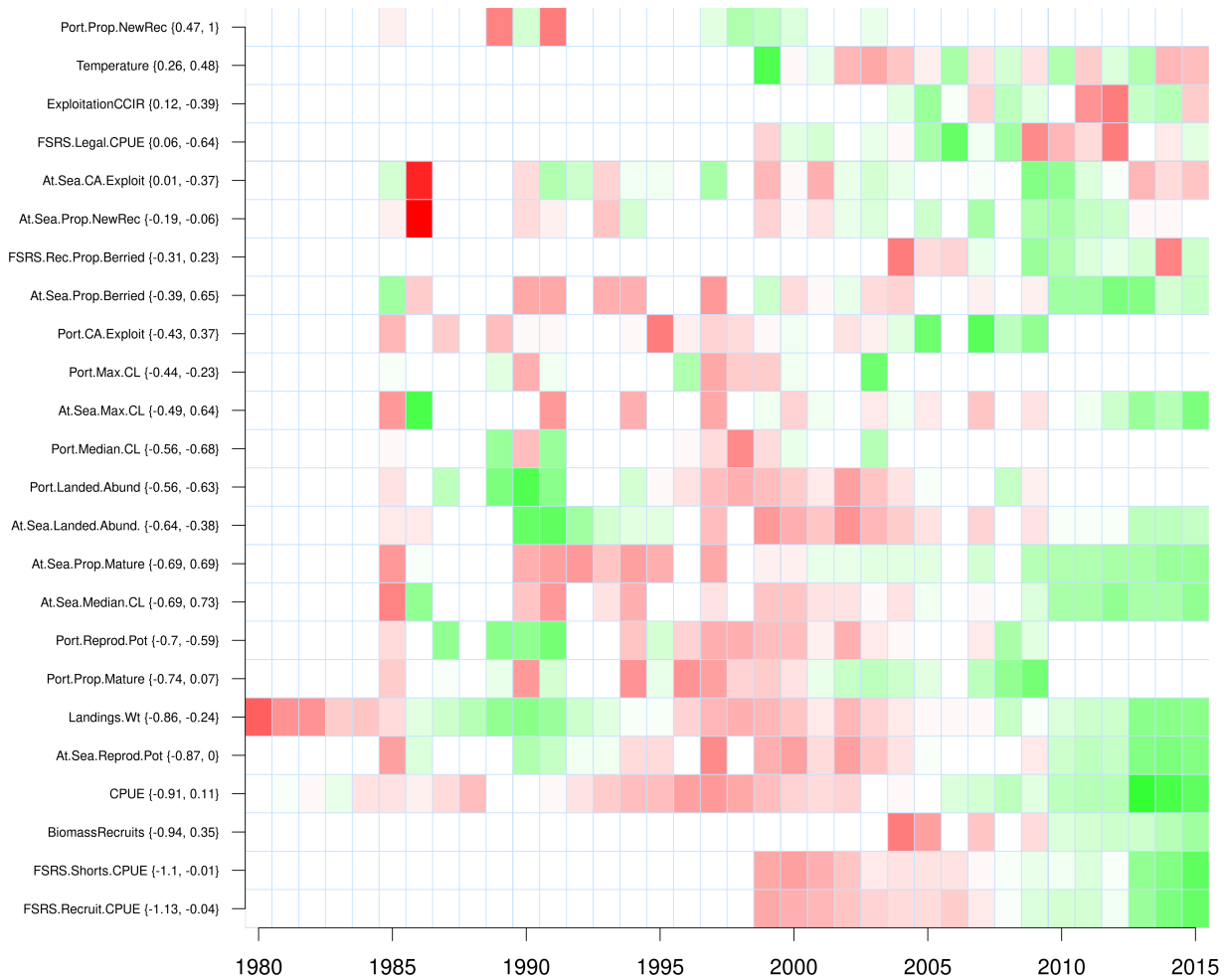


Figure 109: Time series of anomalies of the first principle component of a multivariate ordination of indicators representing the lobster stock and fishery in LFA 27. The values in brackets beside indicator names represent component scores for PC1 and PC2 respectively.

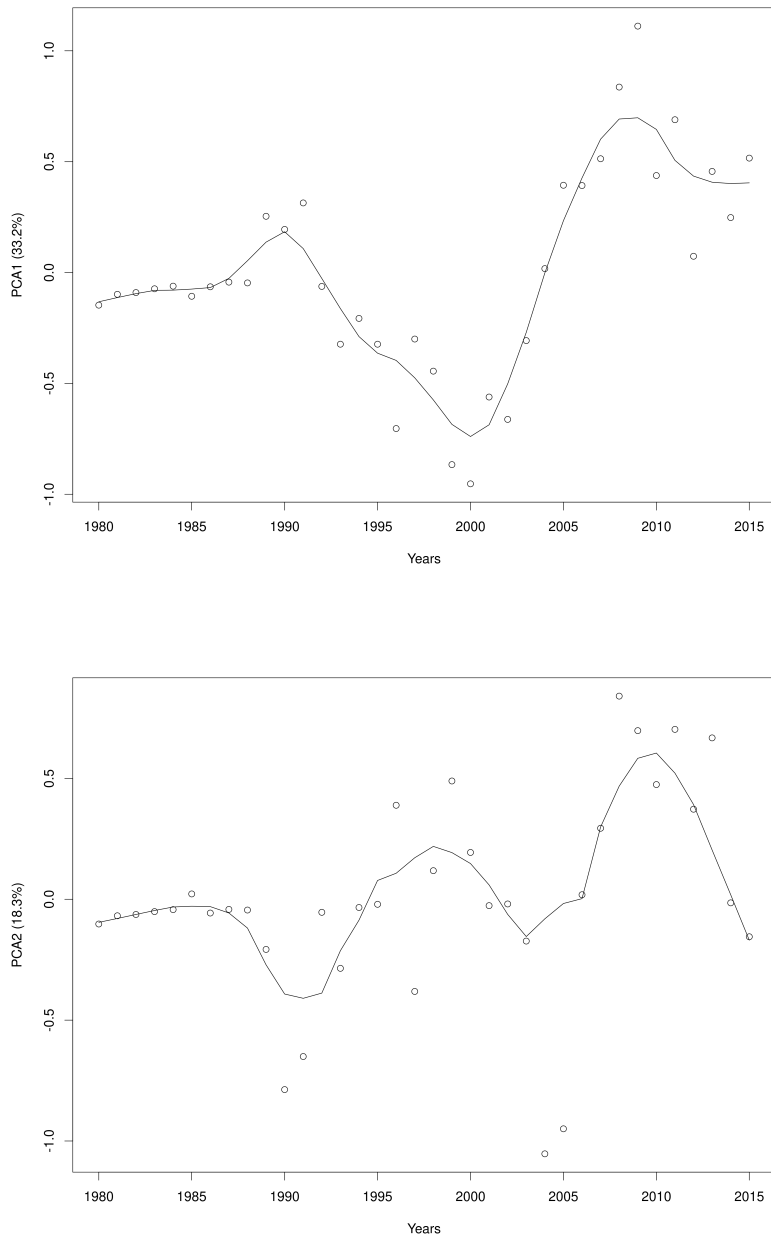


Figure 110: The first two principle components of a multivariate ordination of indicators representing the lobster stock and fishery in LFA 29. Solid line represents a loess smooth.

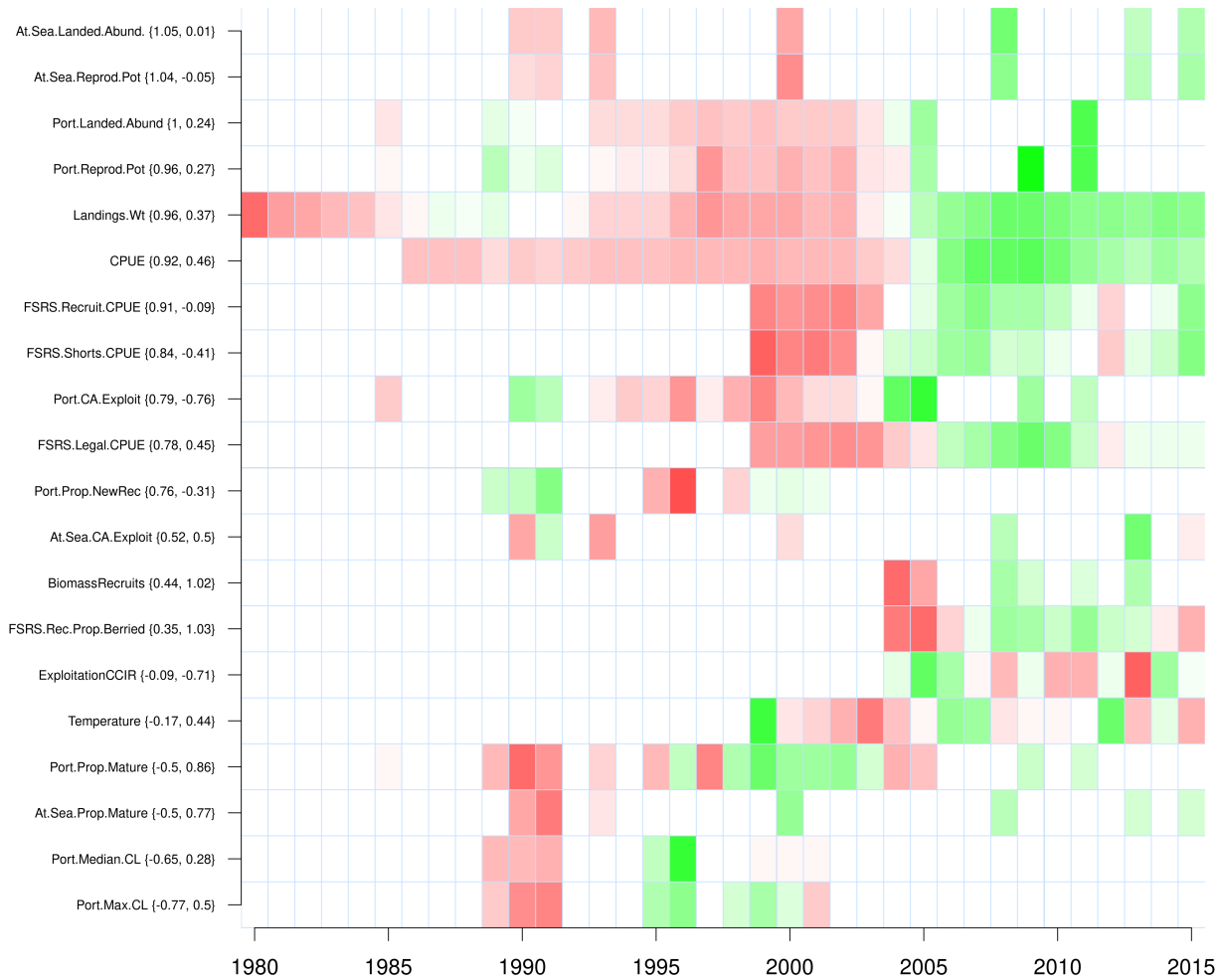


Figure 111: Time series of anomalies of the first principle component of a multivariate ordination of indicators representing the lobster stock and fishery in LFA 29. The values in brackets beside indicator names represent component scores for PC1 and PC2 respectively.

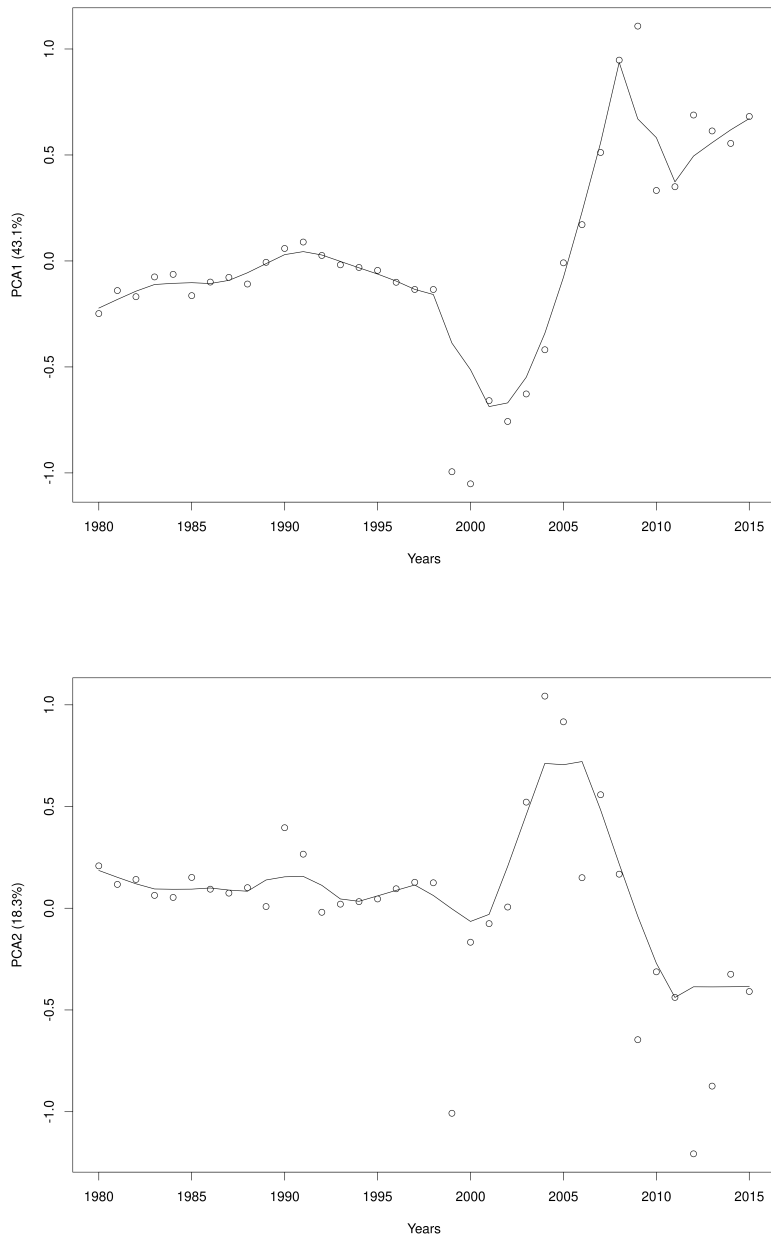


Figure 112: The first two principle components of a multivariate ordination of indicators representing the lobster stock and fishery in LFA 30. Solid line represents a loess smooth.

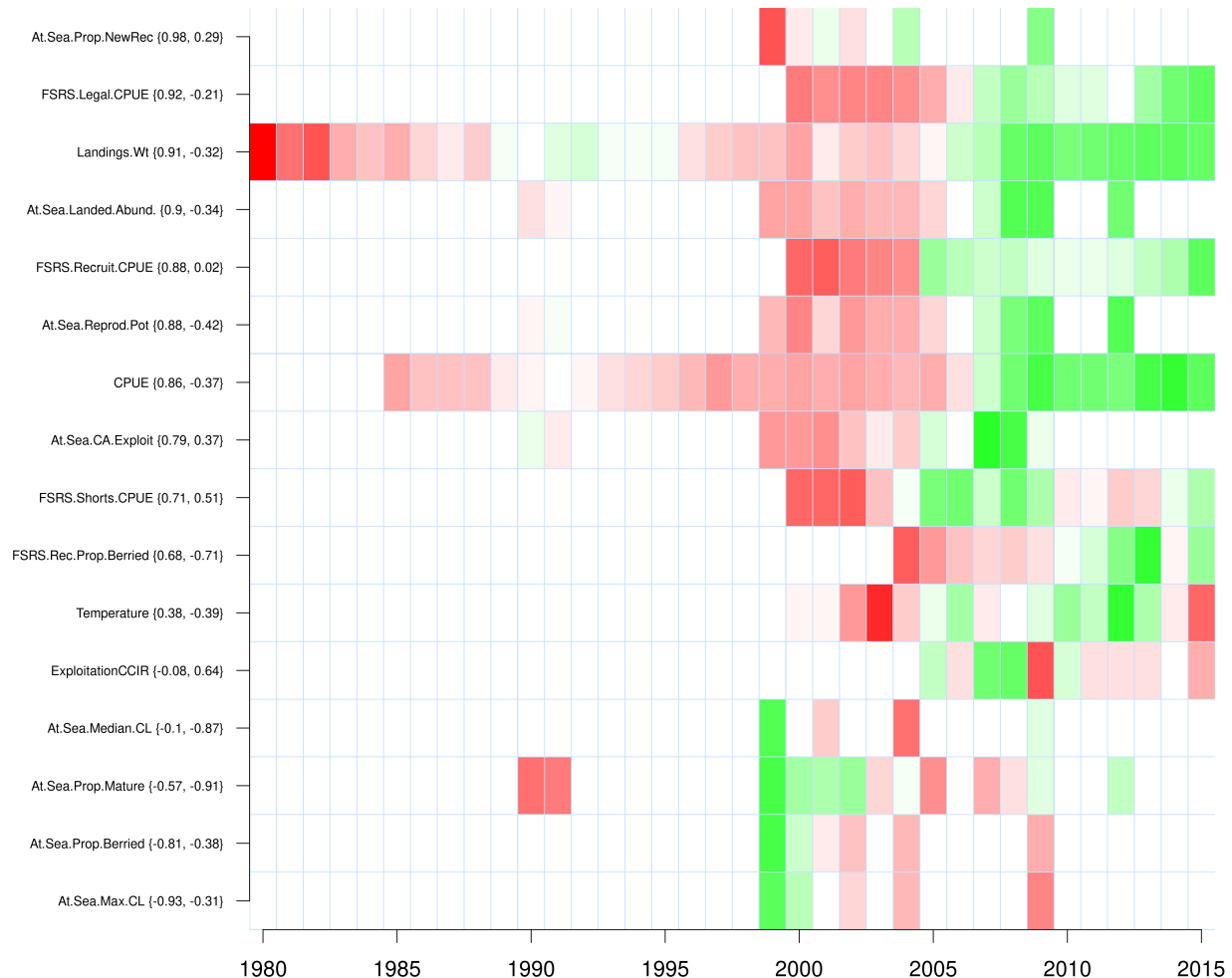


Figure 113: Time series of anomalies of the first principle component of a multivariate ordination of indicators representing the lobster stock and fishery in LFA 30. The values in brackets beside indicator names represent component scores for PC1 and PC2 respectively.

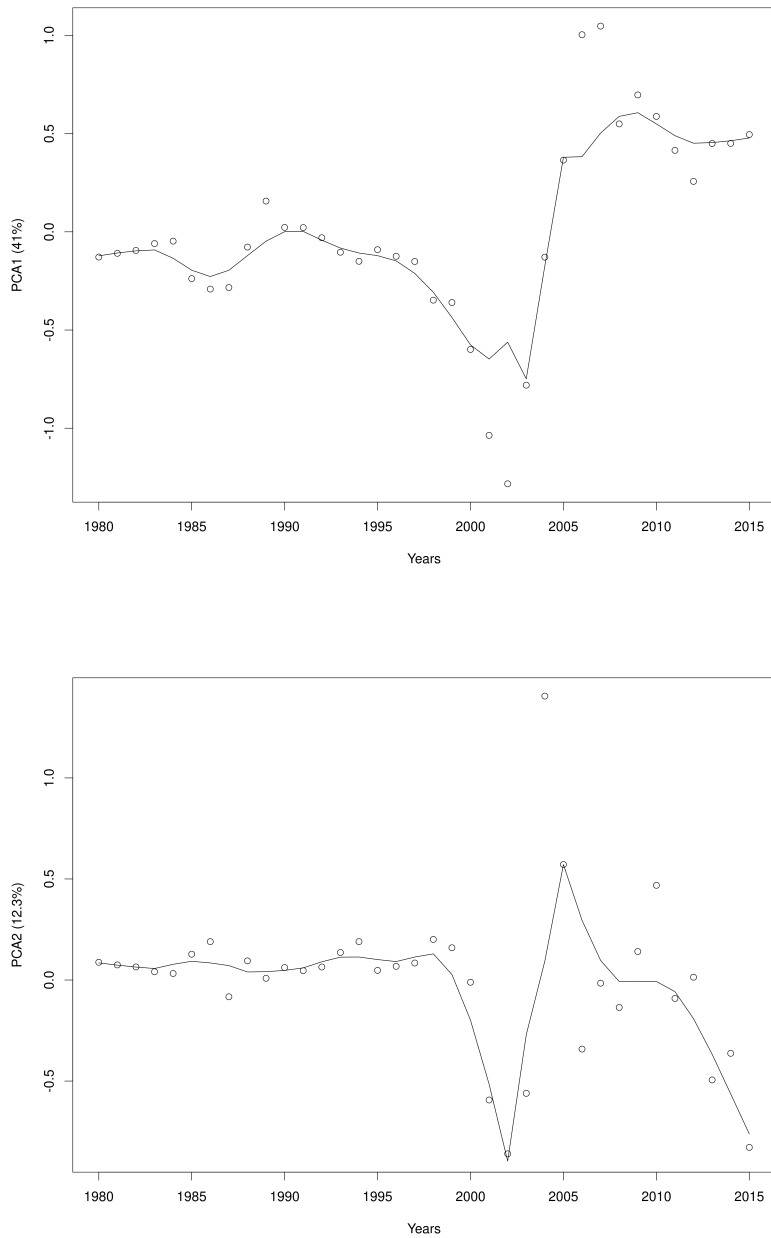


Figure 114: The first two principle components of a multivariate ordination of indicators representing the lobster stock and fishery in LFA 31A. Solid line represents a loess smooth.

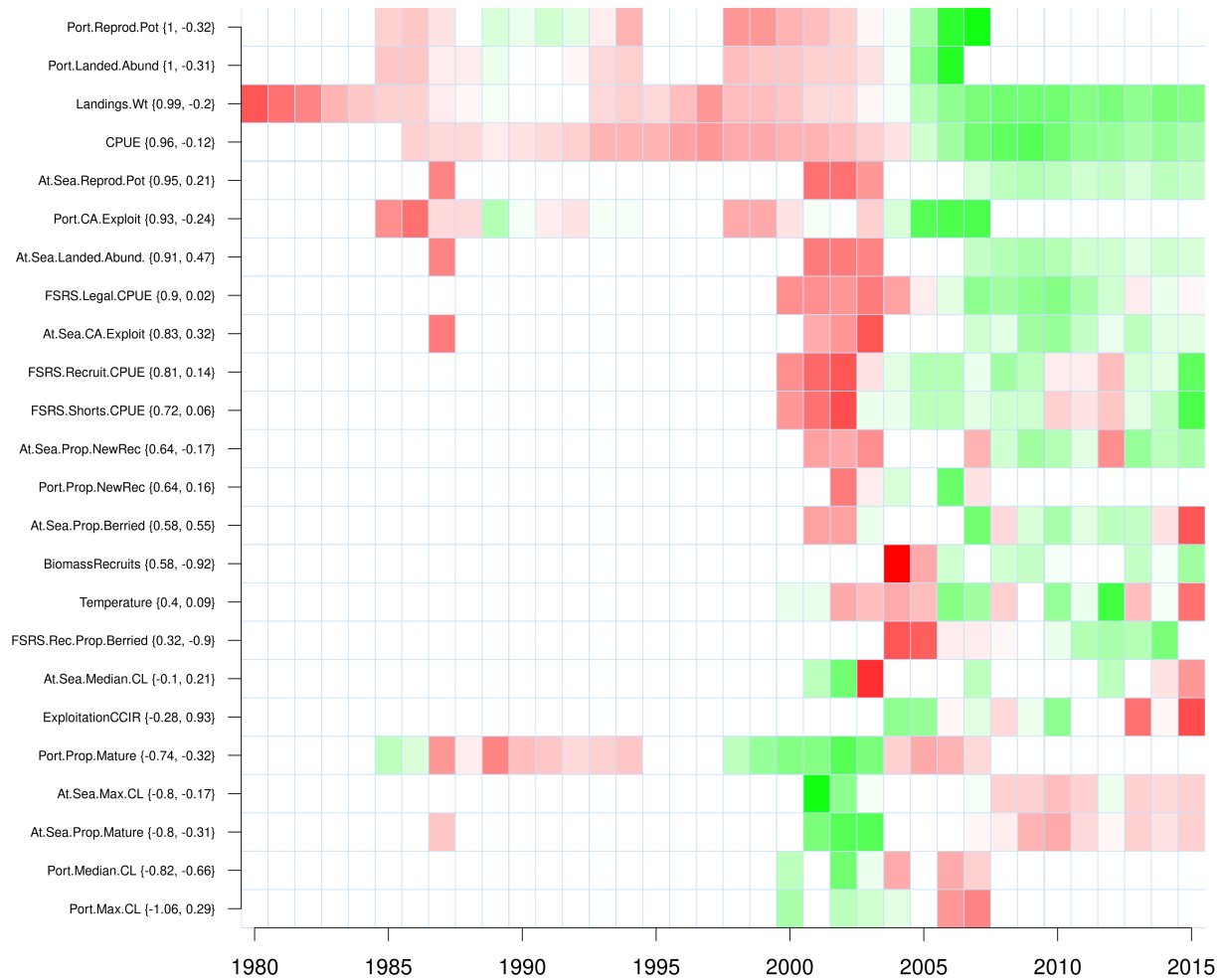


Figure 115: Time series of anomalies of the first principle component of a multivariate ordination of indicators representing the lobster stock and fishery in LFA 31A. The values in brackets beside indicator names represent component scores for PC1 and PC2 respectively.

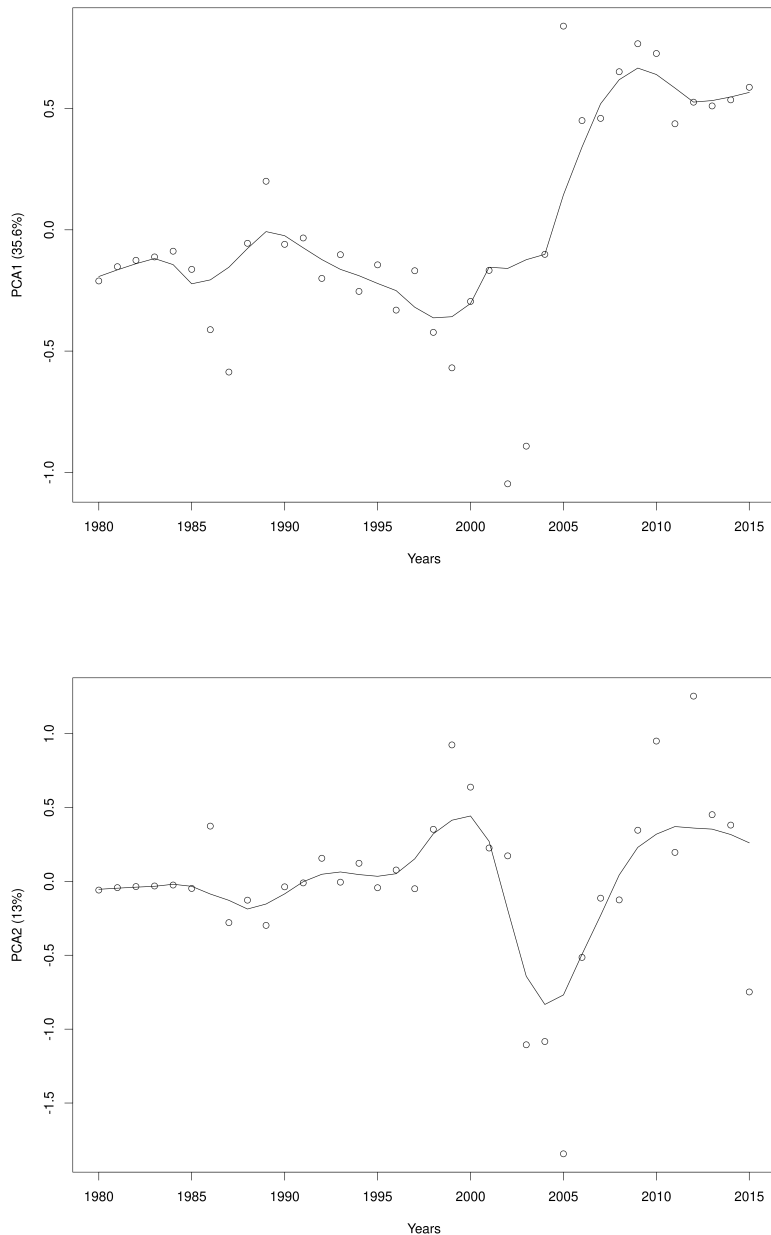


Figure 116: The first two principle components of a multivariate ordination of indicators representing the lobster stock and fishery in LFA 31B. Solid line represents a loess smooth.

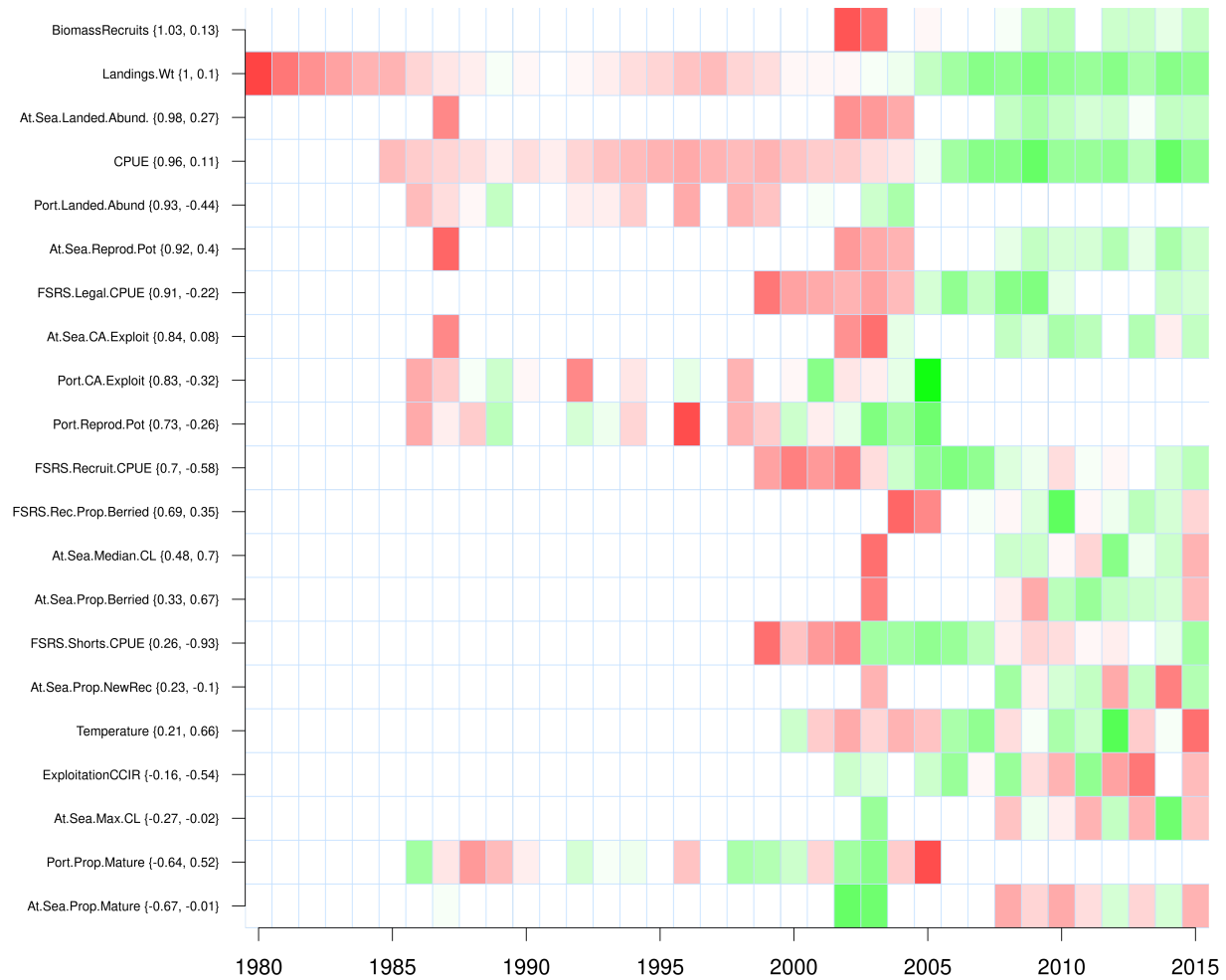


Figure 117: Time series of anomalies of the first principle component of a multivariate ordination of indicators representing the lobster stock and fishery in LFA 31B. The values in brackets beside indicator names represent component scores for PC1 and PC2 respectively.

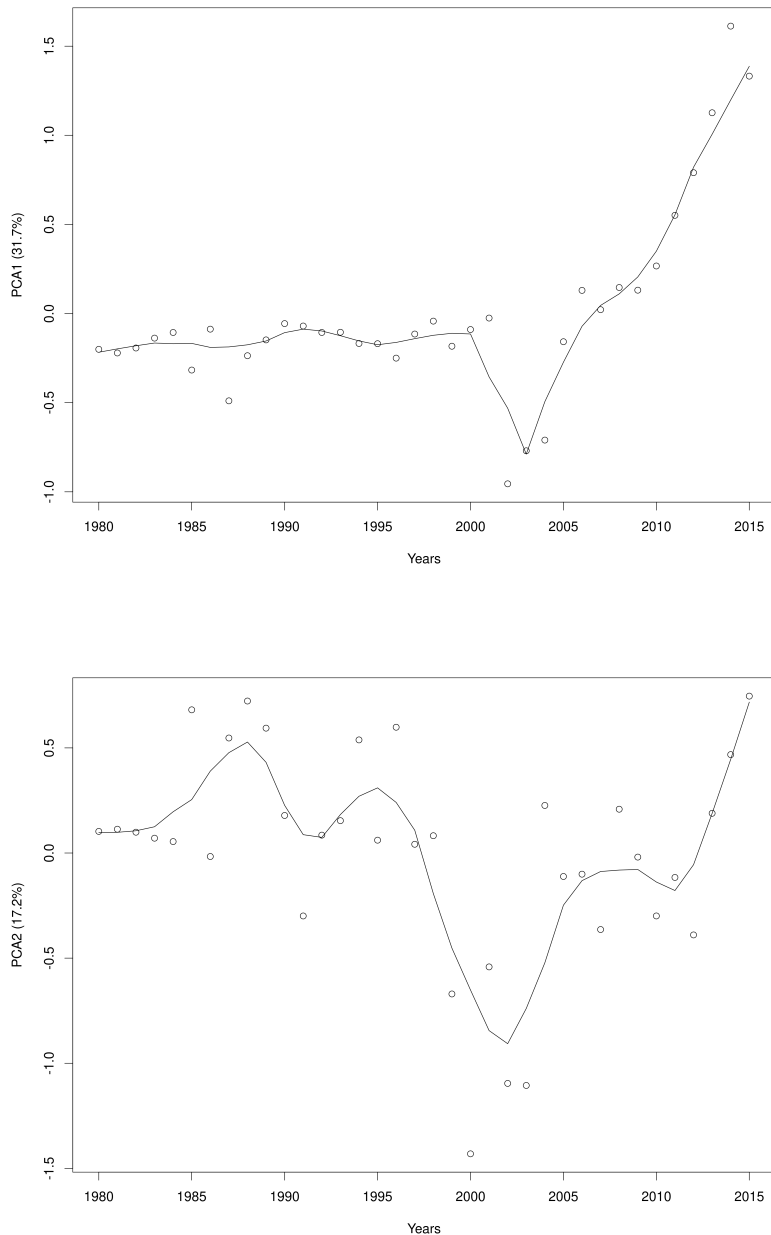


Figure 118: The first two principle components of a multivariate ordination of indicators representing the lobster stock and fishery in LFA 32. Solid line represents a loess smooth.

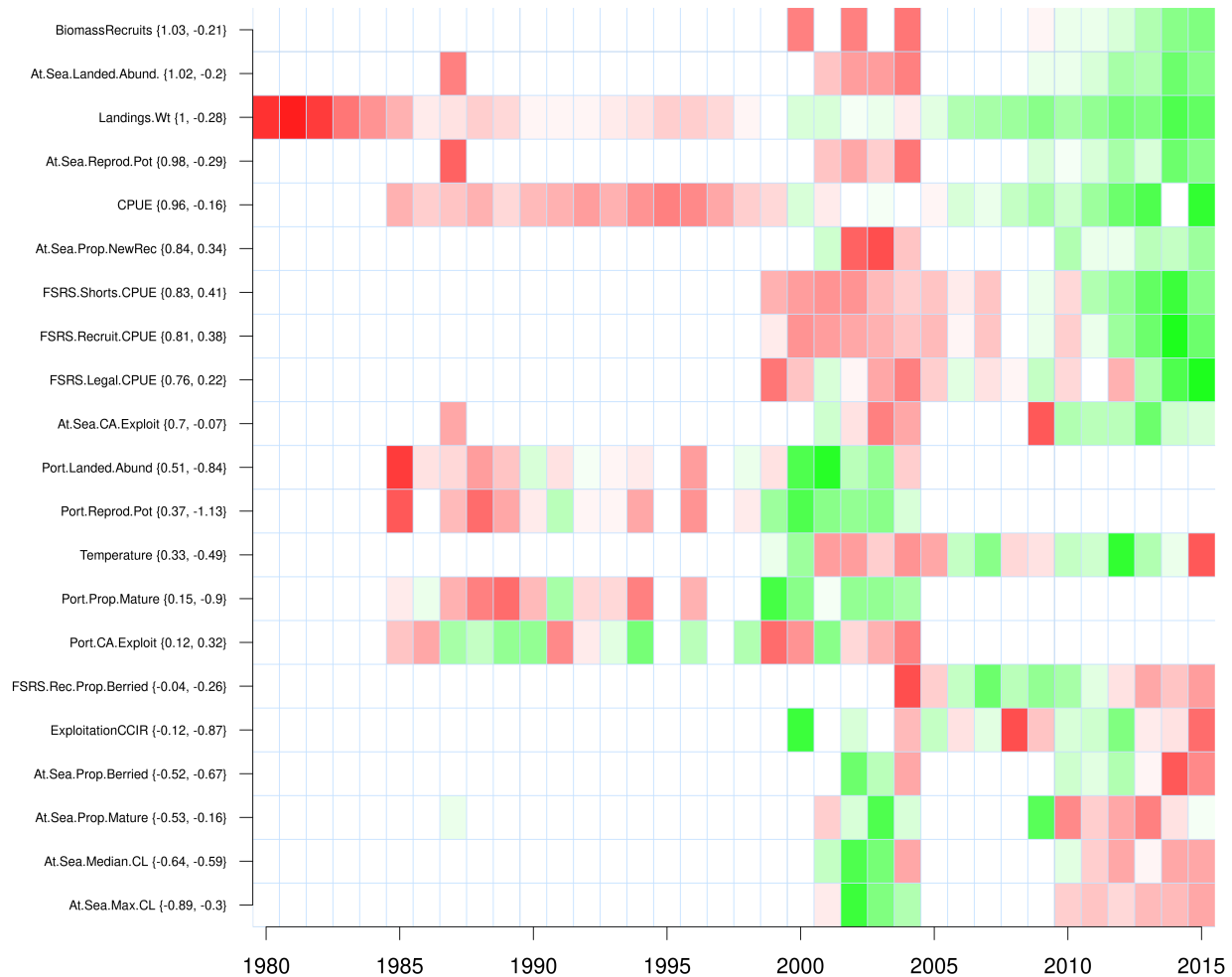


Figure 119: Time series of anomalies of the first principle component of a multivariate ordination of indicators representing the lobster stock and fishery in LFA 32. The values in brackets beside indicator names represent component scores for PC1 and PC2 respectively.

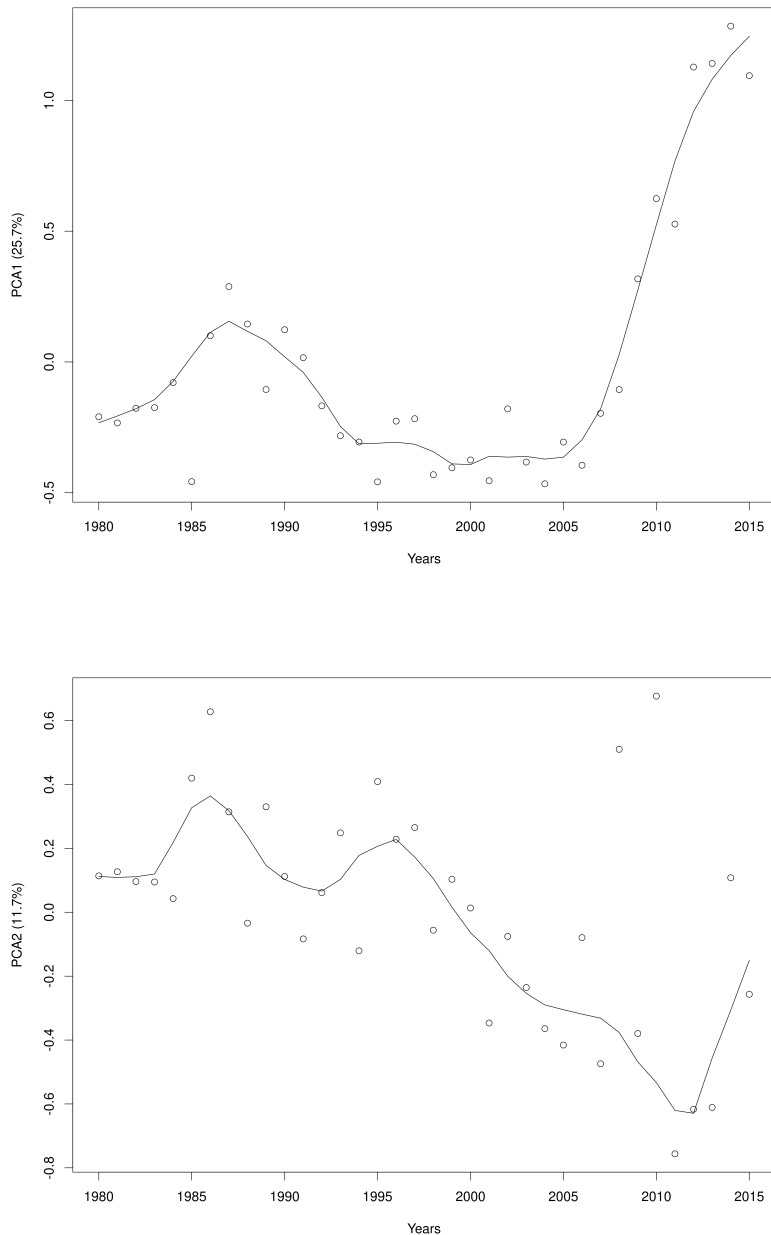


Figure 120: The first two principle components of a multivariate ordination of indicators representing the lobster stock and fishery in LFA 33. Solid line represents a loess smooth.

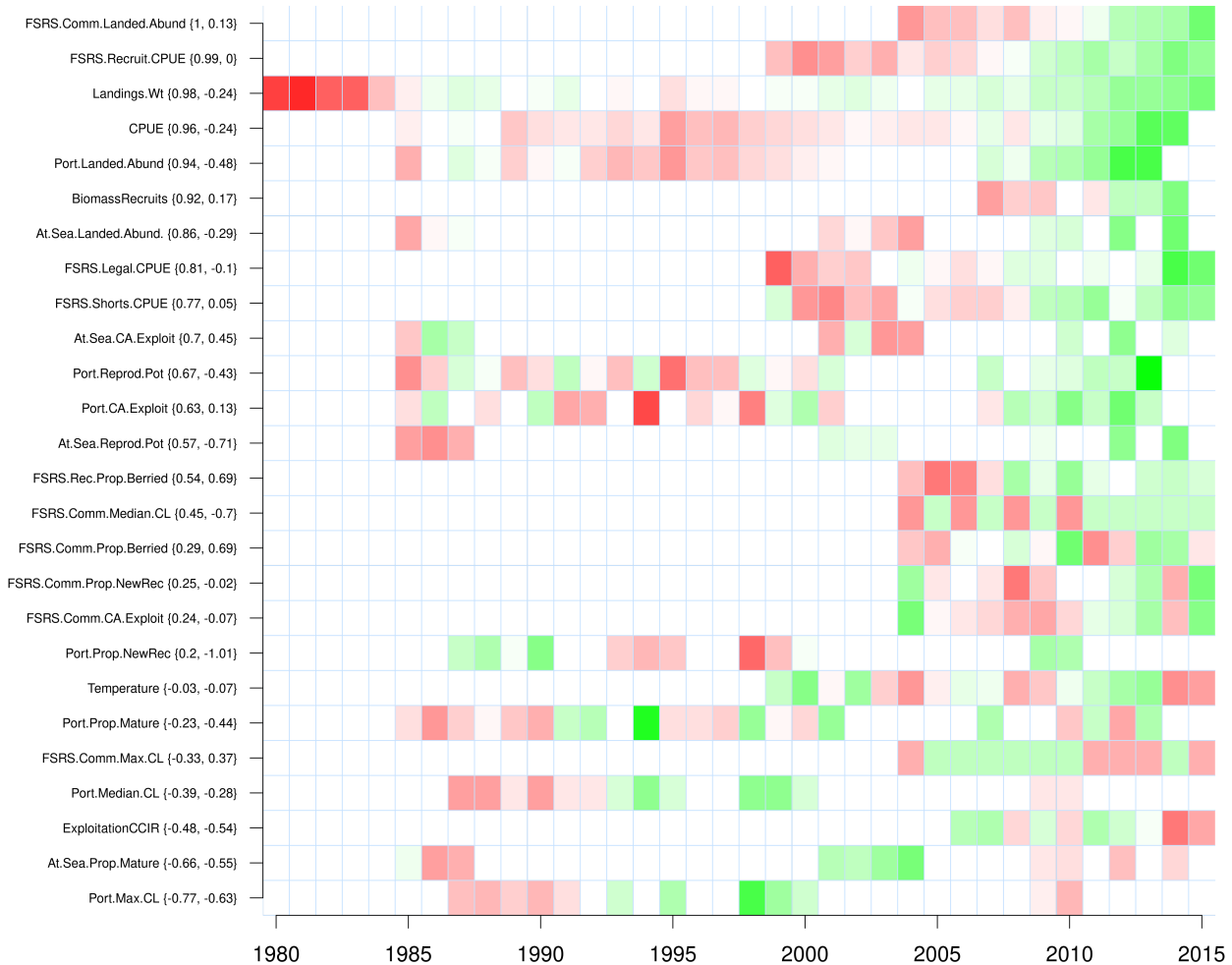


Figure 121: Time series of anomalies of the first principle component of a multivariate ordination of indicators representing the lobster stock and fishery in LFA 33. The values in brackets beside indicator names represent component scores for PC1 and PC2 respectively.

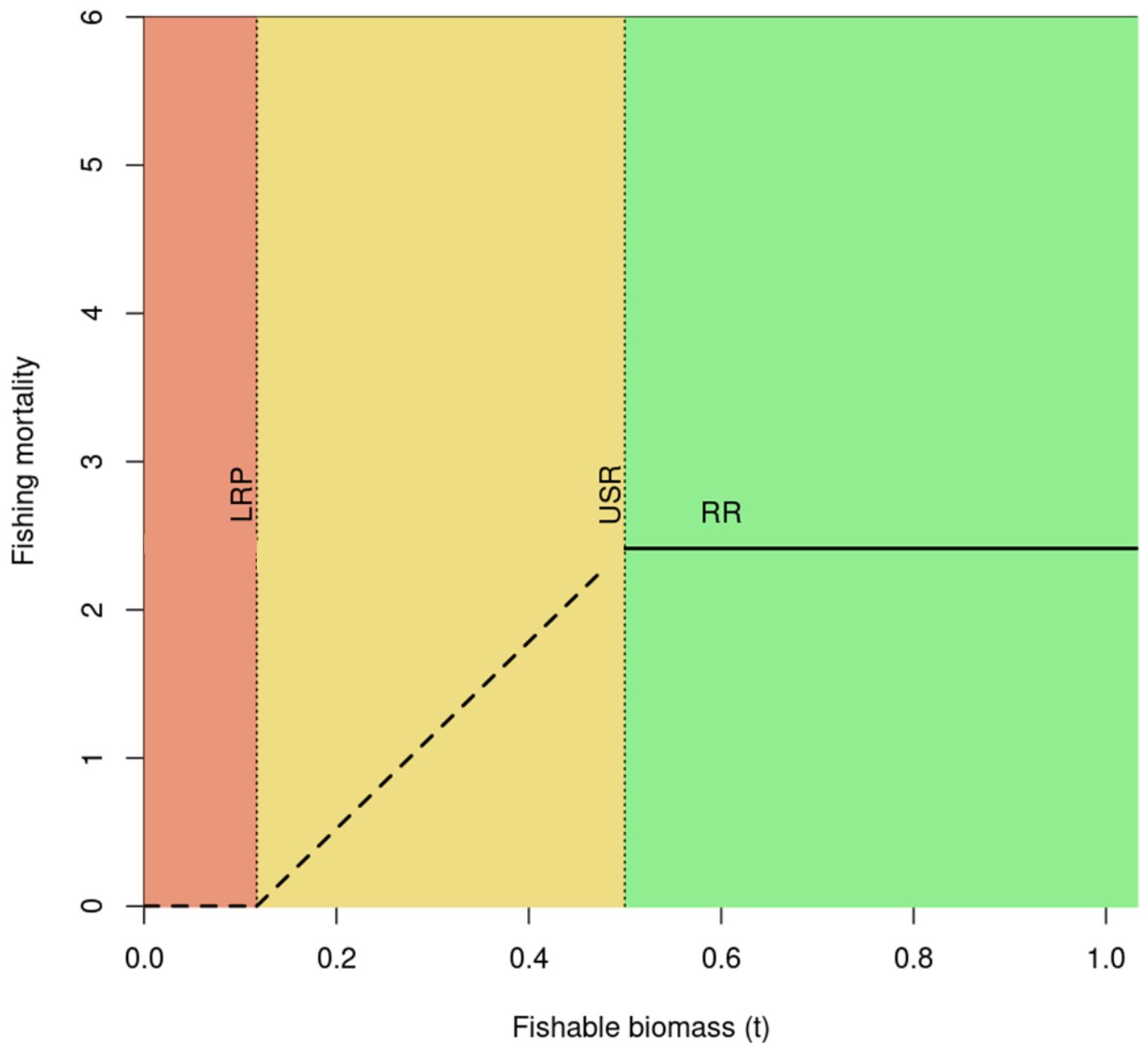


Figure 122: Example precautionary approach phase plot delimiting the healthy zone (green) above upper stock reference (USR) the cautious zone (yellow), between the USR and the limit reference point (LRP) and critical zone (red), below the LRP. The removal reference (RR) is shown as a solid black line in all three zones, however in practice the RR should be reduced in the cautious zone (black dashed) to allow stock rebuilding and set to 0 in the critical zone.

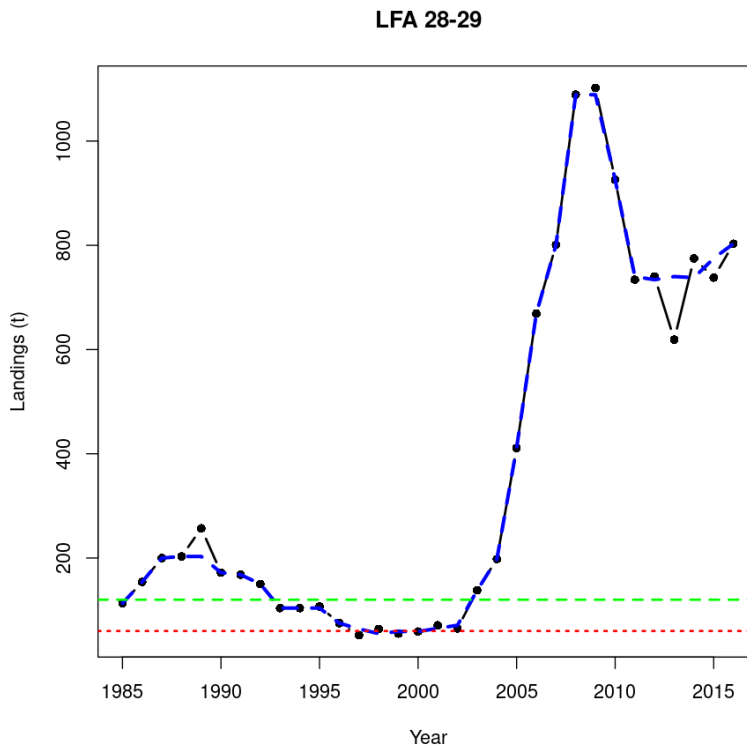
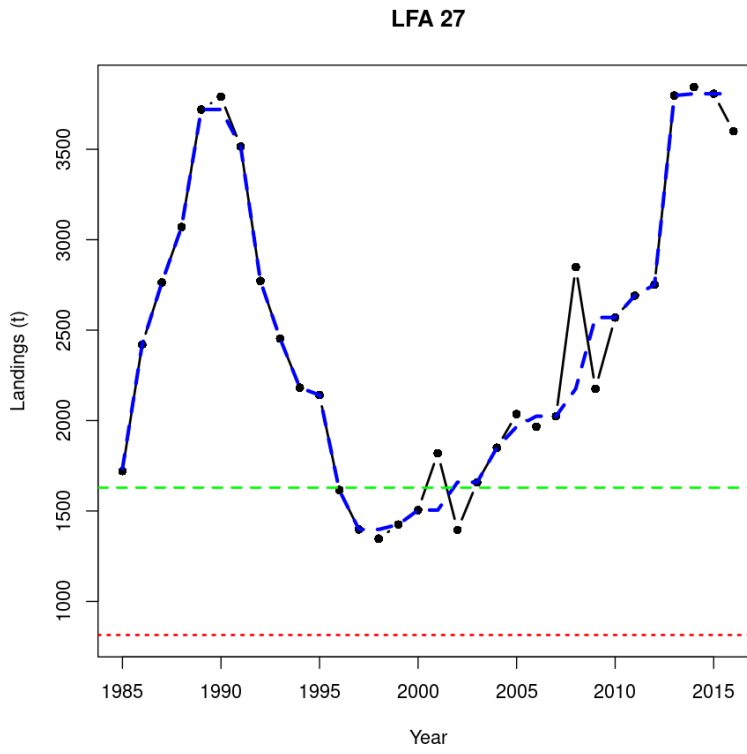


Figure 123: Time series of landings (black), three year running median of landings (blue) with currently approved upper stock (dashed green line) and limit reference (dotted red line) points by LFA.

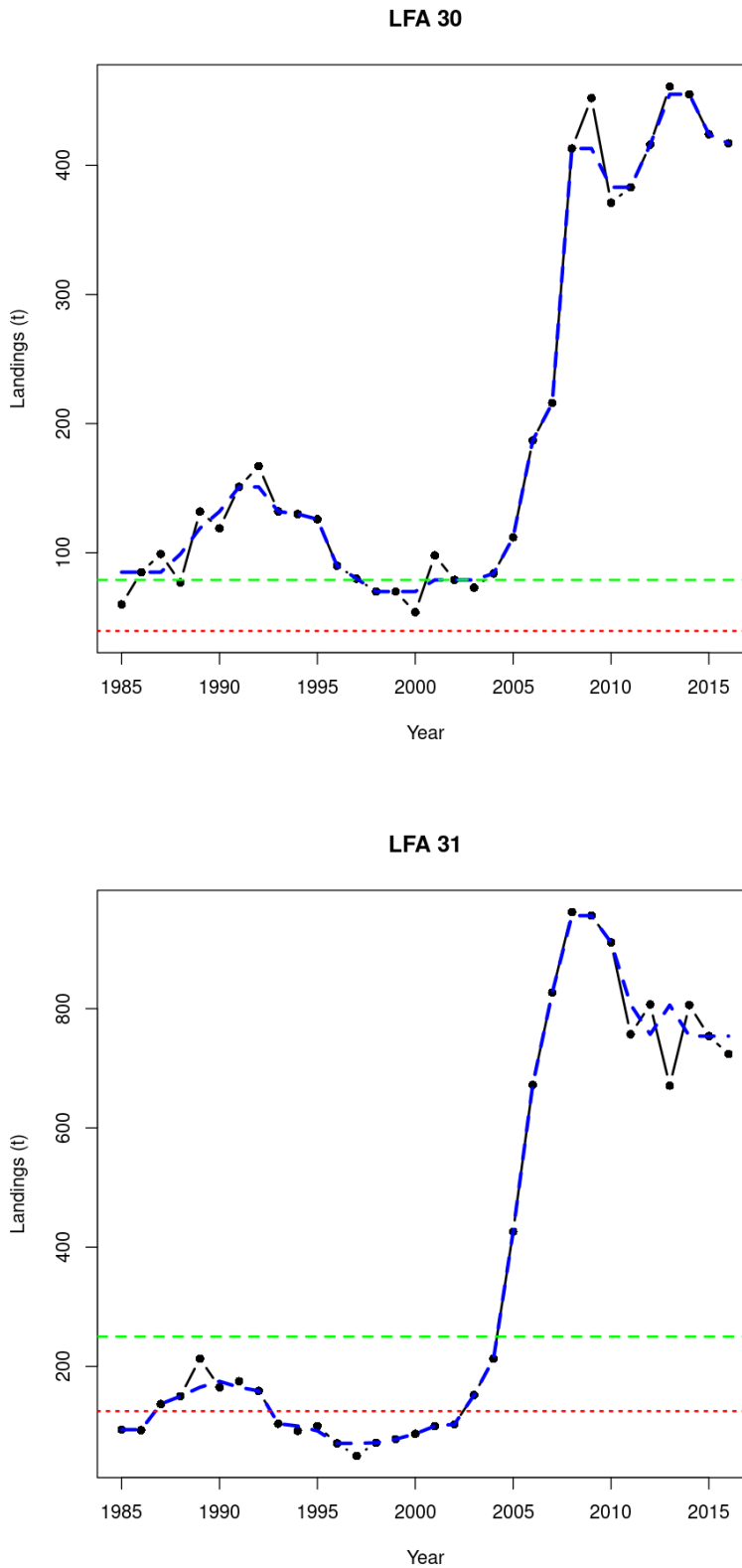


Figure 124: Time series of landings (black), three year running median of landings (blue) with currently approved upper stock (dashed green line) and limit reference (dotted red line) points by LFA.

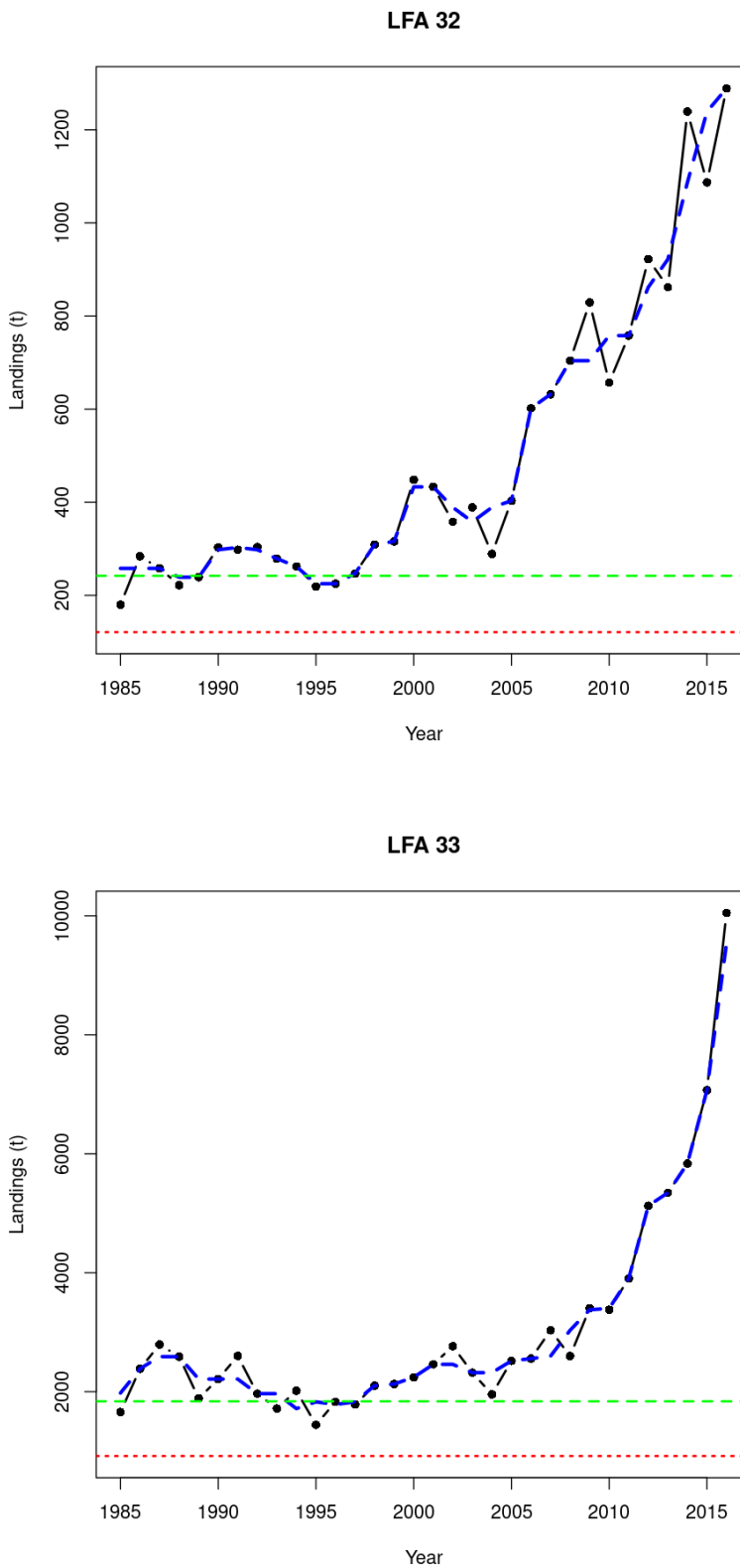


Figure 125: Time series of landings (black), three year running median of landings (blue) with currently approved upper stock (dashed green line) and limit reference (dotted red line) points by LFA.

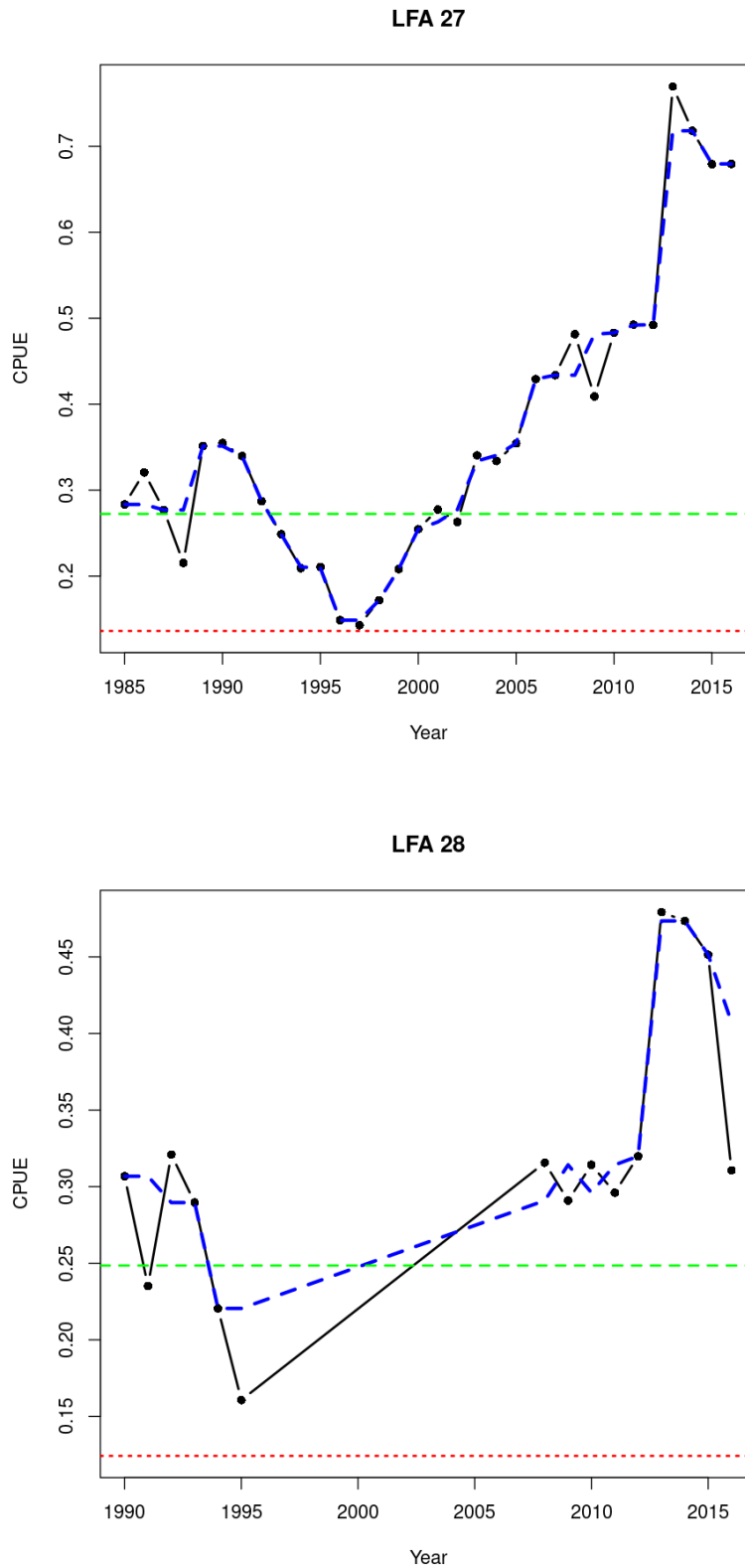


Figure 126: Time series of commercial catch rates (black), three year running median (blue) with proposed upper stock (dashed green line) and limit reference (dotted red line) points by LFA.

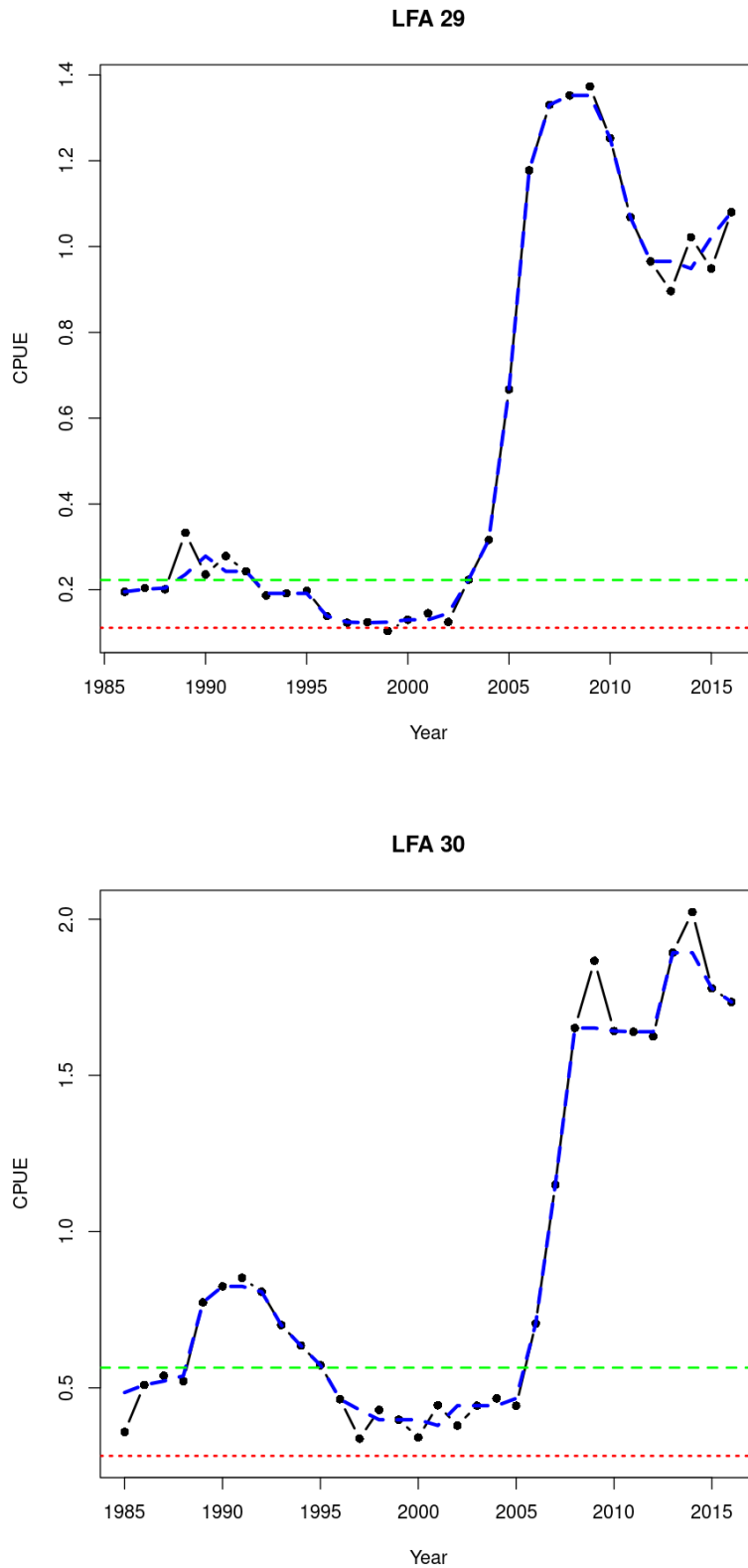


Figure 127: Time series of commercial catch rates (black), three year running median (blue) with proposed upper stock (dashed green line) and limit reference (dotted red line) points by LFA.

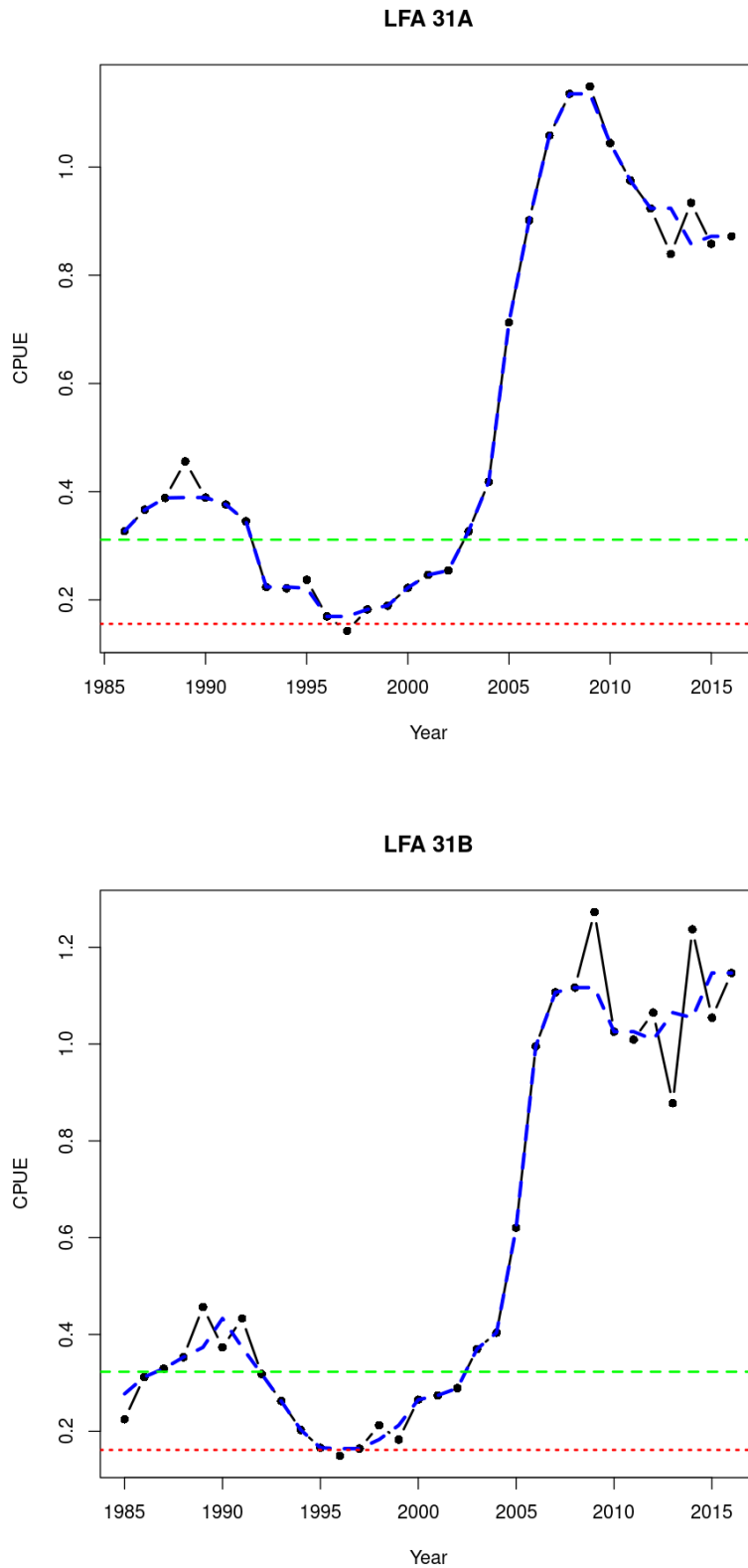


Figure 128: Time series of commercial catch rates (black), three year running median (blue) with proposed upper stock (dashed green line) and limit reference (dotted red line) points by LFA.

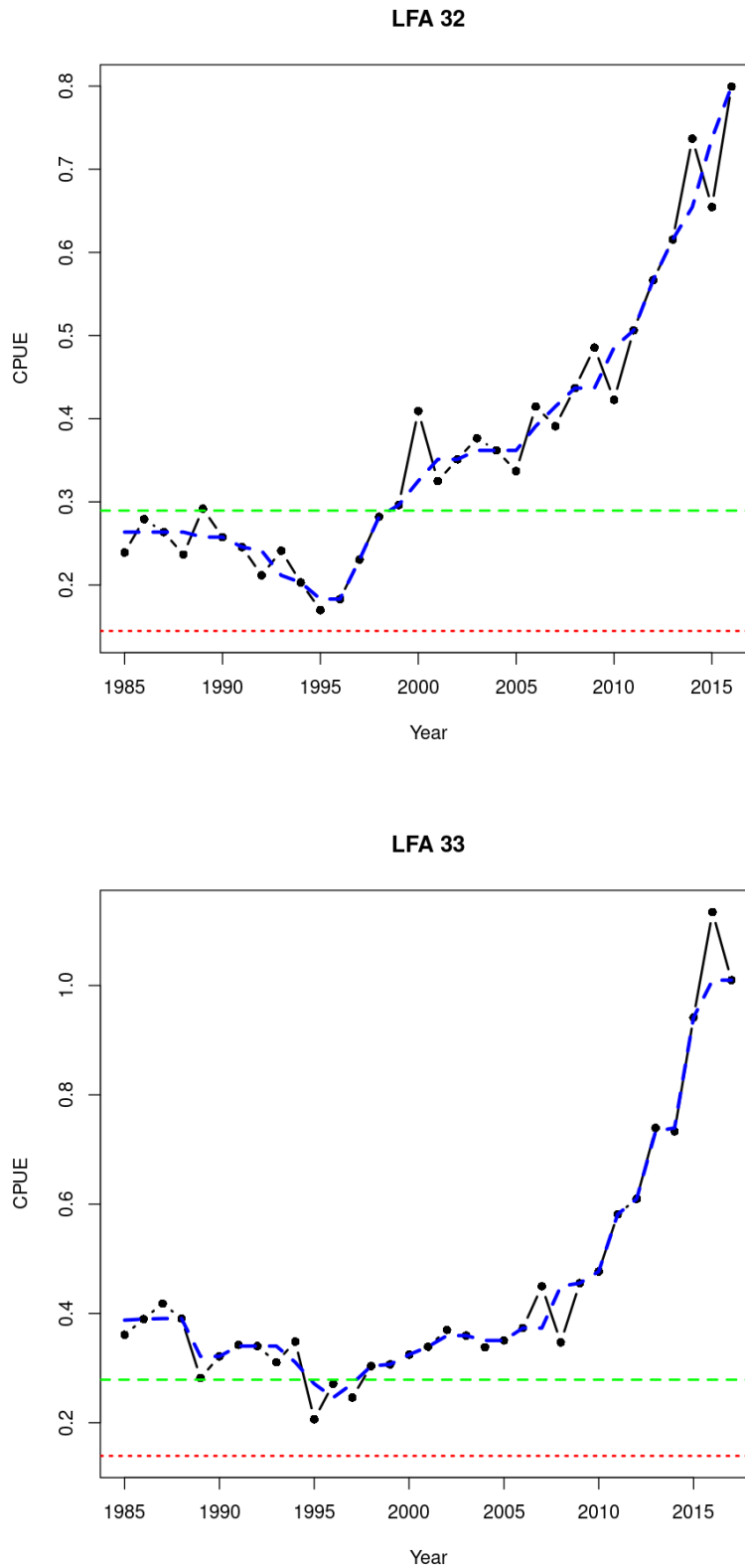


Figure 129: Time series of commercial catch rates (black), three year running median (blue) with proposed upper stock (dashed green line) and limit reference (dotted red line) points by LFA.

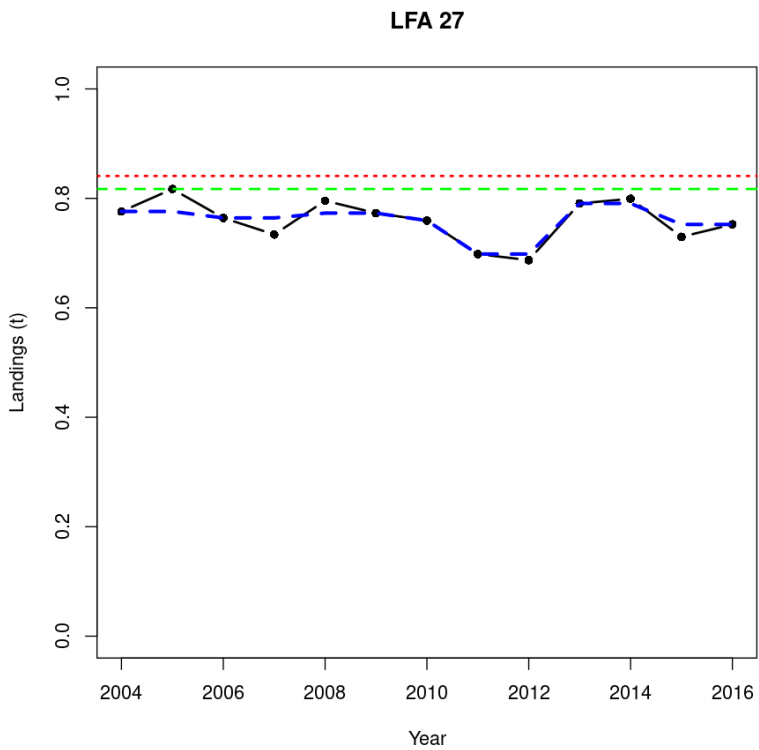


Figure 130: Time series of CCIR exploitation indices (black), three year running median (blue) with removal references (RRc = dashed green line; RR₇₅ = dotted red line)

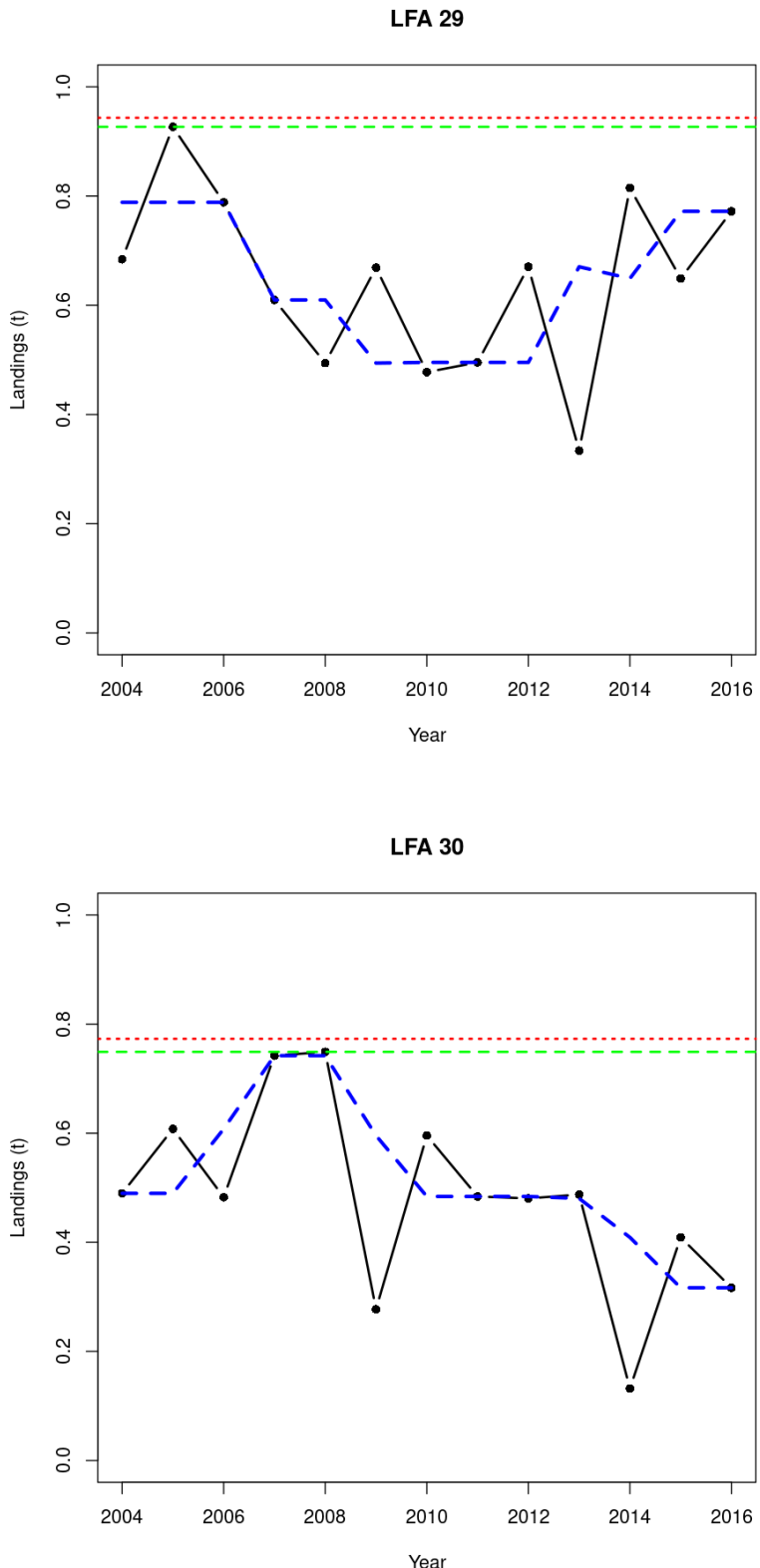


Figure 131: Time series of CCIR exploitation indices (black), three year running median (blue) with removal references (RRc = dashed green line; RR_{75} = dotted red line)

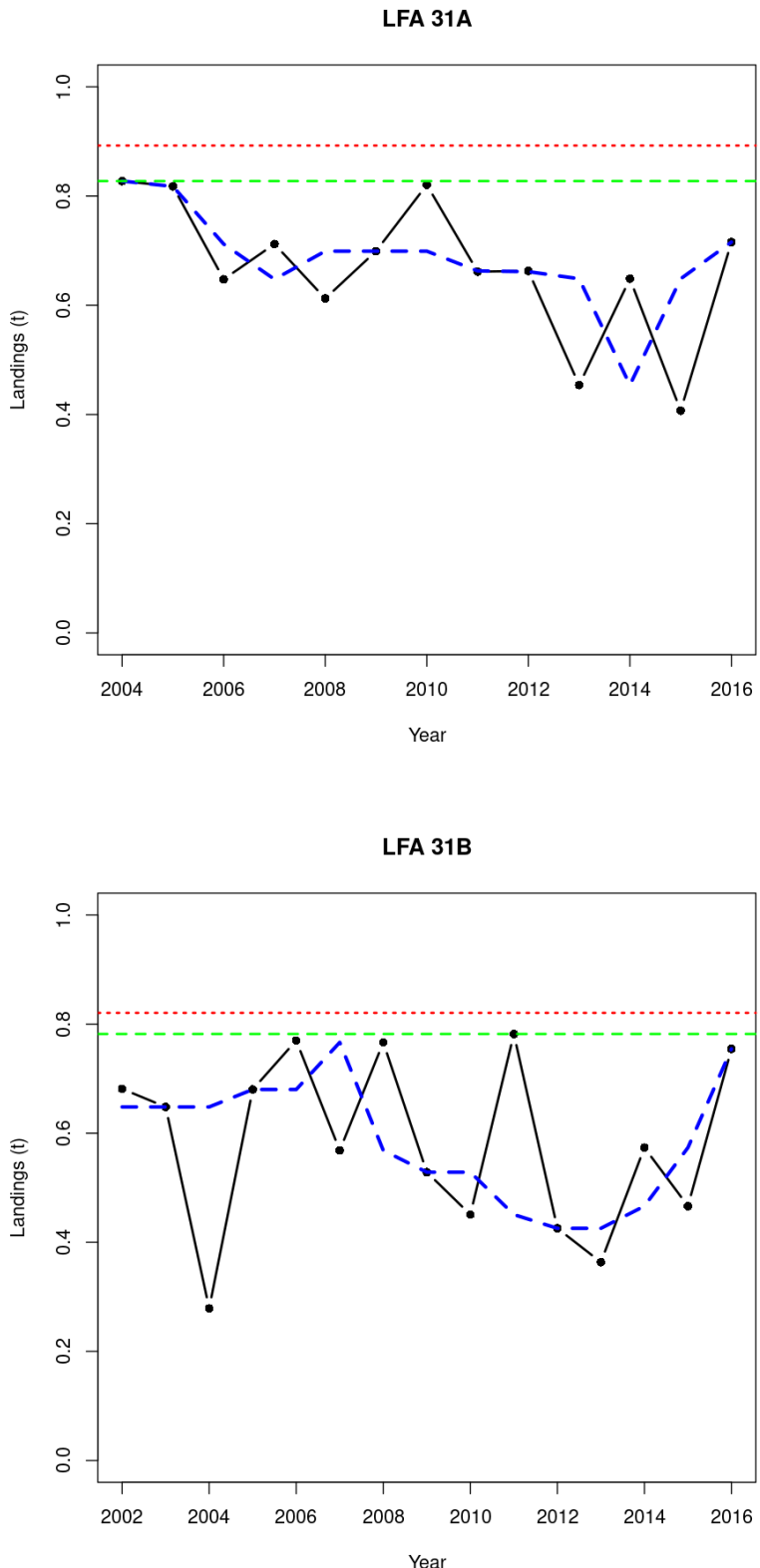


Figure 132: Time series of CCIR exploitation indices (black), three year running median (blue) with removal references (RRc = dashed green line; RR₇₅ = dotted red line)

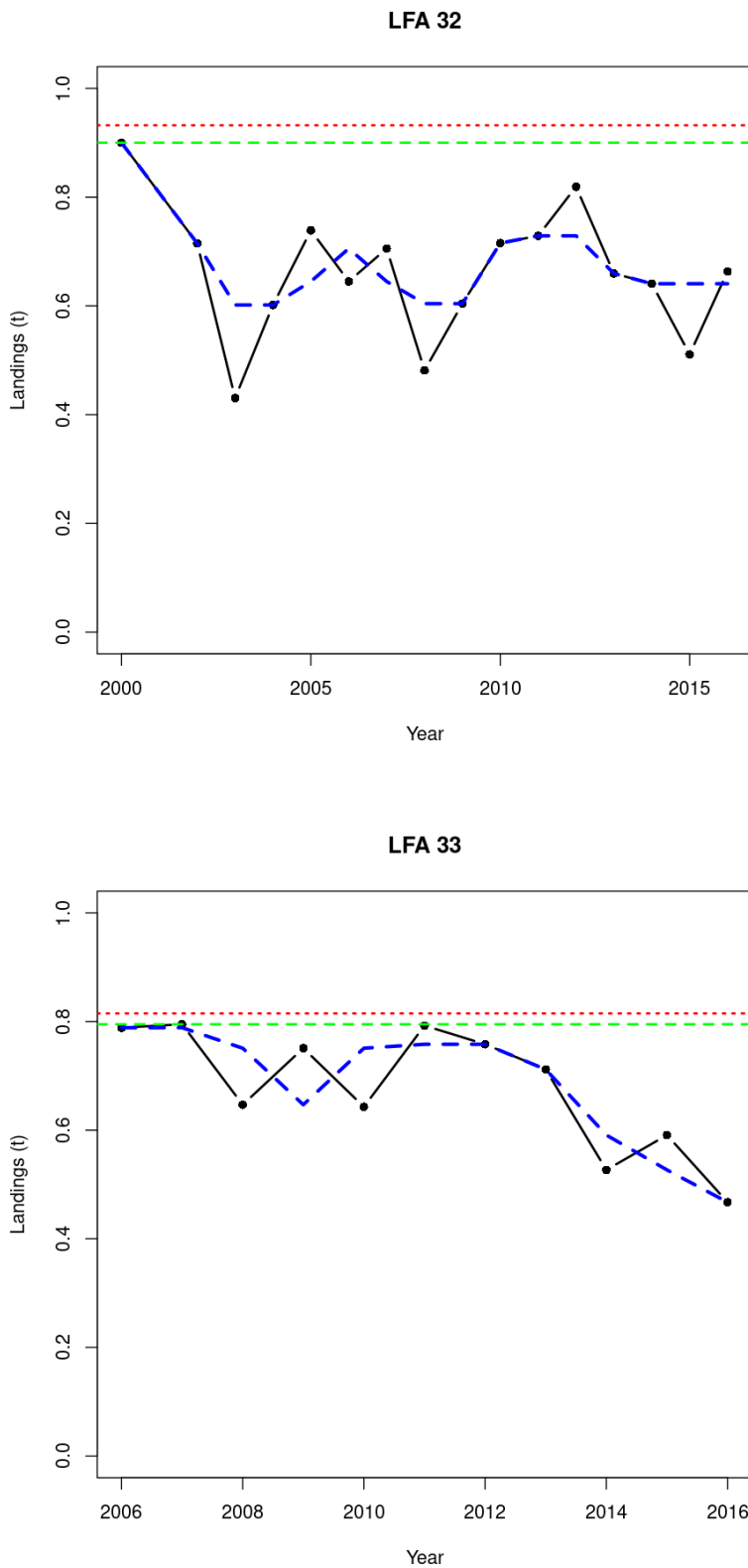


Figure 133: Time series of CCIR exploitation indices (black), three year running median (blue) with removal references (RRc = dashed green line; RR₇₅ = dotted red line)

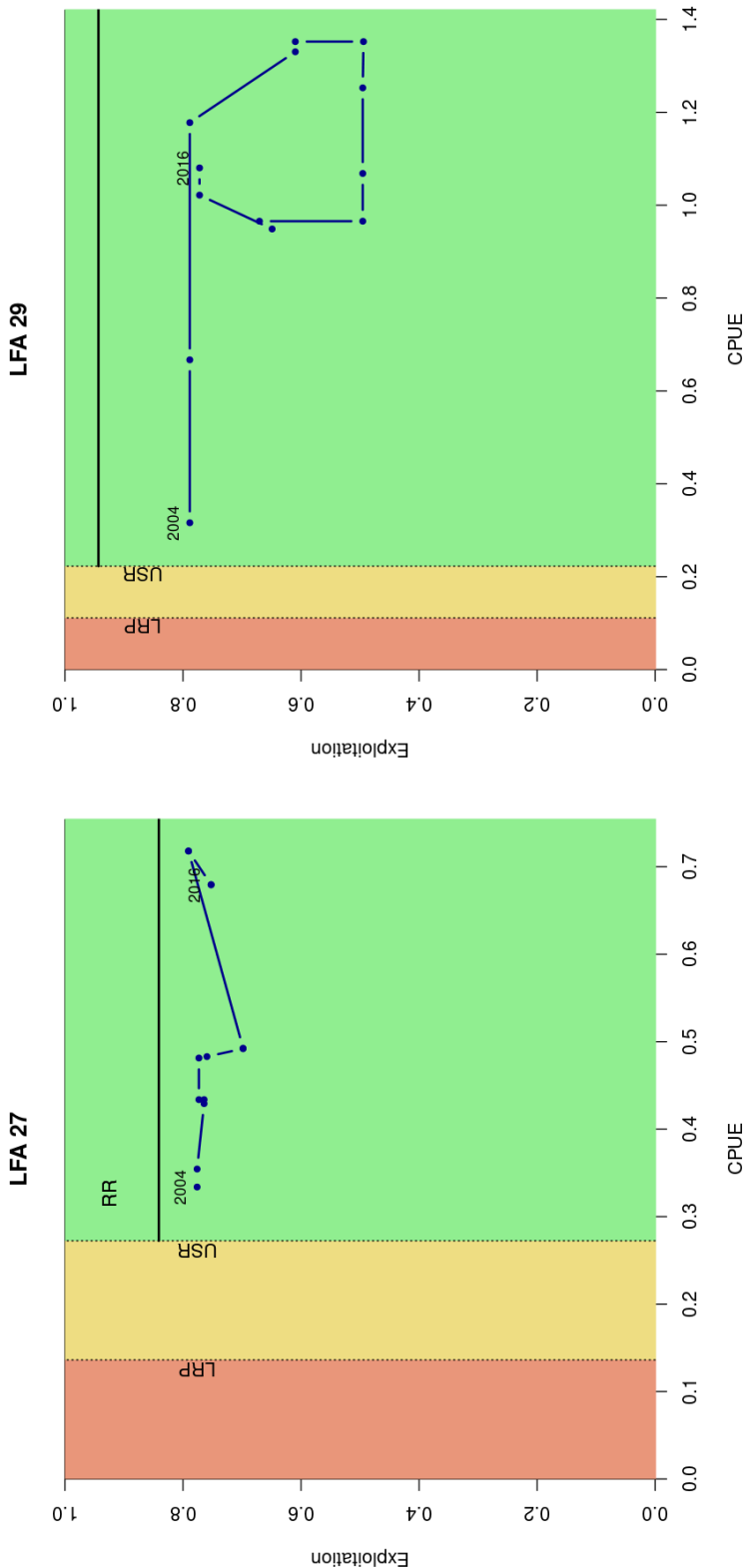


Figure 134: Phase plot using the three year running median of CCIR exploitation index compared against the proposed upper stock and limit reference points based on commercial catch rates. The removal reference proposed represented the 75th quantile break of the posterior distribution for the maximum exploitation index respectively.

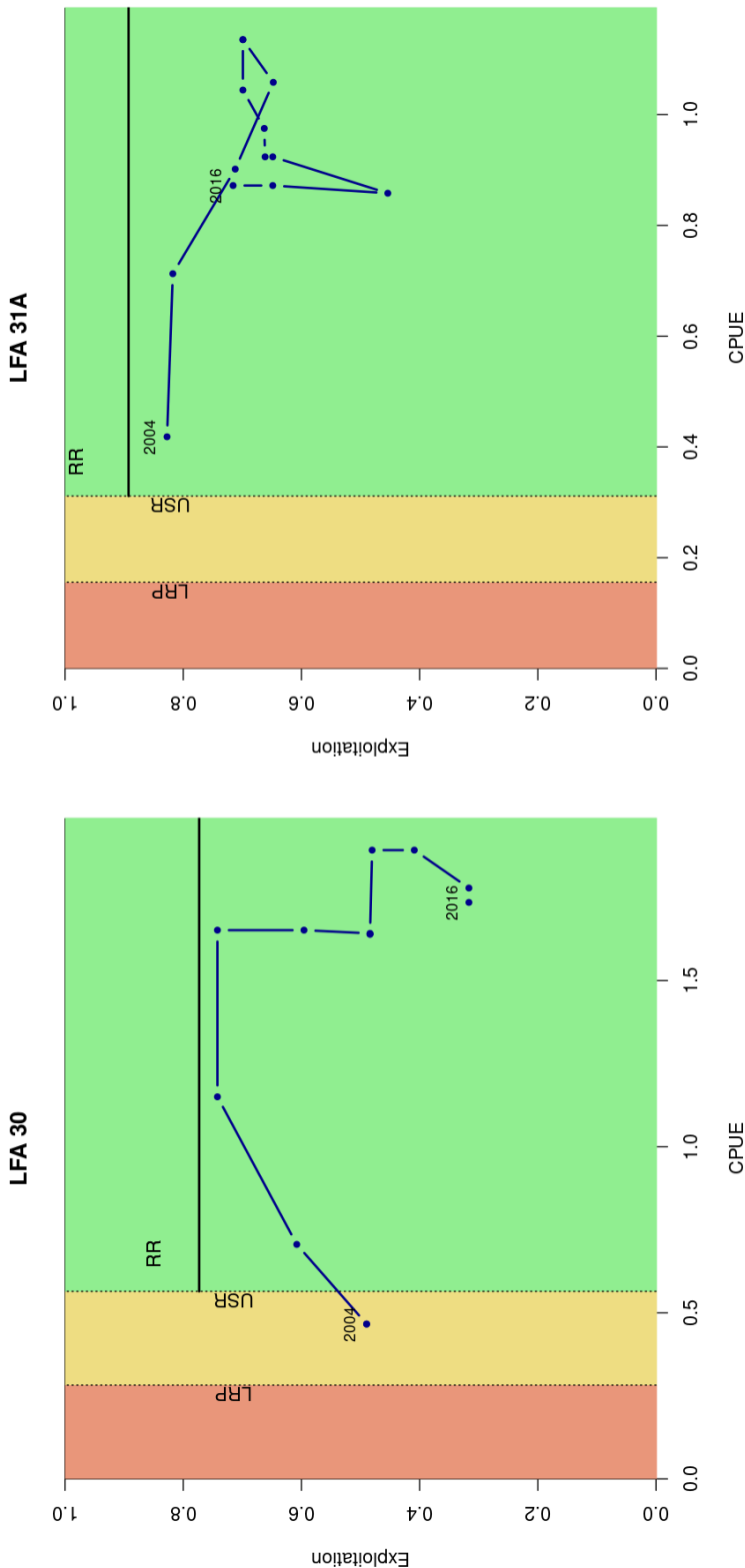


Figure 135: Phase plot using the three year running median of CCIR exploitation index compared against the proposed upper stock and limit reference points based on commercial catch rates. The removal reference proposed represented the 75th quantile break of the posterior distribution for the maximum exploitation index respectively.

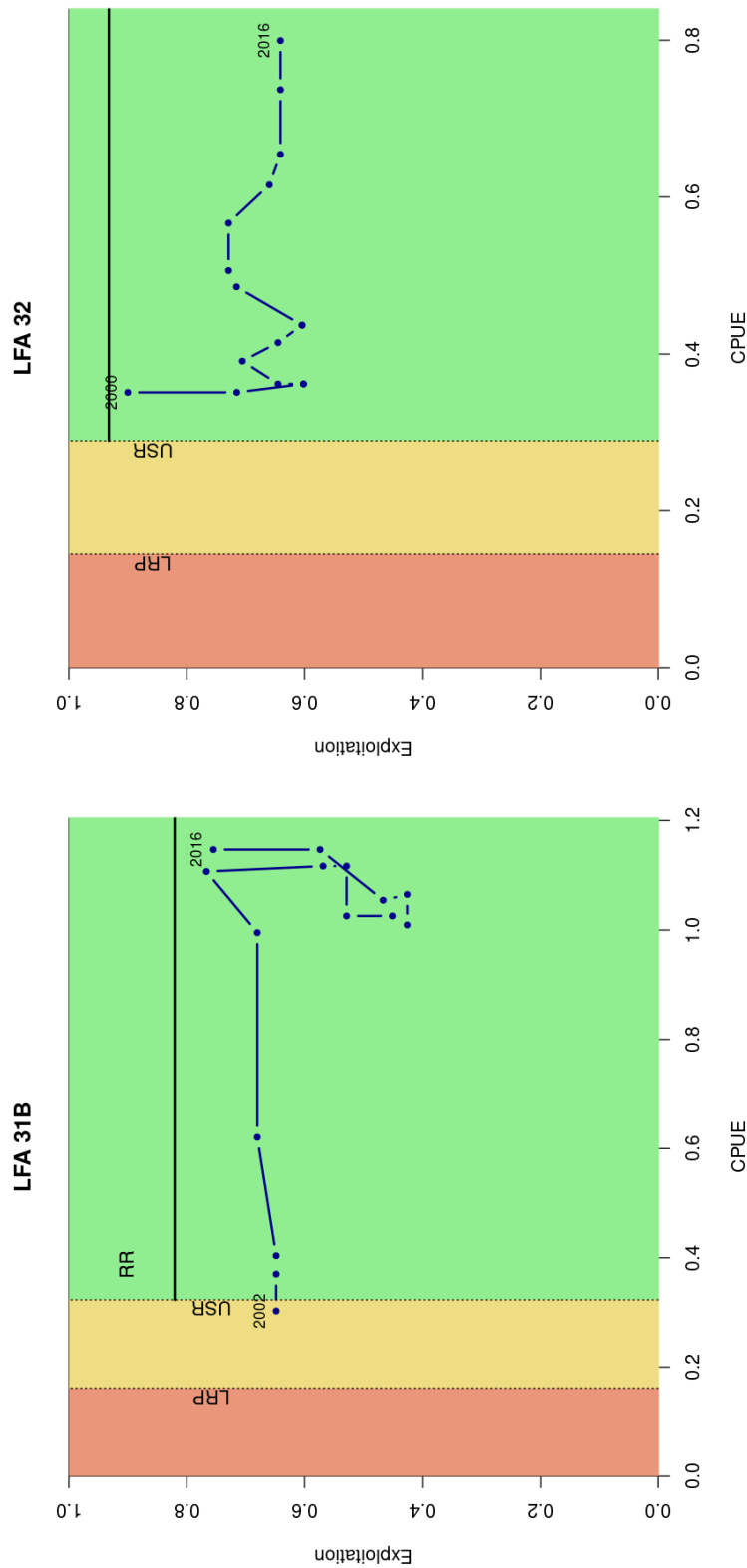


Figure 136: Phase plot using the three year running median of landings and three year running median of CCIR exploitation index compared against the proposed upper stock and limit reference points based on commercial catch rates. The removal reference proposed represented the 75th quantile break of the posterior distribution for the maximum exploitation index respectively.

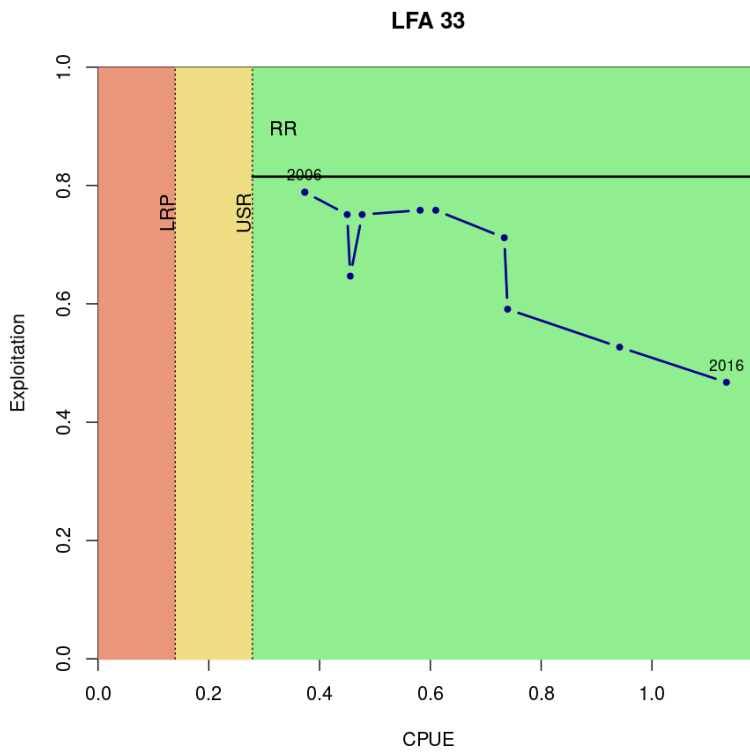


Figure 137: Phase plot using the three year running median of landings and three year running median of CCIR exploitation index compared against the proposed upper stock and limit reference points based on commercial catch rates. The removal reference proposed represented the 75th quantile break of the posterior distribution for the maximum exploitation index respectively.

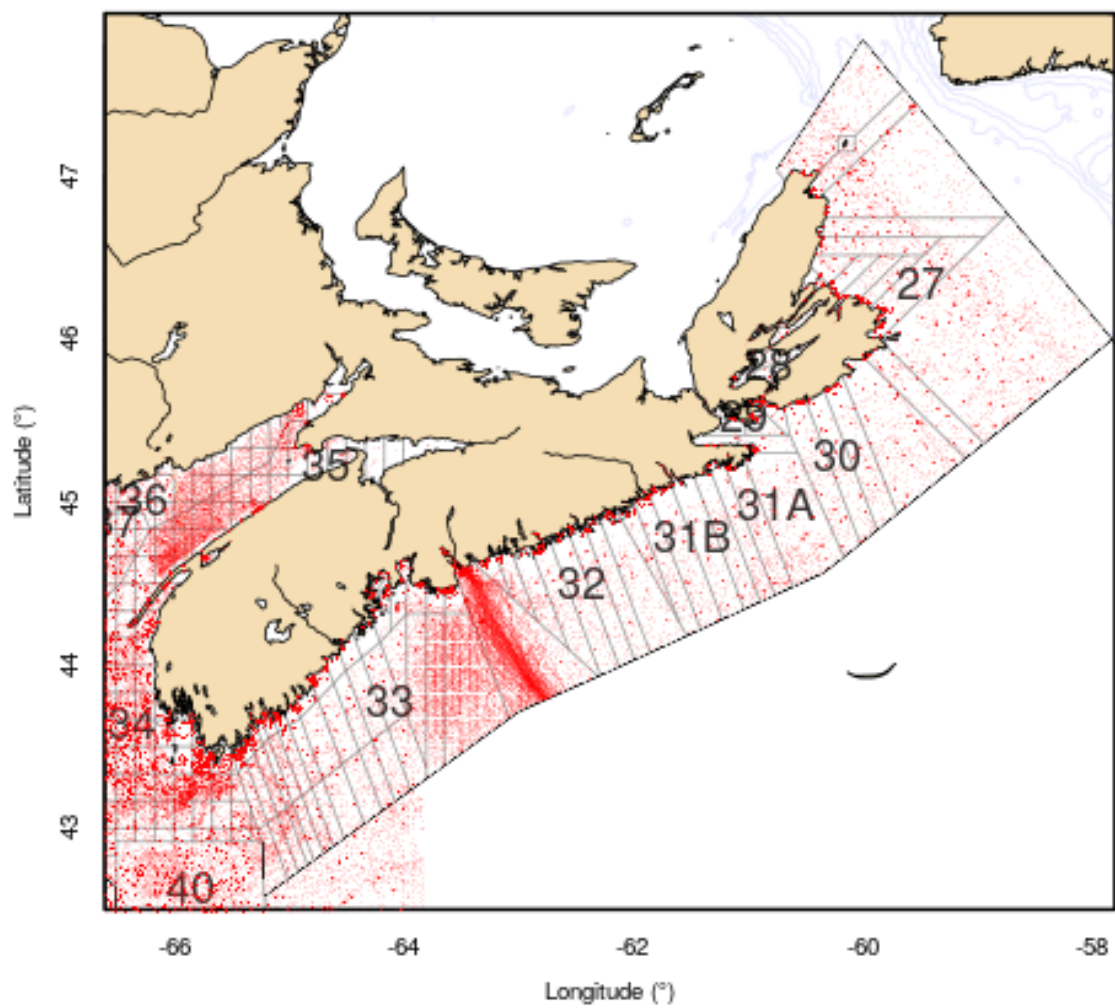


Figure 138: Locations of all temperature data used in the temperature model.

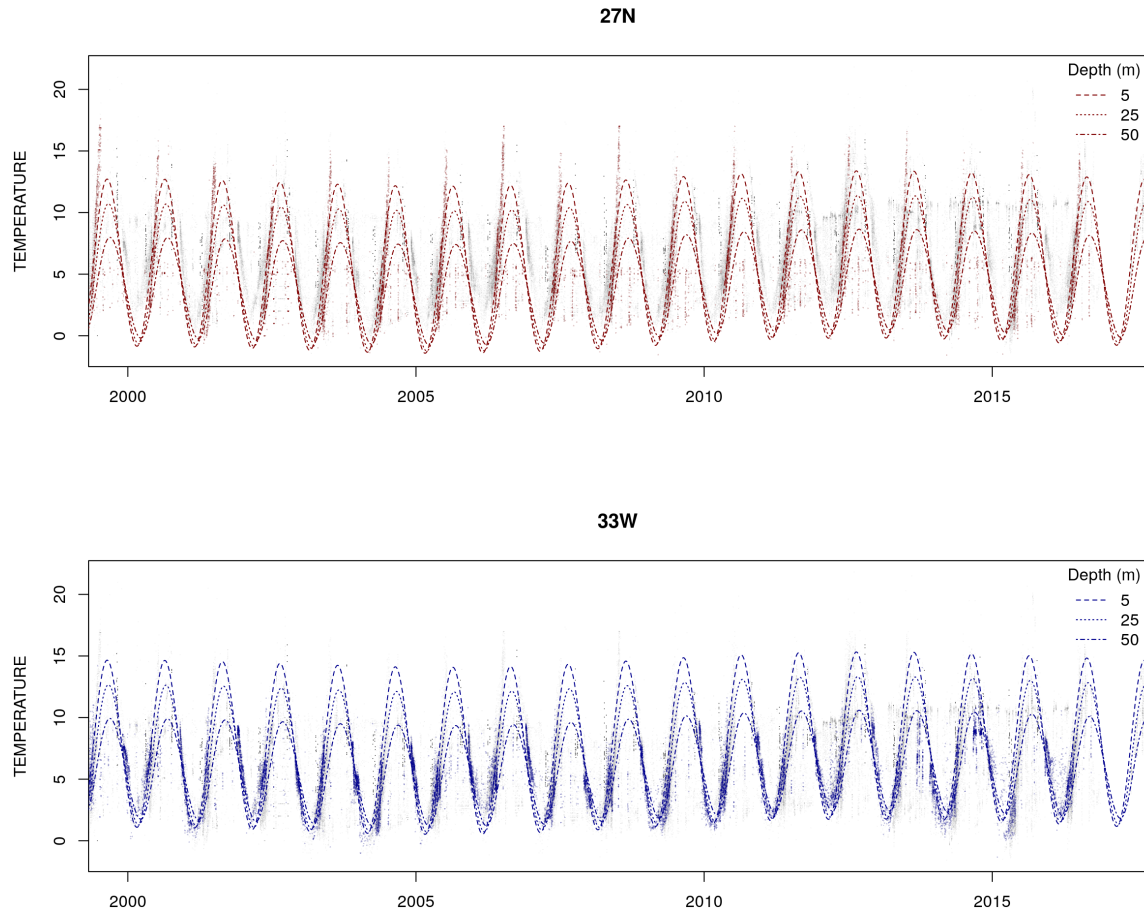


Figure 139: Time series of temperature data overlaid with predictions from the temperature model showing seasonal trends in LFA 27N (top, red) and LFA 33W (bottom, blue) at various depths.

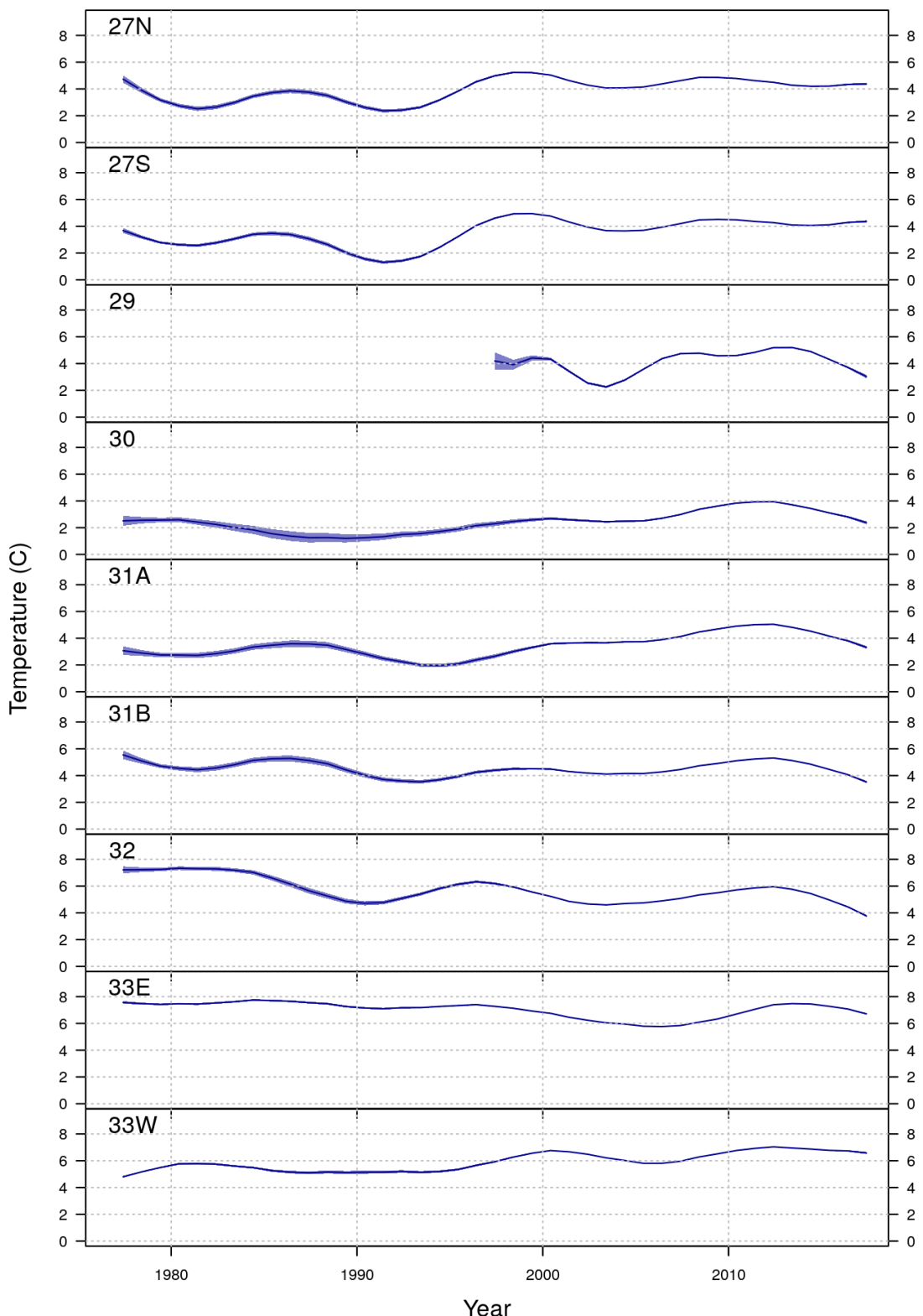


Figure 140: Predictions from the temperature model for June 1st at 25 m to show the annual trends in each LFA. Light blue band represents the standard error of the prediction.

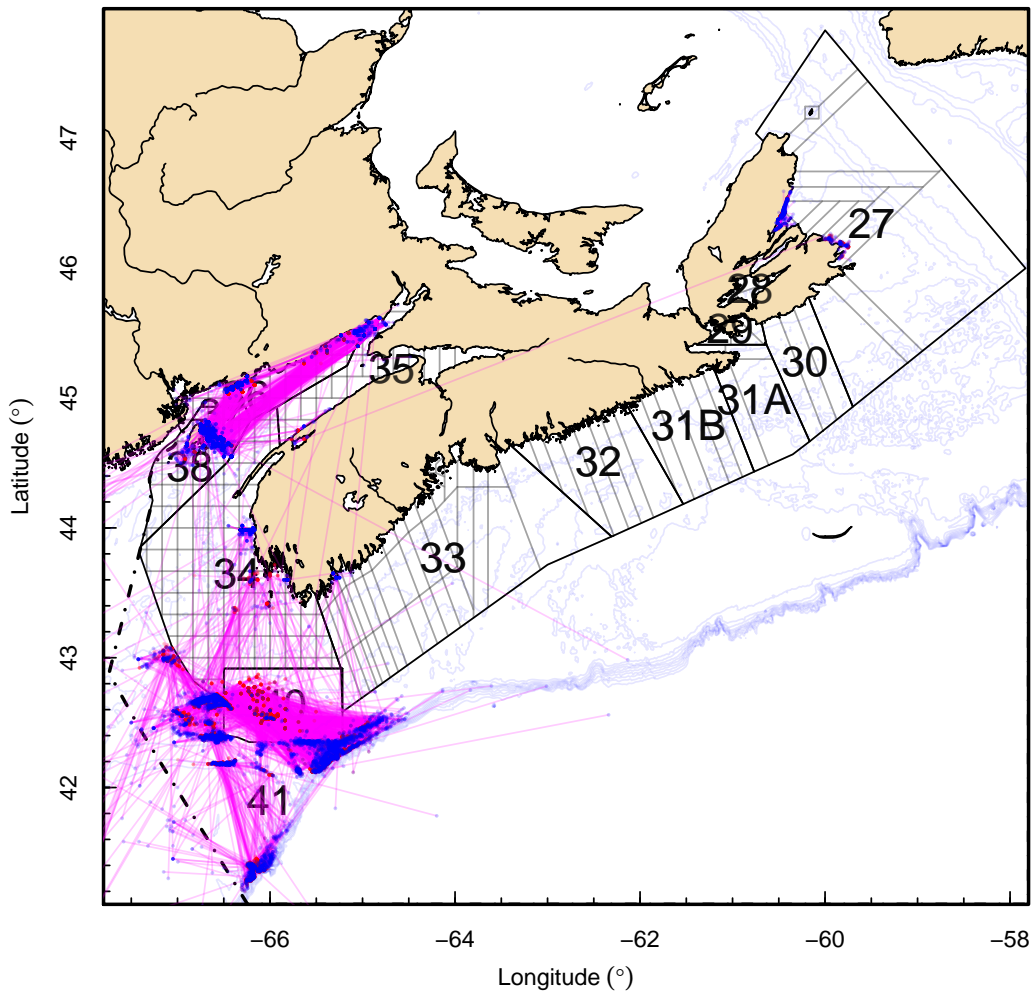


Figure 141: Locations of tagging mark-recapture data used for estimating moult probability and increment. Releases (red dots) are connected to their recaptures (blue dots) with a purple line.

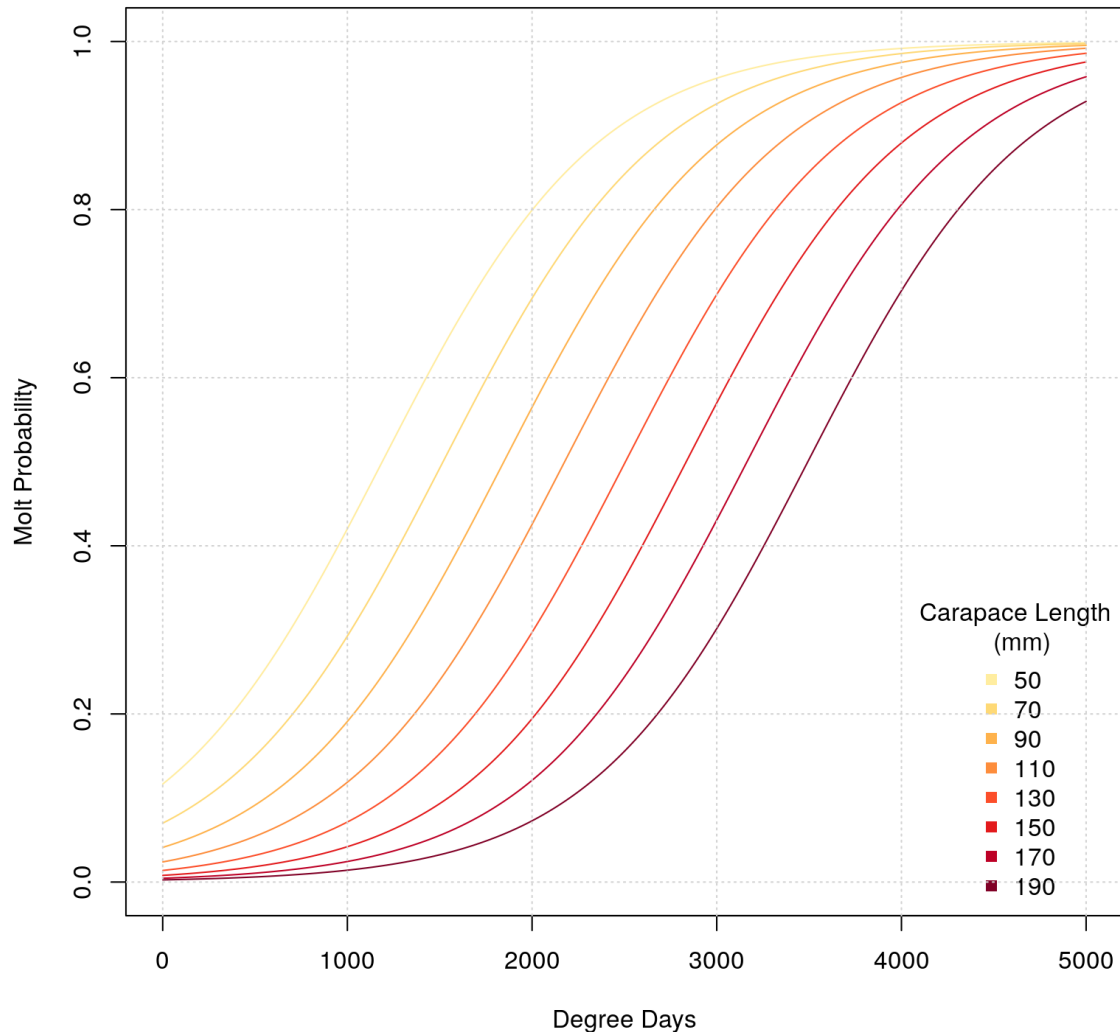


Figure 142: Predicted molt probabilities by number of degree days above 0°C since last molt for various initial carapace lengths from the molt probability model.

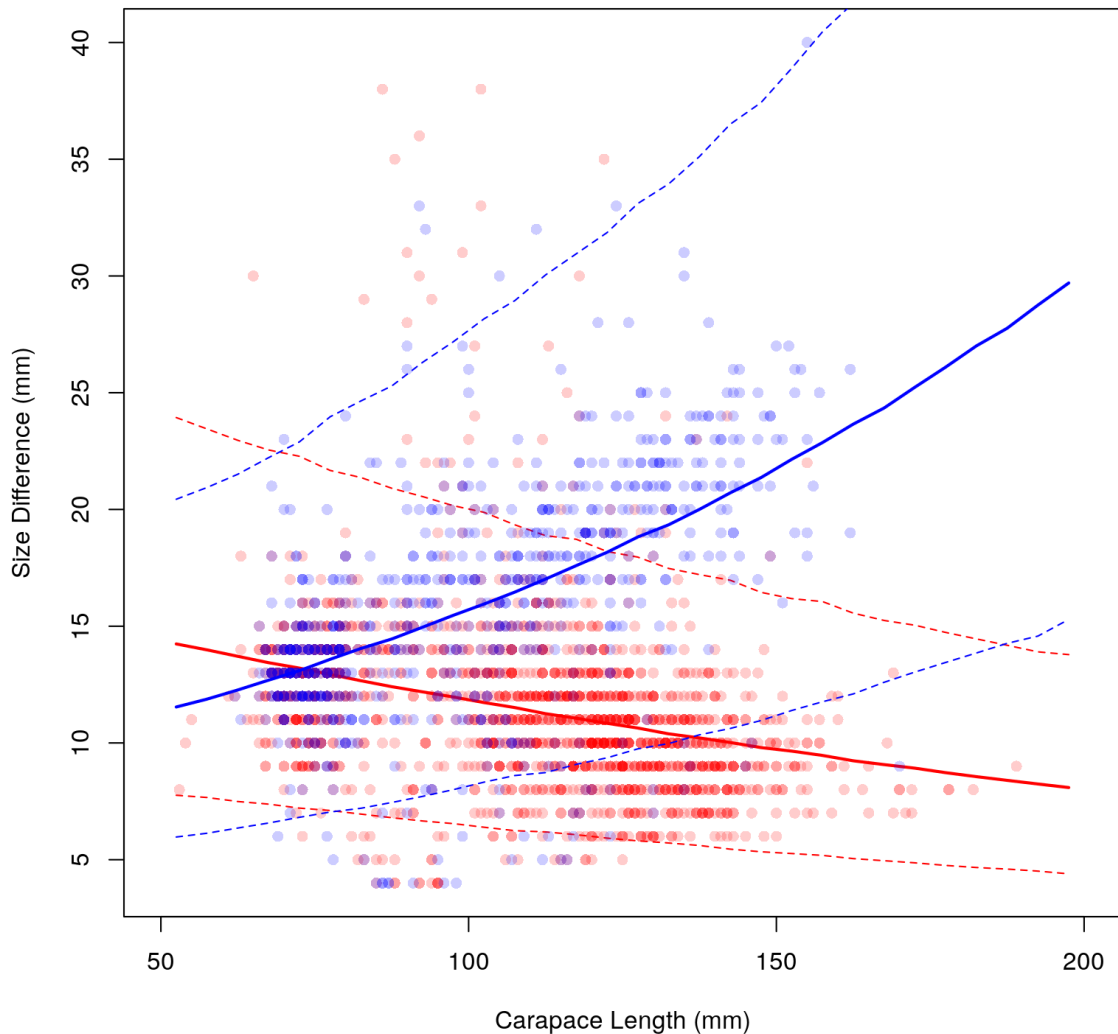


Figure 143: Molt increment as the size difference versus initial carapace length for males (blue) and females (red) from tagging data. Lines represent the fits and 95% credible interval of the molt increment model for each sex.

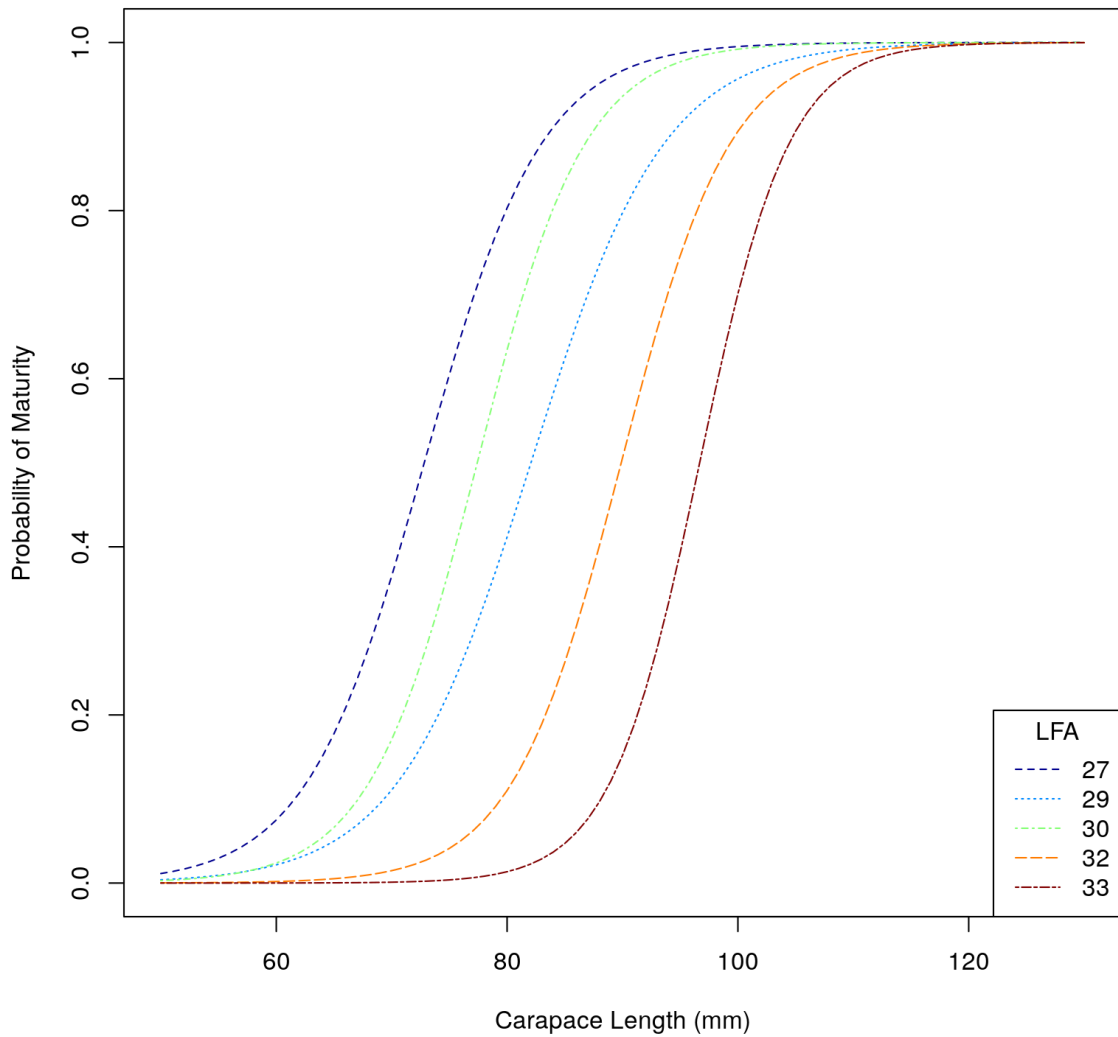


Figure 144: Size at maturity ogives applied for selected LFAs.

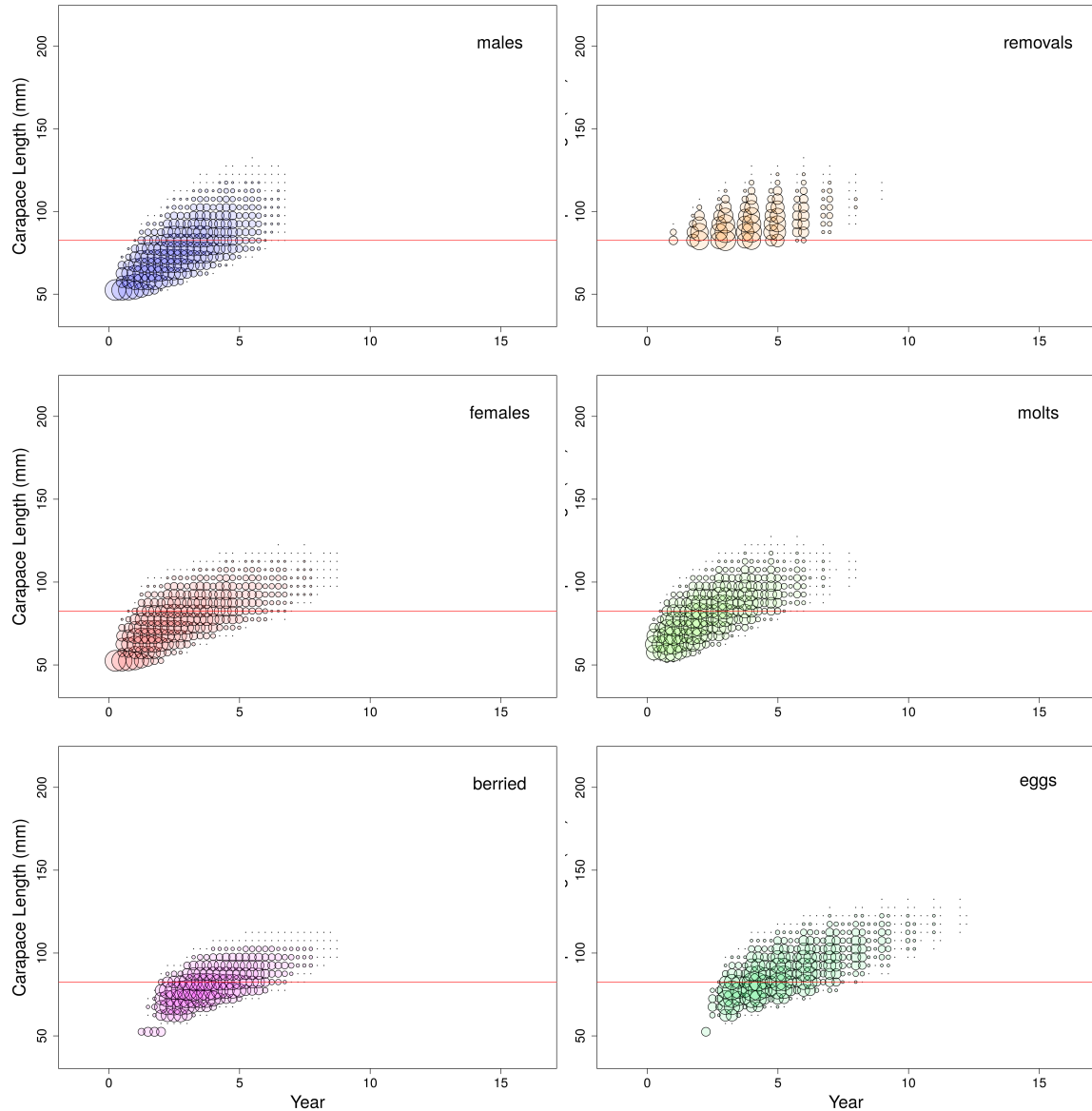


Figure 145: Bubble plots showing the simulated population under the current management regime for LFA 27N. The diameter of the bubbles are proportional to the log number of lobsters in a given size bin and time step.

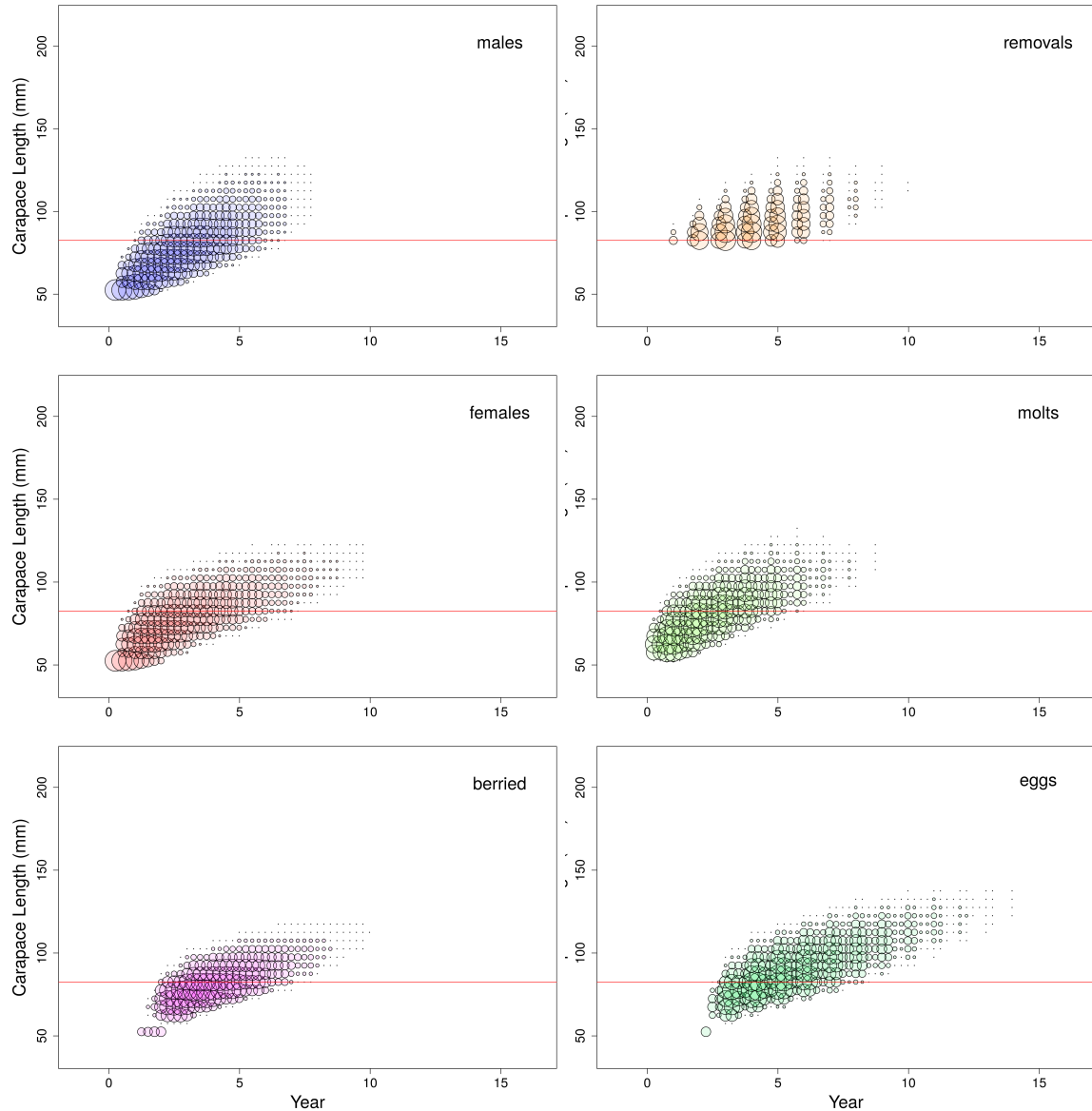


Figure 146: Bubble plot showing the simulated population under the current management regime for LFA 27S. The diameter of the bubbles are proportional to the log number of lobsters in a given size bin and time step.

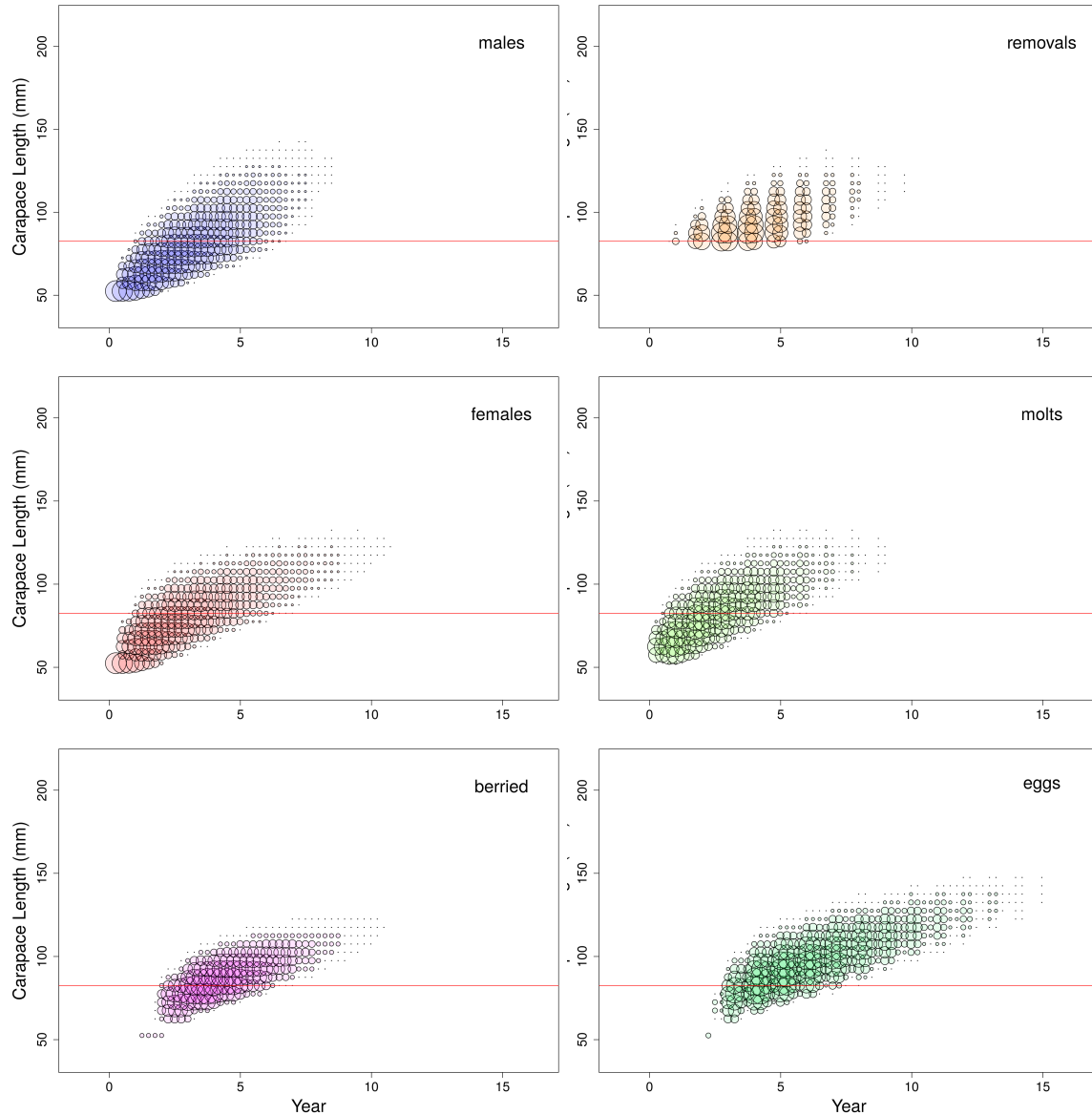


Figure 147: Bubble plot showing the simulated population under the current management regime for LFA 29. The diameter of the bubbles are proportional to the log number of lobsters in a given size bin and time step.

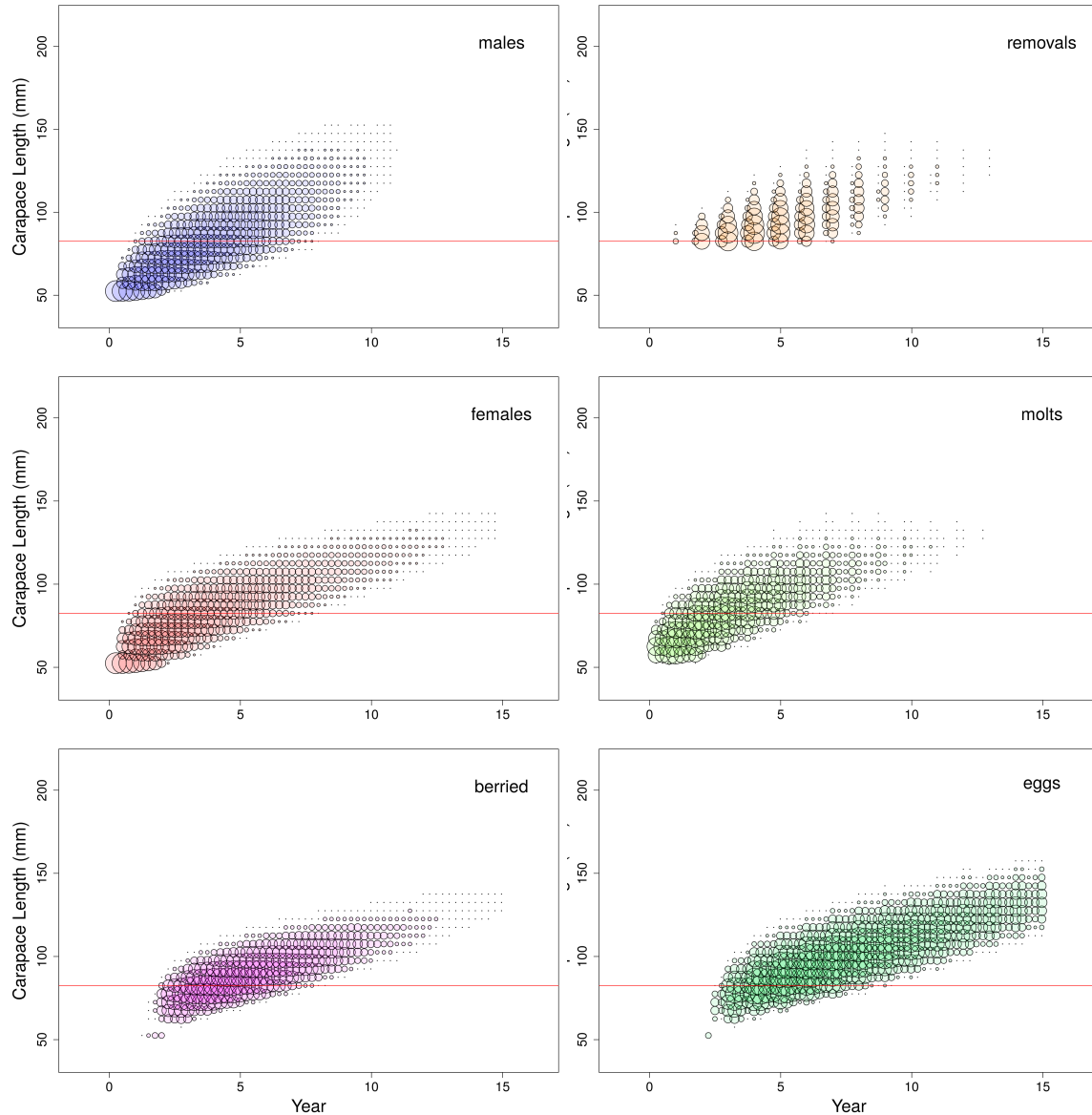


Figure 148: Bubble plot showing the simulated population under the current management regime for LFA 30. The diameter of the bubbles are proportional to the log number of lobsters in a given size bin and time step.

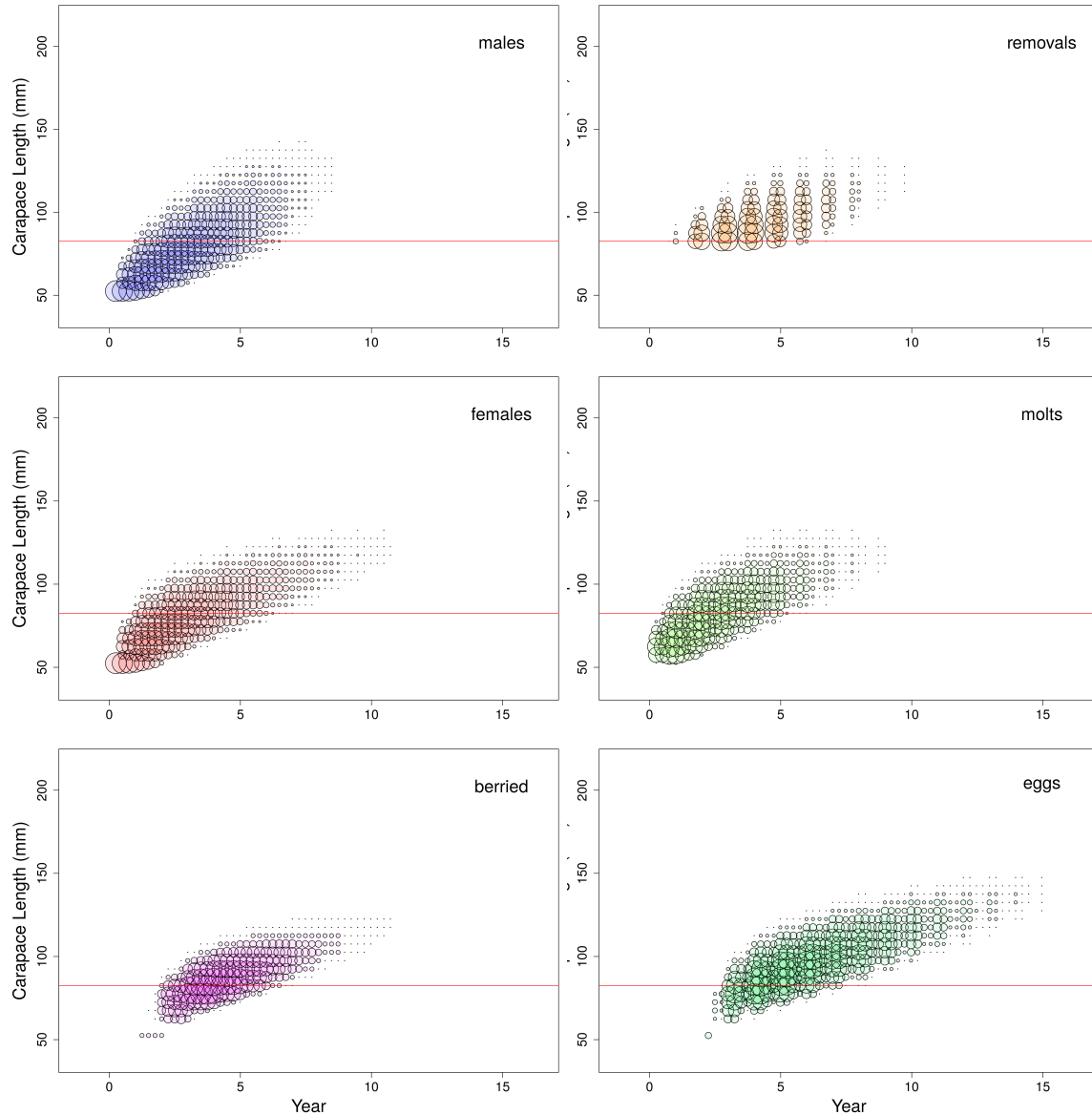


Figure 149: Bubble plot showing the simulated population under the current management regime for LFA 31A. The diameter of the bubbles are proportional to the log number of lobsters in a given size bin and time step.

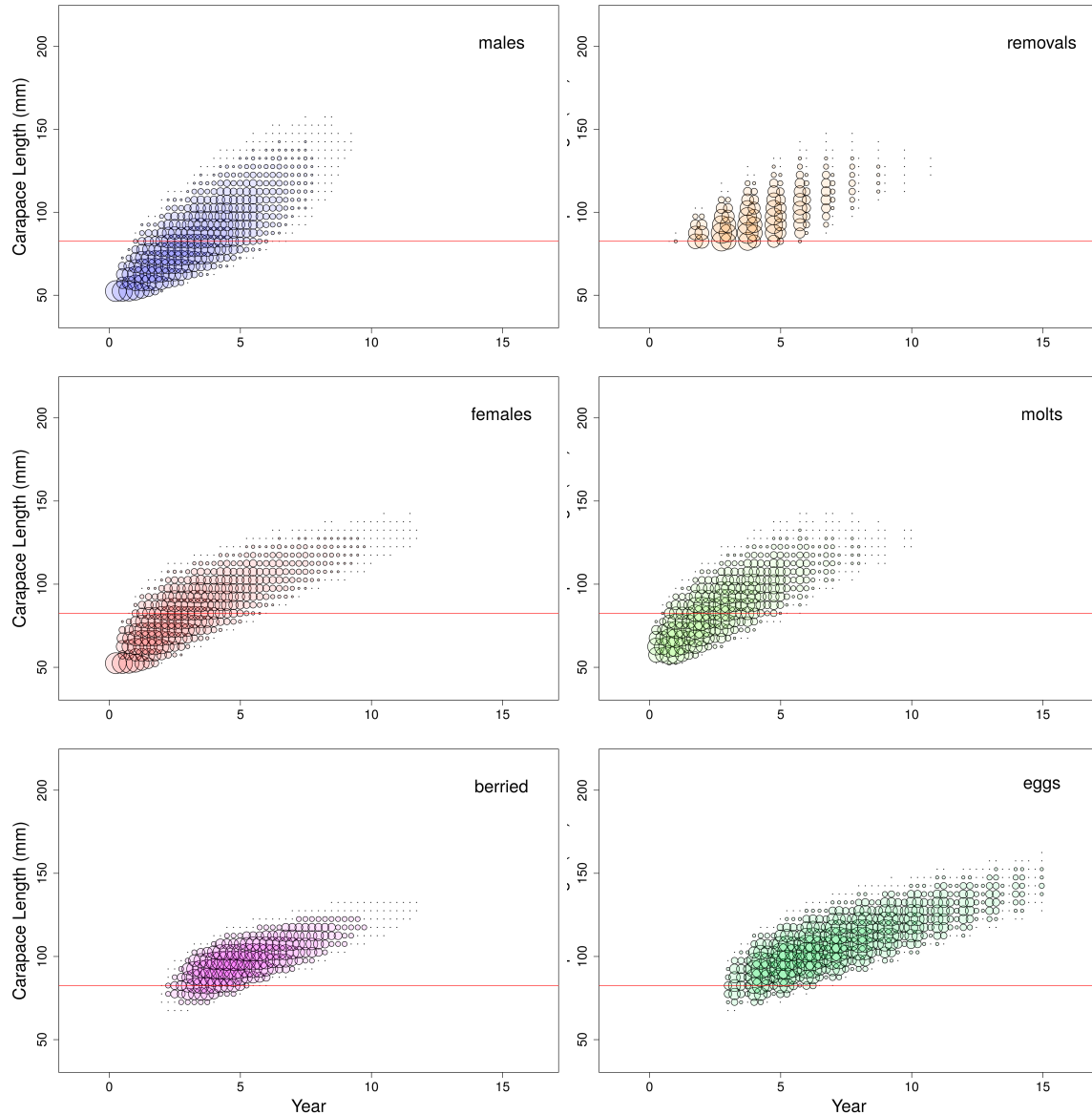


Figure 150: Bubble plot showing the simulated population under the current management regime for LFA 31B. The diameter of the bubbles are proportional to the log number of lobsters in a given size bin and time step.

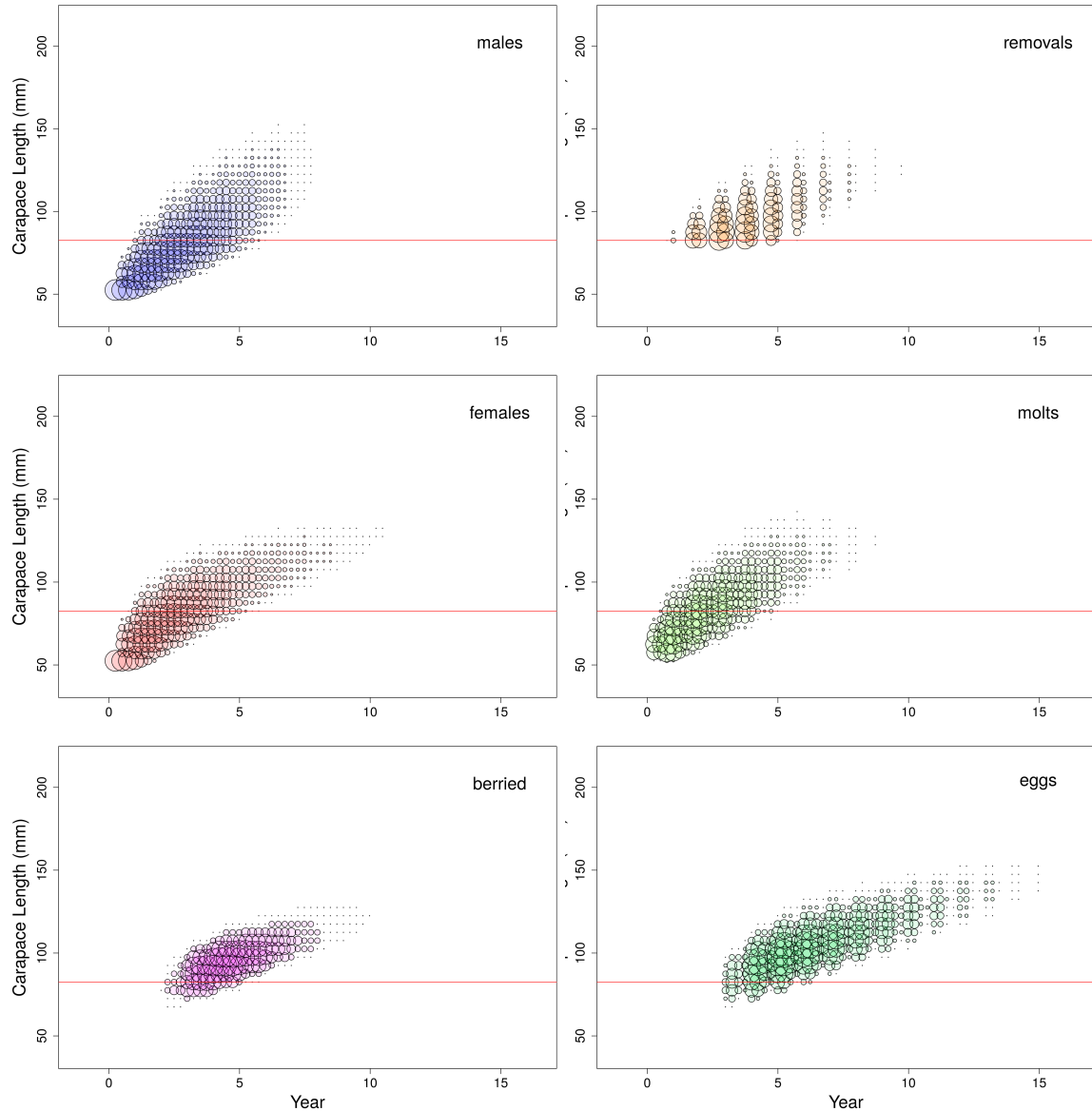


Figure 151: Bubble plot showing the simulated population under the current management regime for LFA 32. The diameter of the bubbles are proportional to the log number of lobsters in a given size bin and time step.

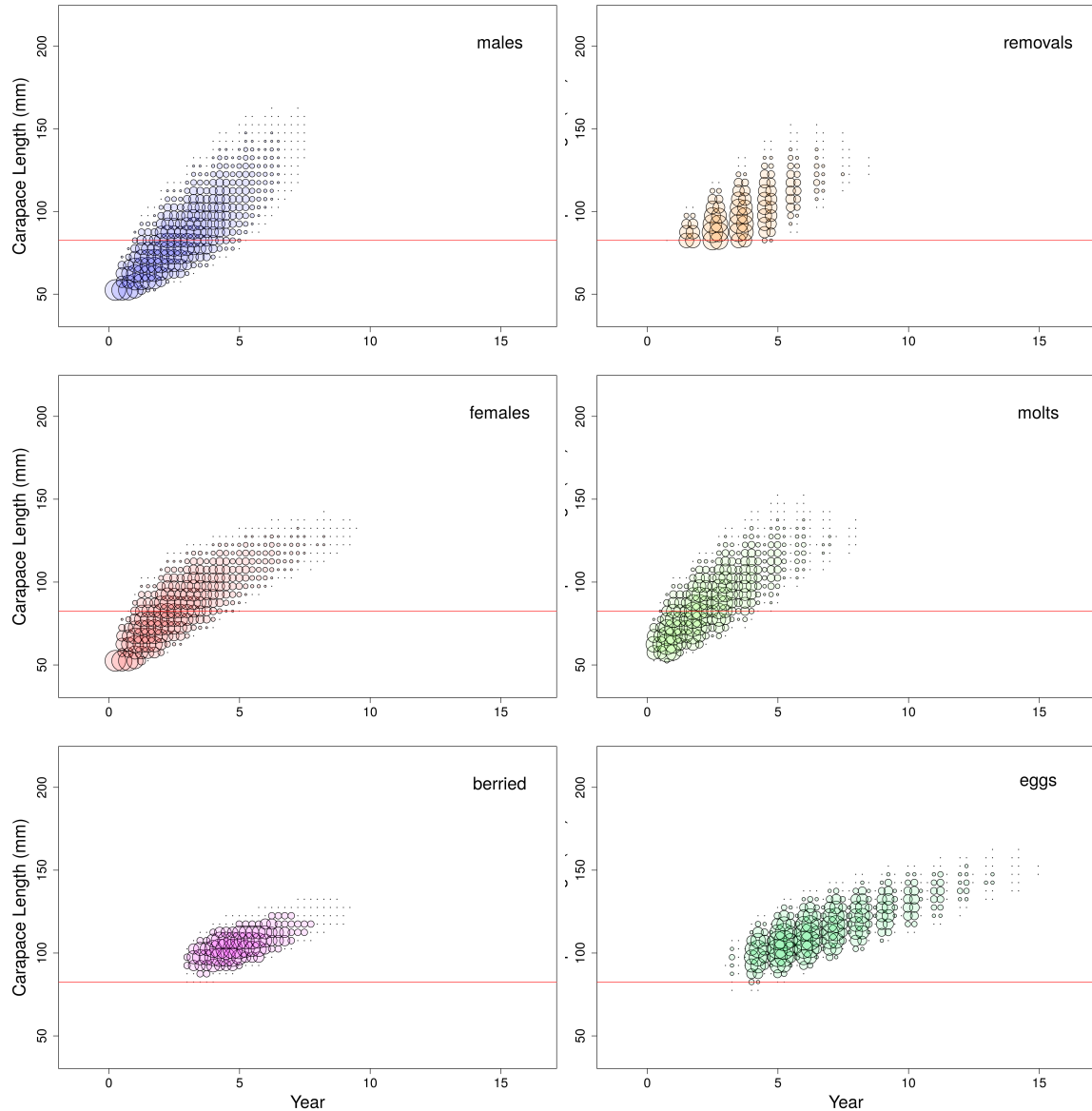


Figure 152: Bubble plot showing the simulated population under the current management regime for LFA 33E. The diameter of the bubbles are proportional to the log number of lobsters in a given size bin and time step.

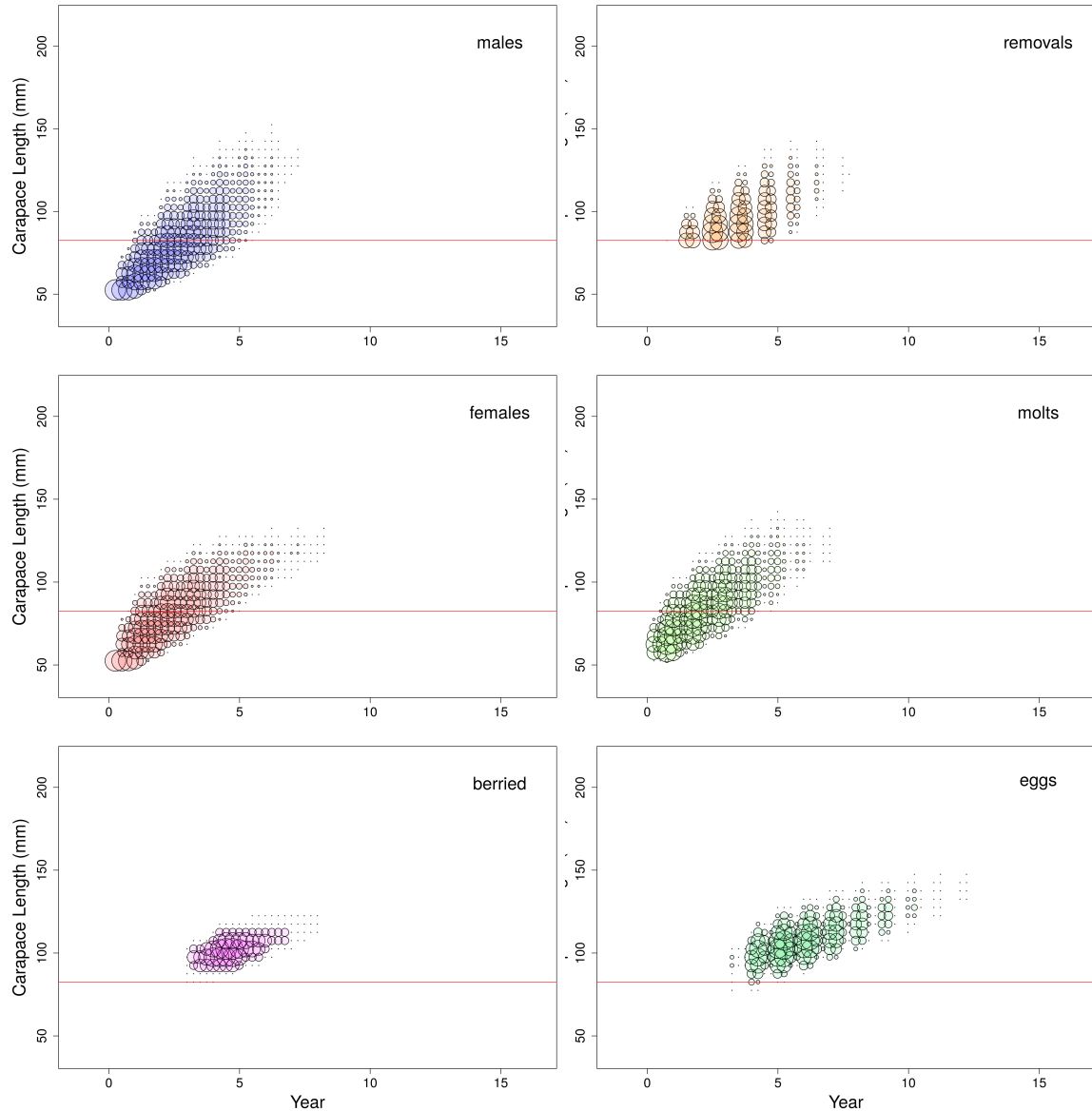


Figure 153: Bubble plot showing the simulated population under the current management regime for LFA 33W. The diameter of the bubbles are proportional to the log number of lobsters in a given size bin and time step.

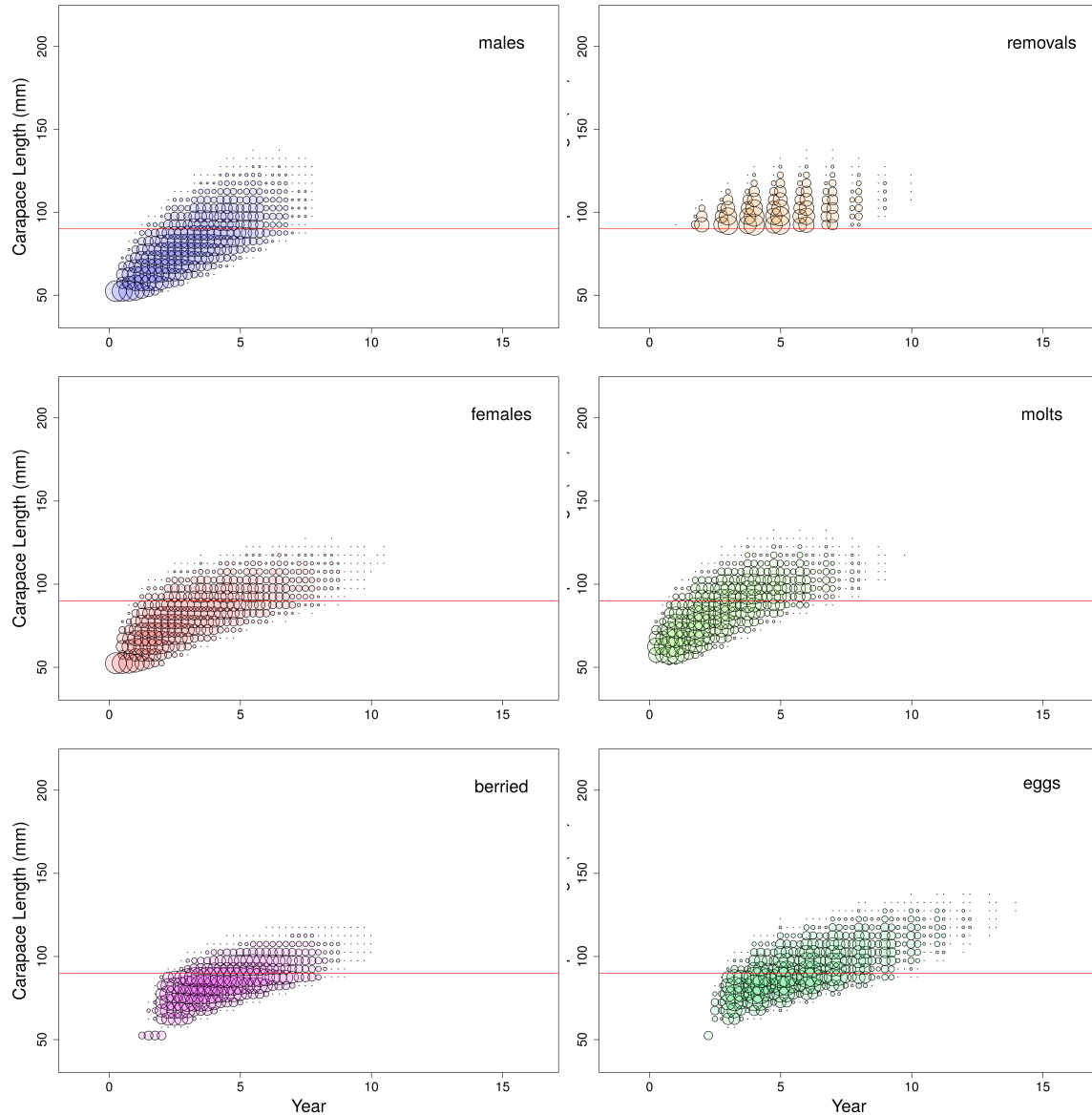


Figure 154: Bubble plots showing the simulated population where MLS was increased to 90mm for LFA 27N. The diameter of the bubbles are proportional to the log number of lobsters in a given size bin and time step.

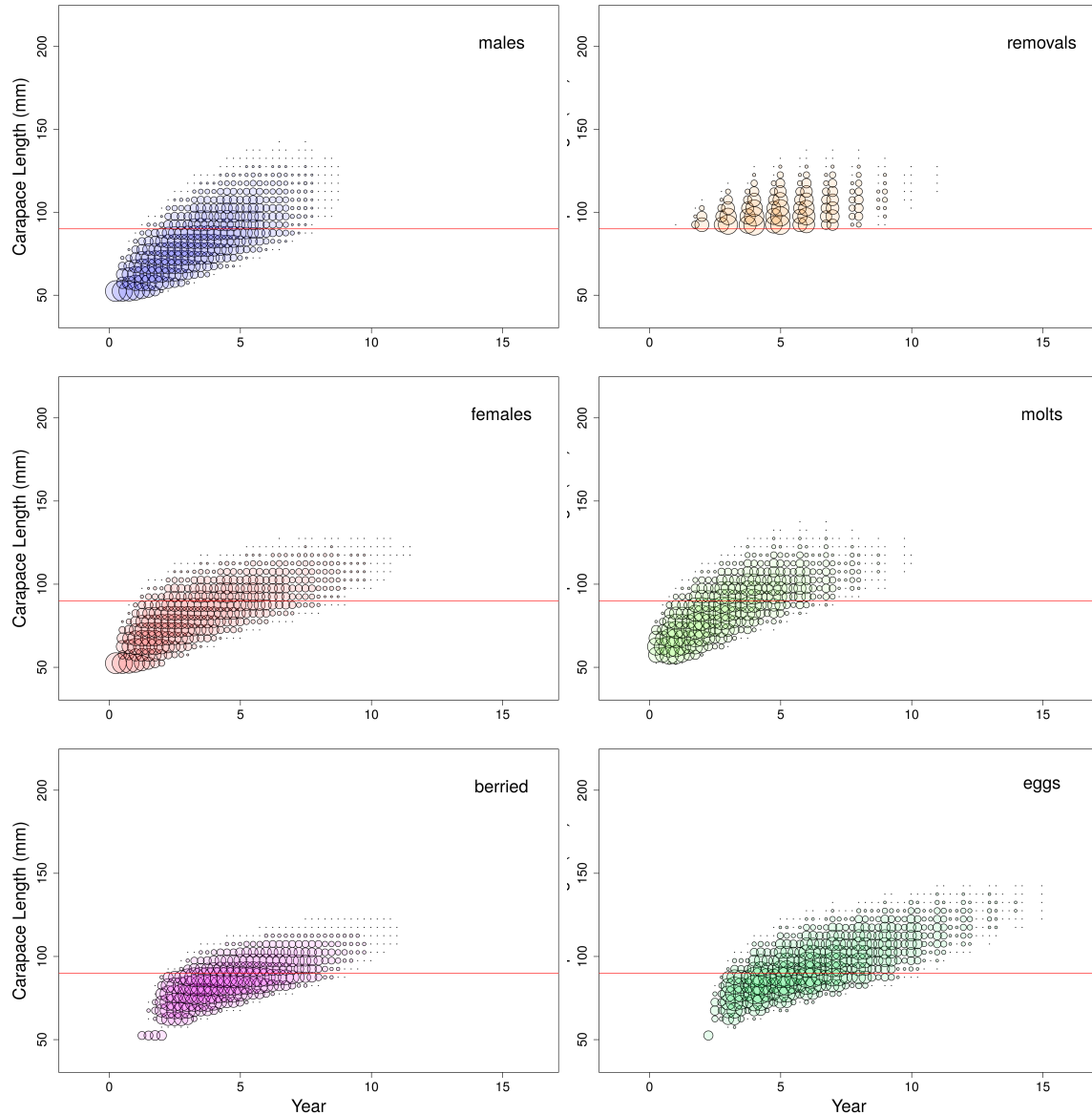


Figure 155: Bubble plot showing the simulated population where MLS was increased to 90mm for LFA 27S. The diameter of the bubbles are proportional to the log number of lobsters in a given size bin and time step.

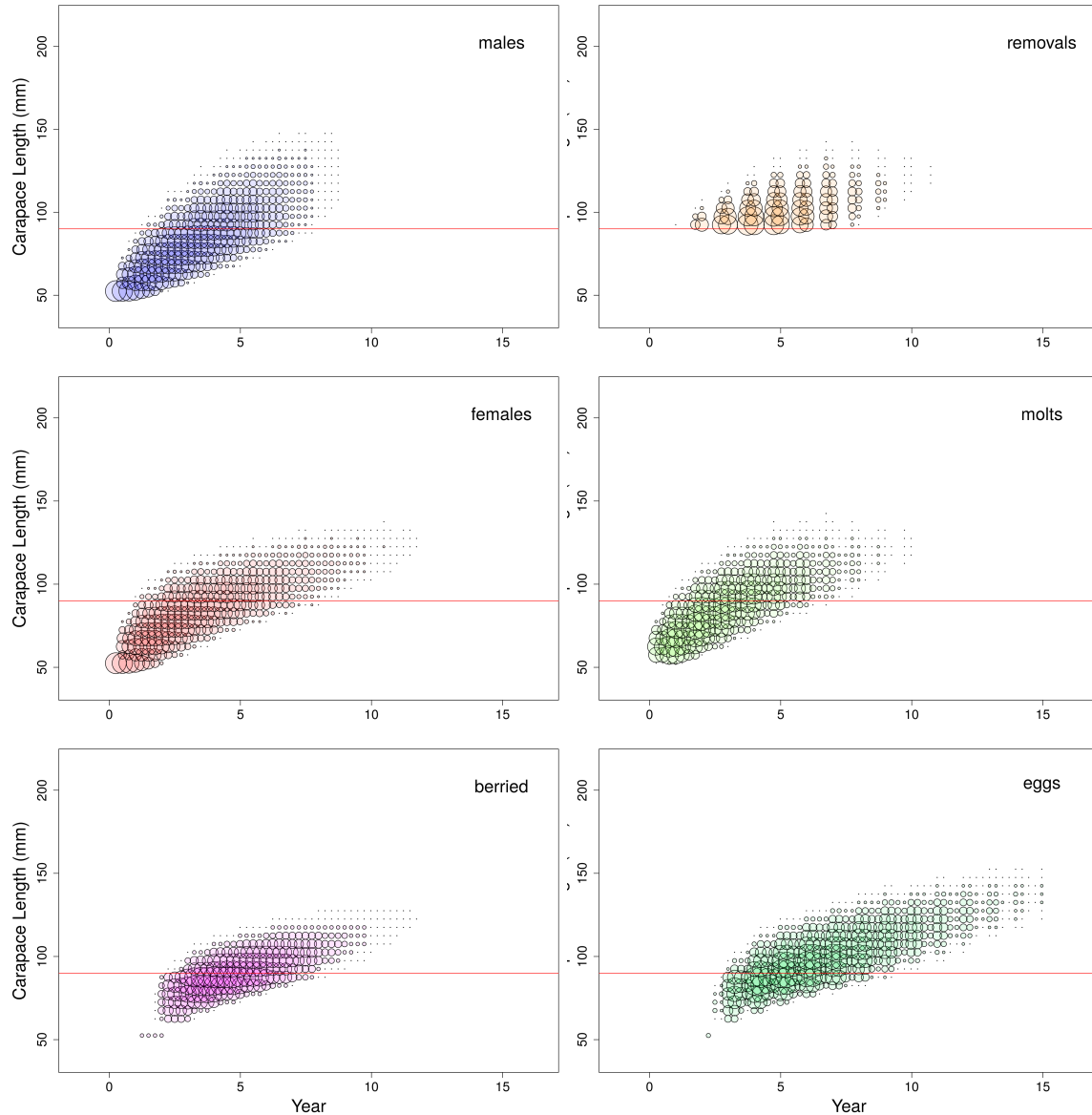


Figure 156: Bubble plot showing the simulated population where MLS was increased to 90mm for LFA 29. The diameter of the bubbles are proportional to the log number of lobsters in a given size bin and time step.

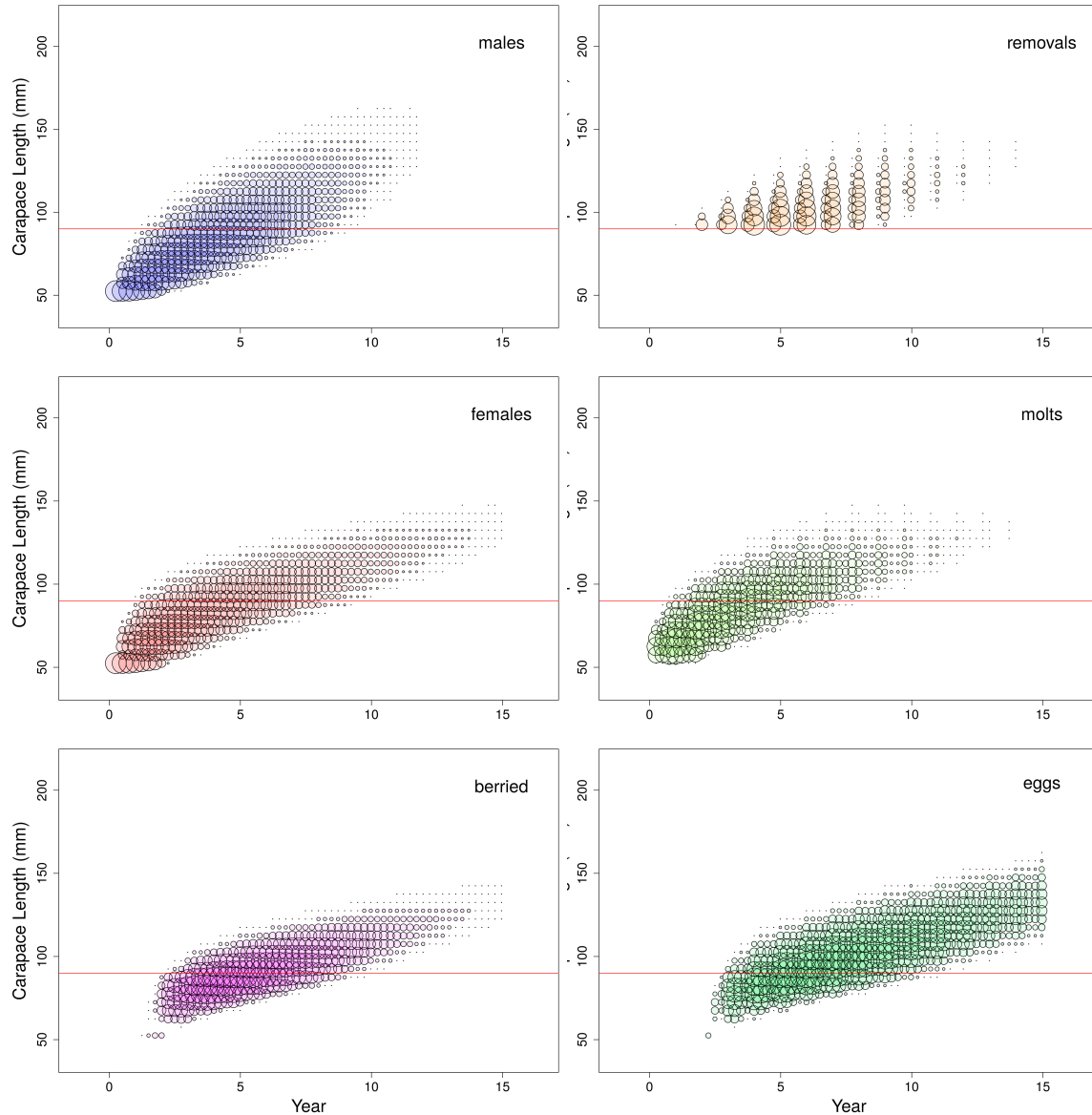


Figure 157: Bubble plot showing the simulated population where MLS was increased to 90mm for LFA 30. The diameter of the bubbles are proportional to the log number of lobsters in a given size bin and time step.

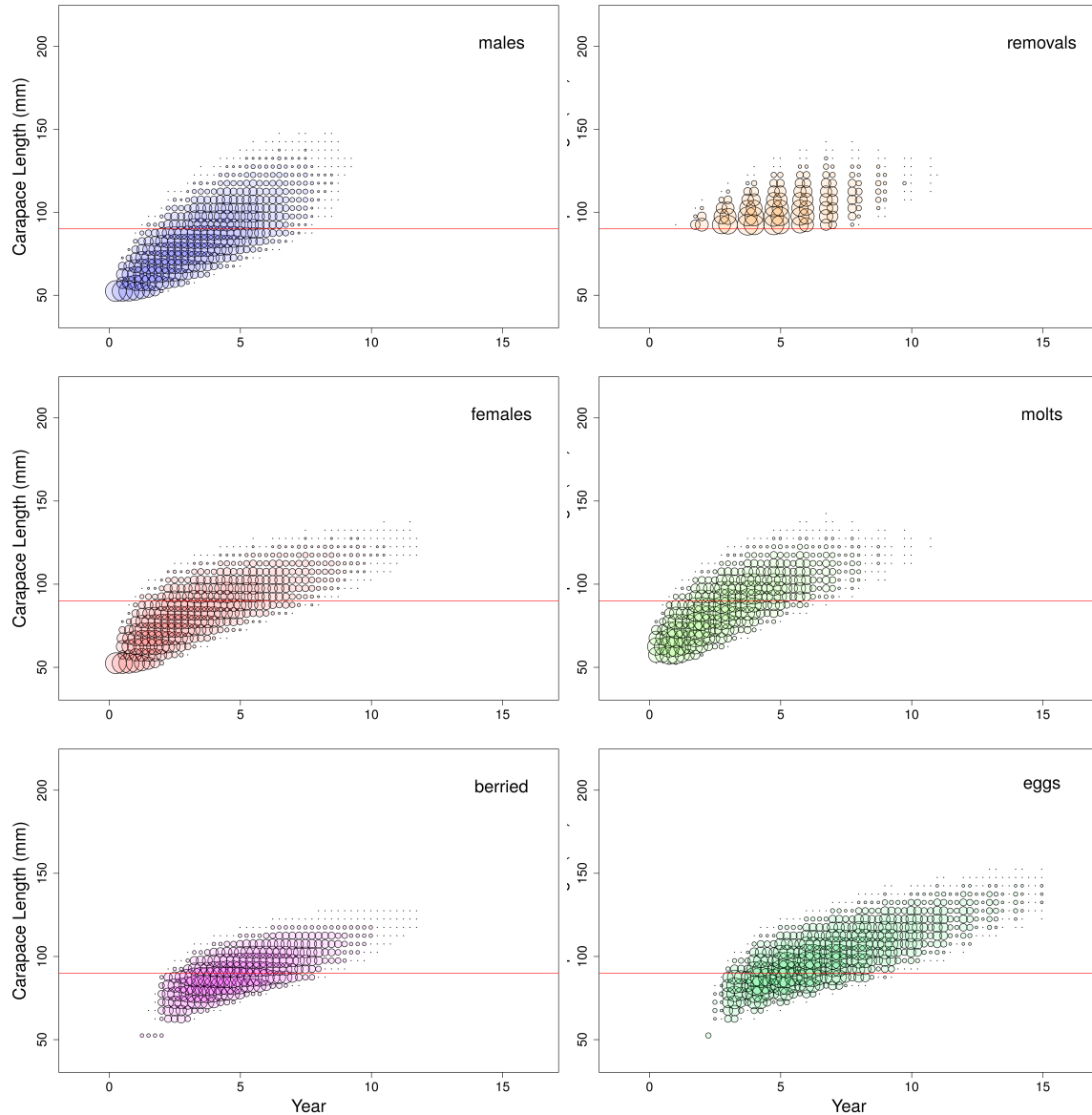


Figure 158: Bubble plot showing the simulated population where MLS was increased to 90mm for LFA 31A. The diameter of the bubbles are proportional to the log number of lobsters in a given size bin and time step.

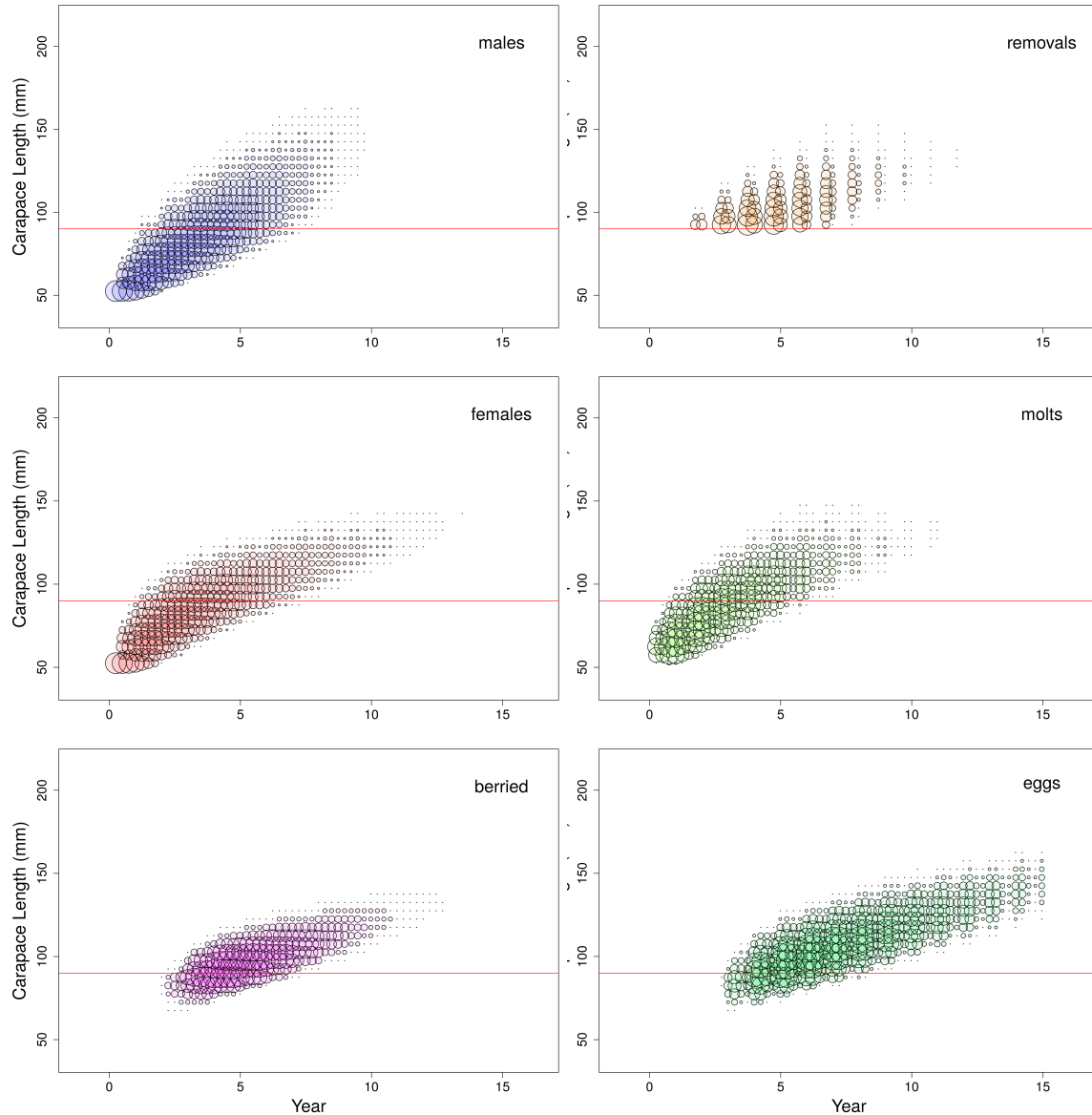


Figure 159: Bubble plot showing the simulated population where MLS was increased to 90mm for LFA 31B. The diameter of the bubbles are proportional to the log number of lobsters in a given size bin and time step.

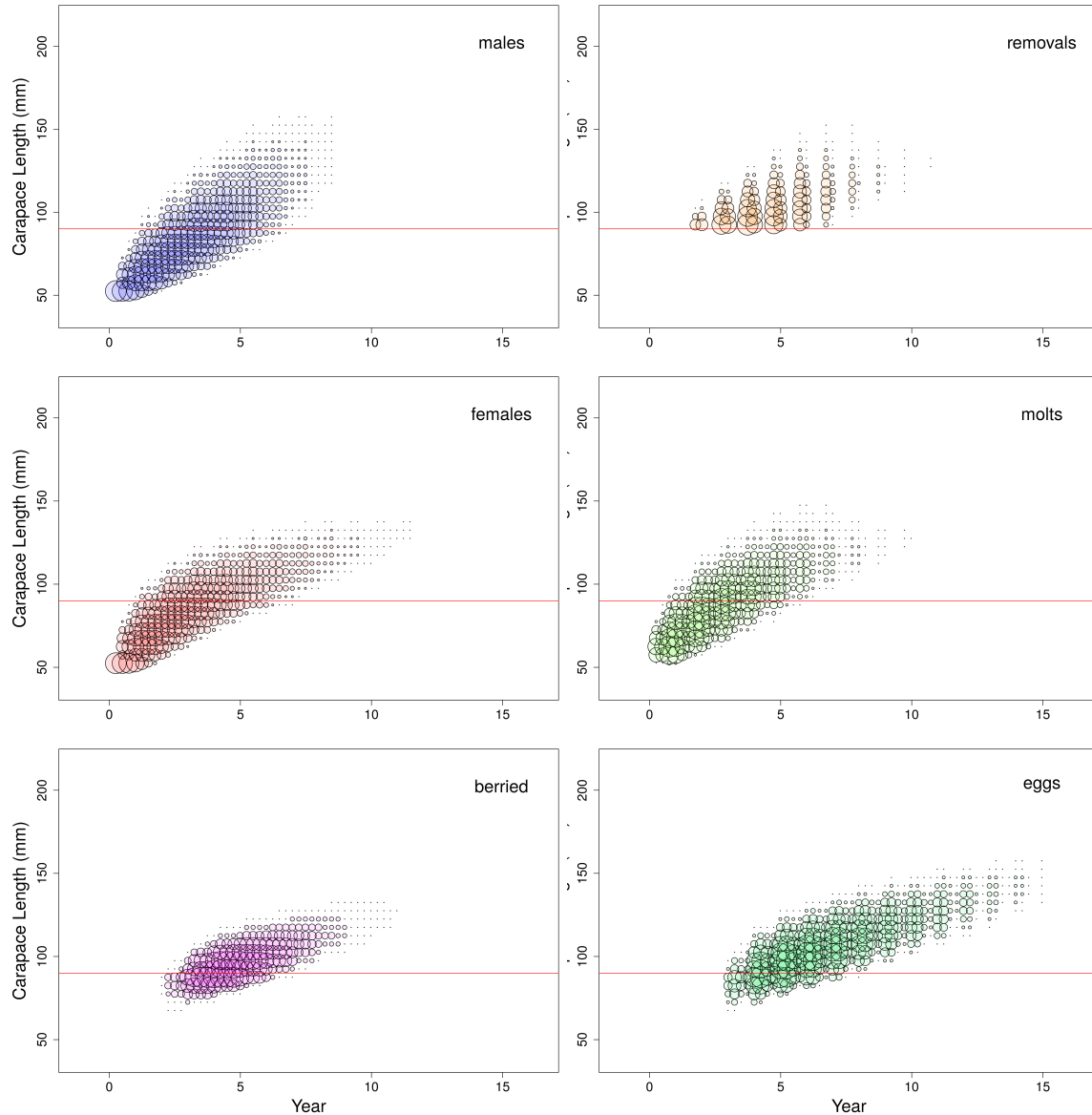


Figure 160: Bubble plot showing the simulated population where MLS was increased to 90mm for LFA 32. The diameter of the bubbles are proportional to the log number of lobsters in a given size bin and time step.

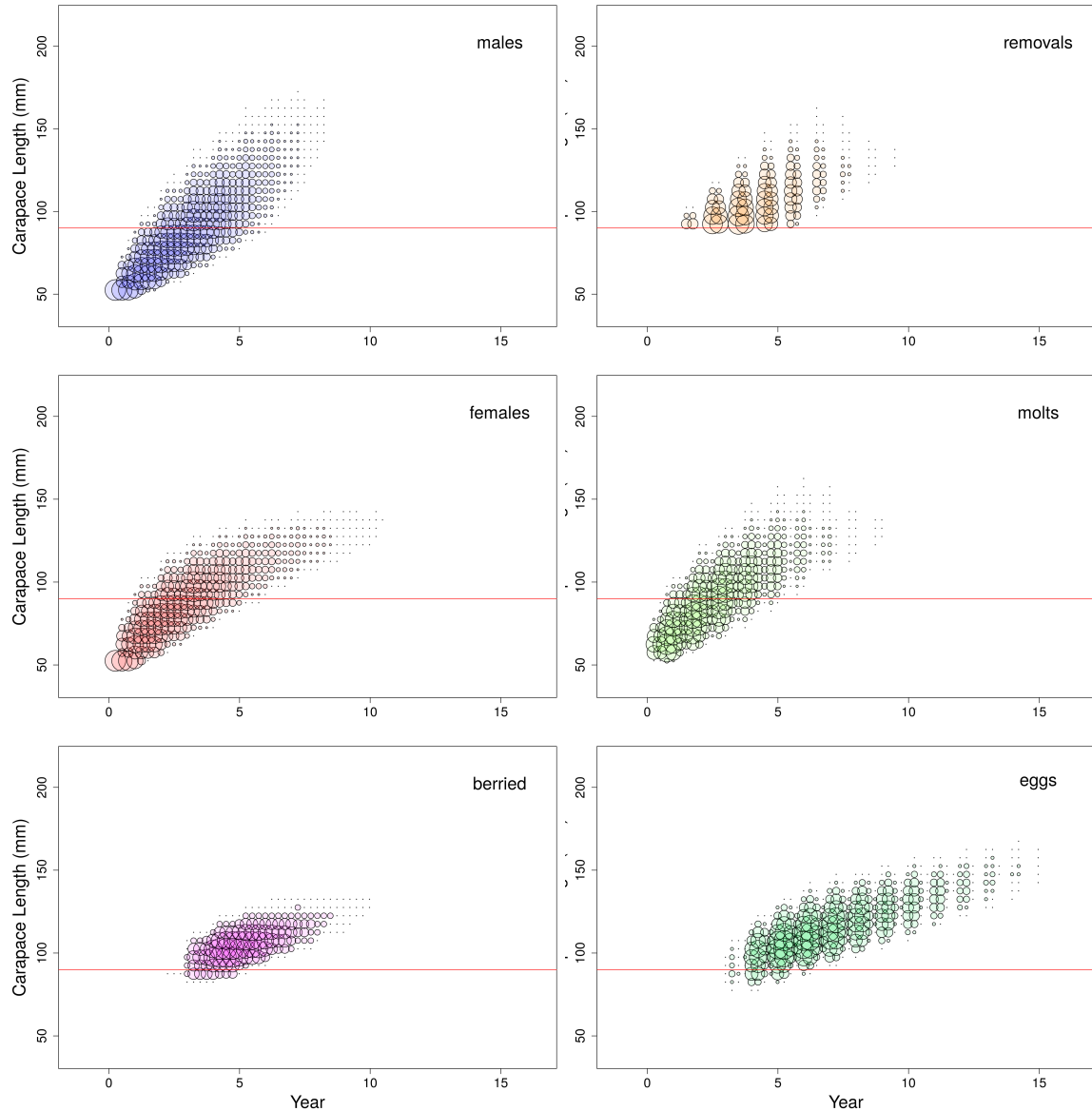


Figure 161: Bubble plot showing the simulated population where MLS was increased to 90mm for LFA 33E. The diameter of the bubbles are proportional to the log number of lobsters in a given size bin and time step.

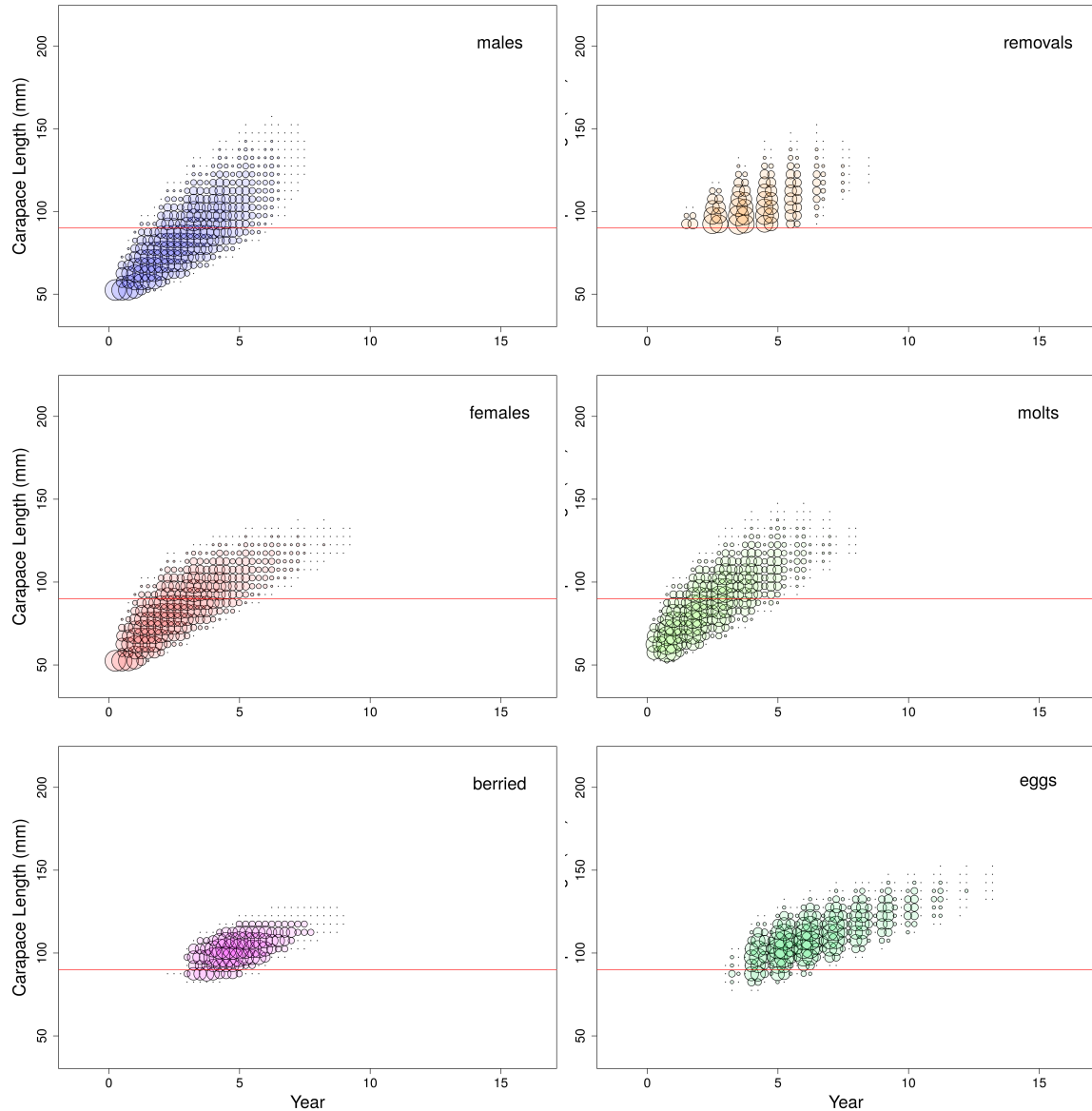


Figure 162: Bubble plot showing the simulated population where MLS was increased to 90mm for LFA 33W. The diameter of the bubbles are proportional to the log number of lobsters in a given size bin and time step.

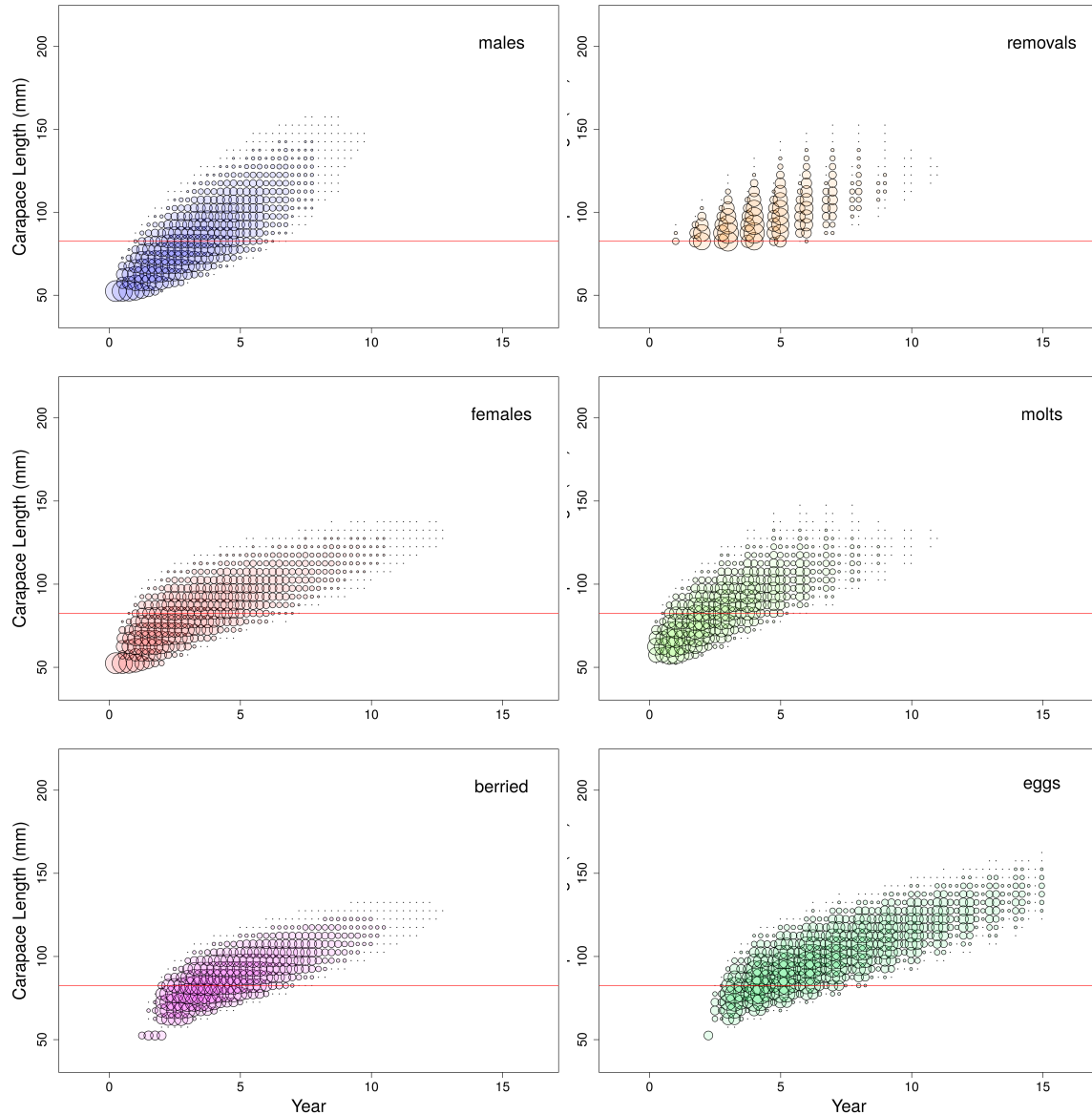


Figure 163: Bubble plots showing the simulated population where the season was shortened by 50 percent for LFA 27N. The diameter of the bubbles are proportional to the log number of lobsters in a given size bin and time step.

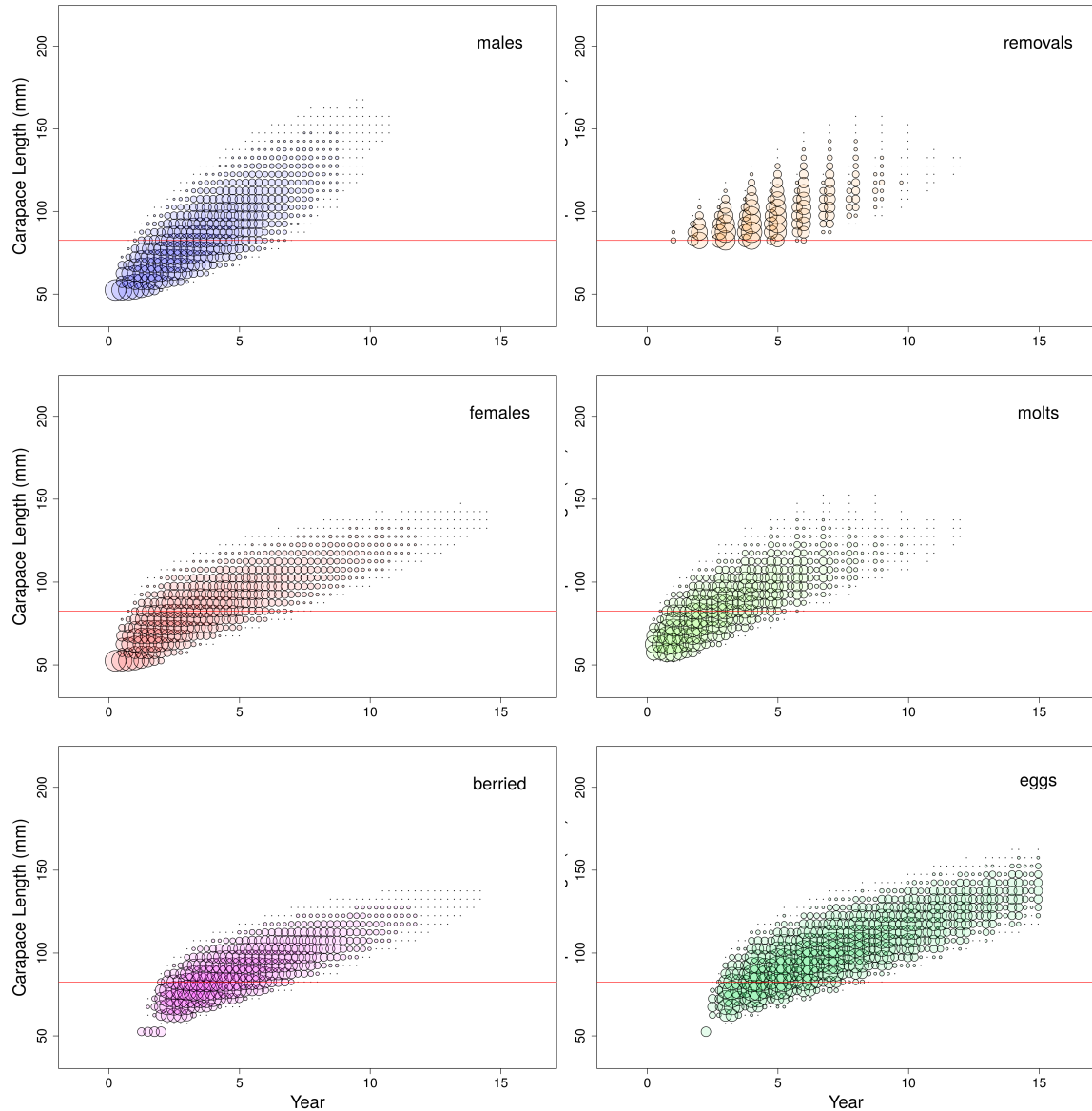


Figure 164: Bubble plot showing the simulated population where the season was shortened by 50 percent for LFA 27S. The diameter of the bubbles are proportional to the log number of lobsters in a given size bin and time step.

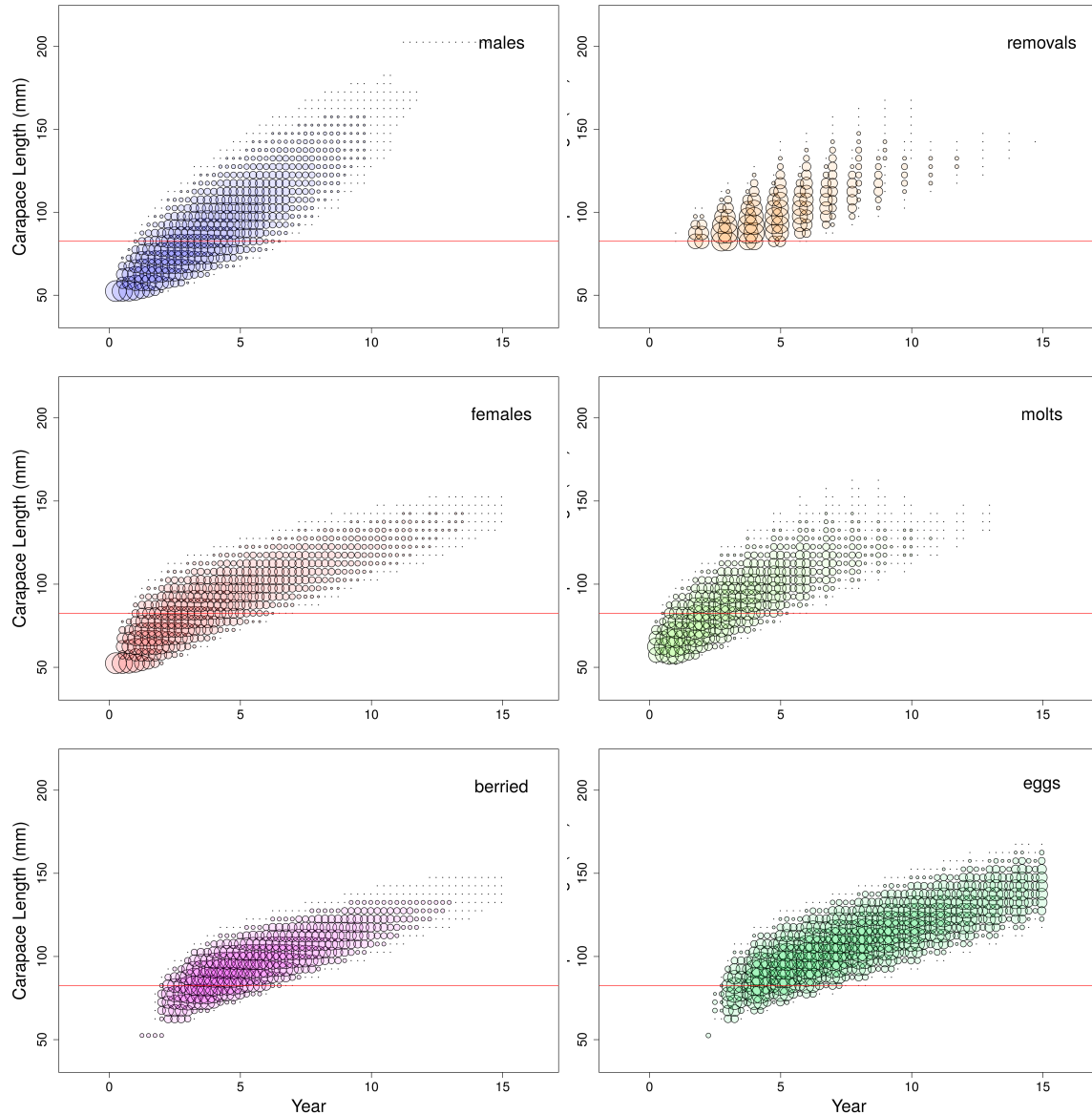


Figure 165: Bubble plot showing the simulated population where the season was shortened by 50 percent for LFA 29. The diameter of the bubbles are proportional to the log number of lobsters in a given size bin and time step.

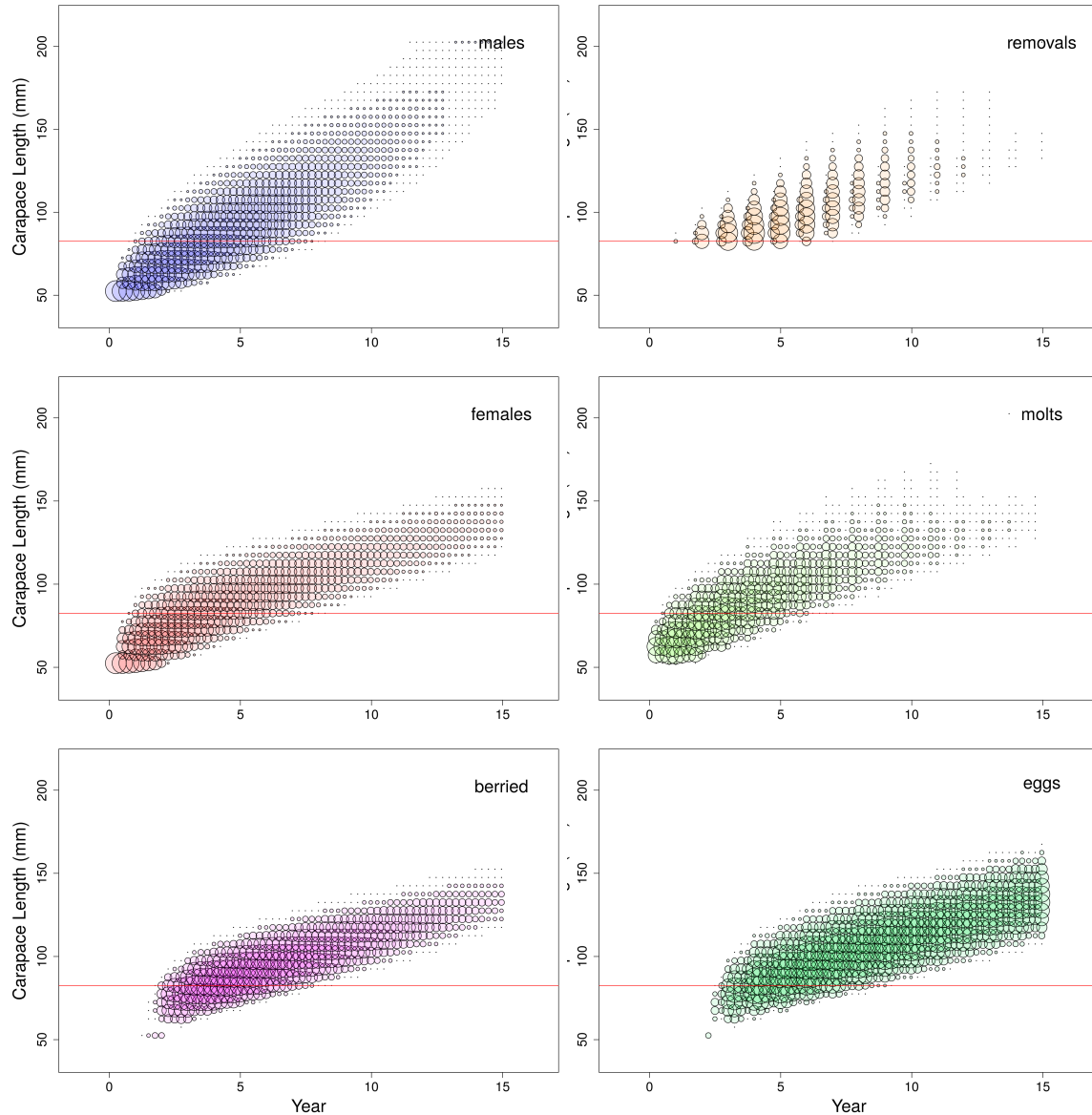


Figure 166: Bubble plot showing the simulated population where the season was shortened by 50 percent for LFA 30. The diameter of the bubbles are proportional to the log number of lobsters in a given size bin and time step.

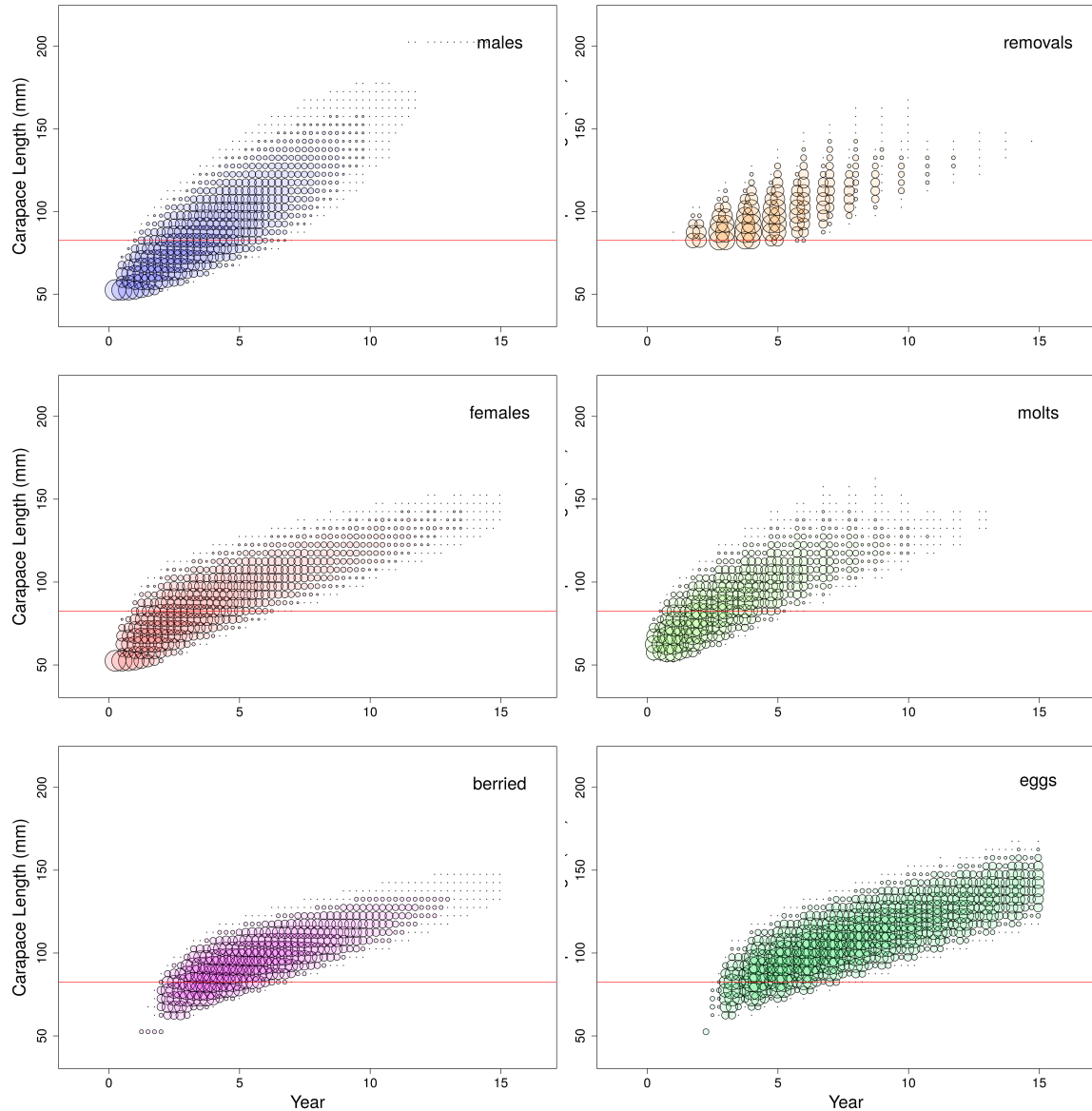


Figure 167: Bubble plot showing the simulated population where the season was shortened by 50 percent for LFA 31A. The diameter of the bubbles are proportional to the log number of lobsters in a given size bin and time step.

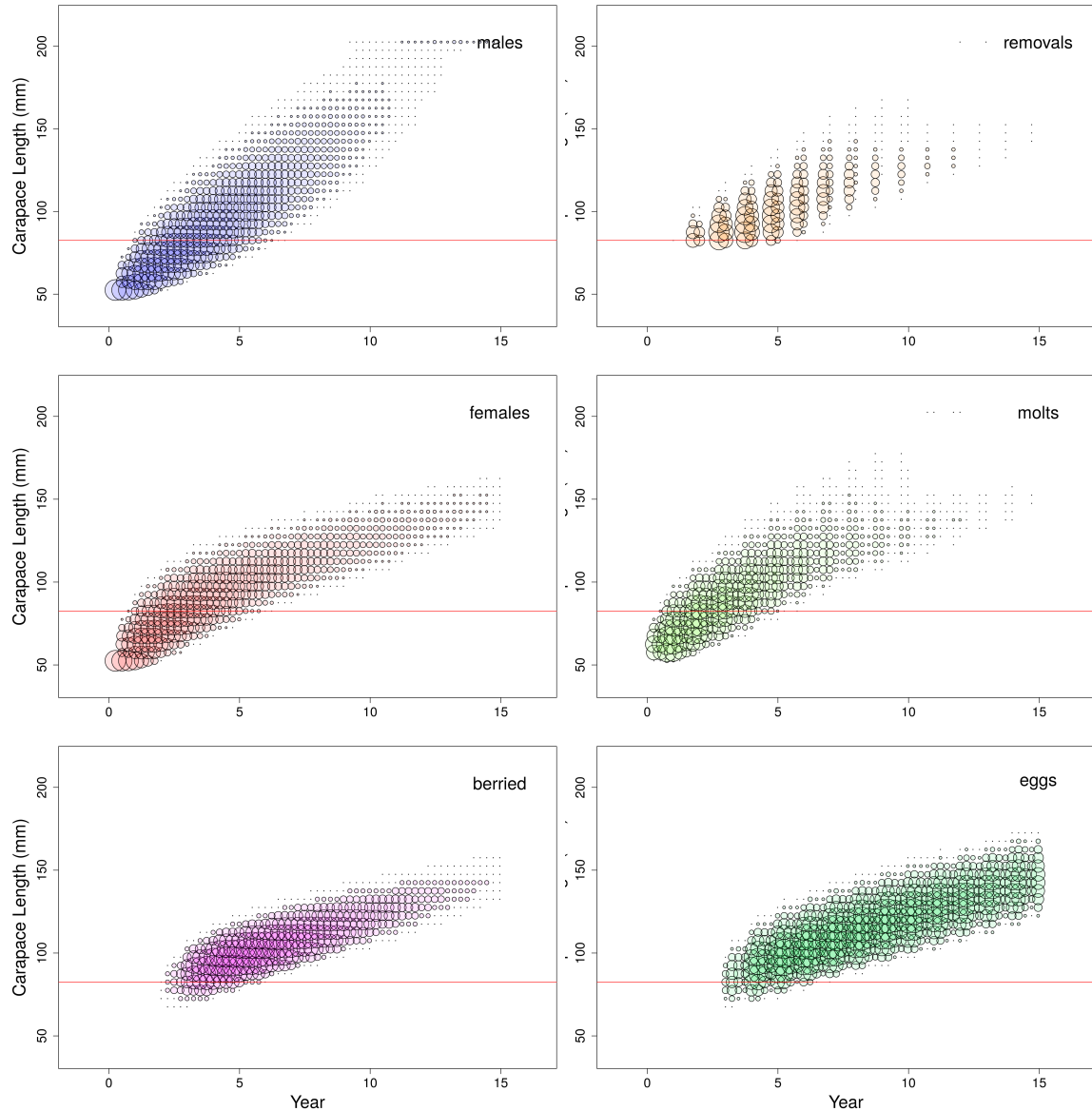


Figure 168: Bubble plot showing the simulated population where the season was shortened by 50 percent for LFA 31B. The diameter of the bubbles are proportional to the log number of lobsters in a given size bin and time step.

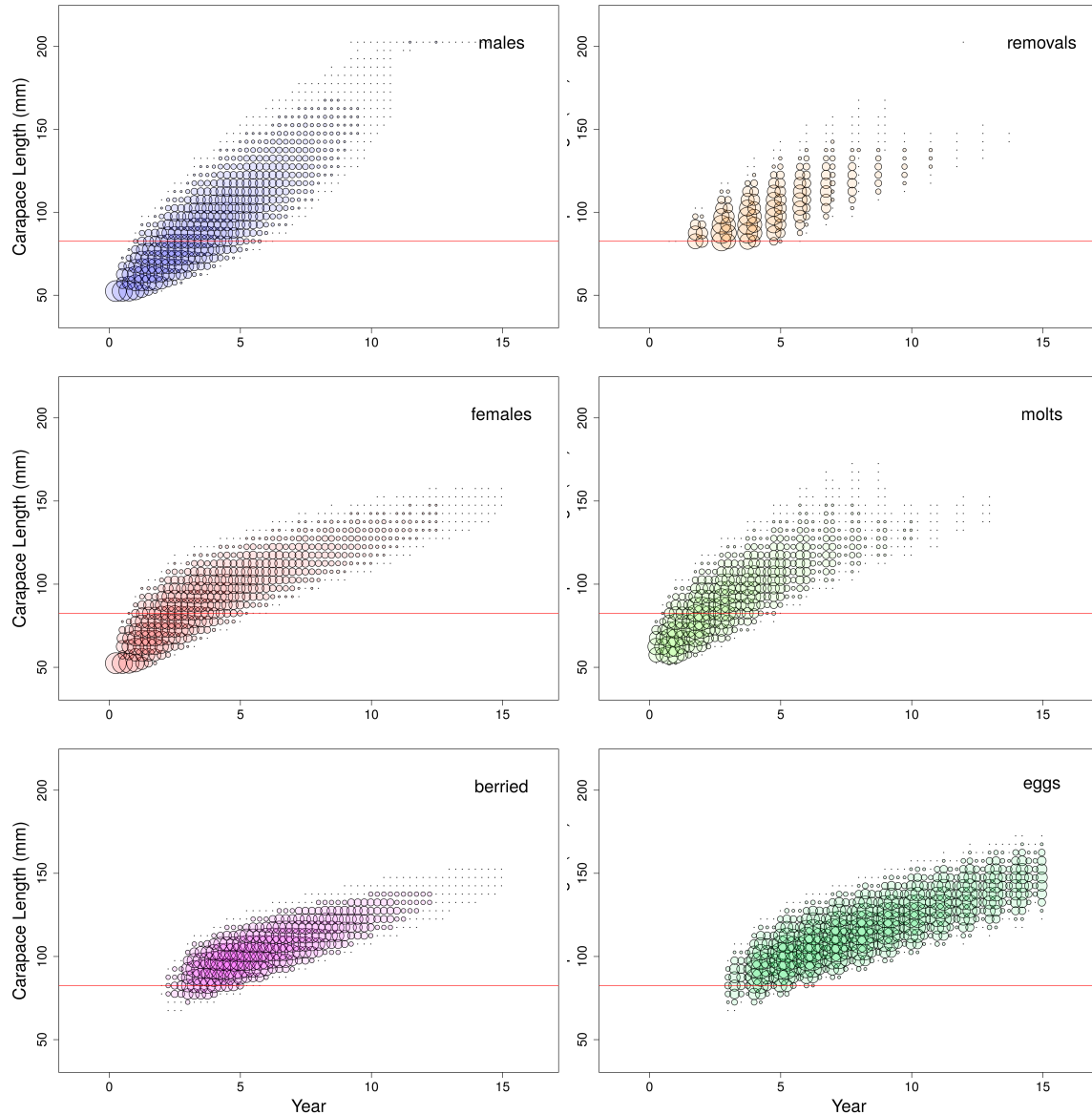


Figure 169: Bubble plot showing the simulated population where the season was shortened by 50 percent for LFA 32. The diameter of the bubbles are proportional to the log number of lobsters in a given size bin and time step.

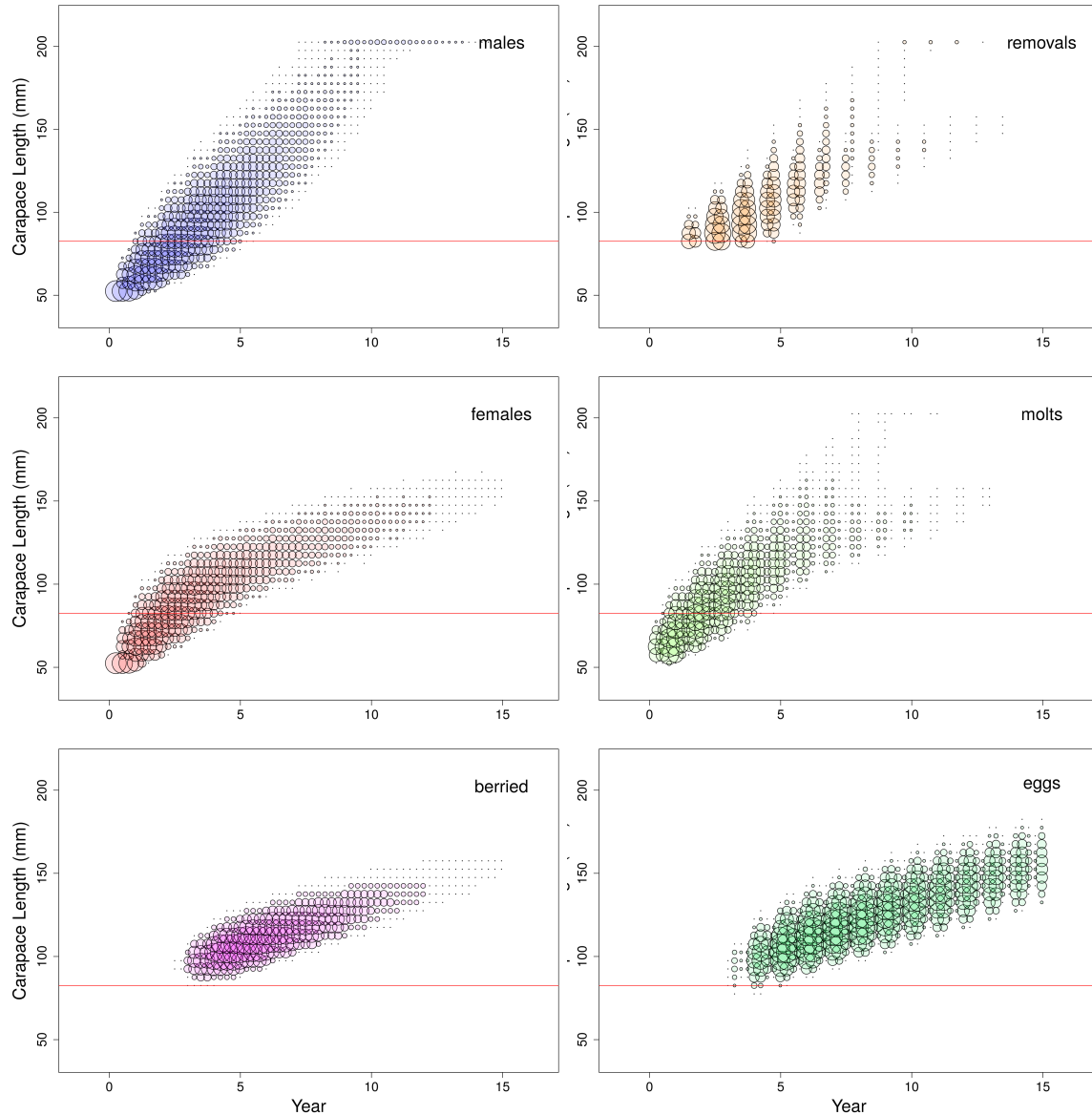


Figure 170: Bubble plot showing the simulated population where the season was shortened by 50 percent for LFA 33E. The diameter of the bubbles are proportional to the log number of lobsters in a given size bin and time step.

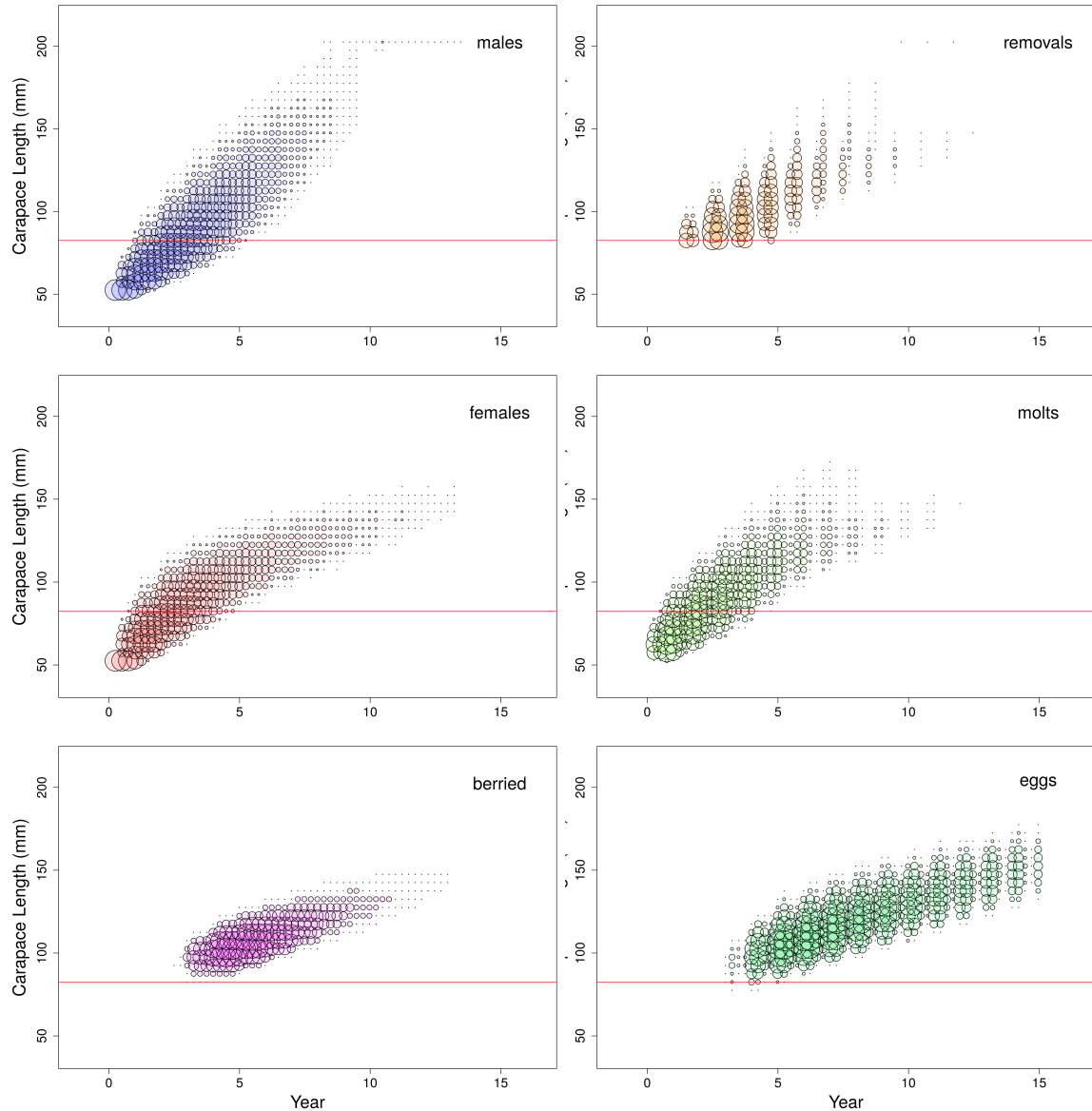


Figure 171: Bubble plot showing the simulated population where the season was shortened by 50 percent for LFA 33W. The diameter of the bubbles are proportional to the log number of lobsters in a given size bin and time step.

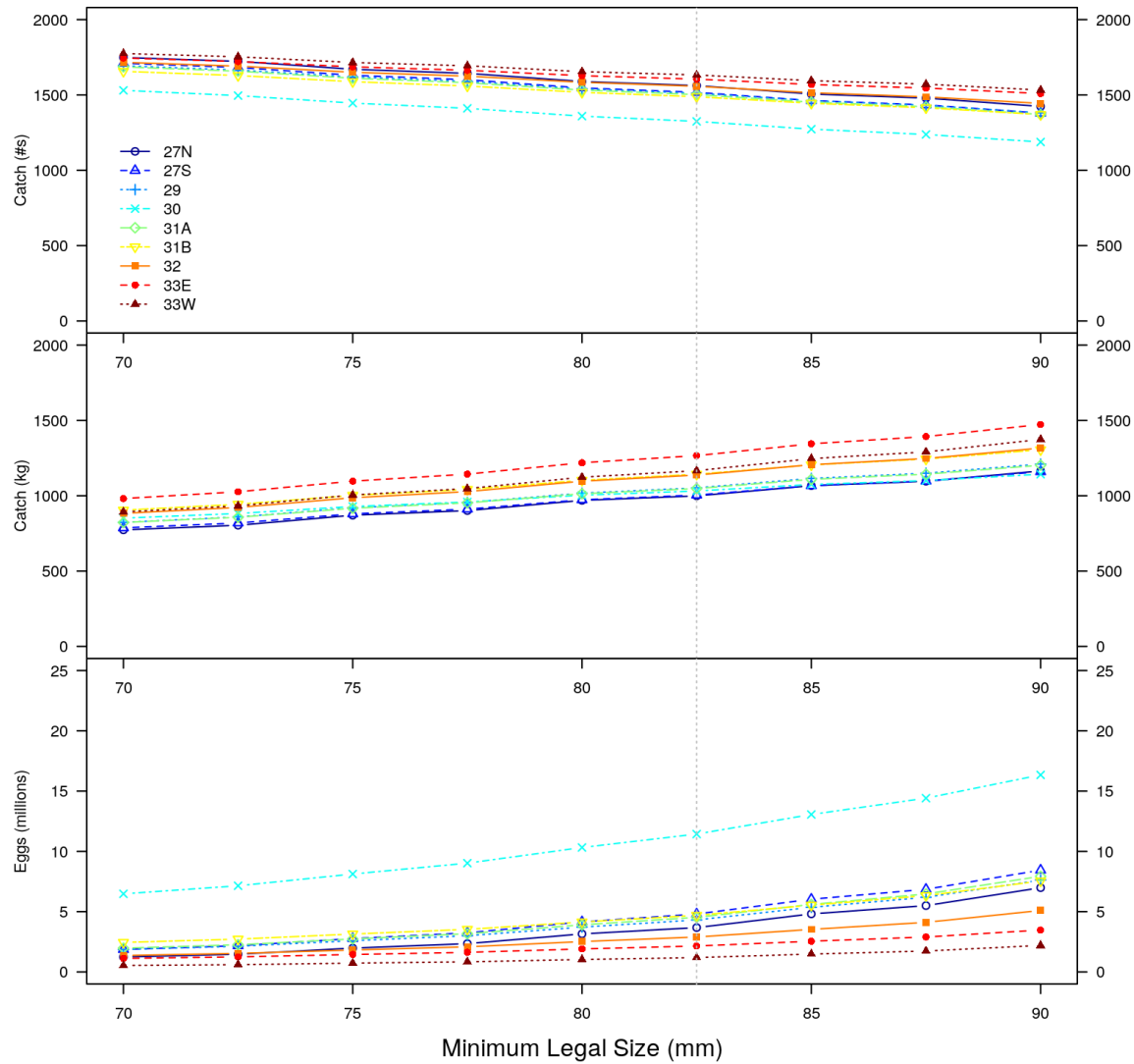


Figure 172: Summary of simulation model results for changes in Minimum Legal Size for each LFA.

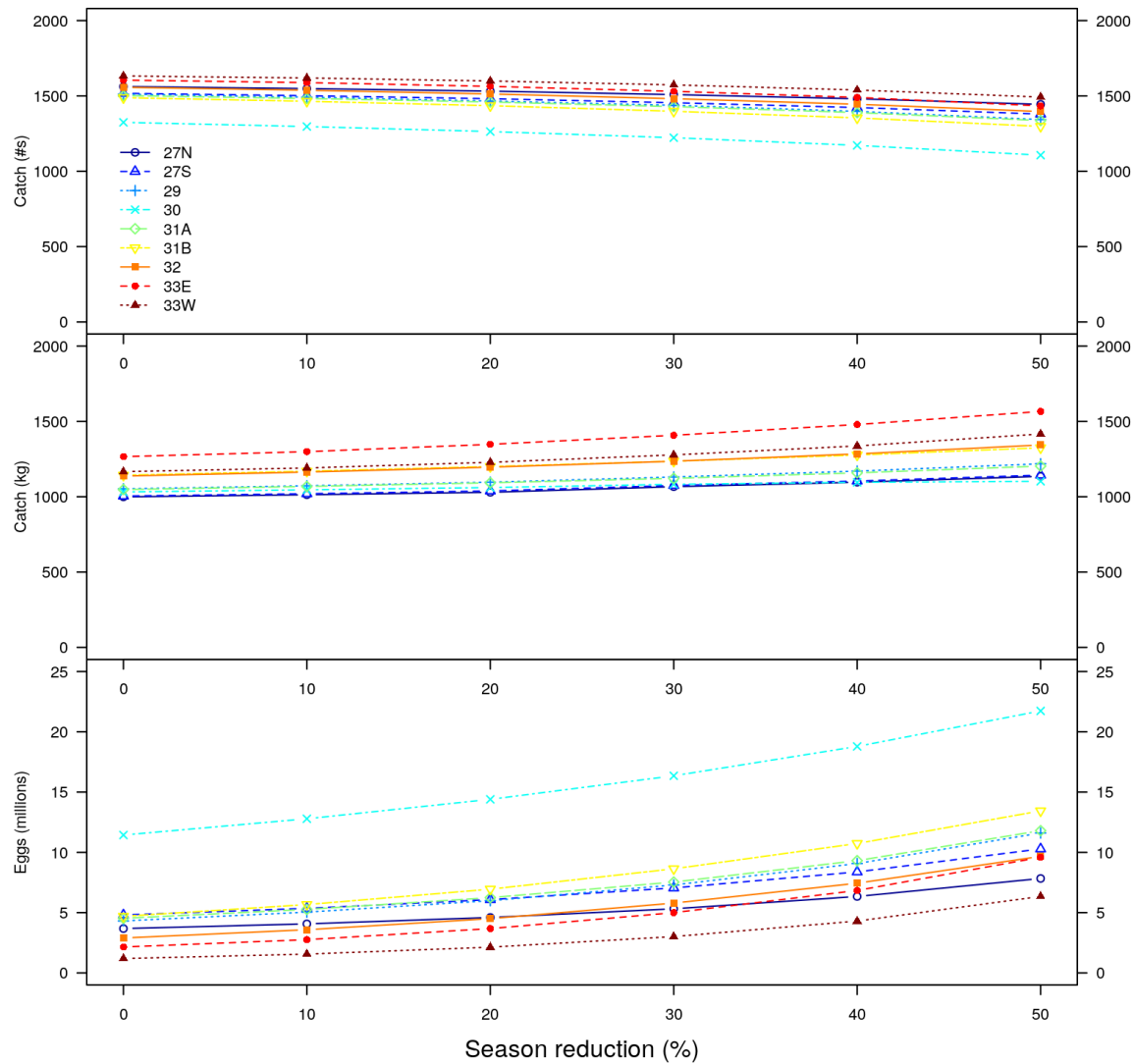


Figure 173: Summary of simulation model results for season reduction in each LFA.